EFFECT OF PHOSPHATE AVAILABILITY AND NUTRITIONAL STATUS ON THE WHEAT TRANSCRIPTOME

ASTRID GRÜN

Thesis submitted to the University of Nottingham

for the degree of Doctor of Philosophy

JULY 2015

Abstract

Economic, political and environmental factors have prioritized the need for research on phosphate (P_i) acquisition efficiency (PAE), P_i use efficiency (PUE) and P_i fertilizer uptake efficiency in crops. However, the coordination of molecular responses to P_i starvation and the mechanisms of P_i starvation tolerance have been investigated predominantly in model plants but remain elusive in grain crops, especially in wheat. This project investigates transcriptional profiles in wheat, particularly in the roots, as a response to nutrient availability focusing on phosphate (P_i). Furthermore, appropriate screening approaches and the difficulties in crop improvement, particularly for wheat, are discussed.

P_i acquisition by plants is mediated by members of P_i transporter families. The roles of these P_i transporters in P_i partitioning and re-translocation is complex and the knowledge about their functioning in wheat still limited. Here, members of the Pht1 family in wheat were identified, their expression profiles determined when exposed to different nutrient regimes in roots and ear tissues at various developmental stages and their potential role as targets for genetic improvement discussed. In addition to P_i transporters, regulatory genes including transcription factors, signalling pathways and apparently other P_i-responsive genes with unknown function are also of critical importance. Therefore, the genome-wide responses to limited nutrient availability were investigated for the first time in roots of field-grown wheat exposed to limited nutrient availability resulting in the identification of several candidate genes for PAE/PUE improvement on the molecular level. These data were validated against other studies and across a wider wheat germplasm. Furthermore, the correlation of candidate gene expression to the nutritional status, P_i availability and PAE/PUE properties revealed four potential target genes which may be major contributors to genotypic diversity of this trait. However, there are still some agronomic bottlenecks which impede implementing P_i efficient crops and the application of molecular tools and marker genes.

Publications list

Gruen, A., Broadley, M.R. and Buchner, P. (2015) Efficient mineral nutrition: genetic improvement of phosphate uptake and use efficiency in crops (2015) In: Nutrient use efficiency in plants - concepts and approaches (Hawkesford, M.J., Kopriva, S. and De Kok, L.J., eds.), Springer International Publishing, Switzerland, pp. 93-132.

Acknowledgements

Firstly, I have to say that I am very grateful to my supervisors, Martin R. Broadley, Malcolm Hawkesford and Peter Buchner, for advice and support during my project. Especially, I would like to thank Malcolm and his group for the welcoming, encouraging and enjoyable atmosphere. I am particularly grateful to Peter Buchner, Saroj Parmar and Andrew Riche for helping me to carry out my ideas and my work in the laboratories and the field. They were a great team and wonderful to work with.

I would like to thank the long-term experiments national capability, particularly the curators Andy McDonald and Margaret Glendining, which provided the datasets from the Classical Experiments and the on-site meteorological records from the electronic Rothamsted Archive (eRA).

Furthermore, I have to thank Jane Coghill who did the hybridization for the transcriptome analysis at the University of Bristol and Neil Graham for providing access to the Genespring software and advice for conducting the statistical analysis of these data at the University of Nottingham.

The work at Rothamsted Research is supported via the 20:20 Wheat® Programme by the UK Biotechnology and Biological Sciences Research Council (BBSRC). The contribution was supported by BIONUT-ITN and the research leading to these results has received funding from the European Union Seventh Framework Programme (FP7/2007-2013) under grant agreement no. 264296.

I would like to thank all the BIONUT-ITN partners for a very enjoyable time together. It was stimulating to meet so many different people with so various backgrounds. I am also thankful to all my friends and colleagues at Rothamsted, my friends and family at home and particularly my husband, Emanuel Reim, who followed and encouraged me during these last three years.

This work is dedicated to my mother, Friederike v. Hantelmann-Grün, and my farther, Helmut Grün, who I love so dearly and who have always supported me in this journey to make it real whatever happened.

Table of Contents

List of Figures

CHAPTER 1: GENERAL INTRODUCTION

CHAPTER 2: TAPHT1 FAMILY IDENTIFICATION

CHAPTER 3: TRANSCRIPTOME ANALYSIS

CHAPTER 4: CANDIDATE GENE SCREENING

List of Tables

CHAPTER 2: TAPHT1 FAMILY IDENTIFICATION

CHAPTER 3: TRANSCRIPTOME ANALYSIS

CHAPTER 4: CANDIDATE GENE SCREENING

List of Abbreviations

ABA	Abscisic acid
Al	Aluminium
AM	Arbuscular mycorrhiza
ANOVA	Analysis of variance
sAPase	Secreted acid phosphatase
As	Arsenic
A.tauschii	Aegilops tauschii, Tausch`s goatgrass
Ath	Arabidopsis thaliana, thale cress
ATP	Adenosine triphosphate
AxC	Avalon x Cadenza mapping population
BBSRC	Biotechnology and Biological Sciences Research Council, UK
Bd	Brachypodium distachyon, purple false brome
bHLH	Basic helix–loop–helix protein
BIONUT-ITN	Initial Training Network - Biochemical and Genetic Dissection of Control of Plant Mineral Nutrition
BLAST	Basic Local Alignment Search Tool
Bn	Brassica napus, oilseed rape
bp	Base pair
Ca	Calcium
CaDe	T. aestivum cv. Capelle Desprez
$Ca(NO_3)_2$	Calcium nitrate
Cd	Cadmium
CDC48	Cell division protein 48; chaperone of the AAA-ATPase family
cDNA	Complementary DNA
Co	Cobalt
Con	T. aestivum cv. Conqueror
Contig	Contiguous; DNA consensus region
COP	Critical Olsen P
Cr	Chromium
Cu	Copper
$CuCl_2$	Copper chloride
cv.	Cultivar

d	Day
DEFRA	Department for Environment, Food and Rural Affairs
DEPC	Diethylpyrocarbonate
df	Degrees of freedom
DH	Double haploid
DM	Dry matter
DNA	Deoxyribonucleic acid
DNase	Deoxyribonuclease
dNTP	Deoxyribonucleotide
dT	Deoxythymidine
DTT	Dithiothreitol
EDTA	Ethylenediaminetetraacetic acid
EMBL	European Molecular Biology Laboratory
eRA	Electronic Rothamsted Archive
ESTs	Expressed sequence tags
exp	Exponential
EXS	(ERD1/XPR1/SYG1) domain containing proteins
FAO	Food and Agricultural Organization of the United Nations
FASTA	Protein sequence alignment software package, sequence format
Fe	Iron
GAPDH	Glycerinaldehyd-3-phosphate-dehydrogenase
GEO database	Gene expression omnibus database
GDPD	Glycerophosphoryl diester phosphodiesterase
Glu-6-P	Glucose-6-Phosphate
Gm	Glyxine max; soybean
G3P	Glycerol-3-phosphate
GPX-PDE	Glycerophospho diester phosphodiesterases
GTP	Guanosine-5`-triphosphate
h	Hour
HAD	Haloacid dehalogenase-like hydrolase superfamily
H^+-ATPase	Proton-adenylpyrophosphatase
H_3BO_3	Boric acid
HCl	Hydrochloric acid
He	T. aestivum cv. Hereward

HGCA	Home grown cereals authority, United Kingdom
H_2O	Water
$H_2PO_4^-/HPO_4^{2-}$	Orthophosphate
Hv	Hordeum vulgare; barley
IAA	Isoamylalcohol
ICP-AES	Inductively Coupled Plasma Atomic Emission Spectrometer
ITPG	Isopropyl-β-D-1 thiogalactopyranoside
IWGSC	International Wheat Genome Sequencing Consortium
JIC	John Innes Centre
˚K	Kelvin
K	Potassium
KCl	Potassium chloride
KH_2PO_4	Monopotassium phosphate
K_m	Affinity value in Michaelis-Menten kinetics
KNO_3	Potassium nitrate
Le	Solanum esculentum; tomato
LEA	Late embryogenesis abundant proteins
LiCl	Lithium chloride
Log	Logarithmic
LSD	Least significant difference
M	Million
MAS	Marker-assisted selection
MCM6	Mini-chromosome maintenance protein 6
MDH	Malatedehydrogenase
MFS	Major facilitator superfamily
Mg	Magnesium
$MgSO_4$	Magnesium sulphate
Mn	Manganese
$MnCl_2$	Manganese chloride
Mo	Molybdenum
MPSS	Massive parallel signature sequencing
mRNA	Messenger RNA
miRNAs	Micro RNAs
MW	T. aestivum cv. Maris Widgeon

MYB-TF	Member of the MYB-transcription factor superfamily; MYB derived from an oncogene (v-myb) avian myeloblastosis virus (AMV)
N	Nitrogen
Na	Sodium
Na_2MoO_4	Sodium molybdate
$NaNO_3$	Sodium nitrate
NaOCl	Sodium hypochlorite solution
NaOH	Sodium hydroxide
NAS	Nicotianamine synthase
NCBI	National Center for Biotechnology Information
Ni	Nickel
Olsen P	mg P_i kg^{-1} air dried soil
Os	Oryza sativa, rice
P	Phosphorus
Pa	T. aestivum cv. Paragon
PAE	Phosphate acquisition efficiency
PAP	Purple acid phosphatase
Pb	Lead
P1BS	PHR1 specific binding sequence
PCA	Principal component analysis
PCR	Polymerase chain reaction
PEP	Phosphoenolpyruvate
PEPC	Phosphoenolpyruvate carboxylase
PHF	Phosphate transporter traffic facilitator 1
Pho1	Phosphate1 gene, contains SPX and EXS domains
Pho2	Phosphate2 gene; ubiquitin-conjugating E2 enzyme
PHR	Phosphate starvation responsive; transcription factor
PHS	Phosphate:H^+ symporter
Pht	Phosphate transporters
P_i	Phosphate
PLEXdb	Plant expression database
PP2C	Phosphoprotein phosphatase
PPCK	Phosphoenolpyruvate carboxylase kinase

PP_i	Pyrophosphate
PP_iase	Pyrophosphatase
PSI	Phosphate starvation induced genes
PSR	Phosphate starvation response
PTF1	Phosphate starvation induced transcription factor 1
PUE	Phosphate use efficiency
Pup1	Phosphate uptake 1 (QTL)
QTL	Quantitative trait loci
r	Correlation coefficient
R^2	Percentage variance accounted with a model (%)
RAN GTPase	GTP-binding nuclear protein RAN-B1
REML	Residual maximum likelihood
RIL	Recombinant inbred lines
RNA	Ribonucleic acid
RNAse	Ribonuclease
S	Sulphur
SAGE	Serial analysis of gene expression
SAMD	S-adenosylmethionine decarboxylase
SDS	Sodium dodecyl sulphate
Se	Selenium
SE	Standard error
SED	Standard error of the difference
S. italic	Setaria italic; foxtail millet
SIZ1	E3 SUMO-protein ligase
SPX	(SYG1, PHO81, XPR1) domain containing proteins
SPS	Sucrose phosphate synthase
SQD1	UDP-sulfoquinovose synthase 1
ssp.	Subspecies
S. tritici	Septoria tritici; Septoria leaf blotch
SUMO	Small ubiquitin-like modifier
SUC2	Sucrose transporter
Ta	Triticum aestivum, wheat
TAE	Tris acetate EDTA
TaG3Pp	Wheat glycerol-3-phosphate permease

TCA	Tricarboxylic acid cycle
TF	Transcription factor
TGW	Thousand grain weight
TM	Transmembrane domains
T. monococcum	Triticum monococcum, einkorn
Tris	Tris (hydroxymethyl) aminomethane
T. ssp. durum	Triticum turgidum subspecies durum, durum wheat
T. turgidum	Triticum turgidum
UBC24	Member of the E2 ubiquitin conjugase (UBC) family
UDP	Uridine diphosphate
V_{max}	Maximum velocity in Michaelis-Menten kinetics
WT	Wild type
WISP	Wheat Improvement Strategic Programme
Zm	Zea mays, maize
Zn	Zinc
$ZnCl_2$	Zinc chloride
18sRNA	18S ribosomal RNA

Chapter 1: Dissection of efficient mineral nutrition and targets for genetic improvement of phosphate acquisition and phosphate use efficiency in crops

1.1. Project outline

1.1.1. PhD project within the BIONUT – objectives of the ITN

This PhD project is part of a Marie Curie Initial Training Network "Biochemical and Genetic Dissection of Control of Plant Mineral Nutrition" (BIONUT-ITN)[1] which aims to dissect three main areas: "Genetic control of nutrient use efficiency", "Functions of genes affecting plant mineral nutrition" and "Candidate gene evaluation in crops under agronomic conditions". This project is focused on gene expression in wheat as a response to the availability of phosphate (P_i).

1.1.2. Context, hypothesis and project outline

Economic, political and environmental factors have prioritized the need for research on P_i acquisition efficiency (PAE), P_i use efficiency (PUE) and P_i fertilizer uptake efficiency in crops. However, plants take up phosphorus (P) as P_i, which has critical functions in plants and complex interactions in soils, and deficiencies can be a major constraint for agricultural productivity. Exploitation of genetic variation and gene modification of target genes are routes for future crop improvement including efficient use of nutrients. The coordination of molecular responses to low P_i availability and the mechanisms of P_i starvation tolerance have been investigated predominantly in model plants, but less so in grain crops, especially in wheat. However, P_i efficiency strategies may not be conserved between species and genetic diversity responsible for P_i starvation tolerance may be the basis for crop improvement.

Importantly, wheat is an essential staple food, a major contributor to the global phosphorus cycle and exposed to P_i limited conditions in many regions of the world. However, wheat research is challenging due to the complexity of its

[1] http://www.bionut-itn.eu/
[2] http://faostat.fao.org/
[3] http://www.nutrientstewardship.com/; supported by the International Plant Nutrition Institute,

genome and the difficult task of applying molecular tools in the breeding effort.

To consider root traits in the selection process is another challenging task, even if it might significantly improve nutrient acquisition and agricultural productivity.

Therefore, the main aims of this study were to:

- Determine transcriptional responses to macronutrient limitations in wheat and identify genes linked to these responses
- Dissect specific gene expression in the roots as a response to limited P_i availability and the nutritional status of the shoot
- Quantify the molecular responses to P_i availability in the roots, focusing on P_i uptake processes
- Determine the molecular responses to P_i availability in ear tissues, focusing on translocation processes during grain filling
- Screen wheat germplasm for potential P_i efficiency traits
- Assess the expression of potential target genes and link them to P_i efficiency traits and to the nutritional status of the plant
- Identify candidate genes which may be used for future crop improvement

1.1.3. Experimental approaches

Due to the complex interactions of P_i in soils, field experiments are more suitable to assess applicable traits for increasing P_i efficiency in crop production rather than using liquid culture systems. Therefore, three experimental approaches were used to distinguish between short-term strategies to cope with local P_i depleted soil patches and longer-term adaptation to P_i starvation. These approaches used hydroponic culture and soil-grown plant material derived from two field experiments at Rothamsted Research station: Broadbalk (2011 and 2012) and the P_i field trial at Sawyers (2012 and

2013). The Broadbalk experiment is characterized by long-term withdrawal of N, P_i, K, Mg and S fertilizers. The P_i field trial at Sawyers consists of a wheat germplasm collection growing at different plant-available soil-P_i. Further differentiation was made between wheat genotypes and physiological stages throughout the seasons.

PAE and PUE are usually linked to each other, are difficult to dissect and there is a lack of consistent screening methodologies in the literature. Hence, a selection process considering P_i acquisition, translocation processes and crop P_i requirements during different growth stages is required. Therefore, a tissue-specific approach was used to evaluate across the diverse genotypes available for studying in field experiments at Rothamsted.

The effect of P_i starvation on the ionome, i.e. macro- and micronutrient concentrations, were chemically determined via ICP-AES. Candidate gene selection was based on a transcriptome analysis using the Affymetrix Wheat Gene Chip® array and gene expression studies using real-time quantitative polymerase chain reaction (PCR) techniques. Candidate gene validation was performed by linking gene expression data to ionome and PAE/PUE data.

1.1.4. Thesis structure

The thesis consists of five main parts: Chapter 1 provides a general overview of the context and the difficulties for improving complex traits in crops such as PAE/PUE. Genes mediating either the P_i starvation signalling response or posttranslational modifications, morphological, metabolic or biochemical responses that enhance P_i solubility in the soil and facilitate acquisition including root plasticity, secretion processes and symbioses will be discussed. P_i acquisition is mediated by members of P_i transporter families and their roles as well as enzymes involved in P partitioning and re-translocation is complex. In Chapter 2, members of the P_i transporter family were identified in wheat and their potential role as targets for genetic improvement investigated. In Chapter 3, the genome-wide response of field-grown wheat roots to limited nutrient availability was investigated. The impact of P_i starvation and other essential

macronutrient limitations on ionomic and transcriptional responses is presented. The data were further compared with previously published transcriptome data from model plants and other crops exposed to P_i starvation. There is a critical importance of regulatory genes including transcription factors, signalling pathway genes and P recycling responsive genes which were investigated and validated as candidates across a wider wheat germplasm in Chapter 4. Furthermore, PAE/PUE traits were determined for these genotypes and the potential linkage of candidate gene expression to the nutritional status and to PAE/PUE are discussed. The potential application of the acquired molecular data from current research on P_i nutrition in crop improvement strategies, including breeding and production, is discussed in Chapter 5, emphasising which aspects are already exploitable or which require further knowledge or are difficult to implement.

1.2. Phosphate nutrition in plants

1.2.1. Wheat as target crop

Wheat is one of the most important staple food crops worldwide (Shewry 2009). In terms of production quantity, with 670 M t harvested in 2012, wheat ranks in fourth place behind sugar cane (1832 Mt), maize (872 Mt) and rice (719 Mt) (FAOStat, 2012)[2]. Over the past decades wheat production has risen due to an increase in yield, rather than an increase of cultivation area (Figure 1A). However, the annual rates of gain in global wheat production during the last ten years were at about 1 %, much less than it was between 1960 and 1990 during the green revolution. Annual rates were > 3 % during that period (Figure 1 A and B), which was achieved through the adoption of semi-dwarf cultivars, favouring more productive varieties rather than landraces together with increased cropping intensity through fertilizer use (Peng et al. 1999, Phillips and Norton 2012).

Currently, wheat yields are facing a plateau in many countries with high production intensity, for example in the United Kingdom (UK) (Figure 1B), France and Germany, which are amongst the top ten of world producers in terms of wheat grain yields (Phillips and Norton 2012). Increasing yields without raising the production area is crucial for ensuring global food security, improving the sustainability of crop production, and decreasing energy and fertilizer resource use (Gregory and George 2011); this may be achieved through a combination of improved wheat genetics and agricultural practices (Phillips and Norton 2012). Particularly, as global P_i fertilizer consumption is still increasing (Figure 1C) and 15 % of the total nutrient applications through fertilizers are applied in wheat production (Phillips and Norton 2012). Although nutrient acquisition, such as P_i via the plant root system, is a crucial factor for agricultural productivity and crop yield (Lynch 1995), root systems of green revolution wheat have been suggested to be significantly smaller compared to landraces (Waines and Ehdaie 2007). Therefore, root traits should indeed be reconsidered and integrated into the breeding effort and the process of genetic selection (Vance et al. 2003, Waines and Ehdaie 2007).

[2] http://faostat.fao.org/

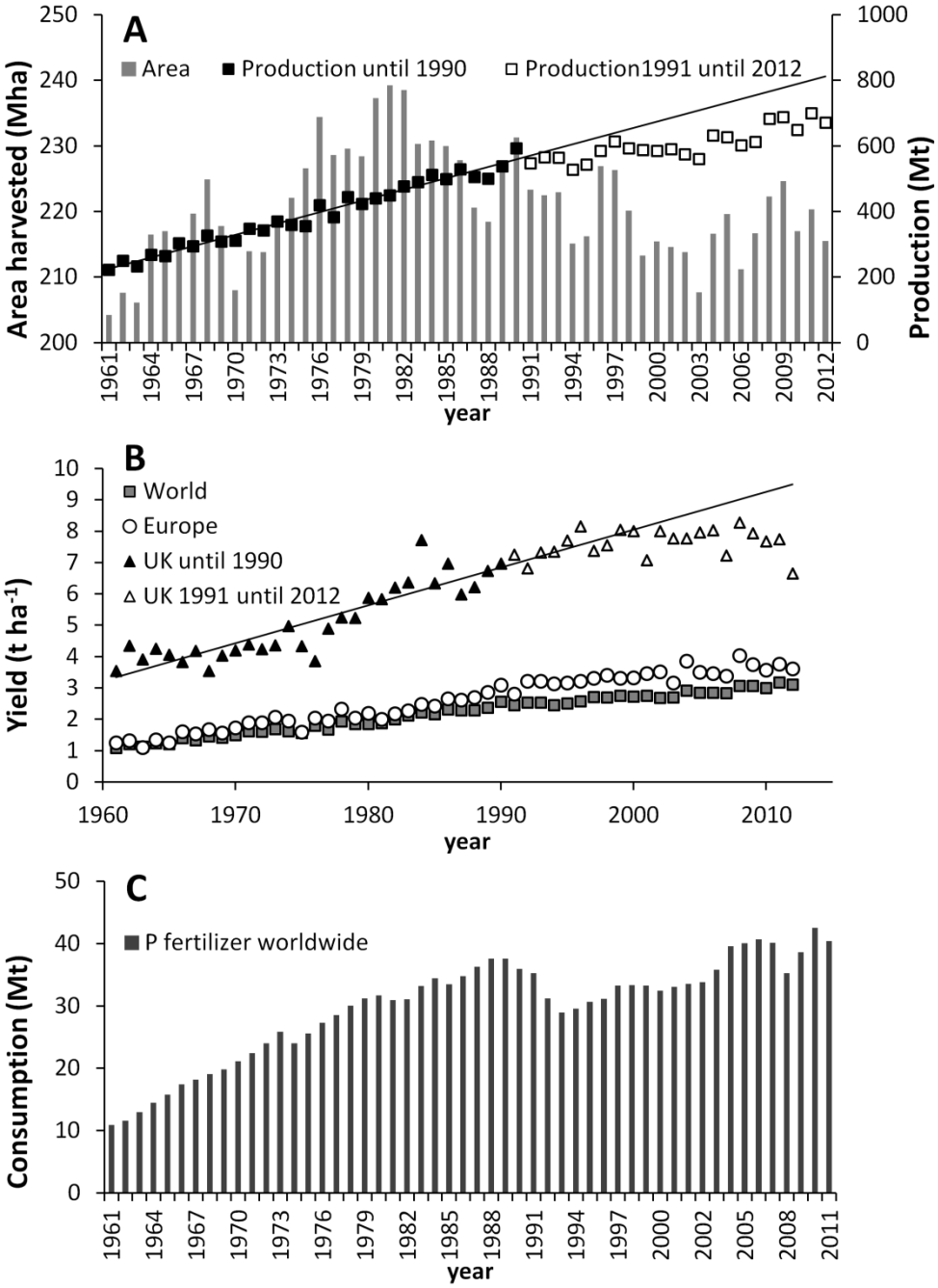

Figure 1: (A) World wheat production (Mt) and production area (Mha), (B) grain yields (t ha-1) and (C) P_i fertilizer consumption (Mt) (FAOStat, 2012).

Wheat is allohexaploid (2n=6x=42; AA BB DD) with a genome size of up to 17,000 Mbp containing around 100,000 genes (Brenchley et al. 2012). Furthermore, the wheat genome it is not yet fully sequenced. It has a large repeat content of around 80 % with genes arranged in gene-rich regions for which assigning functions is a major challenge (Lagudah et al. 2001, Choulet et al. 2010, Brenchley et al. 2012). To date, due to the complexity of its genetics, there is still a huge knowledge gap in the understanding of which alleles or allelic variants are controlling many important agricultural traits in wheat and where they are located on the genome (Bagge et al. 2007, Coram et al. 2008). Therefore, increasing wheat yields without comprising on sustainability through (molecular) breeding is a long and demanding task in comparison to maize or rice, due to the difficulties in implementing molecular and genomic tools (Bagge et al. 2007, Coram et al. 2008, Aversano et al. 2012).

1.2.2. The nutritional importance of phosphate for crops

Phosphorus (P) is an essential macronutrient with multiple functions in plant macromolecular structures: as a component of nucleic acids and phospholipids, with crucial roles in energy metabolism, participation in signal transduction pathways via phosphorylation/dephosphorylation and controlling key enzyme reactions (Theodorou and Plaxton 1993, Schachtman et al. 1998, Marschner 2012). Plants acquire P in its inorganic form as orthophosphate (P_i) $H_2PO_4^-$ /HPO_4^{2-} from the soil solution (Bieleski 1973, Holford 1997, Schachtman et al. 1998, Marschner 2012). In many agricultural systems, P_i is one of the most limiting nutrients for crop production and is a major constraint for yield (Vance et al. 2003, Raghothama 2005, Kirkby and Johnston 2008), with shoot growth, tiller number and tiller weight all influenced by P_i availability (Römer and Schilling 1986, Bollons and Barraclough 1997). P concentrations in wheat ranging from 0.5 to 0.4 % in dry matter (DM) at tillering and 0.2 to 0.3 % in DM at booting are indicative for sufficient P_i supply (Finck 1991, Marschner 2012). The amount of readily available P_i may be raised through P_i fertilization and different agronomic strategies (Bahl and Singh 1986, Strong et al. 1997,

Kirkby and Johnston 2008, Syers et al. 2008) which complement fertilizer recommendation schemes.

1.2.3. Fertilizer recommendation schemes

Fertilizer recommendations in Europe are based on soil testing and their calibration against relative crop response curves (Jordan-Meille et al. 2012). Such response curves are usually determined using grain yield as target for determining the critical soil-P_i concentration (e.g. Olsen P) which is reflected by at least 90 % of the maximum yield according to an appropriate fitting procedure (Bollons and Barraclough 1999, Teng et al. 2013) (Figure 2 A). However, the recommended P_i fertilizer application rate for reaching the critical soil-P_i concentration varies according to soil type, the local environment, P_i export quantity via the crop and crop sensitivity (Jordan-Meille et al. 2012). Soil tests use a diversity of chemical extractants according to a specific soil type (acid dissolution, anion exchange, cation complexation and cation hydrolyses) aiming to reflect the labile and plant available soil-P_i concentration (Sanchez 2007, Jordan-Meille et al. 2012). However, due to large interactions between soil tests and soil types, extractant methods are controversial and can result in very different amounts of "extractant-available P_i" for similar soil samples (Neyroud and Lischer 2003). Therefore, the amount of extractable soil-P_i is just an approximation to the actual amount of plant available soil-P_i, This is one of the main reasons why recommended fertilizer rates are empirical calculations (Jordan-Meille et al. 2012). There exist mechanistic models, which require more input information such as soil pH, soil-buffer capacity, initial water soil content, field capacity, temperature, rainfall, etc. (Greenwood et al. 2001) or the interaction of the main fertilizers applied in arable production such as NPK (Zhang et al. 2007). However, the large data requirement prevented the implementation of mechanistic models until now (Kirkby and Johnston 2008).

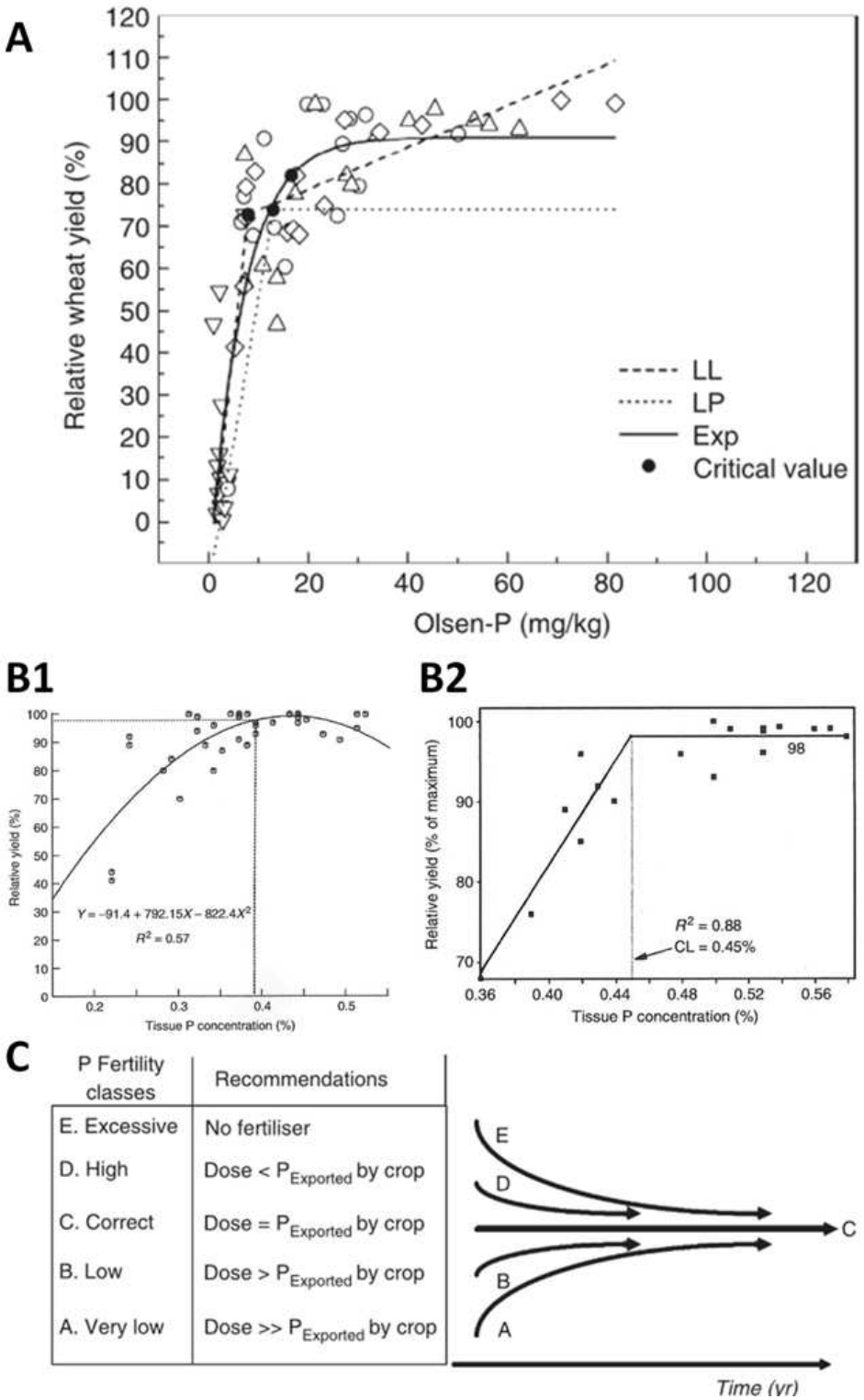

Figure 2: Concepts for fertilizer recommendations schemes according to (A) soil-testing calibration curves, (B) plant tissue calibration curves and (C) the maintenance method.

Data from Jordan-Meille et al. (2012) (Figure A and C) and Sanchez (2007) (Figure B). Jordan-Meille et al. (2012): LL = Linear-linear model, LP = Linear-plateau model, Exp. = Mitscherlich-model, Δ, ∇, o and ◊ symbols refer to different treatments, • = critical Olsen P (Olsen et al. 1954). B1 = curvilinear model using the midribs of endive at the 8-leaf stage, B2 = linear response and plateau model at 98 % using radish leaves (Sanchez 2007).

There is a second way of obtaining calibration curves using tissue testing instead of soil testing (Sanchez 2007) (Figure 2 B). However, this method is quite costly, diagnostic standards are very diverse, depending on the growth stage and the plant part sampled, and a diagnosed deficiency is normally difficult to remedy quick enough for potential yield losses (Finck 1991, Sanchez 2007). Therefore, in arable cropping, preplant application of P_i fertilizer is common and tissue testing is usually only used for diagnosing a systematic nutrient starvation in the production system itself.

Sustainable P_i fertilizer management considers the target critical soil-P_i concentration for each crop rotation, the need to maintain this concentration, the responsiveness of a crop and the quantity of nutrient which will be removed from the field at harvest (Defra 2012). In the UK, an index system is in place recommending Index 2 as target for arable crops using sodium bicarbonate as extractant at a pH of 8.5 (Olsen et al. 1954): Index 0 = 0-9 Olsen P; Index 1 = 10-15 Olsen P; Index 2 = 16-25 Olsen P; Index 3 = 26-45 Olsen P; Index 5 = 71-100 Olsen P (Defra 2012; Fertilizer Manual RB209). There are additional agronomic concepts to improve the sustainability of fertilizer application and the fertilizer recover efficiency such as minimum tillage, precision agriculture tools, fertilizer band placement and seed priming (Kirkby and Johnston 2008, Syers 2008, McBeath et al. 2012). These concepts are in concordance with the 4R nutrient stewardship (Phillips and Norten 2012), a fertilizer guideline concept[3], which provides information on management practices based on four principles: the right fertilizer source, at the right rate, at the right time, with the right placement. However, maintaining the soil on a target soil-P_i concentration and replacing only the harvest product off takes is a general strategy across Europe (Figure 2 C) and the basis for all fertilizer recommendation schemes.

[3] http://www.nutrientstewardship.com/; supported by the International Plant Nutrition Institute, The Fertilizer Institute, The Canadian Fertilizer Institute, and the International Fertilizer Industry Association

1.2.4. Implication for phosphate nutrition in crops

Grain crops like rice, maize, wheat and oilseed rape are essential major staple foods (FAO 2011) and major contributors to the global P cycle (Rose and Wissuwa 2012). Global P flows such as the rock mineral fertilizer trade and manure-delivering livestock production are unevenly distributed, resulting in massive agronomic imbalances and spatial surplus or deficit patterns across regions and countries (Tiessen 2008, MacDonald et al. 2011) (Figure 3). Additionally, large amounts of applied P_i are removed in harvested products from the fields (Lott et al. 2009), and nutrient recycling, especially organic P sources, from urban areas or returning biomass is rare (Cordell et al. 2009).

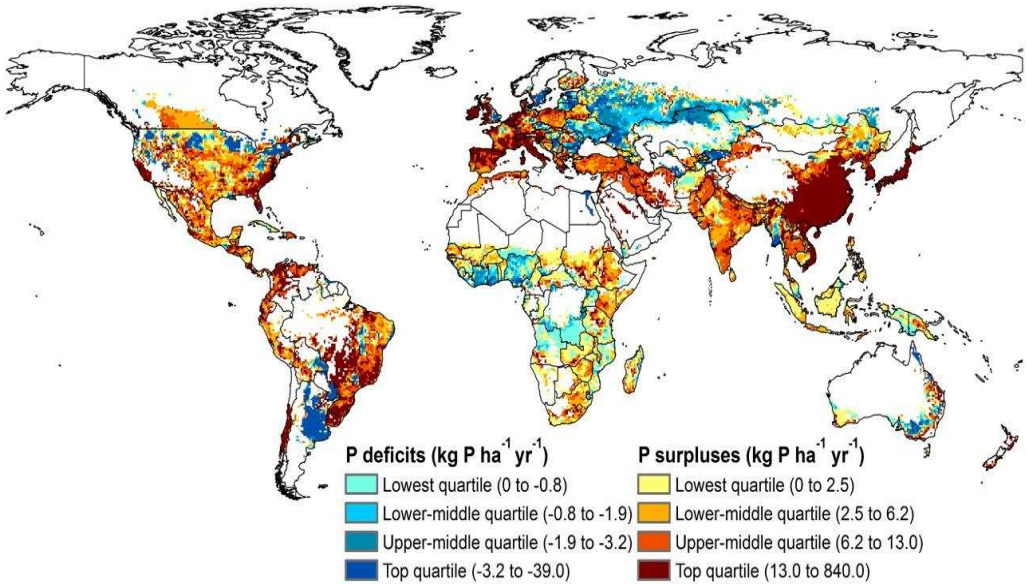

Figure 3: Global map of agronomic P imbalances for the year 2000. Imbalances are shown per unit of cropland area in each 5˚grid cell. The surpluses and deficits are each classified according to quartiles globally (0-25th, 25-50th, 50-75th, and 75-100th percentiles); figure and data taken from MacDonald et al. 2011.

Rock P_i fertilizers are extracted and exported from only a few countries worldwide, which carries geopolitical risks (Tiessen 2008, Cordell et al. 2009, FAO 2011). Furthermore, phosphate fertilizer derived from rock phosphate is a finite and non-renewable resource (Cordell et al. 2009) and nonetheless, the demand is estimated to be increasing 1.9 % yearly from 2011 to 2015 (FAO

2011). To meet the requirement for future demands of an increasing world population, bearing in mind that rock P_i reserves are limited and deposits cannot be exploited infinitely (Kirkby and Johnston 2008), it is necessary to enhance P_i fertilizer use efficiency of crops (Gregory and George 2011). Furthermore, fertilizer derived P_i may cause environmental problems associated with eutrophication (Gaxiola et al. 2001), especially as a result of overuse (McDowell 2012). Hence, a major challenge for future crop production will be to produce higher yields with lower inputs (Gregory and George 2011). One strategy would be to develop crop genotypes that require smaller amounts of fertilizer and consequently use nutrients more efficiently, bred based on trait-focused screens of germplasm collections (Gregory and George 2011). Nevertheless, little progress has been made in breeding cultivars with high P_i use efficiency or P_i acquisition efficiency (Calderón-Vázquez et al. 2011, Rose et al. 2011), and recovery (acquisition) rates of applied P_i between 25 to 60 %, depending on the method used, are still modest (Syers et al. 2008).

1.2.5. Phosphate acquisition via the root system

Nutrient acquisition via the plant root system is a crucial factor for agricultural productivity and crop yield (Lynch 1995). The amount of available P_i in the soil solution is determined by the ability of the soil to replenish P_i ions from the exchangeable P_i pool, but also by the extent and efficiency of root acquisition by the plant. Thus, cropping system specific such as soil cultivation and plant-specific approaches such as crop species, crop rotations must also be taken into account in order to raise P_i acquisition efficiency and P_i use efficiency. Furthermore a consideration of root traits in genetic selection might result in significant improvements for crops (Vance et al. 2003). Soil-P is the most immobile, inaccessible and unavailable of all macronutrient elements (Holford 1997), and is taken up by plants in its inorganic form (P_i) (George and Richardson 2008). Edaphic and climate factors and/or cropping systems have a strong impact on the rate of replenishment of the available P_i pool which can be recovered by the plant. P_i movement from the soil to the root proceeds mainly by diffusion rather than mass flow, with slow diffusion rates at around 10^{-15} m s^{-1} (Hinsinger 2001, Rausch and Bucher 2002), resulting in a depletion

zone of 1 to 2 mm around the root (Jungk 2001). Soil-P_i concentrations are extremely low, being generally < 10 µM and typically around 2 µM (Bieleski 1973, Barber 1984, Holford 1997), whereas in plants, concentrations on a fresh weight basis of > 40 mM can be achieved (Bollons and Barraclough 1997). Hence, plants take up P_i faster than it is supplied by diffusion (Bieleski 1973).

Soil pH, buffer capacity, soil moisture and soil structure affect P_i solubility and sorption capacity (Holford 1997, Syers et al. 2008); P_i can be absorbed on the surface of clay minerals, iron (Fe) - and aluminium (Al) - hydrous oxide surfaces and organic matter complexes or be fixed in acidic soils as Al-/Fe phosphates or Ca/Mg-phosphates in alkaline soils (Barber 1984, Bahl and Singh 1986, Holford 1997, Hinsinger 2001). Significant amounts of P in soils (20 to 80 %) are bound in organic forms such as nucleic acids, phospholipids and predominately monophosphate esters, as phytic acid and its derivatives (Richardson 1994). These organic forms have to be mineralized and/or solubilized into inorganic forms in order to be available for plants; a process which is either microbiological or plant mediated.

1.2.6. Phosphate transporters mediate P_i acquisition and translocation

Phosphate acquisition from the soil solution is mediated by plasma-membrane localized phosphate transporters (Pht) which have been suggested to function as H^+ co-transporters (Daram et al. 1998, Smith et al. 1999, Mimura 2001, Rae et al. 2003, Raghothama 2005). Consistent with the pH in many agricultural soils, maximal Pi uptake rates occur in a pH range 5 to 6 (Ullrich-Eberius et al. 1981, Furihata et al. 1992, Rae et al. 2003). A constitutively expressed low-affinity P_i uptake system with a K_m of 50 to 300 µM and a high-affinity uptake system, which is regulated by P_i availability with a K_m of 3 to 7 µM have been proposed (Ullrich-Eberius et al. 1981, Furihata et al. 1992). P_i transporters are classified into distinct families: Pht1, Pht2, Pht3 and Pht4 (Bucher et al. 2001, Liu et al. 2011). Pht1 are high-affinity transporter homologues to the yeast PHO84 P_i transporter and other fungal high affinity P_i transporters (Pao et al. 1998). However, the functional characterization of the Pht1 transporter family

in rice and barley (Rae et al. 2003, Ai et al. 2009) revealed kinetic properties that are within a high- and low affinity range.

Pht1 transporters belong to the distinct phosphate: H+ symporter (PHS) family which is a member of the major facilitator superfamily (MFS) of proteins (Pao et al. 1998). All these transporters exhibit high sequence similarity with each other, being similar in size and having 12 predicted transmembrane domains (TMs) with a large hydrophilic loop between TM6 and TM7 that results in a 6+6 configuration (Liu et al. 2011). The N- and C-termini are oriented towards the inside of the cell and they contain potential sites for phosphorylation and N-glycosylation (Smith et al. 1999).

Transporters of the Pht2 family have been cloned in Arabidopsis, and it has been suggested they have roles as constitutively expressed low-affinity proton symporters (H^+/P_i co-transporter) for P_i loading in green shoot organs and predominantly leaf tissues (Daram et al. 1999, Versaw and Harrison 2002). The Pht2;1 protein is structurally similar to the Pht1 members, but is more closely related to the putative P_i transporters from bacteria and mammalian Na^+/P_i transporters. However, its amino acid sequence and primary structure is distinct to Pht1 transporters and it has a large hydrophilic loop between TM8 and TM9 (Daram et al. 1999). In wheat, TaPht2;1 was predominantly expressed in a photoperiod-dependent manner in the leaves, which was significantly enhanced during P_i starvation (Guo et al. 2013). GFP-fusion studies localized TaPht2;1 to the chloroplast envelope, suggesting a regulatory role mediating P_i translocation from the cytosol to the chloroplast as low-affinity transporter with a K_m of 225 µM P_i (Guo et al. 2013).

The Pht3 transporters belong to the mitochondrial transporter family (Rausch and Bucher 2002) and the Pht4 family has been suggested to play a role in P_i translocation between the cytosol, chloroplast, plastids and the Golgi apparatus (Guo et al. 2008, Liu et al. 2011).

1.2.7. Morphological and biochemical adaptations of plants during P_i limitation

When sensing nutrient starvation, plants have developed broad morphological and biochemical strategies to deal with the heterogeneous availability of soil resources. Root plasticity (morphology, topology and architecture) is a crucial but neglected factor which is linked with immobile nutrients such as P_i (Lynch 1995).

Plant roots typically respond to P_i starvation through allocation of more carbohydrates towards the roots, which enhances root growth to maximize the soil volume exploited and increases root to shoot ratio (Hermans et al. 2006, Hammond and White 2008). Root hair formation (numbers, length and surface area) is strongly related to P_i starvation (Bates and Lynch 1996, Gahoonia et al. 1997, Jungk 2001, Zhu et al. 2005), emphasizing a strong role in P_i acquisition from the soil (Gahoonia and Nielsen 1998, Gahoonia et al. 2001). Topsoil foraging, which is characterized by enhanced lateral root branching over primary root growth, contributes to efficient P_i acquisition (Lynch and Brown 2001, Williamson et al. 2001, Pérez-Torres et al. 2008).

Phosphate acquisition is enhanced through symbioses with arbuscular mycorrhizal (AM) fungi (Barber 1984, Fitter 2006), by substantially increased P_i absorbing surface for P_i acquisition (Jakobsen et al. 1992), the ability to access mineralized organic P sources (Koide and Kabir 2000) and increased expression and secretion of plant acid phosphatases (Tarafdar and Marschner 1994). Strigolactones have a facilitating role in symbiosis formation (Gomez-Roldan et al. 2008) and stimulate tiller formation (Hong et al. 2012), an important parameter for yield. A high soil pH has a strong decreasing influence on the bioavailability of soil-P_i (Barber 1984, Hinsinger 2001). Therefore, root excreted protons along with organic acids like malic acid, citric acid or phenolic compounds act as chelators (Raghothama 1999, Vance et al. 2003) acidify the rhizosphere and aid solubilizing rhizosphere P_i. Organic acids displace bound P_i from Al^{3+}-, Fe^{3+}- and Ca^{2+}-phosphates (Dinkelacker et al. 1989, Gerke et al. 1994). In particular, cluster roots, which are brush-like root formations that release large amounts of P_i solubilising compounds such as

carboxylates and extracellular acid phosphatases, are an adaptation strategy to low soil-P_i availability of many plant species such members of the Proteaceae, Fabaceae, Casuarinaceae and Myricaceae family (Neumann and Martinoia 2002, Shane and Lambers 2005).

Plants also respond to P_i starvation through the induction of various metabolic processes e.g. induction of a bypass pathway of glycolysis and mitochondrial electron transport to replace ATP as an energy resource and increase internal P_i utilization (Duff et al. 1989, Theodorou and Plaxton 1993).

1.3. Phosphate efficiency in model plants and crops

1.3.1. The concept of P_i efficiency in crops and cropping systems

Phosphate acquisition and use efficiency (PAE, PUE) represent a plant`s ability to cope with either P_i limiting conditions or maintain growth under P_i starvaion due to morphological, biochemical and molecular changes without sacrificing yields (Chiou and Lin 2011). However, P_i efficiency is a complex trait and the genetic determinants which are involved in enhanced P_i starvation tolerance or P_i efficiency are still not clearly understood. In addition, there is an essential need for agronomic P_i efficiency criteria to be defined in order to be able to exploit and screen genetic variation in grain crops (Rose and Wissuwa 2012). As discussed previously, the focus of molecular research lies mainly on P_i starvations responses of individual genotypes or model plants and it is questionable if these findings are general applicable for crops in an agricultural context. Genotypic differences in P_i efficiency might rarely be conserved between species (Calderón-Vásquez et al. 2008, Hammond et al. 2009, Calderón-Vásquez et al. 2011, Niu et al. 2012, Alexova and Millar 2013) and need to be identified before they can be exploited for breeding.

From an agronomic and economic point of view, improved P_i efficiency is defined by the cropping area and seeks to improve P_i fertilizer recovery and a higher exploitation of availably soil-P_i (Sattelmacher et al. 1994). This concept takes into account the low P_i availability in e.g. tropical soil (Wissuwa et al.

2009), limited access to P_i fertilizers in some regions of the world (Tiessen 2008), costs for fertilization (FAO 2011) and environmental aspects like impaired water quality by run-off or drainage due to agricultural intensification (McDowell 2012). P_i efficiency properties which are based on the plant itself can be divided into P_i acquisition efficiency (PAE) and P_i use efficiency (PUE) (Wang et al. 2010). Both traits are usually linked and can be negatively associated with each other and are hard to distinguish (Su et al. 2006, Su et al. 2009, Rose and Wissuwa 2012). Furthermore, in contrast to PAE, PUE is much less well understood, lacks clearly defined and consistent terminologies across the literature, and has become a bottleneck for P_i efficiency improvement in crops (Hammond et al. 2009, Wang et al. 2010, Rose and Wissuwa 2012). There is a strong economic interest not to over mine the soil by increasing P_i export from the field via the grain via enhanced P_i acquisition (Batten 1992, Rose and Wissuwa 2012). Therefore, a selection technique achieving an appropriate distinction is required (Batten 1992) which considers a positive correlation of biomass ratios with increasing PUE (Rose and Wissuwa 2012).

Increasing PUE is especially interesting in regions of high cropping intensity facing plateaued yields during the last decade. When P_i efficiency is intended to be evaluated across a range of distinct or heterogeneous genotypes e.g. high yielding modern varieties and low-yielding land races, a tissue-specific approach should be most suitable (Rose and Wissuwa 2012). Using this approach, presupposes knowledge about the different P pools as well as about the changing P_i requirements depending on the growth stage of the crop (Veneklaas et al. 2012).

1.3.2. Screening approaches

Phosphate is compartmentalized within plant cells and exists in two main P pools (Veneklaas et al. 2012). The first P pool consists of free inorganic orthophosphate (P_i) which is either metabolically active in the cytoplasm or stored in the vacuole to buffer P_i demands of the cytoplasm (Lauer et al. 1989, Mimura et al. 1996). The second P_{org} pool represents organic forms as P-esters,

comprising nucleic acids, phospholipids, phosphorylated proteins and low relative molecular mass metabolites (Veneklaas et al. 2012).

Over 90 % of total P in cells is present as P_i when plants are adequately P_i supplied (Marschner 2012). Therefore, vacuolar storage P_i can have a diagnostic value (Bollons and Barraclough 1997, Bollons and Barraclough 1999), although, shoot growth seems to be reduced before severe P_i depletion of the vacuolar storage pool occurs (Mimura et al. 1996, Rouached 2011).

In the nucleic acid pool, RNA is usually the largest component with 40-60 % of this P_{org} pool, (Bieleski 1968) and ribosomal RNA (rRNA) having the biggest share, adjusting with growing patterns (Hensel et al. 1993, Kanda et al. 1994, Suzuki et al. 2010). Nucleic acid and protein turnover and repair has a large P cost (Raven 2012). Hence, plants cannot reduce DNA or RNA without affecting growth (Raven 2008); a target for P_i use efficiency would be the optimizing of the ribosomal pool size, protein biosynthesis and especially protein turnover (Veneklaas et al. 2012). Phospholipids in cell membranes fulfill structural roles, serve as substrates for biochemical signals and are required in abundance by photosynthetic tissues and cell-expanding/-dividing tissues. The replacement of phospholipids by glycolipids (galactolipids, sulfolipids) in plastids, as result of P_i starvation, is known (Essigmann et al. 1998, Andersson et al. 2003, Wasaki et al. 2003, Oono et al. 2011). However, the total area of membranes can not be decreased substantially for the sake of economizing P (Veneklaas et al. 2012). In cyanobacteria and algae, their replacement can be complete (Van Mooy et al. 2006, Van Mooy et al. 2009) or partial in rhizobial symbionts (Gaude et al. 2004), but in plants the consequences of such a replacement remain speculative (Veneklaas et al. 2012).

Phosphate acquisition seems to be most critical during vegetative growth. In the late vegetative or early reproductive stage remobilization and optimal allocation becomes another resource of P_i (Römer and Schilling 1986, Rose et al. 2007, Veneklaas et al. 2012). There are wheat genotype screenings in the literature focusing on P_i efficiency during early growth (Liao et al. 2008) or

contrastingly, on grain yield (Jones et al. 1992). P concentrations in the grain of crops are usually much higher than in vegetative tissues (Veneklaas et al. 2012), and seed P reserves occur predominately as phytate (Lott et al. 2009, Raboy 2009, White and Veneklaas 2012), which are the salts of phytic acid with high affinity to zinc (Zn) and iron (Fe) (Michael et al. 1980).

Seed P content as well as phytate content differs between wheat genotypes (Batten 1992) and declines with decreasing P_i supply (Mengel and Kirkby 2001). High P grain content, especially phytate, is not particularly desirable, as it acts as an anti-nutrient in monogastric animal and human diet, due to chelatization with Zn and Fe in the gut, which aggravates the global problem of mineral malnutrition (White et al. 2012). Furthermore, P_i rich manure or sewage causes environmental problems (Raboy 2009). However, whether low seed P content or concentration could be an appropriate selection criteria for improved PUE, is controversial. Grain or seed P reserves support initial seedling growth until it is supplemented through P_i acquisition by the developing root system (White and Veneklaas 2012) and correlated with the initial root biomass (Zhu et al. 2005). It is questionable if seed coating or P_i fertiliser placement could compensate low grain P (Rebafka et al. 1993), even if lower root development due to lower seed P reserves can be overcome due to mycorrhizal infection (Zhu and Smith 2001).

1.3.3. Exploiting genetic differences

There are studies showing genotypic differences for P_i starvation tolerance suggesting that P_i efficiency mechanisms may differ among wheat, rye and triticale genotypes (Manske et al. 2001, Osborne and Rengel 2002, Ozturk et al. 2005, Gunes et al. 2006). Hammond et al. (2009) observed a considerable diverse species-wide variation for shoot P concentrations and several PUE measures in Brassica oleracea landraces and commercial varieties. Manske et al. (2001) argued that under P_i depleted conditions P_i acquisition efficiency plays the key determinant for yield, whereas P_i use efficiency was more relevant under high P_i supply conditions. There are also several investigations

in other Brassica plants aiming to exploit genetic diversity (Solaiman et al. 2007, Akhtar et al. 2008, Yang et al. 2010, Yang et al. 2011). Batten (1992) pointed out that selection of more P_i efficient wheat occurs unconsciously during breeding when selecting for higher yields at suboptimal P_i availability. Chin et al. (2010) mentioned a similar observation of an unconscious selection for major P_i starvation tolerance rice QTL, Pup1, in drought-tolerant varieties developed under unfavourable conditions. Hammond et al. (2009) similarly implicated inadvertent selection in B. oleracea breeding programmes. The selection process resulting in modern (Brassica) crop varieties with increased grain yield per mg shoot P (Hammond et al. 2009) might be a result of higher harvest index (Batten and Khan 1987). Chin et al. (2010) support that hypothesis by observing a lower frequency of the P_i starvation tolerant QTL Pup1 in modern irrigated rice varieties compared to traditional varieties.

There are further studies showing that enhanced P_i starvation tolerance in wheat was due to enhanced P_i acquisition rather than enhanced P utilization (Gahoonia et al. 1996, Gahoonia et al. 1999). A comparison of modern wheat varieties from the International Maize and Wheat Improvement Centre (CIMMYT) with an older Mexican variety showed that PUE did not differ (Egle et al. 1999). However, P_i acquisition under P_i starvation was improved mainly due to a better root length density, especially during the period during anthesis and grain filling (Egle et al. 1999). With P_i fertilization, root length density was not significantly different between the older and the modern varieties, but higher P_i acquisition rates, especially during grain filling, of the modern varieties seemed to have contributed to higher P_i acquisition ability at appropriate P_i supply. A higher shoot growth and a subsequently higher sink capacity of more kernels might have contributed to that effect (Egle et al. 1999, Wang et al. 2012). In maize, several studies have identified variation in P_i acquisition amongst genotypes (DaSilva and Gabelman 1992, Zhu and Lynch 2004, Chen et al. 2009a, de Sousa et al. 2012), without providing large amounts of potential target genes for exploiting crop biodiversity (Calderón-Vázquez et al. 2008).

1.4. Potential targets for genetic crop improvement

1.4.1. Characterization of potential candidate genes

The design of phenotypic screens for dissecting P_i acquisition or P_i utilization differences in crops requires an understanding of the underlying molecular mechanism of P_i starvation tolerance. This section highlights mechanisms known in crops that may be potential targets for a breeding approach, integrating physiological, molecular and genetic strategies. Genes will be listed that come from model organisms and were subsequently investigated in crop species.

A potential candidate target would be characterized by being a key factor in the molecular mechanism of the P_i starvation response, adaptation and genetic diversity responsible for P_i starvation tolerance, keeping in mind that there is a need for different strategies in low-input and high-input systems, focusing more on PAE or PUE respectively.

Teng et al. (2013) investigated the expression profiling of known PSI genes in wheat under different rates of P_i fertilizer and soil Olsen P, proving that the turning point for the genetic response was the critical soil-P_i availability. This observation leads to a general model (Figure 4) which raises the question which strategy would be the most suitable to shift the onset of target gene expression for the P_i starvation signalling response into lower soil-P_i availabilities and would therefore decrease the crop demand for equal yield performance? There were three main scientific strategies adressing this problem.

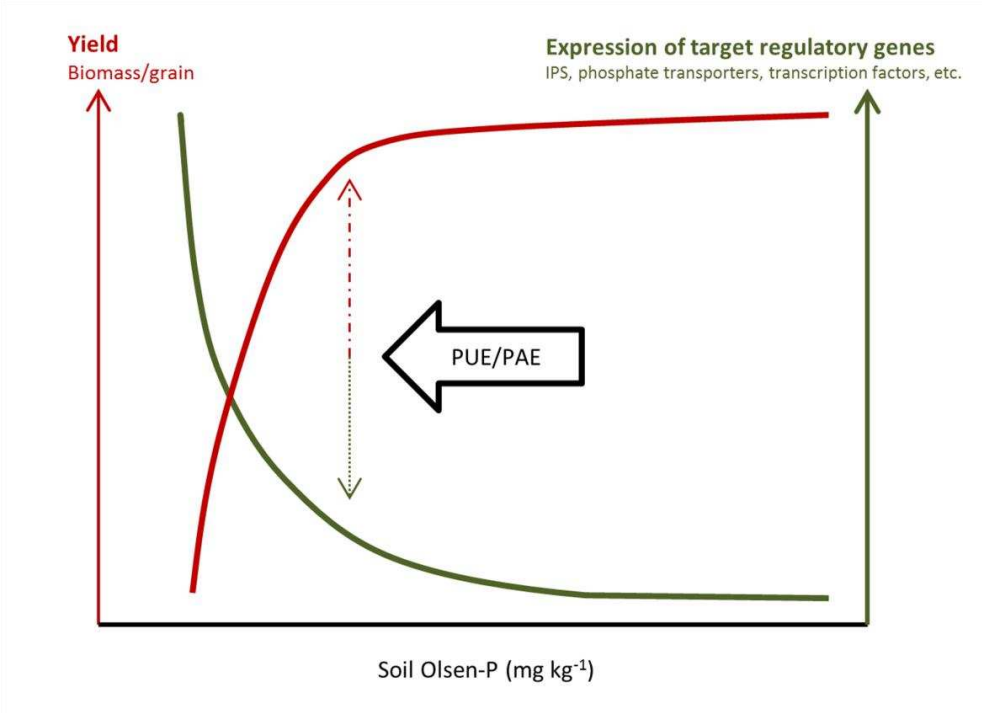

Figure 4: Model for improved P_i efficiency traits.
The optimal yield (red arrow) coinciding with the induction of P_i starvation marker genes (green arrow) in field-derived wheat roots are shifting towards a lower P_i availability (soil Olsen P) with improved P_i efficiency traits (Teng et al. 2013).

1.4.2. Approaches for candidate gene identification

The first approach comprises the majority of studies which are based on comparisons of P_i starvation tolerant genotypes with more susceptible genotypes or cultivars (Li et al. 2008a, Hammond et al. 2009, Pariaska-Tanka et al. 2009, Zhang et al. 2009, Li et al. 2010, Yao et al. 2011) exposed to a short-term P_i starvation period; especially transcriptome, proteome or metabolite profiling studies (Wang et al. 2002, Wasaki et al. 2003, Hammond et al. 2003, Hammond et al. 2004, Calderón-Vázquez et al. 2008, Huang et al. 2008, Liang et al. 2010, Oono et al. 2011, Oono et al. 2013). Even if these profiling studies provide a useful tool to study the response mechanisms with regards to adaptation to nutrient stresses (Hammond et al. 2004, Nilsson et al. 2010), the majority used hydroponically grown plant material exposed to short-term P_i starvation. However, Hammond et al. (2011) used the transcriptional profiling technology to identify a predictive diagnostic gene set for detecting

the physiological P_i status under field conditions and at a range of P_i fertilizer applications rates. This group of genes were determined from investigating the transcriptional P_i starvation responses in potato leaves grown hydroponically and were validated for exposure to various nutritional and abiotic stresses using the Arabidopsis orthologues (Hammond et al. 2011). This aspect is more focused on increasing the precision of fertilizer application but may also be a potential tool for genotypic screening PAE and PUE under agronomic conditions in the future.

The second approach deals with the over-expression of target genes resulting in partly contradictory observations of their roles in the P_i sensing and regulating network (Rae et al. 2004, Zhou et al. 2008, Ren et al. 2012a, Tian et al. 2012, Guo et al. 2013, Wang et al. 2013a).

The third approach is using quantitative trail loci (QTL) analysis to dissect the genetic basis of P_i efficiency and identifying superior alleles or loci in different germplasm (Wissuwa et al. 2005, Zhu et al. 2005, Su et al. 2006, Liang et al. 2010, Yang et al. 2011, Gamuyao et al. 2012) which could lead, if successful, to marker-assisted selection (MAS) in breeding for improved nutritional traits.

1.5. Molecular phosphate starvation responses in plants

1.5.1. The coordination of P_i starvation responses in model plants

Elicited responses to internal and external nutritional status involve local and systemic signalling (Chiou and Lin 2011). The P_i starvation response (PSR), consisting of the regulation or coordination of the P_i starvation inducible (PSI) genes to maintain P_i homeostasis, has been investigated predominantly in the model plant Arabidopsis, white lupin, rice and maize using forward (mutants) and reverse genetic approaches (Rubio et al. 2001, Uhde-Stone et al. 2003, Aung et al. 2006, Sánchez-Calderón et al. 2006, Shin et al. 2006, Franco-Zorrilla et al. 2007, Nilsson et al. 2007, Calderón-Vázquez et al. 2008, Duan et al. 2008, Bustos et al. 2010, Li et al. 2010, Nilsson et al. 2010, Oono et al. 2011, Alexova and Millar 2013). PSI genes and enzymes which are induced or

suppressed at the molecular level and commonly used as markers for monitoring PSR are described below. Biochemical and morphological changes have been elucidated to a much larger extent, whereas information on phosphate sensing and signal transmission is more limited (Chiou and Lin 2011).

Nonetheless, the lack of studies investigating genotypic variation in a broad spectrum of cultivars, make is difficult to draw conclusion for enhancing PUE in crops (Calderón-Vázquez et al. 2011, Veneklaas et al. 2012, Alexova and Millar 2013).

1.5.2. The importance of PHR1 for P_i starvation signalling

PHR1 (Phosphate starvation responsive 1) plays a pivotal role in sensing P_i availability (Chiou and Lin 2011) and has been examined in detail. PHR1 is a member of the MYB-transcription factor family (15 members) and seems to be a key regulator for downstream PSI genes, through binding to a P1BS cis-element, which is an imperfect palindromic sequence (GNATATNC) (Rubio et al. 2001, Nilsson et al 2007, Bustos et al. 2010, Nilsson et al. 2010). An important downstream target of AtPHR1 is miRNA399, which is involved in the Pho2 regulation as previously mentioned (Miura et al. 2005, Schachtman and Shin 2007). Over-expression of AthPHR1 and OsPHR2 increased miRNA399 transcript abundance, decreased Pho2 expression, increased shoot P_i content and enhanced root hair density in rice and Arabidopsis (Nilsson et al. 2007, Zhou et al. 2008, Bustos et al. 2010). Promoters of several PSR genes, including IPS and some Pht1 transporters, contain the P1BS cis-element (Rubio et al. 2001, Hammond et al. 2003, Schünmann et al. 2004, Bustos et al. 2010, Oono et al. 2011, Guo et al. 2013).

The Athphr1 mutant impairs a broad range of PSR and shows impaired root growth and root hair length (Rubio et al. 2001, Nilsson et al. 2007, Bustos et al. 2010). In rice, two homologues of AtPHR1**,** OsPHR1 and OsPHR2, are involved in P_i-starvation signalling (Zhou et al. 2008, Wang et al. 2009a;b).

However, only OsPHR2 over-expression resulted in increased shoot P_i and altered root morphology (Wu and Wang 2008, Zhou et al. 2008, Bustos et al. 2010). OsPHR2 positively regulates the low-affinity phosphate transporter OsPht1;2 in roots resulting in excessive P_i accumulation in the shoot tissue (Liu et al. 2010). Furthermore, a root-associated purple acid phosphatase (10a) in rice, OsPAP10a, is controlled and induced by OsPHR2 (Tian et al. 2012).

1.5.3. PHR1 mediated P_i-starvation signalling cascades in crops

In Brassica napus, BnPHR1 was predominantly expressed in the roots exposed to P_i limitation and over-expression enhanced the expression of the high-affinity P_i transporter BnPht1;2 (Ren et al. 2012a). In wheat, three TaPHR1 homologues have been identified that have been reported to contain the P1BS element (Wang et al. 2013a). They regulate genes such as TaPht2;1 (Tittarelli et al 2007, Gou et al. 2013) and TaIPS1 (Oono et al. 2013). TaPHR-A1 over-expression activated TaPht1;2 expression (Wang et al. 2013a), which was also more abundant in a P_i efficient genotype than in an P_i inefficient genotype (Miao et al. 2009). Furthermore, TaPHR1-A1 over-expression resulted in an up-regulation of PSR genes, stimulated lateral root branching, enhanced P_i acquisition and P_i translocation and increased grain yield but not P_i distribution from shoot to the grains in pot and field trials under P_i starved conditions (Wang et al. 2013a). Root TaPht1;2 and shoot TaPht1;6 expression increased under high and low P_i conditions, whereas other usually PSI genes such as TaIPS1.2, TaPho or TaSPX3 did not change their expression levels (Wang et al. 2013a). These results indicated that TaPHR1 is an upstream regulator for Pht1 transporters but suggested that other transcriptional factors are relevant for the induction of other wheat PSI genes, as it is the case for OsPHR2 (Zhou et al. 2008). Oono et al. (2013) recently published a transcriptome study using de novo transcript assembly analysis, in order to investigate wheat seedlings, cv. Chinese spring, exposed to 10 days of P_i starvation. Genes of the phosphorylation category including protein kinases were among the up-regulated transcripts (Oono et al. 2013). Furthermore, genes which belong to oxidation-reduction processes, metabolic processes, carbohydrate metabolism,

transcription process, lipid metabolism and transmembrane transport were induced, as well as AtWRKY6 and AtPho1 homologues (Oono et al. 2013).

1.5.4. The importance of other transcription factors for P_i starvation signalling

There are other transcription factors induced by P_i starvation and involved in P_i availability responses including OsPTF1 (Yi et al. 2005), WRKY75 and ZAT6 (Devaiah et al 2007a/b), bHLH32 (Chen et al. 2007), WRKY6 (Chen et al. 2009b) and MYB62 (Misson et al. 2005). Two WRKY box (W-box) elements have been found in the promoter of genes relevant for P_i retranslocation and scavenging, including AtPht1 transporters, AtIPS, acid phosphatase genes (AtPS2), purple acid phosphatase (PAP11) and PHR1 (Devaiha et al. 2007). A basic helix–loop–helix (bHLH) protein, bHLH32, acts a negative regulator for phosphoenolpyruvate carboxylase kinase (PPCK) expression in P sufficiency, root hair formation and anthocyanin production (Chen et al. 2007). Furthermore, positive and negative regulatory roles for transcription factors, PHR1 WRKY75 and bHLH32, have been suggested for root hair formation in Arabidopsis (Chen et al. 2007, Devaiah et al. 2007a, Bustos et al. 2010).

1.5.5. Phosphate starvation signalling mediated by SPX proteins

SPX proteins which containing a SPX domain (SYG1, PHO81, XPR1) at the N-termini, are involved in the downstream responses of PHR1 in Arabidopsis (Duan et al. 2008) and OsPHR2 and Pho2 in rice (Wang et al. 2009a). Members of the SPX protein family in rice (OsSPX3 and SPX1/2/6) have been shown to be highly induced (preferentially) in rice roots and shoots, where they are involved in the regulation of PSI and OsIPS1 (Wang et al. 2009b, Oono et al. 2011). OsSPX1 over-expression suppressed IPS genes, miRNA399 and Pht1 transporter (Wang et al. 2009b) induction. Hürlimann et al. (2009) showed that the SPX domain of two yeast P_i transporters, Pho 87 and Pho90, caused P_i uptake inhibition. In Arabidopsis mutants, AtSPX1-AtSPX4 affected the expression patterns of purple acid phosphatase genes (Duan et al. 2008).

OsSPX1 is positively regulated by OsPHR2 and is involved in the feed-back P_i signalling network in roots by supressing OsPht1;2 and other PSI genes (Liu et al. 2010), and negatively regulates shoot P accumulation (Wang et al. 2009a). In summary, SPX proteins seem to be essential players for maintaining P_i homeostasis and P_i signalling in plants (Rouached et al. 2010, Nilsson et al. 2012, Secco et al. 2012). The regulatory mechanisms of P allocation among different organs during plant development under P stress remain relatively elusive and investigations have been mainly focused on screening Arabidopsis mutants with abnormal P distribution.

1.5.6. IPS genes in model plants

"Induced by P_i-starvation genes" transcripts (IPS) under P_i starvation has been reported in Arabidopsis and rice (Rubio et al. 2001, Oono et al. 2011) and members of the IPS gene family have been widely used as molecular markers of plant P_i nutritional status (Zhou et al. 2008, Tian et al. 2012, Wang et al. 2013a). IPS genes encode non-coding RNAs that interact in the miR399-PHO2 regulatory loop as ribo-regulators (Doerner 2008). They function as miRNA399 antagonists, which negatively alter Pho2 expression at the post-transcriptional level; a regulatory process which is described as "target mimicry" (Franco-Zorrilla et al. 2007). It seems likely that they stabilize the initial decrease of Pho2 transcript to prevent P_i toxicity via P_i accumulation in the shoots (Bari et al. 2006, Chitwood and Timmermans 2007).

Five IPS genes have been found in the Arabidopsis genome (Franco-Zorrilla et al. 2007), two in rice, maize and barley (Hou et al. 2005). Promoters of the Pho4-regulon in yeast have two cis-regulatory elements which were also found in Arabidopsis (At4 /AtIPS4), tomato (TPSI1), Medicago truncula (Mt4) and rice (OsPI1) (Hammond et al. 2003). At4 and AtIPS4 in Arabidopsis are involved in P_i allocation between roots and shoot and enhance lateral root development (Shin et al. 2006, Franco-Zorrilla et al. 2007). The at4 mutant exhibited P_i accumulation in shoots (Shin et al. 2006), whereas over-expression decreased it (Franco-Zorrilla et al. 2007). AtIPS1 modulates PHR expression, a

MYB-CC type transcription factor which is involved in PSR (Rubio et al. 2001).

1.5.7. IPS mediated signalling in crops

In P_i starved wheat plants, the strong induction of TaIPS1 homologues (Oono et al. 2013) suggested that the IPS-mediated signalling cascade is functional similar to the miR399-Pho2 regulatory loop previously identified in model species (Franco-Zorrilla et al. 2007, Doerner 2008, Oono et al. 2011). Furthermore, genetic variation in PUE of barley was correlated with HvIPS1 expression (Huang et al. 2011). However, root TaIPS1 and shoot TaIPS2 transcript levels P_i starved wheat were strongly repressed by N starvation (Li et al. 2008b) providing evidence of an influence on the signalling pathways of P_i homeostasis by the nutritional N status. Furthermore, nine wheat miRNAs were identified in addition to miRNA399 as responsive to P_i starvation in a variety-dependent manner (Zhao et al. 2013). Wheat miRNAs putatively target diverse gene families which are down-regulated during P_i starvation including genes which are important for transcriptional regulation, signal transduction, phytohormone and defence responses among several others (Zhao et al. 2013). Transgenic tomato lines over-expressing miRNA399 from Arabidopsis enhanced the secretion of acid phosphatases and protons in roots (Gao et al. 2010). A further example is the over-expression of a PSI transcription factor, OsPTF1 in rice, which increased tiller number, shoot biomass, panicle weight and P content during P_i starvation (Yi et al. 2005). Genes which are regulated by OsPTF1 (P_i starvation induced transcription factor 1) contain E-box and G-box elements, but do not include high affinity P_i transporters or acid phosphatases (Yi et al. 2005). In addition, total root length and root surface area were increased, resulting in higher P_i acquisition rates (Yi et al. 2005). Both studies provide evidence of a promising method enhancing P_i acquisition in crops, although enhancing tolerance to P_i starvation via this pathway needs a greater understanding of the involvement of other proteins and factors.

1.5.8. The involvement of Pho-like transporters in the P_i starvation signalling cross-talk

The Athpho1 mutant showed severe P_i starvation in above ground shoot tissues due to a disruption in the transfer of P_i to the xylem vessels for subsequent transport to shoot and leaves (Poirier et al. 1991, Liu et al. 2012). Eleven members of the AthPho1 transporter family are known to share the same topology (Wang et al. 2004); a SPX tripartite domain in the N-terminal (SYG1/PHO81/XPR1) and an EXS domain at the C-terminal (ERD1/XPR1/SYG1). The EXS/SPX domains have been identified in yeast as being involved in P_i transport and sorting proteins to endomembranes (Liu et al. 2012, Wang et al. 2004). However, AthPho1 is a membrane-spanning protein which has been localized to the ER and the Golgi, but there is no evidence that it is a transporter itself, and it does not have homology to any other previously known transporter (Hamburger et al. 2002, Liu et al. 2012). AtPho1 seems to mediate P_i efflux out of root stellar cells along its electrochemical gradient (Hamburger et al. 2002) and AthPho1;H1, seems to be regulated by PHR1 (Stefanovic et al. 2007). The roles of the other members, AtPho1;H2 to AtPho1;H9, are unknown (Secco et al. 2010), but show distinct expression patterns from that of AtPho1 and AtPho1;H1 (Hamburger et al. 2002). The AthPho1 family clusters into two clades, and are expressed in a broad range of tissues, including leaves and predominately in vascular tissues of roots, leaves, stems or flowers. Only one clade, which contains AtPho1 and AtPho1;H1, clusters with the three OsPho1 proteins found in rice (Secco et al. 2010). Of these three OsPho1 genes, OsPho1;2, was mostly expressed in roots and mutation affected root-to-shoot P_i transfer, whereas OsPho1;1 was strongest expressed in flowers before and during pollination and OsPho1;3 weakly in leaves and flowers (Secco et al. 2010). AthPho1 is a down-stream component of the AthPho2 regulatory pathway (Liu et al. 2012). AthPho1 degradation is Pho2 dependent and was suggested to occur at the posttranslational level (Aung et al. 2006, Liu et al. 2012).

The Arabidopsis pho2 mutant exhibits excessively high P concentrations in the shoots displaying symptoms of toxicity as a result of enhanced aquisition and root-to-shoot translocation (Delhaize and Randall 1995, Liu et al. 2012).

AthPho2 is predominantly expressed in the root (Chiou et al. 2006) and like Pho1, it is localized to the ER and Golgi (Liu et al. 2012).

AthPho2 is a member of the E2 ubiquitin conjugase family (UBC24) (Bari et al. 2006) and is a target for miRNA399, which supresses AthPho2 expression (Fujii et al. 2005, Aung et al. 2006, Chiou et al. 2006). miRNA399 over-expression or loss-of function of UBC24 resulted both in enhanced P_i accumulation and impairment of P_i remobilization from old to young leaves in Arabidopsis (Chiou et al. 2006). miRNA399 expression is an early response to P_i starvation and a systemic signal of P_i starvation derived from P starved root and shoot tissues (Aung et al. 2006, Bari et al. 2006, Chiou et al. 2006, Lin et al. 2009). The expression of miRNA399 is regulated by PHR1 (Aung et al. 2006, Bari et al. 2006) in a mechanism called "target mimicry" (Franco-Zorrilla et al. 2007). In addition to miRNA399, various other miRNAs could be identified by deep sequencing in Arabidopsis (Hsieh et al. 2009, Lundmark et al. 2010) and other plant species (Chiou and Lin 2011), including, soybean (Zeng et al. 2010), tomato (Gu et al. 2010) and wheat (Zhao et al. 2013). It has been assumed that altered AthPht1;8 expression contributed to the phenotype of Athpho2 mutant and miRNA399 over-expressors because they are up-regulated in these mutants and over-expressors (Aung et al. 2006, Bari et al 2006). In rice shoots, Ospho2 mediated P accumulation was assumed to result from induced expression of high- and low-affinity P_i transporters OsPht1;2, OsPht1;9 and OsPht1;10 (Liu et al. 2010). It has been suggested that AthPho2 encodes an additional regulator for the low-affinity P_i translocator protein, AthPht2;1, in green shoot tissues of Arabidopsis (Daram et al. 1999). Downstream responses of Pho2 are still not completely understood (Liu et al. 2012). Pho1 and Pho2 are both expressed in vascular root tissues (Hamburger et al. 2002) as is miRNA399 (Aung et al. 2006).

1.5.9. Sucrose as a regulator of P_i starvation responses

There are studies providing evidence that sucrose is a global regulator of plant PSR, interacting with P_i starvation signals (Lloyd and Zakhleniuk 2004,

Karthikeyan et al. 2007, Lei et al. 2011) and root architecture alterations (Niu et al. 2012). Sucrose phosphate synthase (SPS) has been reported to be more abundant in P_i starvation tolerant cultivars of Brassica napus (Yao et al. 2011). Exogenously applied sugars or sucrose-enriched growing media could stimulate PSI genes such as acid phosphatases (APase), AtIPS1 (Müller et al. 2005) and APGase subunit in tobacco (Nielsen et al. 1998). P_i transporters such as TaPht1;2 (Miao et al. 2009) seem to belong to a group of sugar-modulated genes under P_i starvation (Jain et al. 2007, Karthikeyan et al. 2007, Hammond and White 2008). The Arabidopsis pho3 mutant exhibited a restricted sucrose translocation from root to shoot caused by a defective sucrose transporter, SUC2, which is involved in sucrose loading of the phloem (Lloyd and Zakhleniuk 2004). Atpho3 further shows altered APase induction/secretion on the root surface reduced P_i accumulation in both leaves and roots (Zakhleniuk et al. 2001) and a strongly induced Glc-6-P/phosphate translocator precursor. This phenomenon is again consistent with the observation that sucrose accumulates in P_i starved leaves of various crops (Hammond and White 2008). Microarray analysis investigating consequences of SUC2 over-expression in the transcriptome of the hypersensitive to phosphate starvation1 (hps1) Arabidopsis mutant revealed the induction of PSI genes under P_i replete conditions (Lei et al. 2011). In conclusion, sugar sensing and signalling is involved in adaptation responses to P_i starvation even if the exact mechanism is not yet understood.

1.5.10. Involvement of plant hormones in the PSR

Plant hormones have also been implicated with P_i signalling mechanisms as changes in P_i availability alters the expression of genes involved in the biosynthesis of phytohormones which in turn may influence PSR (Morcuende et al. 2007, Chiou and Lin 2011). P_i itself might be important in P_i starvation signalling, as is the case for nitrate acting as a signal stimulating root growth (Zhang and Forde 2000). The P_i flow across the peri-arbuscular cortex membranes may be among the mechanisms which allow plants to recognize AM fungi from less beneficial microbes (Yang and Paszkowski 2011).

Compelling evidence is provided by studies using phosphite, which is a phosphate analogue. Phosphite is taken up by plants but cannot be oxidized once inside the cell and mimicks sufficient P_i supply in P_i starving plants, which therefore interferes with PSR at slows-down the plant`s transcriptional and post-transcriptional responses (Chiou and Lin 2011).

1.6. Physiological adaptation mechanisms to P_i starvation

1.6.1. Alteration of root morphology during P_i starvation

Among common responses to P_i starvation are changes in root morphology such as increasing root hair density, reduction of primary root growth and promoted lateral root initiation, which have been well described in Arabidopsis (López-Bucio et al. 2000, Williamson et al. 2001, Sánchez-Calderón et al. 2006) and more recently studied in cereals (Hochholdinger and Zimmermann 2008). For instance, a root-hairless mutant of Arabidopsis (Bates and Lynch 2001) and a barley root-hair-deficient mutant (Gahoonia et al. 2001) grew poorly under P_i starvation. The root cap senses local P_i concentrations initiating spatial changes, comprising inhibition of cell division activity of primary meristematic cells and root cell elongation (Ticconi et al. 2004, Sánchez-Calderón et al. 2005, Franco-Zorrilla et al. 2007, Svistoonoff et al. 2007). However, due to the low mobility of P_i in the soil solution, the root architecture of crops in agricultural systems is strongly related to P_i distribution in the soil profile, determined by tillage, fertilizer and cultivation practices, which influence in turn the chemical dynamics of soil-P_i and the rhizosphere (Niu et al. 2012). Therefore, results from model plant studies using homogenous growth substrate may not be directly transferable to cropping systems.

1.6.2. Genes mediating root morphological changes

Phytohormone-related genes have been reported to mediate root architectural changes under low P_i growing environments, particular auxin-responsive genes (Bates and Lynch 1996, Hammond et al. 2004, Jain et al. 2007, Pérez-Torres et al. 2008, Miura et al. 2011). Comparing the proteome of a P_i starvation tolerant

and a sensitive oilseed rape genotype revealed that proteins related to lateral root formation such as auxin-responsive family proteins and sucrose-phosphate synthase-like proteins were up-regulated in roots and leaves (Yao et al. 2011). Li et al. (2008) observed a significant increase of a phosphatase 2A isoform in the more P_i starvation tolerant genotype. This phosphoprotein family is involved in auxin transport and reduced activity altered lateral root growth in Arabidopsis (Rashotte et al. 2001).

Significant increases of CDC48 protein, regulators of cell division and cell cycle, Ran GTPase, MCM6 and importins, were assumed to be important factors mediating a better root development and accelerated cell proliferation in the meristem under P_i starvation (Li et al. 2008a). Furthermore, expansins are involved in cell wall extension (Zhao et al. 2012), including root-hair formation (Yu et al. 2011) and are stimulated by indole-3-acetic acid and abscisic acid under abiotic stress (Zhao et al. 2012). For instance, Miura et al. (2011) concluded that genes coding for expansin 17, glycosyl hydrolase 19 and UDP-glycosyltransferase are involved in the regulation of cell wall-loosening and elongation in response to P_i starvation in Arabidopsis.

Gene modification is a potential mean of enhancing P_i starvation tolerance (Wang et al. 2013a). For example, a ß-expansin gene in soy bean, Gm-EXPB2, enhanced P_i acquisition when it was over-expressed (Guo et al. 2011). Expansins are involved in cell wall extension (Zhao et al. 2012), including root hair formation (Yu et al. 2011). They are among up-regulated genes during P_i starvation (Calderón-Vázquez et al. 2008), suggesting a remodelling of the cell-wall structure and integrity.

Root morphology related genes in maize, Rtcs (rootless concerning crown and lateral seminal roots; Hochholdinger and Zimmermann 2008), Bk2 (brittle stalk-2; Brady et al. 2007), Rth3 (root hairless 3; Hochholdinger et al. 2008), were determined as being related to differential P_i responses and PAE capability in the seedling stage in two contrasting maize lines (de Sousa et al. 2012). However, even if observable only under P_i starvation, root traits such as surface area, volume, diameter, root length per volume, exhibited high

heritability and low coefficient of variation making them exploitable for breeding (de Sousa et al. 2012). Genes which were investigated belonged to a family of glycosylphophatidylinositol (GPI)-anchored proteins involved in root cell expansion, cell wall biosynthesis and root hair formation (de Sousa et al. 2012).

1.6.3. Genetic factors controlling root architecture

Distinct responsiveness to P_i availability among Arabidopsis ecotypes (Chevalier and Rossignol 2011), and the identification of quantitative trait loci (QTLs) affecting root morphology (Reymond et al. 2006), suggests a genetically determined control of the root growth response to limited P_i availability.

Genetic factors controlling roots plasticity have been investigated recently using low phosphorus insensitive (lpi) mutants (Sánchez-Calderón et al. 2006). The mutation disrupted not only the root developmental response but also altered the induction of PSI genes which are relevant for adaptation to P_i starvation including acid phosphatases (AtPAP1, AtACP5) and phosphate transporters (AtPT1, AtPT2) (Sánchez-Calderón et al. 2006). Furthermore, their findings suggest that the root architectural response as being mediated by a specific nutrient (P) sensing signalling network (Sánchez-Calderón et al. 2006). For instance, two transcription factors WRKY75 (Devaiah et al. 2007a) and ZAT6 (Devaiah et al. 2007b), are among several transcription factors which have a regulatory effect on root architecture of Arabidopsis and were suggested to have an impact on PSR. Genetic selection based on root parameters has been difficult due to their multigenic nature and the lack of appropriate evaluation methods (Vance et al. 2003, Su et al. 2006, Su et al. 2009, De Souza et al. 2012).

Root (architectural) parameters are a difficult selection criteria for breeders as root phenotyping is very time consuming and usually destructive (de Sousa et al. 2012). However, QTL detection based on root phenotyping would benefit

the breeding efforts of marker-assisted selection (MAS) (Liang et al. 2010). Root morphology or primary root growth in maize seems as not affected by P_i availability (Mollier and Pellerin 1999), and the extensive shoot-born root system and different root types of cereals (Hochholdinger and Zimmermann 2008) emphasizes regulatory differences to model plants such as Arabidopsis. Nonetheless, genotypic differences in P_i starvation tolerance or high yield at low soil-P_i availability were often associated with root growth properties or P_i acquisition capability in crops (Gahoonia et al. 1996, Gahoonia et al. 1997, Zhu and Lynch 2004, Zhu et al. 2005, Li et al. 2008a, Hammond et al. 2009, Pariaska-Tanka et al. 2009, Yao et al. 2011), showing that there is a large exploitable genetic variation in root acquisition traits. For example, there is considerable genotypic variation in root hairs in barley and wheat cultivars with root hair length strongly correlated to the rhizosphere P_i depletion (Gahoonia et al. 1997). A root hairless mutant in maize conferred significant grain yield loss (Hochholdinger et al. 2008). Similar observations were made when comparing different maize lines and their root hair length, plasticity and subsequent performance under P_i starvation (Zhu et al. 2010).

Unfortunately, the underlying genetic mechanisms of germplasm variation for root hair traits have not yet been determined. Marker-assisted selection may facilitate root trait selection for breeding more P_i efficient cultivars, exemplified by studies showing that root morphology QTLs are linked to PAE in maize (Zhu et al. 2005), wheat (Ren et al. 2012b) or soybean (Liang et al. 2010).

1.7. Metabolic adaptation mechanisms to P_i starvation

1.7.1. Alteration of the TCA metabolism

Phosphate limitation alters the tricarboxylic acid cycle (TCA) metabolism and has been shown in a broad range of studies. Enzymes involved in the TCA cycle and glycolysis produce organic acids required for P_i recycling from phosphorylated glycolytic intermediates as well as releasing P_i from organic P sources or inorganic bound P_i in the soil (Oono et al. 2011). The

overproduction of citrate in transgenic tobacco (López-Bucio et al. 2000) as well as mitochondrial citrate synthase in A. thaliana (Koyama et al. 2000) enhanced P_i acquisition. Key enzymes which have been studied in A. thaliana are citrate synthase, malic enzyme and aconitase which exhibited variation in protein abundance during P_i starvation between ecotypes (Chevalier and Rossignol 2011).

1.7.2. Organic acid secretion

In other species, the activity of aconitase correlated with organic acid secretion (Neumann and Römheld 1999). The length of exposure to P_i starvation is another factor for enhanced adaptation ability to low P_i. For instance, genes encoding for isocitrate dehydrogenase were supressed in rice roots under longer-term P_i starvation, resulting in a suppression of citrate degradation (Oono et al. 2011), and malate dehydrogenase (MDH) over-expression in alfalfa caused higher shoot P concentrations (Teshafaye 2001).

Root modification and organic acid secretion require a carbon supply which might be to the detriment of yield or growth but being nevertheless beneficial during P_i starvation (Johnson et al. 1996, Zhu and Lynch 2004, Lynch and Ho 2005, Yao et al. 2011). For example, maize lines growing in nutrient solution culture, differences in P_i starvation tolerance were related to proteins that decrease citrate degradation, increased citrate synthesis and malate dehydrogenase activity in the roots (Li et al. 2008a). Furthermore, proteins related to carbon and energy metabolism were expressed to a higher extent in a P_i starvation tolerant Brassica napus genotype compared to a low P_i sensitive one (Yao et al. 2011). It has been hypothesised that transgenic plants that secrete microbial phytases into the rhizosphere have potential for improved acquisition of organic P sources. However, when these plants were grown in soil, growth was not different from to the control plants (Richardson et al. 2001, George et al. 2005). Therefore, results from in vivo studies appear more complex when tested under soil conditions. However, the expression of alfalfa or fungal phytase genes in Arabidopsis and tobacco improved the ability of the

plants to access organic P sources through mineralizing phytate to P_i via phytase secretion (George et al. 2005, Xiao et al. 2005).

Studies on bacterial citrate synthase genes in tobacco (sectreted citrate displaces P_i from insoluble soil complexes) came to contradictory results (López-Bucio et al. 2000, Delhaize et al. 2001) and investigations of genotypic variation in root exuded wheat phosphatase activity could not relate their activity to the P content when plants were grown in soil (George et al. 2008). Nonetheless, Zhang et al. (2009) suggested that improved acquisition and therefore higher P_i efficiency of two Brassica napus genotypes grown in soil was related to the ability to lower the pH or higher acid phosphatase activity in the rhizosphere. However, higher APase activity was observable in roots and especially shoots tissues in P_i scarce conditions in rice but without exhibiting genotypic differences (Yao et al. 2011). Over-expression of a wheat malate transporter, Ta-ALMT1, in barley enhanced P_i acquisition on acid soils in the short-term, but not when the soil was limed (Delhaize et al. 2009). Over-expression of a root-associated purple phosphatase gene in rice, OsPAP10a, could promote better growth and a higher tiller number compared to the wild type under P_i sufficient conditions (Tian et al. 2012). In summary, genotypic variation of P_i starvation tolerance is related to root morphology and secretory traits which may be exploitable.

1.7.3. Replacement of phospholipids

The replacement of phospholipids by galactolipids or sulpholipids is a well-known adaptation process in plants during P_i starvation (Anderson et al. 2003, Hammond et al. 2003, Byrne et al. 2011), even if phospholipid degradation is differently mediated in different species (Calderón-Vázquez et al. 2011). For instance, in potato, an array study identified novel roles for the main storage protein in potato tubers, the patatin like proteins, which also have lipase activity and are potentially involved breakdown of phospholipids for P_i recycling (Hammond et al. 2011). Numerous studies in model plants or crops reported the induction of genes related to an altered lipid metabolism, for

example UDP-sulfoquinovose synthase 1 (SQD1) or glycerophosphoryl diester phosphodiesterase (GDPD) or lipid transfer proteins (Wasaki et al. 2003, Morcuende et al. 2007, Calderón-Vázquez et al. 2008, Hammond et al. 2011, Oono et al. 2011). Glycerophosphodiester phosphodiesterases (GPX-PDE) catalyse the hydrolysis of phospholipids to glycerol-3-phosphate and the corresponding alcohol. Recently, GPX-PDE genes were identified which were highly expressed in cluster roots of white lupin under P_i starvation (Uhde-Stone et al. 2003, Cheng et al. 2011). To date, the knowledge about functional consequences of replacing phospholipids in membranes are very limited (Veneklaas et al. 2012).

1.7.4. Phosphate partitioning and re-translocation within the crop

More P_i efficient genotypes of rice or oilseed rape were characterised by preferential P_i re-translocation from the shoot towards the roots (Wissuwa et al. 2005, Akhtar et al. 2008, Hammond et al. 2009). Higher root to shoot ratios and increased carbohydrate partitioning contributed to genotypic PUE differences in barley (Huang et al. 2011). However, several enzymes and transcription factors are involved in this process: Genes such as PEPC (phosphoenolpyruvate carboxylase), which are involved into the modified glycolysis bypassing ATP requiring reactions were up-regulated in the P_i starvation tolerant but down-regulated in the more susceptible rice genotype (Li et al 2010). Moreover, over-expression of the bHLH transcription factor OsPTF1 increased Glu-6-P translocator, H^+-ATPase and PEP carboxykinase expression in the shoot and enhanced P_i starvation tolerance in rice (Yi et al. 2005). A proteome study on rice showed that 6-phosphogluconate dehydrogenase, an important enzyme of the pentose phosphate pathway, was among the higher over-accumulated proteins in the more P_i starvation tolerant maize genotype (Li et al. 2008a). Hence, the authors assumed that the larger proportion of sucrose in the total soluble sugar fraction fulfilled the requirements of the sugar metabolism better in the P_i starvation tolerant genotype (Li et al. 2008a). Pyruvate phosphate dikinase, pyruvate kinase-like proteins and UDP-glucose pyrophosphorylase which utilize PP_i

(pyrophosphate) to produce ATP or UTP were also more abundant in the P_i starvation tolerant maize line and were assigned to a higher PUE (Li et al. 2008a). Finally, another fundamental issue would be assessing the role or P_i transporters involved in P_i loading into the grain (Rose and Wissuwa 2012).

1.8. Transcriptional and posttranslational adaptation mechanisms to P_i starvation

1.8.1. Expressional response of P_i transporters to limited P_i supply

A strong induction of Pht1 transporters has been reported in the majority of transcript profiling studies where plants were exposed to a short-term P_i starvation period and grown in nutrient solution (Wang et al. 2002, Wasaki et al. 2003, Calderón-Vázquez et al. 2008, Huang et al. 2008, Huang et al. 2011), in the field (Teng et al. 2013), exhibiting a large diversity of expression patterns throughout the plant tissues. Pht1 transporters, which are preferentially or exclusively expressed in roots, were found in barley (Smith et al. 1999, Rae et al. 2003), wheat (Davies et al. 2002, Teng et al. 2013, Wang et al. 2013a), Arabidopsis (Muchhal et al. 1996, Mudge et al. 2002), rice (Paszkowski et al. 2002), maize (Nagy et al. 2006) and tomato (Liu et al. 1998, Muchhal and Raghothama 1999). Furthermore, Pht1 expression in shoot tissues has been reported e.g. in leaves of barley (Rae et al. 2003), in the panicle of rice at heading (Liu et al. 2011), in mature pollen of Arabidopsis (Mudge et al. 2002) or during mycorrhizal infection in roots of rice (Paszkowski et al. 2002, Yang et al. 2012), wheat (Glassop et al. 2005), Brachypodium (Hong et al. 2012) and Medicago (Gaude et al. 2012). The Pht1 expression during arbuscular mycorrhiza (AM) colonization in cereal species was considered symbiosis specific (Harrison et al. 2002, Paszkowski et al. 2002, Glassop et al. 2005, Gutjahr et al. 2008), for example OsPht1;11 (Paszkowski et al. 2002, Gutjahr et al. 2008) and OsPht1;13 (Güimil et al. 2005, Yang et al. 2012) expression in rice. Homologues of both genes occur in Brachypodium (Hong et al. 2012) and maize (Nagy et al. 2006), where transcripts also accumulate in non-colonized roots and leaves, suggesting additional roles during P_i starvation (Yang et al. 2012).

Promoter fusion to fluorescent proteins showed that high expression levels of P_i transporters occur in root trichoblast cells (Daram et al. 1998, Mudge et al. 2002, Schünmann et al. 2004) and remarkably in root tips and root hairs during P_i starvation (Sanchez-Calderon et al. 2006). As variability in P_i depletion profiles in the rhizosphere of wheat genotypes suggest genetic variability in root hair formation (Gahoonia et al. 1996 Gahoonia et al. 1997), varietal expression differences with respect to preferentially root expressed Pht1 are very likely. Until now, there is no evidence that genotypic variation exists that could be exploited in breeding (Rose and Wissuwa 2012), and this has to be investigated in the future.

All these observations make P_i transporters obvious targets for genetic improvement. However, the lack of the whole genome sequence information has hindered detailed investigation in wheat. Enhancing P_i acquisition by overexpressing Pht1 transporter genes has been reported in tobacco cell cultures (Mitsukawa et al. 1997) but could not be confirmed at the plant level (Rae et al. 2004). Furthermore, enhanced induction of TaPht1 transcripts might be a short-term adaptation to local P_i depletion and unevenly distributed patterns of P_i availability. Therefore, high induction maintained during severe long-term P_i starvation as an adaptation mechanism seems questionable and should be investigated on field-grown crops.

1.8.2. Expressional regulation of P_i transporters

The promoters of Pht1 genes contain the target elements for transcription factors of the P_i signalling network, for instance the P1BS (PHR1 specific binding sequence) cis-element as a target for the PHR1-TF (Schünmann et al. 2004, Ren et al. 2012a) or the W-box as a target for the WYRK 75-TF (Devaiah et al. 2007a, Miao et al. 2009), suggesting their embedding in the cross-talk of P_i signalling during P_i starvation to maintain P_i homeostasis. It may be concluded that the regulation of P_i acquistion and P_i transport mediated by Pht1 transporters, for which multiple roles in P_i acquisition and P_i

remobilization have been suggested, are very complex. Their role in the genetically diverse trait of the P_i starvation tolerance or PAE/PUE will be discussed further but remains elusive.

1.8.3. Posttranslational modifications: The role of kinases

Posttranslational modifications may be a very important factor in signalling and metabolic pathways involved in PUE (Alexova and Millar 2013, Plaxton and Tran 2011) and may explain the discrepancies when comparing proteome with transcriptome studies in P_i starved maize (Calderón-Vázquez et al. 2008, Li et al. 2008a) and Arabidopsis (Morcuende et al. 2007). The importance of posttranslational modifications within adaptation to low P_i exposure is underpinned by the potential role of a protein kinase OsPupK46-2 within the Pup1 (phosphate uptake 1) locus, which is a major QTL for P_i starvation tolerance in rice (Gamuyao et al. 2012).

The enhanced synthesis of organic acids allows P_i recycling from phosphorylated glycolytic intermediates, particularly phosphoenolpyruvate (PEP), which is mediated via the enzyme phosphoenolpyruvate carboxylase (PEPC). Phosphorylation via PPCK (PEPC kinase) activates PEPC (Gregory et al. 2009). PPCK has been reported in a few studies as being among up-regulated genes during P_i starvation (Chen et al. 2007, Morcuende et al. 2007, Müller at al. 2007). Therefore, PEP and PEPC are among the metabolites and enzymes being more abundant or active in P_i starved A. thaliana, B. nigra, O. sativa and T. aestivum (Duff et al. 1989, Johnson et al. 1996, Neumann and Römheld 1999, Morcuende et al. 2007, Oono et al. 2011).

1.8.4. Posttranslational modifications: phosphorlyation of Pht1

Pht1 transporter genes are also regulated at the post-transcriptional level through phosphorylation by the recently discovered phosphate transporter traffic facilitator 1 (PHF1) in rice and Arabidopsis (Chen et al. 2011, Bayle et al. 2011, Chiou and Lin 2011), which is connected to a kinase, RAPTOR1B.

Both are up-regulated at the protein level and PHR1 at the transcript level in P_i starved roots of Arabidopsis (Lan et al. 2012).

Targeting the P_i transporters to the plasma membrane via the secretory trafficking pathway is mediated by PHF1, which is expressed strongly in root tissues and in leaf mesophyll cells, mimicking the expression patterns of the Pht1 gene family (Gonzáles et al. 2005, Chen et al. 2011). OsPHF1 and OsPHF1L (Chen et al. 2011) and TaPHF1 (Wang et al. 2013a) in rice and wheat, homologues to AthPHF1 in Arabidopsis (González et al. 2005, Bayle et al. 2011), are localized specifically in the endoplasmic reticulum (González et al. 2005, Bayle et al. 2011). AthPHF1 encodes a plant-specific protein structurally related to SEC12 proteins of the early secretory pathway (González et al. 2005). The phf1 mutation in Arabidopsis impairs P_i acquisition and P_i transport (González et al. 2005). Even under P_i replete experimental conditions, expression of phosphate starvation induced genes (PSI) was induced in rice osphf1-1 mutants due to impaired plasma membrane location of the low-affinity P_i transporter OsPht1;2 and a high-affinity P_i transporter OsPht1;8 (Chen et al. 2011). Furthermore, the N- and C-termini of Pht1 transporter are oriented towards the inside of the cell and they contain potential sites for phosphorylation and N-glycosylation (Smith et al. 1999).

Therefore, Pht1 expression is also dependent on PHF1 expression and its phosphorylation status (Bayle et al. 2011) even if the role of this modification is not yet understood.

1.8.5. Posttranslational modifications: Sumoylation of PHR

In Arabidopsis, PHR1, which initiates P_i starvation signalling responses, was hypothesized to be a target for the conjugation of the SUMO superfamily of proteins via SUMO ligases (sumoylation) (Miura et al. 2005, Wang et al. 2013a). The sumoylation is mediated by a small ubiquitin like modifier SUMO E3 ligase, AtSIZ1, which is localized in the nucleus of the cells (Miura et al. 2005) predominantly in the root. The homologue, OsSIZ1, has also been

detected among transcripts of P_i starved rice (Oono et al. 2011). AtIPS induction was reduced in siz1 mutants, indicating a positive regulation with AtSIZ1 (Miura et al. 2005), which strengthens the hypothesis that posttranslational modifications are essential for the initial stages of P_i starvation signalling cascades. Additionally, AtSIZI negatively regulates P_i starvation-dependent primary root growth inhibition (increased root hair number and length) through the control of auxin patterning (Miura et al. 2011), whereas the phr1 mutant does not exhibit affected root architecture (Rubio et al. 2001). In conclusion, posttranslational modifications appear to be essential for P economy (Raven 2008) and potentially for enhancing PUE in crops.

1.9. Conclusion

Phosphorus is an essential macronutrient with crucial functions in macromolecular structure, energy metabolism and signal transduction and can be a major constraint for high yield when limiting in crop production. There are economic, political and environmental reasons why P_i efficiency and P_i fertilizer use in crops should be investigated for improvement. Therefore, scientific interest in finding underlying molecular mechanisms for adaptability to P_i starvation and identifying targets to achieve high-yielding and P_i starvation tolerant crops has increased. Agronomic strategies for raising the amount of available fertilizer are constantly under assessment. However, the polygenetic basis of P_i starvation tolerance is still not yet understood.

Field selection and screening for PUE traits, is difficult due to the complex effects of soil-P_i availability and agronomic practice on root properties and other traits. Another critical point is the shift from P_i acquisition to translocation processes when crops become generative and redistribution to grain and seeds becomes predominant. Several approaches for investigating crops, comprising the comparison of individual genotypes exposed to a short-term P_i starvation period, the over-expression of target genes and QTL analysis, resulted in partly contradictory observations. But many potential target genes, which have been identified previously in model organisms using

forward and reverse genetic approaches, are also found in crops and are potentially exploitable. Phosphate transporters, several transcription factors, genes coding for proteins of the TCA cycle metabolism, phospholipid degradation, transfer and post-translational modifications are among the candidates who have been emphasised even if their role in the genetically diverse P_i starvation tolerance or PUE context seems complex and still elusive.

Chapter 2: Identification and expression profiling of family 1 P_i transporters in wheat as targets for P_i efficiency improvement

2.1. Introduction

2.1.1. The P_i transporter family 1

Members of the P_i transporter family 1 (Pht1) which mediate P_i acquisition in plants (Rausch and Bucher 2002, Raghothama 2005) were previously suggested as potential targets for genetic improvement, although their role in P_i acquisition, P partitioning and P_i re-translocation is very complex (Chapter 1).

Root expressed Pht1 transporters, predominantly induced in root tips and root hairs (Daram et al. 1998, Mudge et al. 2002, Schünmann et al. 2004, Glassop et al. 2005), have been identified in a broad range of different plant species including wheat, indicating their involvement in initial root P_i acquisition from the soil solution (Smith et al. 1999, Davies et al. 2002, Mudge et al. 2002, Paszkowski et al. 2002, Rae et al. 2003, Glassop et al. 2005, Nagy et al. 2006, Wang et al. 2013a). The expression patterns of some Pht1 transporters are related to root arbuscular mycorrhiza (AM) colonization in rice, wheat, Brachypodium and Medicago (Harrison et al. 2002, Paszkowski et al. 2002, Glassop et al. 2005, Güimil et al. 2005, Gutjahr et al. 2008, Gaude et al. 2012, Hong et al. 2012, Yang et al. 2012). Apart from the initial root P_i acquisition, a large diversity of expression profiles throughout different plant tissues indicates that Pht1 transporters are also involved in P_i translocation as well as P_i remobilization in the aerial plant parts, especially during generative growth. For example, translocation of P_i from leaves into other developing organs has been shown in Arabidopsis (Himelblau and Amasio 2001) suggesting an involvement of Pht1 transporters in that redistribution process. In barley, weak expression of root-expressed HvPht1;2 and HvPht1;1 has been reported in leaves (Schünmann et al. 2004), and the authors suggested that the methods used in previous studies (Smith et al. 1999, Rae et al. 2003) were insufficient in sensitivity to detect these low expression levels. However, HvPht1;2 was expressed most in vascular tissues near the root apex and at the site of secondary root emergence in barley (Schünmann et al. 2004).

Furthermore, HvPT1;6 was predominantly and strongly expressed in old leaves and flag leaves of barley with an expression hardly responsive to external P_i concentrations (Rae et al. 2003). Affinity (K_m) values of HvPht1;6 suggested that it might be involved in P_i re-translocation, functioning as a low-affinity P_i transporter located on the plasma membrane of epidermal cells (Rae et al. 2003, Preuss et al. 2010). In rice, OsPht1;1 was abundantly expressed in epidermal root cells, but also in stele cells of leaves and weakly in pikelets and emerging buds (Sun et al. 2012). OsPht1 transporter expression was further observed in the panicle and flag leaves in rice (Liu et al. 2011) or in flowers of soybean (Qin et al. 2012). Apart from spatial variation, physiological development plays another role for transcriptional profiles of P_i transporters. OsPht1;2 expression was low in all tissues except roots, and was highest at mature stages of rice plants (Paszkowski et al. 2002).

2.1.2. The involvement of Pht1 transporters within the P_i starvation signalling crosstalk

Increasing Pht1 transporter expression was reported when plants were exposed to a short period of P_i starvation or to mycorrhizal infection (Daram et al. 1998, Smith et al. 1999, Wang et al. 2002, Rae et al. 2003, Wasaki et al. 2003, Tittarelli et al. 2007, Calerón-Vázquez et al. 2008, Huang et al. 2008, Ai et al. 2009, Miao et al. 2009, Pariasca-Tanaka et al. 2009, Qin et al. 2012). Furthermore, P_i nutrition and regulators of the P signalling crosstalk influence root P_i acquisition, P_i translocation and P_i partitioning between roots and aerial tissues in a differentiated manner and alter P_i acquisition mechanisms via altered Pht1 transporter expression: Nagy et al. (2006) determined a differential regulation and responsiveness of ZmPht1 transporters to decreasing concentrations in external P_i availability. AthPht1;5 and OsPht1;1 over-expression increased root hair development at P_i replete conditions in Arabidopsis and rice (Nagarajan et al. 2011, Sun et al. 2012).

OsPht1;1 over-expression altered the expression of other OsPht1 transporters, including OsPht1;4 and OsPht1;8 (Sun et al. 2012), whereas OsPht1;8 over-

expression did not affect OsPht1;1 in the roots but significantly enhanced many others including OsPht1;2 or OsPht1;6 (Jia et al. 2011), indicating that the cross-talk between P_i transporter expression is quite complex and may involve other key regulators to determine the extent of transcriptional alteration. Furthermore, OsPht1;1 was strongly induced in Ospho2, but not Osphr1 mutants (Sun et al. 2012), whereas OsPht1;2 is up-regulated in OsPHR2 over-expressing lines, an effect which can be counteracted through OsSPX over-expression (Liu et al. 2010). Some Pht1 promoters contain the target elements for PHR1 (Schünmann et al. 2004, Ren et al. 2012a), WYRK 75 (Devaiah et al. 2006, Miao et al. 2009), both important transcription factors of the P_i starvation signalling network, and other conserved cis-acting elements (Tittarelli et al. 2007).

Arbuscular mycorrhizal fungi, which are abundant in agricultural soils and are influenced greatly by P_i fertilizer application (Abbot and Robson 1994), have been shown also to change Pht1 expression patterns (Paszkowski et al. 2002, Glassop et al. 2005, Yang et al. 2012). This suggests an important role of these transporters in relation to AM symbiosis. These results provide evidence that the cross-talk of P_i transporter regulation is complex and is mediated through multiple regulatory genes with different effects.

2.1.3. The importance of Pht1 transporters in wheat

Obtaining high grain yields without wasting fertilizer resources will challenge future crop production (Kirkby and Johnston 2008, Gregory and George 2011). As a major grain crop and staple food (FAO 2011), wheat is contributing to the global P cycle (Rose and Wissuwa 2012). Nonetheless, little progress has been made to increase P_i efficiency traits in cereal crops (Syers et al. 2008, Calderón-Vázquez et al. 2011, Rose et al. 2011, Veneklaas et al. 2012). Therefore, this study aims to identify all putative members of the Pht1 family in wheat (TaPht1) based on genomic sequence information and homologies in model plants and other cereal species. This approach complements prior studies on TaPht1 genes which investigated the specifically root-expressed

(Davies et al. 2002, Tittarelli et al. 2007, Miao et al. 2009) and mycorrhiza-associated TaPht1 genes (Glassop et al. 2005, Miao et al. 2009, Sisaphaitong et al. 2012, Teng et al. 2013). However, the lack of whole genome sequence information in wheat has hindered detailed investigations on the TaPht1 family and the determination of their importance in agronomic systems as targets for enhancing tolerance to P_i starvation, especially in regards to genotypic variation (Davies et al. 2002, Pariasca-Tanaka et al. 2009, Huang et al. 2011, Rose and Wissuwa 2012).

Soil properties and soil cultivation are highly relevant for root growth and P_i acquisition mechanisms (Holford 1997, Hinsinger 2001, Syers et al. 2008, Niu et al. 2012), and may influence Pht1 expression. Therefore, induced TaPht1 transporter expression, as an adaptation mechanism of field-grown crops during severe long-term P_i starvation, rather than a quick short-term response to patchy patterns of P_i availability, is determined in this study predominantly for root and ear tissues. The involvement of TaPht1 transporters in the translocation of P_i from leaves into other tissues could not be accurately tested due to the formation of secondary products during real-time qPCR analysis when RNA from using leaf samples. Apart from spatial variation, physiological development and nutritional status may also alter Pht1 transcription. Therefore, TaPht1 expression profiles in wheat root and ear tissues exposed to different nutrient regimes, including N, P_i, K, Mg and S, and different stages of development were determined, which allowed the comparison between individual transporters across time, tissues and experiments.

2.2. Material and Methods

2.2.1. Identification of TaPht1 genes and phylogenetic analysis

Gene and mRNA sequence searches for putative members of the Pht1 gene family in Triticum aestivum were based on BLASTn analysis (Altschul et al. 1990) of different wheat sequence databases using sequence data of phylogenetically closely related Pht1 family members in barley (Rae et al. 2003), Brachypodium distachyon (Hong et al. 2012) and rice (Paszkowski et al. 2002). These sequences were identified and assigned to the A, B or D genome and specific chromosome using the International Wheat Genome Sequencing Consortium (IWGSC) wheat survey sequence data base[4] with the basic default BLAST parameter settings "blastn" and "wheat survey sequence / chromosome 1, 2, 3, 4, 5, 6 and 7 ABD genome". For incomplete nucleotide sequences, a second database, the Chinese Spring wheat database Cerealsdb BLAST[5] was used with default settings: 'unassembled 454 reads'/e-value cut-off e-05. All matching sequences were downloaded in FASTA format, assembled using the CAP3 programme (Huang and Madan 1999) and consensus region of DNA sequences, 'contigs', were compared for sequence identity using the ExPASy SIB Bioinformatics Resource Portal Lalign tool[6]. The D-genome sequences of TaPht1;1 and TaPht1;2 were completed in this manner.

Previously published putative TaPht1 sequences (Davies et al. 2002, Glassop et al. 2005, Sisaphaithong et al. 2012) were extracted from the NCBI Pubmed database and allocated by multiple sequence aliment to those identified in this study. Multiple sequence alignments of the coding Pht1 genome DNA sequences were done using the ClustalX v 2.0 (Larkin et al. 2007) and visualized with GeneDoc v. 2.7.000 (Nicholas and Nicholas, 1997). The wheat sequences used originated from the chromosome for which the sequences were the most completely available which was mostly chromosome D. The same genome DNA sequences were used for generating a sequence indentity table.

[4] http://www.wheatgenome.org/
[5] http://www.wheatbp.net/CerealsDB/Documents/DOC_search_reads.php
[6] http://www.ch.embnet.org/software/LALIGN_form.html

The initial phylogenetic analysis which illustrates the phylogenetic relationships between the distinct Pht1 transporters of each cereal species was performed by constructing a Bootstrap Neighbour-Joining tree and assessed with TreeView (Win 32) 1.6.6. using the coding nucleotide sequences. However, MEGA 5.05 (Tamura et al. 2011) was used for calculation of phylogenetic trees (the neighbour-joining method (Saitou and Nei 1987). Bootstrap values for the trees were calculated as a percentage of 1000 trials with a seed number for the random number generator of 1000 (Felsenstein 1985). The evolutionary distances (expressed as number of amino acid differences per site) used the number of differences method (Nei and Kumar 2000). TaPht1 transporters were classified according to the barley nomenclature when putative homologues were identified.

2.2.2. Plant material from a hydroponic culture

Seeds of T. aestivum cv. Hereward, a semi-dwarf winter wheat were surface-sterilised by 10 min immersion in a solution containing 1 % sodium hypochlorite solution (NaOCl), rinsed with sterile water and incubated over night (> 10 h) at 4 ˚C. Seed were germinated for 5 days on sterile water-soaked paper tissue, 1st to 6th of December 2011, and seedlings were then transferred to a completely randomized single plant 1 L aerated hydroponic culture in a controlled environment facility at Rothamsted Research, Harpenden, UK: 12 h day length, 70 % humidity, 20 ˚C, photon flux rate of 500 µmol photons m^{-2} s^{-1} and night with 16˚C and 80 % humidity. The plants were grown hydroponically for 18 days, from 6th to 24th of December 2011, in a Letcombe nutrient solution modified for wheat (Drew and Saker 1984) at a pH of 7 containing 1.5 mM Ca $(NO_3)_2$, 5 mM KNO_3, 2 mM $NaNO_3$, 1 mM $MgSO_4$, 1 mM KH_2PO_4, 25 µM FeEDTA, 160 µM $CuCl_2$, 9.2 mM H_3BO_3, 3.6 mM $MnCl_2$, 16 µM Na_2MoO_4, 5 mM KCl, 770 µM $ZnCl_2$. The water used for the nutrient solutions was deionised by reverse osmosis at < 30 µs cm^{-1} and additionally UV treated (service provided by the controlled environment building facilities). The nutrient solution was exchanged three times per week. P_i starvation was imposed by replacing 1 mM KH_2PO_4 with 1 mM KCl after

day 6 of culture for a period of 12 days and plant roots rinsed before the transfer to the P_i starvation treatment. Roots and shoots were harvested in triplicates from the P_i starvation and P_i supplied treatment on day 0, 3, 6, 9 and 12 after onset of the P_i starvation between 9 and 11 am. Roots were rinsed in deionized water, dried briefly on paper towels before freezing in liquid nitrogen and being stored at -80 ˚C. Biomass was not recorded in order to prevent a limitation of plant material for molecular analysis. All samples were ground with a mortar and pestle in liquid nitrogen and 1 ml aliquots for RNA extraction and for chemical analysis were stored at -80 ˚C in Eppendorf tubes. The remaining shoot material was used for mineral analysis (Chapter 2, Section 2.5.)

2.2.3. Field derived plant material from the Broadbalk site 2011 and 2012

Field grown T. aestivum cv. Hereward was harvested in two growing seasons, 2010/11 and 2011/12, from sections 0 and 1 plots (representing continuous wheat plots) of the "Broadbalk" field experiment (Rothamsted Research 2006[7], Watts et al. 2006) where the plots have been exposed to different nutrient deficiencies since 1843. The field experiment comprises an area of 4.8 ha divided in 20 strips of 6 m width which are further divided into 10 cropping sections 0 to 9 (Watts et al. 2006). Five sections contain continuously grown wheat (Section 0, 1, 6, 8 and 9) and three sections contain wheat grown in rotations with oats and maize (2 to 5 and 7). Except on section 0, straw is removed from the sections post-harvest. The soil of this field site is a flinty, silty clay loam (Luvisol) with a clay content ranging from 25 to 35 % and calcareous layers below 2 m depth in the sampling area (Watts et al. 2006). The harvested plant material was exposed to multiple long-term nutrient deficiencies through the omission of N, P_i, K, Mg and S fertilizers (Table 1 and 2).

[7] http://www.rothamsted.ac.uk/Content.php?Section=Research&Page=Publications

Table 1: Fertilizer treatments at the Broadbalk field site.
Plant material from these plots was used for gene expression studies on TaPht1 transporter expression (2011 and 2012) and microarray analysis (2011). Plot 19 was used as P_i starvation treatment in 2011 and plot 20 in 2012. Source: Guide to classical experiments; Rothamsted Research (2006).

Fertilizer treatment (Plot no.)	Fertilizer supply	Fertilizer forms, timing and amount
Control plot (BB 0**9**)	N4, (P_i), K, Mg	**N (nitrogen)**, applied as ammonium nitrate either as a single application mid-April;192 kg N ha^{-1} (**N4**) or splited mid-March, mid-April and mid-May applying 48 kg N ha^{-1} respectively (**N1+1+1)** **P_i (phosphate)**, applied as a single application of triple superphoshate in autumn; 35 kg P ha^{-1}, (P) no P application since 2000 **K (potassium)**, applied either as a single application of potassium sulphate; 90 kg K ha^{-1} (**K**) or as potassium chloride; 90 kg K ha^{-1} (**K***) **Mg (magnesium)**, applied as magnesium sulphate until 1973, then either as kiserit; 35 kg Mg ha^{-1} every 3rd year or as kiserit 30 kg Mg ha^{-1} every 3rd year until 2000 (**Mg***)
No P_i application (BB **19**); since 2001*	N1+1+1, K, Mg	
No P_i application (BB **20**)	N4, K, Mg	
No S application (BB **14**)	N4, P_i, K* (Mg*)	
No Mg application (BB **13**)	N4, P_i, K	
No K application (BB **11**)	N4, P_i, Mg	
No N application (BB **06**)	N1, (P_i), K, Mg	

* Previously, castor meal supply (96 kg N)

Table 2: Soil and yield data from plots at the Broadbalk field site (eRA data8).

Olsen P, K, Mg, pH and % organic matter determined for air-dried soil < 2 mm top soil (0-23 cm) sampled in autumn 2010 from compacted stubble from Section 0 (straw incorporated) and Section 1 at Broadbalk. Yields (grain + straw with 85 % DM) are from year 2011 and 2012 (eRA data). Plot numbering refers to the data reference: Rothamsted Research (2006). Plot 19 was used in 2011 and plots 20 in 2012 for sampling of P_i starved plants. The classification of Olsen P concentrations (mg P_i kg^{-1} soil) into the Index system is according to Defra (2012)*.

Plot (no. – Sec.)	**Olsen P** mg kg^{-1}	**Index***	**Exch K** mg kg^{-1}	**Exch Mg** mg kg^{-1}	**pH**	**% Org C**	**2011 Grain** t ha^{-1}	**2011 Straw** t ha^{-1}	**2012 Grain** t ha^{-1}	**2012 Straw** t ha^{-1}
Control (**9** - 0)	72	5	358	82	8.0	1.19	5.42		6.10	
Control (**9**-1)	55	4	308	76	8.0	1.10	4.83	1.74	6.36	3.52
No P_i (**19** - 0)	20	2	191	66	7.8	1.23	3.84		5.91	
No P_i (**19** - 1)	18	2	191	80	8.1	1.26	3.96	1.93	5.67	3.23
No P_i (**20** - 0)	4	0	386	83	8.2	1.09	1.56		1.12	
No P_i (**20** - 1)	3	0	382	78	8.2	1.09	0.78	0.25	0.14	no straw
No S (**14** - 0)	97	5	261	144	7.6	1.11	5.56		6.45	
No S (**14** - 1)	87	5	220	126	7.7	1.07	5.33	2.04	6.15	3.18
No Mg (**13** - 0)	92	5	339	34	7.8	1.13	4.75		6.55	
No Mg (**13** - 1)	90	5	289	28	7.9	1.04	4.62	1.8	6.12	3.03
No K (**11** - 0)	89	5	94	63	7.5	1.14	4.89		5.47	
No K (**11** - 1)	96	5	79	54	7.5	1.05	4.33	1.54	3.29	1.28
No N (**06** - 0)	80	5	436	93	7.7	1.02	2.59		3.63	
No N (**06** - 1)	86	5	437	95	7.7	1.00	2.62	1.03	3.32	1.44

* Index 0 = 0-9 Olsen P; Index 1 = 10-15 Olsen P; Index 2 = 16-25 Olsen P; Index 3 = 26-45 Olsen P; Index 5 = 71-100 Olsen P

[8] http://www.era.rothamsted.ac.uk/

2.2.4. On-site soil, yield and weather data

Soil and yield data from Broadbalk in during the growing season 2010/11 and 2012/13 and on-site meteorological records were provided by the long-term experiments national capability and data sets requested from the electronic Rothamsted Archive (eRA data) (Table 2, Figure 5). Soil-P_i availability was determined as Olsen P (Olsen 1954).

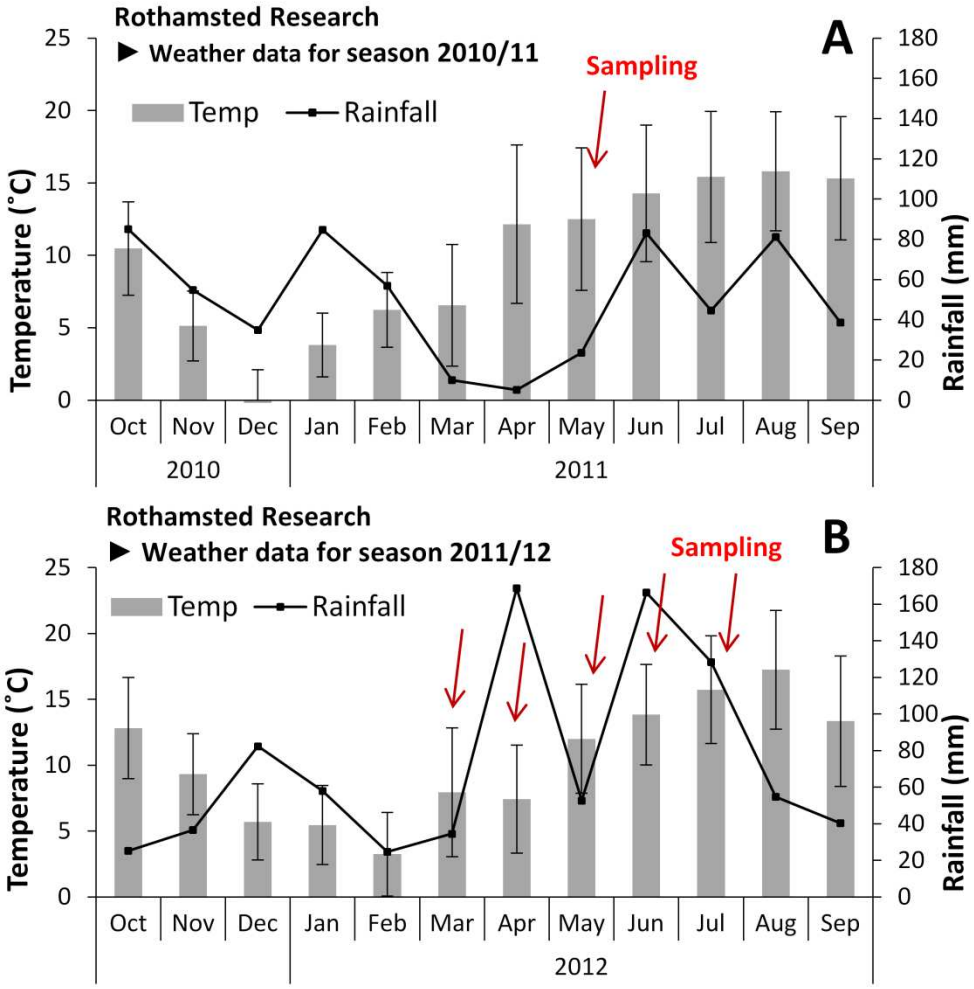

Figure 5: Meteorological data (eRA) from the growing season (A) autumn 2010 to autumn 2011 and (B) autumn 2011 to autumn 2012 at Rothamsted Research, Harpenden, UK.

Temperature and rainfall are presented as average monthly values. Monthly maximal and minimal temperatures are represented as bars with SE. Sampling of plant material from the Broadbalk field trial was done (A) 11th May in 2011 and (B) at booting (GS 45), 28th March (GS 24), 4th April (GS 31/32), 30th May (GS 45), 11th June (GS 49), 15th and 22th June (GS 65), 5th and 11th July (GS 75) in 2012; GS = growth stage according to Zadoks et al. 1974 (see also Table 3). The average temperature and rainfall at Rothamsted is 10 °C and 704 mm (Rothamsted 2006).

In May 2011, plants were excavated with a fork-like spade in triplicates (n = 3) from each plot, including plot 19 for P_i starved plants, at growth stage 45 (Zadoks et al. 1974). Sampling was done between 9 to 12 am. Roots were rinsed with de-ionized water, dried briefly on paper towel before freezing in liquid nitrogen and being stored at -80˚C. The remaining shoot material was used for chemical analysis (Chapter 2, Section 2.5.). In 2012, five replicates (n = 5) of root and shoot tissues were sampled from section 0 and 1 using the previously described procedure at five different growth stages (Table 3) from plot 20 which did not receive P_i fertilizer ('P_i starved') and a control plot which received 35 kg P_i ha^{-1} as triple superphosphate and therefore likely to yield P_i replete plants (plot 09-0/09-1 'P_i supplied').

Table 3: Wheat tissues sampled from the Broadbalk field trial in 2012.
Sampling dates for plant material used in gene expression studies on TaPht1 transporters and for chemical analysis.

Harvest (Zadoks et al. 1974)	Date	Tissues
Tillering (24)	28th March	Root, Shoot
Elongation (31/32)	4th April	Root, Shoot
Booting (45)	30th May	Root, Leaves, Ears
Late booting (49)	11th June	Rachis, Inflorescence
Anthesis (65)	15th June, P_i supplied 22th June, P_i deplete	Root, Leaves, Rachis, Inflorescence
Ripening (75); 20 days post-anthesis	5th July, P_i supplied 11th July, P_i deplete	Roots, Leaves, Rachis, Glume, Grain

Plant growth over the growing season was seriously affected on the 'P_i starved' plots exposing severe symptoms of P_i starvation e.g. fewer tillers, purple coloration and a stronger greening (no systematic recording). The shoot tissues were kept on ice and sorted into whole shoot samples for chemical analysis. Separated samples of different plant parts (depending on growth stage) were frozen in 50 ml tubes in liquid nitrogen and stored at -80 ˚C until further use. Glumes and leaves were ground with mortar and pestle in liquid nitrogen. Root, ears, rachis and grain samples were ground with SPEX SamplePrep 6870

Freezer/Mill (Metuchen USA) for 1 min precool, 2 min run and a rate of 5 cycles per seconds in order to obtain a sufficient pulverization of the samples, particularly the soil-excavated roots. Aliquots were stored in 2 ml tubes at -80 ˚C for RNA extraction (Chapter 2, Section 2.6.).

2.2.5. Chemical analysis

Oven-dried (72 h / 80 ˚C) shoot material sampled was ground using ZM 200 Retsch mill, Haan, Germany. Aliquots of 500 g were stored for chemical analysis in glass vials at room temperature in the dark. Chemical analysis was performed to check whether the actual nutritional status of the plant material corresponded to the expected nutrient starvation status. Total concentrations of micro- and macronutrients as well as trace elements were determined for each oven-dried sample via 'Inductively Coupled Plasma Atomic Emission Spectrometer' (ICP-AES; Perkin Elmer LAS, Seer Green, UK). Aliquots of 250 mg of ground shoot material, including an "in-house" standard, technical replicates and blanks positioned randomly during the procedure, were digested during 2 h of incubation with 5 ml of 70 % nitric (Primar Plus Trace analysis grade) / 70 % perchloric acid (Trace Metal grade) mixture (vol. 15 to 85) (Fisher Scientific, UK) in 25 ml glass vials. All pure acids were diluted using water which had been deionised by reverse osmosis at 18 µs cm^{-1} and additionally UV treated. The 25 ml vials were then placed into a temperature controlled carbolite heating block. In this block, a heating regime carried out over night: 60 ˚C for 3 h, 100 ˚C for 1 h, 120 ˚C for 1 h and 175 ˚C for 2 h, then cooling down to room temperature. During the heating cycles, the organic matter of the plant material is digested and dissolved by the added acids. After adding 5 ml of 25 % HCl (Analytical reagent grade) (Fisher Scientific, UK) into the cool tubes, the block was reheated to 80 ˚C for 1 h for dissolving and volatilisation of the residues. Subsequently, 20 ml of deionised H_2O was added, tubes were vortexed and heated for another 30 min at 80 ˚C. The vials were removed from the heating block to cool and deionised H_2O added to give a final volume of 20 ml.

Nitrogen concentrations in wheat shoots from Broadbalk in 2011 were determined using 300 mg subsamples of ground shoot material in a LECO CNS analyser in which the sample is combusted and any elemental C, S and N converted to CO_2, SO_2, N_2 and NO_x. NO_x containing gas passing the catalyst heater is then reduced to N_2 and measured in a thermo conductivity cell.

Samples were analysed in the Agilent 7500 ICP-MS (Stockport, Cheshire, UK) and the Leco Combutions analyser (LECO TruMac, Stockport, UK) by the "Analytical Unit of the Sustainable Soil and Grassland Systems Department" at Rothamsted.

2.2.6. Total RNA isolation, cDNA synthesis

Total RNA was isolated from ~300 mg of homogenized plant material using a modified protocol from Verwoerd et al. (1989). The extraction is performed with 1 ml of hot (80 ˚C) phenol/extraction buffer [phenol - 0.1 M Tris/HCl, 0.1 M LiCl, 1 % SDS, 10 mM EDTA, pH=8 (1:1)] (Sigma-Aldrich, St. Louis, USA) and 500 µL chloroform/isoamylalcohol (24:1) (Sigma-Aldrich). After 30 s of homogenization, mixtures were centrifuged for 5 min using the maximal speed of 15,000 rpm (HeraeusBiofuge primo R, Kendro, Hanau, Gemany). A second extraction with the RNA containing aqueous phase was performed in a new Eppendorf tube by adding 1 ml chloroform/isoamylalcohol (24:1) (Sigma-Aldrich), vortexing for 30 s and centrifuging 5 min at 15,000 rpm. Subsequently, the supernatant was again transferred to a new Eppendorf tube. The RNA was precipitated over night at 4 ˚C by adding 4 M LiCl (Sigma-Aldrich). RNA was collected by a 20 min centrifugation and washed with 70 % ethanol (Sigma-Aldrich). After a DNase treatment with 5 µl RNase free DNase (Promega, Madison, USA), 15 µl DNase buffer (Promega) and 130 µL H_2O_{DEPC} (= diethyl pyrocarbonate-treated water) which was added to the dried sample, pellets were dissolved on ice before starting the incubation for 30 min at 37 ˚C. Afterwards, 150 µL H_2O_{DEPC} was added to the sample and purification via phenol/chloroform/isoamylalcohol extraction (300 µL) was done. Subsequently another extraction with 300 µl chloroform/isoamylalcohol

followed. The RNA was precipitated at -80 ˚C for 2 h by adding 1/10 volume of 3 M NaOH and 2.5 volume of ethanol. After the incubation, the RNA was collected by 20 min of centrifugation and washed with 70 % ethanol. The final air-dried pellet was dissolved in an appropriate volume of H_2O_{DEPC}. RNA concentration (µg µL^{-1}) was measured for 2 µL of each sample with NanoDrop™ photo-spectrometer; ND-1000 V3 3.0 (Thermo Scientific, Wilmington, USA). Potential DNA contamination was checked by TAE-agarose electrophoresis (1 % w/v; 60 V; 30 min) of 1 µg total RNA per sample. cDNA was synthesised from mRNA using 2 µg aliquots of total RNA, 1 µL 10 mM dT-adapter primer and 1 h synthesis time according to the standard protocol for Superscript III Reverse transcriptase (Invitrogen, Carlsbad, USA). 2 µg of total RNA, 1 µL 10 mM dT-adapter primer and the appropriate volume of H_2O_{DEPC} was used up to a volume of 13 µL, which was mixed and incubated at 70 ˚C for 10 min to denature the template RNA. After cooling on ice, 4 µL of 5x first strand buffer, 1 µL of 0.1 M DTT, 1 µL of dNTP mix and 1 µL of Superscript III Reverse transcriptase were added. The sample was mixed and incubated for 5 min at 20 ˚C, followed by 60 min at 50 ˚C to initiate the cDNA synthesis. Samples were then incubated at 70 ˚C for 15 min to terminate reverse-transcription and stored at -20 ˚C ready for real-time qPCR analysis.

2.2.7. Expression analysis by quantitative real-time PCR

Quantitative real-time qPCR was performed using a 96 well plate (Starlab) in an Applied Biosystems 7500 Fast Real-time PCR System and the corresponding AB7500 Software 2.0.5. Each 25 µL reaction in a 96 well plate contained 10.2 µL SYBR® Green JumpStart™ Taq ReadyMix™ (Sigma-Aldrich), 0.025 µL of ROX reference dye, 1 µL of cDNA, 250 mM (0.63 µL sense/antisense), 150 mM (0.5 µl sense/antisense) or 100 mM (0.37 µL sense/antisense) of gene-specific primer depending on the gene of interest and appropriate amounts of H_2O_{DEPC} (Table 4). Each reaction was prepared in a 1.5 ml Eppendorf tube containing the appropriate amounts of reaction components and cDNA (Table 5).

Table 4: Primer sequences used for TaPht1 transporter expression analysis via real-time qPCR: Amplicon size (bp), primer concentration (mM) appropriate annealing temperature (˚C), and primer efficiency (%). The optimal concentrations with the corresponding annealing temperatures and average efficiencies were determined for each primer pair by $\log_{10}$ dilutions dilution series in triplicates (n=3) using the equation: ($E = 10^{(-1/slope)}$-1) and the LinRegPCR package (Tuomi et al. 2010). TaQhnRNP (Ta.10105.1.S1_at) was used as reference gene (Long et al. 2010).

Gene	Absolute real-time qPCR primer (5' → 3'): Forward, reverse	bp	mM	˚C	%
TaPht1;1	TCCAAGGAGAACGTCGGCGA SCAAACACTTGTGCATGACTCT	51 ABD	150	58	101
TaPht1;2	CGACACCATTGCTCCGACTG TCAARCACACCAACMATGCACG	78 A,75 BD	200	58	106
TaPht1;5	AGGCAACGGCGCCAATAAAGTC GTATGCGTGTGTTGCCTTCTCG	89A, 85DB	200	60	111
TaPht1;6	CAGGACGGTGCCCGTGTGA CCAAACCATGAAAAGCATCCATAC	108A,100B	200	60	108
TaPht1;7*	CAAGTCCTTGGAGGAGATGTC AGTGTTCACSGACAGTCATCTAG	118D*	150	60	130
TaPht1;8	TCRCTGGAGGAGGTGTCCG AGTGGTGCACACAGCCTACG	110 ABD	150	59	109
TaPht1;10	CTAACTCTGACGCCCAAGAG CGGAACTGCTTATGCGTSG	128A, 127BD	200	58	108
TaPht1;11	GCGACCCCAAGCACATGAAG GATCGGCCCATCGTCTCAG	100 ABD	150	60	104
Reference genes					
TaQhnRNP	TTGAACTTGCCCGAAACATGCC, CACCTTCGCCAAGCTCAGAAC	123	200	59	

*TaPht1;7 AB genome sequence not available yet

Table 5: Master mix (MM) pipetting scheme used for TaPht1 transporter expression analysis via real-time qPCR according to the appropriate primer concentrations.

Primer concentration:	250 mM	Working solution	200 mM	Working solution	150 mM	Working solution
Components (µl):	MM (1x)	**MM (1.1x)**	MM (1x)	**MM (1.1x)**	MM (1x)	**MM (1.1x)**
H_2O	12.5	13.75	12.73	14.0	12.985	14.28
SYBR®Green	10.25	11.275	10.25	14.0	10.25	11.28
Rox	0.025	0.0275	0.025	0.03	0.025	0.03
primer/s	0.627	0.69	0.5	0.55	0.37	0.41
primer/as	0.627	0.69	0.5	0.55	0.37	0.41
Master mix (µl):	24	**26.4**	24	**26.4**	24	**26.4**
cDNA	1	1.1	1	1.1	1	1.1
total vol. (µl):	25	**27.5**	25	**27.5**	25	**27.5**

Primers were all tested with genomic DNA before starting the analysis. The primer design for performing accurate real-time q PCR analysis has been prepared according to Udvardi et al. (2008).For each primer pair, the amplification efficiency ($E = 10^{(-1/slope)}-1$) was also determined via $\log_{10}$ dilutions dilution series in triplicates (n=3) for different tissues and treatments and considered acceptable within a range of ≥ 85 % to ≤ 115 %. The average efficiencies of each primer pair are presented for plasmid and standardized root samples in Table 4. For further accuracy of each individual PCR run, the mean primer efficiency was estimated using the linear phase of all individual reactions amplification curves (Ramakers et al. 2003) calculated by using the LinRegPCR package (Tuomi et al. 2010). However, individual PCR reaction efficiencies for each run will not shown in the thesis.

The accuracy of real-time qPCR analysis also depends on appropriate transcript normalization (Guénin et al. 2009). Therefore, a heterogeneous nuclear ribonucleoprotein Q (hnRNP Q) / Ta.10105.1.S1_at was used as reference gene (Long et al. 2010). hnRNP Q belongs to a gene family without poly A tail. However, hnRNP Q expression was successfully checked across all samples, confirming Long et al. (2010) which used a similar RNA isolation technique for identifying novel reference genes in wheat. Conventionally reference genes such as GAPDH and 18sRNA were strongly influenced by P_i fertilizer treatments and were not considered as appropriate for normalization in these experiments.

The real-time qPCR regime followed a standard protocol: 50 ˚C for 2 min, 95 ˚C for 10 min followed by the cycling stage in a total of 40 cycles. Each cycle starts with 95 ˚C for 15 sec (denaturation, annealing) followed by a decrease to 60 ˚C (extension) for 1 min. For some primers, the annealing temperature period had to be adjusted to 20 sec (Table 4) before the extension for 40 sec at 60˚C. SYBR Green is a non-specific binding dye which detects any double-stranded DNA which can be primer-dimers or unspecific amplified products due to low specificity to the desired gene of interest. Therefore, a melting curve was performed expecting a single peak at temperature above 80 ˚C.

Primer concentrations were either decreased in the case of primer-dimer formation or primers redesigned when non-specific products were still detected. Additionally, each run included two non-template controls which would detect primer dimer formation, and two probes containing only SYBR Green, H_2O and ROX which would to detect contamination of solutions or during the preparation process. In some cases "no-reverse transcriptase" controls were included as well to check the cDNA amplification specificity.

Each TaPht1 real-time qPCR amplicon was cloned and sequenced in order to verify if primers amplified specifically the members of the gene family they were designed for (Table 5). Around 500 bp cDNA fragments covering the expression amplicon of each analysed TaPht1 gene were amplified (Mastercycler® gradient, Eppendorf Scientific) using gene specific primers (Table 6) and RedTAQ ready PCR-mix (Sigma-Aldrich, UK).

Amplified DNA fragments were and cloned into pGEM-Teasy vector system (Promega, UK) and finally sequenced (MWG-Eurofins, Ebersberg, Germany). Sequences were submitted to EMBL-data base[9] and accession number entries published on the 14th of December 2013 (Table 6). Due to the lack of expression, cDNA fragments for TaPht1;9 and TaPht1;14 were not cloned. Although cDNA fragments for TaPht1;3 and TaPht1;4 were amplified, cloned and sequenced, no suitable real-time qPCR primer combination for expression analyses were found.

The sequenced plasmids were also used for determining standard curves in qRT-PCR studies to quantify gene expression on an absolute scale. Based on the molecular weight of the plasmid and PCR fragment, the mRNA copy number per μL cDNA was calculated after reference gene normalization of Ct values.

[9] http://www.ebi.ac.uk/ena/

Table 6: TaPht1 gene names, accession numbers, chromosome and genome localization for previously published and identified TaPht1 transporter sequences (NCBI Pubmed database).

( ) indicates when data were incompletely available. Primer sequences used for cloning PCR amplified an average product size of 500 to 550 bp at an annealing temperature of 60˚C.

TaPht1 Gene	T. aestivum accession numbers of previously published TaPht1 transporter	Genome Chromosome location	Primer used for fragment isolation and sequencing: Forward, reverse	T. aestivum accession numbers of identified and sequenced TaPht1 transporters
TaPht1;1	AY293828	chr4 (AL, BL, DL)	GTTCACCGTCGCCTTCATCG CACTTGTGCATGACTCTGTGTC	HG764732 (putative A)
TaPht1;2	AJ344242, AJ344241, AJ344240	chr4 (AL, BL, DL)	TTCACCGTCGCCTTCATCGAC TCAARCACACCAACMATGCACG	HG764733 (D), HG764734 (A)
TaPht1;3	AJ344243, AK333026	chr5 (BL), DL	CCAGCTCATGGGCTTCTTCATG CACTAGCACGCACGAGTTGTG	HG764735 (D), HG764736 (B)
TaPht1;4		chr4 AL	GCTTCGCCATCCAGCTCATG CACGCACGCACGAGTTGTGA	HG764737 (putative A)
TaPht1;5		chr5 AL, BL, (DL)	GTCGTCGGAAGGTTCTGGATC CATGCACGTATGCGTGTGTTGC	HG764738 (putative A)
TaPht1;6	AF110180, AJ344247	chr5 AL, BL, DL	CAACTCCACCACCTTCATCGTG AACYCGACCAGCAACTCTRATG	HG764739 (D), HG764740 (B)
TaPht1;7		chr4 (DL)	CCAGCTCATGGGCTTCTTCATG AGTGTTCACSGACAGTCATCTAG	HG764741 (putative D)
TaPht1;8	AJ830009	chr6 AL, BL, DL	GATGAAGGGACTCATGCTCGTC AGTGGTGCACACAGCCTACG	HG764742 (putative ABD)
TaPht1;9		chr2 AS, BS, DS	CAATTGCTCGGCTTCACCATGA TGACTGATTGGTCTAGATGTGTG/ A genome GCAACCTATTGAGTACAAGACACA /B and D genome	not submitted
TaPht1;10	CD871730	chr7 (AS), BS, DS	CTGGTACATCGTGCTCTACG CGGAACTGCTTATGCGTSG	HG764743 (putative BD)
TaPht1;11	AB753269, AB753270, AB753271	chr4 AL, BS, DS	GTCACCGTGGCMCTCATCGA CGACRTCCTTGTCCACATGC	HG764744 (putative ABD)
TaPht1;12		chr2 (AS), BS, DS	GACAGAATTGGTCGAATCAAGATG CCACATGGTATATTCTTTGGCAC	not submitted
TaPht1;13	AJ344248, AJ344244, AJ344249	chr2 AS	ACGGTGTTCCTCATCGACGTC ACTTCTATCAAACGTCTGGTGCC	HG764745 (putative A)
TaPht1;14		chr4 AL	CGCATCAAGATCCARCTCATG ACACTAAAAYCAKCAACSGGGA	not submitted

Transcript abundance was expressed as normalized copy numbers in 0.1 µg total RNA from the appropriate number of biological replicates. Calculation for absolute quantification was as follows:

A Standard curve determination:

1) Molecular weight (g mol^{-1}) of double stranded plasmid + fragment
2) Calculation of g mol^{-1}: 1/(mol. weigh x 10^{12})
3) Calculation of molecules fg^{-1}: (6.02 x 10^{-23}) x mol fg^{-1} = double strand
4) Molecules fg^{-1} x 0.5 = single strand

B Assessing the copy number for each sample:

5) Normalization:

   Ct_{sample} x ($Ct_{Reference\ gene}$/highest$Ct_{Reference\ gene}$) = $Ct_{normalized\ sample}$

6) Determination of the equivalent of amount of plasmid for each normalized sample by using the standard curve for each transporter:

   Standard curve: **y = mx + b**
   y = amount of plasmid in log_{10}fg,
   m = slope of the standard curve,
   x = Ct value of the normalized sample which was analysed,
   b = y intercept; where the line of the standard curve crosses the y-axis.

   Log_{10}fg plasmid = slope x $Ct_{normalized\ sample}$ + b
   Fg plasmid = 10^ $^{Log10fg\ plasmid}$

7) Determination of the transcript abundance of the gene of interest:

   Number of molecules in 0.1 µg total RNA[10]
   = fg plasmid x (molecules fg^{-1} plasmid single strand)

[10] As cDNA synthesis was done using 1µg total RNA in 10 µl of solution

2.2.8. Cloning and Sequencing of transcripts

A PCR (Mastercycler® gradient, Eppendorf Scientific) was performed using cDNA synthesised from total RNA of root, grain or inflorescence for each gene of interest. In order to obtain sufficient amounts of PCR product, the reaction volume of 15 µL was used four times: 1 µl template cDNA, 0.3 µL of sense and antisense primer (Eurofins) (Table 6), 7.5 µL RedTaq mix (Sigma-Aldrich) and 5.9 µL H_2O_{DEPC}. PCR parameters were 2 min at 94˚C for initial denaturation followed by 40 cycles of denaturation of the cDNA stands at 94 ˚C for 30 s and 20 s at 57 ˚C for the primer annealing and 40 s at 72 ˚C for extension. Final extension was performed for 5 min at 72 ˚C. The final reaction volume of 60 µL PCR products was separated by 1.2 % (w/v) TAE - agarose gel electrophoresis (60 V, 50 min) which contained 3 µl ethidiumbromide (10 µg μL^{-1}).

The amplified target gene product was visualised with a digital image system GeneSnap 6.00.21 and GeneTools 3.02.00 (Syngene, Synoptics Ltd, Cambridge, UK). Amplicons were recovered by cutting out the gel band under UV light and purified using the NucleoSpin®Gel and PCR Clean up kit (Macherey-Nagel). The eluate was stored at -20 ˚C until ligation into a pGEM®-T Easy Vector System (Promega) according to the manufacturer´s protocol.

A reaction volume of 10 µL contained 3.5 µl H_2O, 2 µL of 5x ligation buffer, 1 µL of T4-DNA ligase, PCR fragment and plasmid (pGEM®-T Easy Vector) in a molecular weight ratio of 1:3 and incubated at 16 ˚C for 1 h and at 4 ˚C for 8 h. For the transformation, 5 µL of the ligation product was kept on ice and transferred to 100 µL competent E. coli cells (DH5α strain) which were kept on ice for 20 min and gently flicked in between. The cells were heat shocked for 1 min at 42 ˚C and then directly cooled on ice of further two min in order to perforate the bacterial cell wall. 1 mL of SOC medium consisting of 3.6 g L^{-1} glucose (20 mN), 20 g L^{-1} tryptone, 5 g L^{-1} yeast extract, 0.5 g L^{-1} NaCl, 2.44 g

L^{-1} $MgSO_4$, 15 g L^{-1} agar with a final pH of 7.0 ± 0.2 at 25 °C (ForMedium, Hunstanton, UK) was added and incubated for 1 h at 37 ˚C in a shaking (200 rpm) incubator. 200 µL of E. coli colonies were cultivated on a YT-plate consisting of 16 g L^{-1} tryptone, 10 g L^{-1} yeast extract, 5 g L^{-1} NaCl, 15 g L^{-1} agar with a final pH 7.0 ± 0.2 at 25 °C and 30 mL/petri dish (ForMedium, Hunstanton, UK). All YT-plated also contained ampicillin (50 mg ml^{-1}), IPTG (100 mM) and X-Gal (40 ng mL^{-1}). Positive transformations could be detected by white-blue screening and corresponding plasmids incubated over night at 37 ˚C in in YT media. The plasmids were isolated with the GeneJET™Plasmid Miniprep Kit (Fermentas) using 4 mL of culture. 50 µL of purified plasmid elute was stored at -20 ˚C.

A control PCR was conducted (30 cycles) with previously described parameter settings and amplicons visualized using (1 %) TAE-agarose gel electrophoresis (70 V, 30 min). Sample plasmid DNA concentrations (µg $µL^{-1}$) were measured with NanoDrop™ photo-spectrometer; ND-1000 V3 3.0 (Thermo Scientific, Wilmington, USA) and adjusted to 100 ng $µL^{-1}$ (total vol. of 10 µL) according to the sequencing requirements (Eurofins MWG operon).

2.2.9. Statistical analysis

All chemical and expression data was statistically analysed using GenStat (2013, 16th edition, VSN International Ltd, Hemel Hempstead, UK). For the majority of data, an analysis of variance (ANOVA) was applied. However, to apply an ANOVA as a statistical test is only appropriate if residuals are following a normal distribution. Therefore, residual plots were always checked before performing the statistical tests.

The effect of P_i supply and harvest date on shoot mineral composition in liquid culture plant material were analysed performing an unbalanced ANOVA. For determining the impact of P_i supply on TaPht1 expression with time a two-way ANOVA ($P \leq 0.05$) was performed using a nested treatment structure: Type / (P_supply * Harvest date) with ‘Type’ being either the control when the

experiment started (day 0) or the treatment after day 0. For comparing the expression of all TaPht1 transporters with each other, a factorial treatment structure (P_supply*Pht) and values on a $\log_{10}$ scale were used.
A two-way ANOVA ($P \leq 0.05$) was performed comparing the effect of each fertilizer treatment on macro, micronutrient or trace element concentration in 2011 using "nutrient" as treatment structure. The effect of nutrient starvation on TaPht1 expression in the roots from the Broadbalk site in 2011 was determined using a two-way ANOVA ($P \leq 0.05$). Expression values were transformed to a $\log_{10}$-scale in order to take into account the heterogeneity of variance and resulting in predicted means for each measurement. Therefore, all statistical properties applied are additionally displayed.

Shoot mineral composition in 2012 was analysed for each harvest time point (n=3) from P_i fertilized and non-P_i fertilized plots individually performing a two-way ANOVA ($P \leq 0.05$). The effect of P_i starvation, tissue and harvest time was compared for each specific nutrient (treatment structure: P_supply.tissue_sampled.Harvest_date).

TaPht1 expression in 2012 was analysed by fitting it into a linear mixed model using the method of residual maximum likelihood (REML) for which the data had to be $\log_{10}$-transformed. Means were compared using the standard error of difference (SED) on the relevant degrees of freedom (df) and least significant difference (LSD) values at 5 % level of significance ($p \leq 0.05$) displayed as back-transformed means. For comparing the effect of physiological stage and P supply in specific tissues, approximate F-tests were used.

A two-way ANOVA was used for comparing TaPht1 transporter expression in roots at elongation using $\log_{10}$-values and a factorial treatment structure. The design is a split-plot, with plants as main plots and the gene copy numbers as subsamples. The main effects and interaction between P_i supply and genes as the treatment factors were assessed and means compared using the SED on the corresponding df invoking the LSD value at the 5 % level of significance.

2.3. Results

2.3.1. Identification of the wheat P_i transporter family 1

Analysis of public database data revealed a total of 14 wheat TaPht1 genes (Table 7, Figure 6). The majority of the TaPht1 genes are located on the long-arm of chromosome 4, wheareas a three are located on chromosome 2 (TaPht1;9, TaPht1;12 and TaPht1;13) and chromosome 5 (TaPht1;3, TaPht1;5 and TaPht1;6), respectively (Table 7). This is indicative of gene duplication, especially as TaPht1 transporters located on chromosome 4 and 5 share higher degrees of nucleotide and protein sequence similarity (TaPht1;1 to TaPht1;7) compared to those located on chromosome 2 (TaPht1;9) or 7 (TaPht1;10) (Tables 8, Figure 6). The only exceptions are TaPht1;11 and TaPht1;14 which show lower sequence similarity to the other TaPht1 genes located on chromosome 4 and 5 (Table 8, Figure 6). Furthermore, TaPht1;11 is located on the long arm of the A genome but on the short arm of the B and D genome of chromosome 4 (Table 7).

All 14 TaPht1 transporters share a high degree of sequence similarity in their amino acids of the proteins (Figure 6). TaPht1;1 and TaPht1;2 share the same chromosome localiation (Table 7) and a high degree of sequence similarity of > 95 % (Table 8, Figure 6) which is indicative for a recent gene duplication. Both genes are showing further the highest sequence similarity to TaPht1;3 and TaPht1;4 (Table 8, Figure 6). However, TaPht1;1 and TaPht1;2 share a much lower degree of sequence similarity with any other TaPht1 tranporter (< 70 %), especially with TaPht1;10 (< 45 %) (Table 8). In general, TaPht1;10 does not show a high sequence similarity to any of the other TaPht1 transporters (< 45 %). TaPht1;9, TaPht1;12 and TaPht1;14 exhibit low sequence similarity to any of the other transporters except to each other (~60 %) (Table 8). TaPht1;3 and TaPth1;4 are putatively located on two different chromosomes, 5 and 4, respectively (Table 7). Nonetheless, the coding region of TaPht1;3 and TaPth1;4 differ only in a few bases leading to a > 97 % sequence similarity

between the nucleotide and > 99 % sequence similarity between protein sequence of both transporters (Table 8, Figure 6).

Table 7: Contig sequences of TaPht1 genes available in the IWGSC database.

The data was generated by inputting known Pht1 sequences in Brachypodium, rice, baley and wheat in the IWGSC database. The hit with the highest sequence similarity assigned to A, B and D genome was selected for each gene.

Gene	Sequence name
TaPht1;1	IWGSC_**chr4AL**_ab_k71_contigs_0_7063798, IWGSC_**chr4AL**_ab_k71_contigs_7089469 IWGSC_**chr4BL**_ab_k71_contigs_longerthan_200_6980733 IWGSC_**chr4DL**_V2_ab_k71_contigs_longerthan_200_14415770, IWGSC_**chr4DL**_V2_ab_k71_contigs_longerthan_200_14320716
TaPht1;2	IWGSC_**chr4AL**_ab_k71_contigs_7137440 IWGSC_**chr4BL**_ab_k71_contigs_longerthan_200_6980732 IWGSC_**chr4DL**_V2_ab_k71_contigs_longerthan_200_14415769
TaPht1;3	IWGSC_**chr5BL**_ab_k71_contigs_10794849 IWGSC_**chr5DL**_ab_k71_contigs_4520523
TaPht1;4	IWGSC_**chr4AL**_ab_k71_contigs_4484253
TaPht1;5	IWGSC_**chr4AL**_ab_k71_contigs__141305 IWGSC_**chr4BL**_ab_k71_contigs_longerthan_200_6978840 IWGSC_**chr4DL**_V2_ab_k71_contigs_longerthan_200_14452103
TaPht1;6	IWGSC_**chr5BL**_ab_k71_contigs_longerthan_200_10879329 IWGSC_**chr5DL**_ab_k71_contigs_longerthan_200_4608340
TaPht1;7	IWGSC_**chr4DL**_V2_ab_k71_contigs_longerthan_200_7691254
TaPht1;8	IWGSC_**chr6AL**_ab_k71_contigs_longerthan_200_5786477 IWGSC_**chr6BL**_ab_k71_contigs_longerthan_200_196133, IWGSC_**chr6BL**_ab_k71_contigs_longerthan_200_4336728 IWGSC_**chr6DL**_ab_k71_contigs_longerthan_200_601360
TaPht1;9	IWGSC_**chr2AS**_ab_k71_contigs_longerthan_200_5281078 IWGSC_**chr2BS**_ab_k71_contigs_longerthan_200_5197123 IWGSC_**chr2DS**_ab_k71_contigs_longerthan_200_1056254, IWGSC_**chr2DS**_ab_k71_contigs_longerthan_200_3411524, IWGSC_**chr2DS**_ab_k71_contigs_longerthan_200_791522, IWGSC_**chr2DS**_ab_k71_contigs_longerthan_200_2659001
TaPht1;10	IWGSC_**chr7AS**_ab_k71_contigs_longerthan_200_4249767 IWGSC_**chr7AS**_ab_k71_contigs_longerthan_200_4228753 IWGSC_**chr7BS**_ab_k71_contigs_longerthan_200_3140394 IWGSC_**chr7BS**_ab_k71_contigs_longerthan_200_3163651 IWGSC_**chr7BS**_ab_k71_contigs_longerthan_200_3077373 IWGSC_**chr7DS**_ab_k71_contigs_longerthan_200_3920729
TaPht1;11	IWGSC_**chr4AL**_ab_k71_contigs_longerthan_200_7045368 IWGSC_**chr4BS**_ab_k71_contigs_longerthan_200_4893305 IWGSC_**chr4DS**_ab_k71_contigs_longerthan_200_2325503
TaPht1;12	IWGSC_**chr2AS**_ab_k71_contigs_longerthan_200_5201274 IWGSC_**chr2BS**_ab_k71_contigs_longerthan_200_5155483 IWGSC_**chr2DS**_ab_k71_contigs_longerthan_200_5319819
TaPht1;13	IWGSC_**chr2AS**_ab_k71_contigs_longerthan_200_5227437
TaPht1;14	IWGSC_**chr4AL**_V2_ab_k71_contigs_longerthan_200_7016297

Table 8: Sequence similarity (%) of TaPht1 transporter transcripts and proteins.

The table was generated using nucleotide sequences (italic) and **protein sequences (bold)** identical to those of the phylogenetic analysis. The coding nucleotide sequences which were used are predominantly from the D genome, except for TaPht1;4, TaPht1;13 and TaPht1;12 for which sequences were derived from the A genome and for TaPht1;5 from the B genome.

TaPht1:	1;1	1;2	1;3	1;4	1;5	1;6	1;7	1;8	1;9	1;10	1;11	1;12	1;13	1;14
TaPht1;1 chr4 DL	100	**98**	**69**	**69**	**68**	**56**	**68**	**60**	**50**	**31**	**45**	**55**	**66**	**53**
TaPht1;2 chr 4 DL	97	100	**69**	**69**	**68**	**56**	**67**	**60**	**50**	**31**	**45**	**55**	**65**	**53**
TaPht1;3 chr5 DL	73	72	100	**99**	**76**	**61**	**72**	**62**	**53**	**31**	**45**	**55**	**73**	**55**
TaPht1;4 chr4 AL	73	72	97	100	**76**	**60**	**72**	**62**	**53**	**31**	**45**	**55**	**73**	**55**
TaPht1;5 chr5 BL	70	70	79	79	100	**58**	**69**	**58**	**49**	**30**	**44**	**53**	**70**	**51**
TaPht1;6 chr5 DL	66	66	72	72	67	100	**57**	**48**	**41**	**32**	**33**	**43**	**59**	**44**
TaPht1;7 chr4 DL	71	70	76	76	73	70	100	**59**	**49**	**32**	**44**	**52**	**68**	**52**
TaPht1;8 chr6 DL	65	65	71	72	67	64	68	100	**46**	**30**	**39**	**49**	**58**	**47**
TaPht1;9 chr2 DS	54	54	58	57	55	53	53	**53**	100	**28**	**37**	**55**	**52**	**55**
TaPht1;10 chr7 DS	42	41	44	44	43	40	46	44	37	100	**21**	**29**	**33**	**29**
TaPht1;11 chr4 DL	60	60	65	65	61	57	61	58	49	39	100	**40**	**42**	**38**
TaPht1;12 chr2 DS	59	58	60	60	57	54	57	56	62	38	51	100	**54**	**60**
TaPht1;13 chr2 AS	67	67	75	75	71	72	42	67	57	42	59	58	100	**55**
TaPht1;14 chr4 AL	58	58	62	62	59	55	39	57	61	39	53	64	61	100
TaPht1:	1;1	1;2	1;3	1;4	1;5	1;6	1;7	1;8	1;9	1;10	1;11	1;12	1;13	1;14

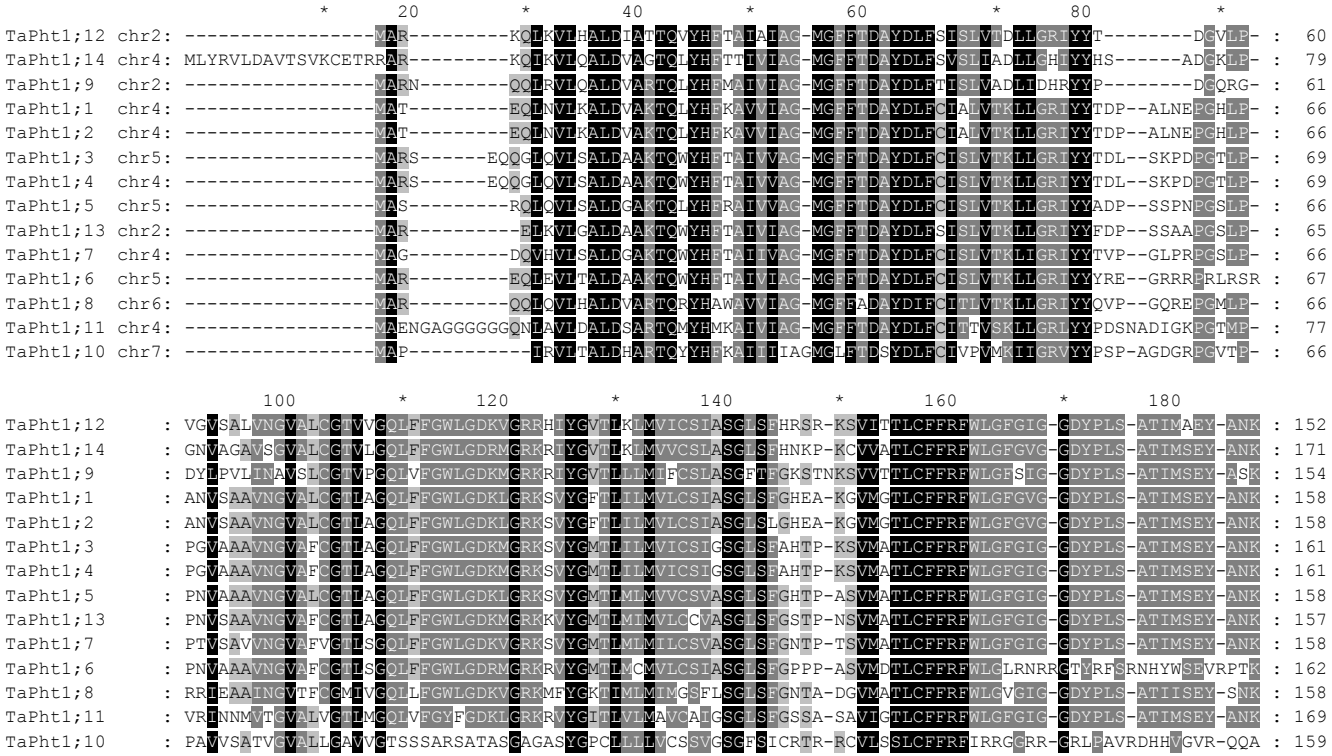

Figure 6: Multiple alignments of TaPht1 transporter protein sequences.
Allocation of identified TaPht1 sequences by multiple alignment (ClustalX version 1.81). Protein sequences were derived from the coding nucleotide sequences predominantly from the D genome, except for TaPht1;14, TaPht1;13 and TaPht1;12 for which sequences were derived from the A genome and for TaPht1;5 from the B genome.

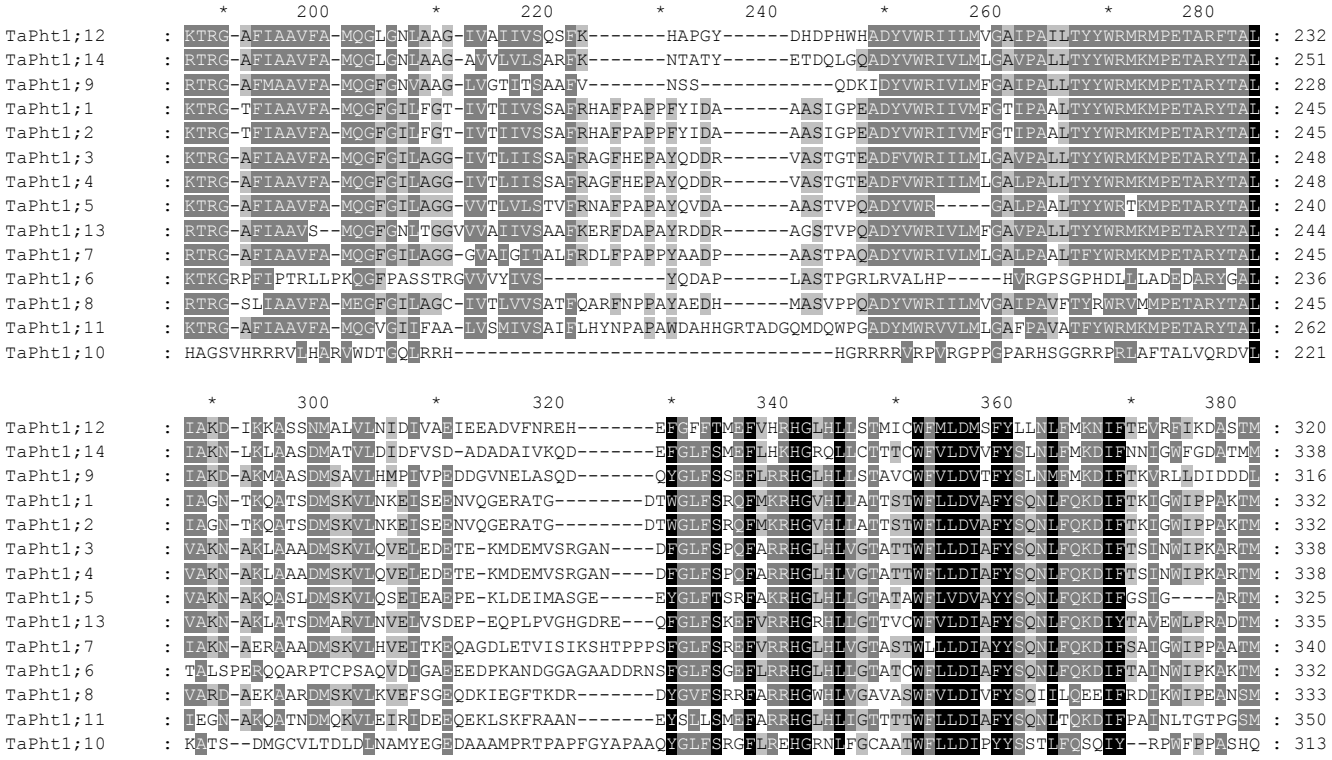

Figure 6 continued.

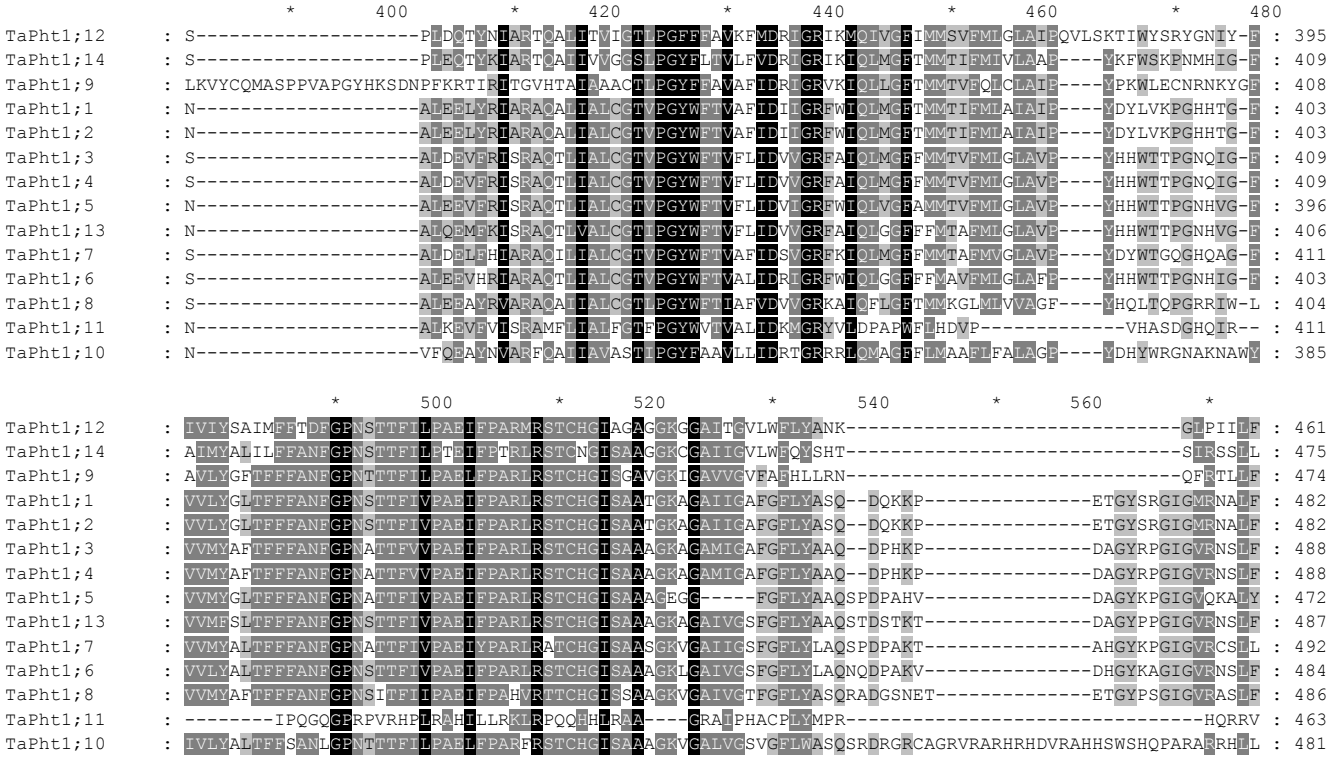

Figure 6 continued.

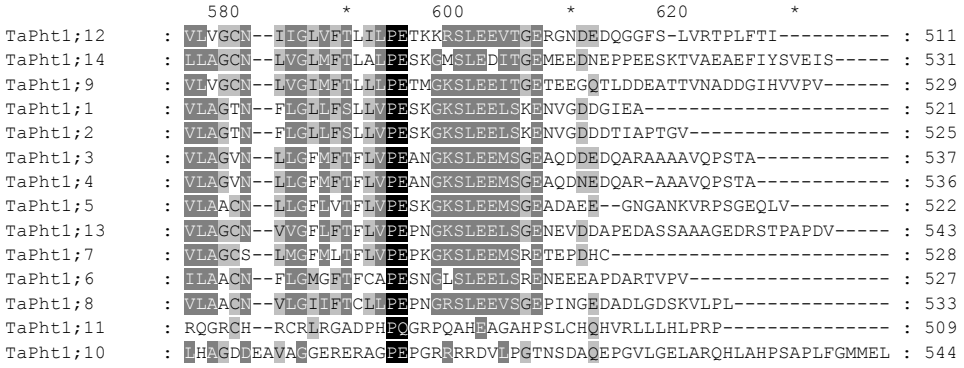

Figure 6 continued

Furthermore, TaPht1;3 and TaPth1;4 exhibit only an average sequence similarity with TaPht1;5, TaPht1;7 and TaPht1;13 (~78 %) and followed by TaPht1;1, TaPht1;2 (~70 %), TaPht1;6 and TaPht1;8 (~65 %) (Table 8). TaPht1;12 and TaPht1;13 share ~60 % sequence similarity with TaPht1;14 and TaPht1;9 (Table 8).

2.3.2. Phylogenetic analysis of cereal Pht1 transporters

Most TaPht1 transporters have one Brachypodium homologue, expect TaPht1;1 and TaPht1;2 which share one homolog in Brachypodium (Figure 7). However, TaPht1;1, TaPht1;12, TaPht1;7, TaPht1;10 and TaPht1;13 have more than one rice homologue which is indicative for rice specific gene duplication (Figure 7). TaPht1;6, TaPht1;8, TaPht1;12 and TaPht1;14 have no rice homologue and TaPht1;9, TaPht1;10, TaPht1;12, TaPht1;13 and TaPht1;14 have no barley homologue (Figure 7). In regards to the phylogenetic relationship of cereal Pht1 genes, they may be subdivided into five clusters (Figure 7).

Cluster one contains TaPht1;1 and TaPht1;2 and corresponding cereal homologous/orthologous genes; OsPht1;1, OsPht1;2 on the rice chromosome 3 and OsPht1;3 on rice chromosome 10 (Figure 7). Phylogenetically related are further HvPh1;1 and HvPh1;2 in barley, but only one Brachypodium gene, BdPht1;4 (Figure 7).

TaPht1;1 and TaPht1;2 are phylogenetically related to TaPht1;3, TaPht1;4 and TaPht1;5 which form a second cluster together with two rice, two Brachypodium and three Pht1 genes in barley (Figure 7). The Pht1;3 and Pht1;4 gene in wheat and barley have only one homologue in rice and Brachypodium (Figure 7). Furthermore, the 97 % sequence similarity of TaPht1;3 and TaPht1;4 in wheat (Table 8) and its homologues in barley (Figure 7) is indicative for a gene duplication particularly in these two species. TaPht1;5 has only one homologue in rice, Brachypodium and barley.

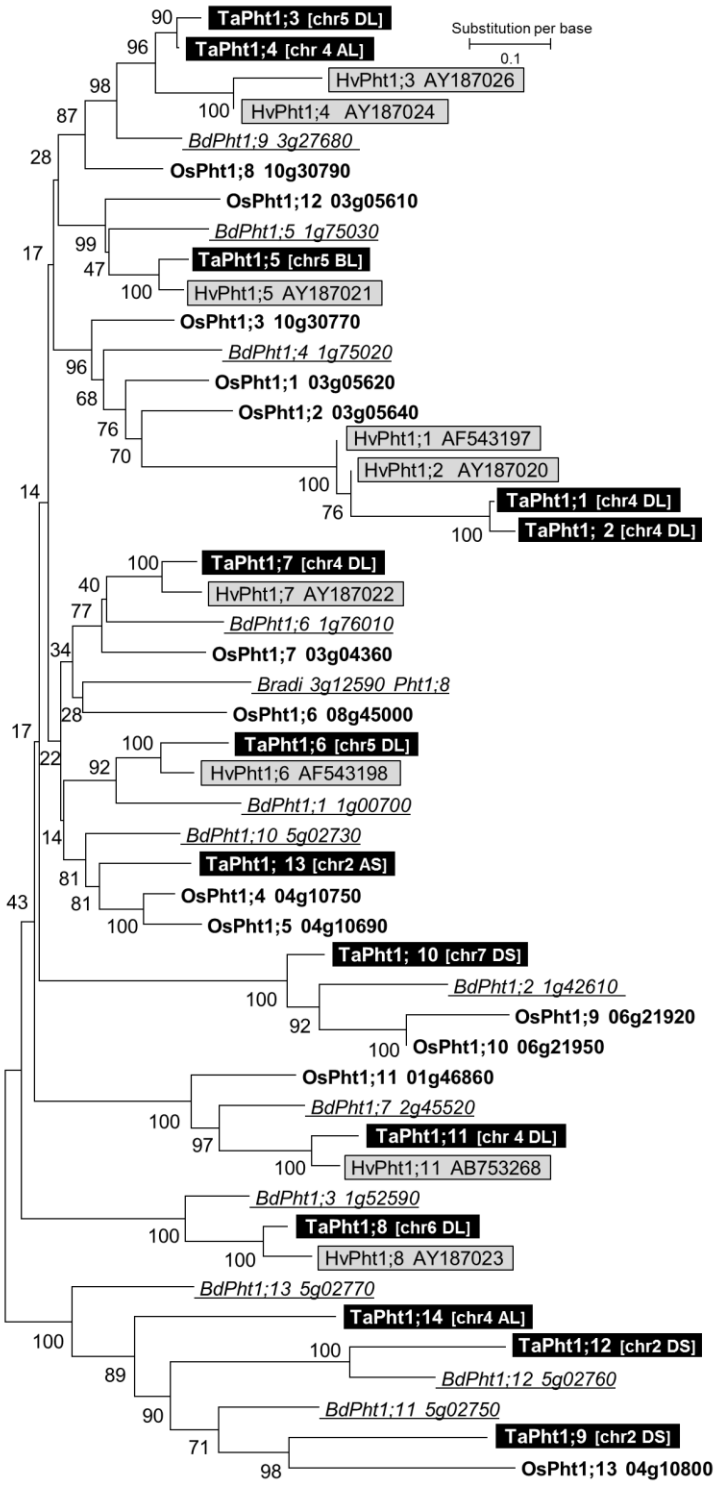

Figure 7: Phylogenetic analysis of the Pht1 family in cereals.
A Neighbour joining tree was generated for Brachypodium (Bradi), rice (Os), barley (Hv) and wheat (Ta) Pht1 transporters with the MEGA5 (v.5.2) software (Bootstrap method and the maximum composite Likelihood model) from the multiple alignment (ClustalX version 1.81) using the coding nucleotide sequences. The bootstrap values, expressed as percentages, were obtained from 1000 replicate trees. Wheat accession numbers are displayed in Table 6.

Cluster three contains the three wheat Pht1 genes TaPht1;7, TaPht1;6 and TaPht1;13, four rice genes, three Brachypodium and only two barley Pht1 genes (Figure 7). The two rice genes to TaPht1;13, OsPht1;4 and OsPht1;5 are indicative for a rice specific gene duplication (Figure 7). Furthermore, there seems to be no rice or barley homologue, except BdPht1;10 in Brachypodium, for TaPht1;6 (Figure 7). TaPht1;7 has one homologue in rice, Brachypodium and barley (Figure 7).

Even with low nucleotide sequence similarity (Table 8), TaPht1;8 and TaPht1;11 genes are in close phylogenetic proximity (Figure 7). Both genes are in the fourth cluster, including TaPht1;10 (Figure 7). There is no rice or barley homologue for TaPht1;8 but one Brachypodium homologue, BdPht1;3 (Figure 7). TaPht1;10 has one homologue in Brachypodium, BdPht1;2, but two in rice, OsPht1;9 and OsPht1;10, and no in barley (Figure 7). The two OsPht1 genes are in close phylogenetic proximity indicating again a rice specific gene duplication. TaPht1;11 has one homologue in rice, Brachypodium and barley (Figure 7).

In the last cluster, cluster five, are more distantly related Pht1 genes, including TaPht1;9, TaPht1;12 and TaPht1;14 (Figure 7). These three wheat Pht1 genes have three corresponding homologues/orthologues in Brachypodium, respectively (Figure 7). In contrast, there is only one homologue in rice for TaPht1;9, OsPht1;13, but no other homologue genes in barley for any of these three genes in cluster five (Figure 7).

2.3.3. TaPht1 expression studies using real-time qPCR

For gene expression studies, reverse primers were designed according to positions in the 3'-non-coding region (Figure 8) due to the high sequence homology of the coding region of the Pht1 genes, considering all distinct A/B/C genome isoforms sequences to cover amplification of all three genomes transcripts. However, only seven members of the fourteen TaPht1 family members were characterised by real-time qPCR.

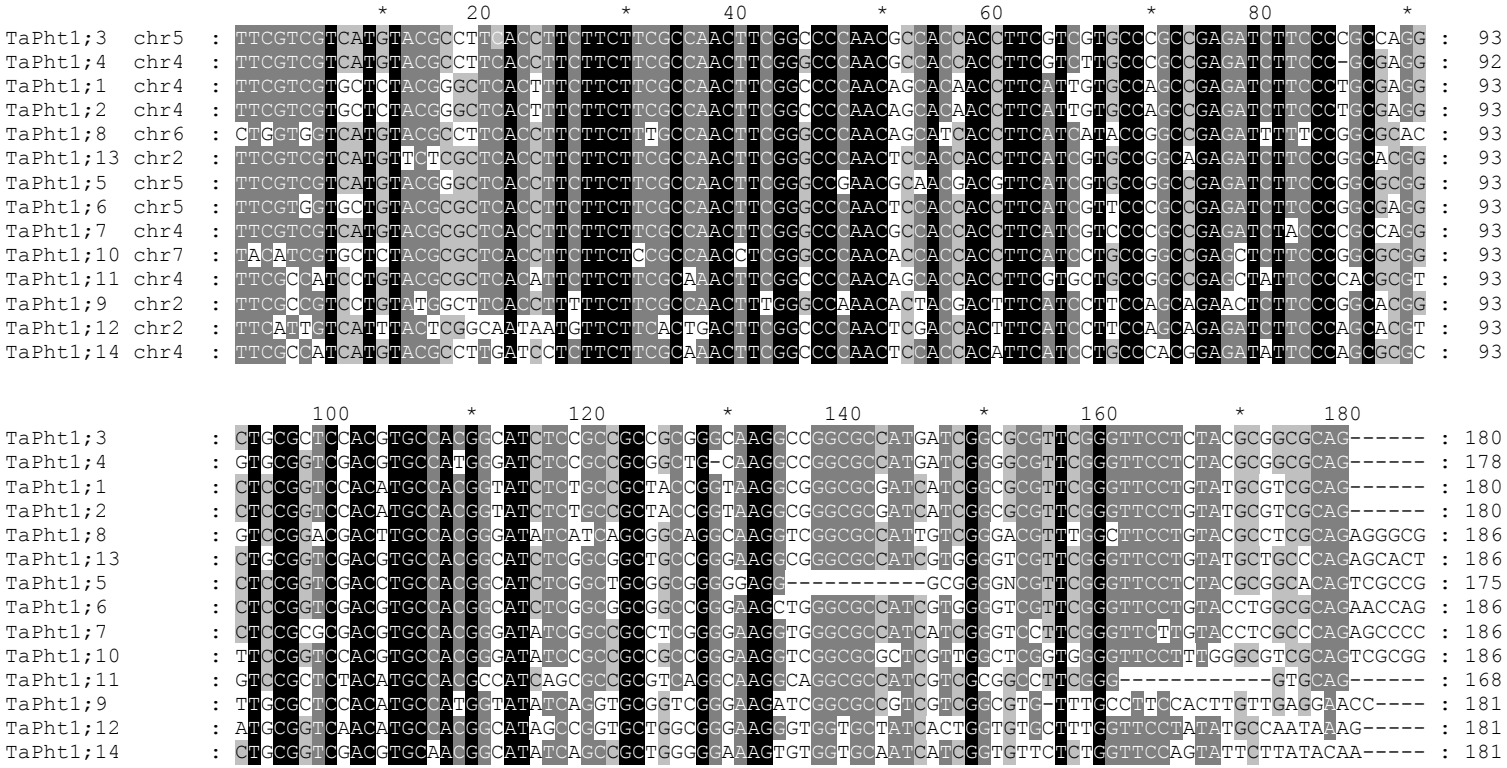

Figure 8: Multiple alignments of TaPht1 transporter genes and primer location.

Alignment generated with the ClustalX v. 1.81 software using the last part of the coding nucleotide sequences (~ 400 bp) and the non-coding, transcribed but not translated 3` region. Primer sequences and stop-codon positions are displayed in red for each TaPht1 transporter gene respectively.

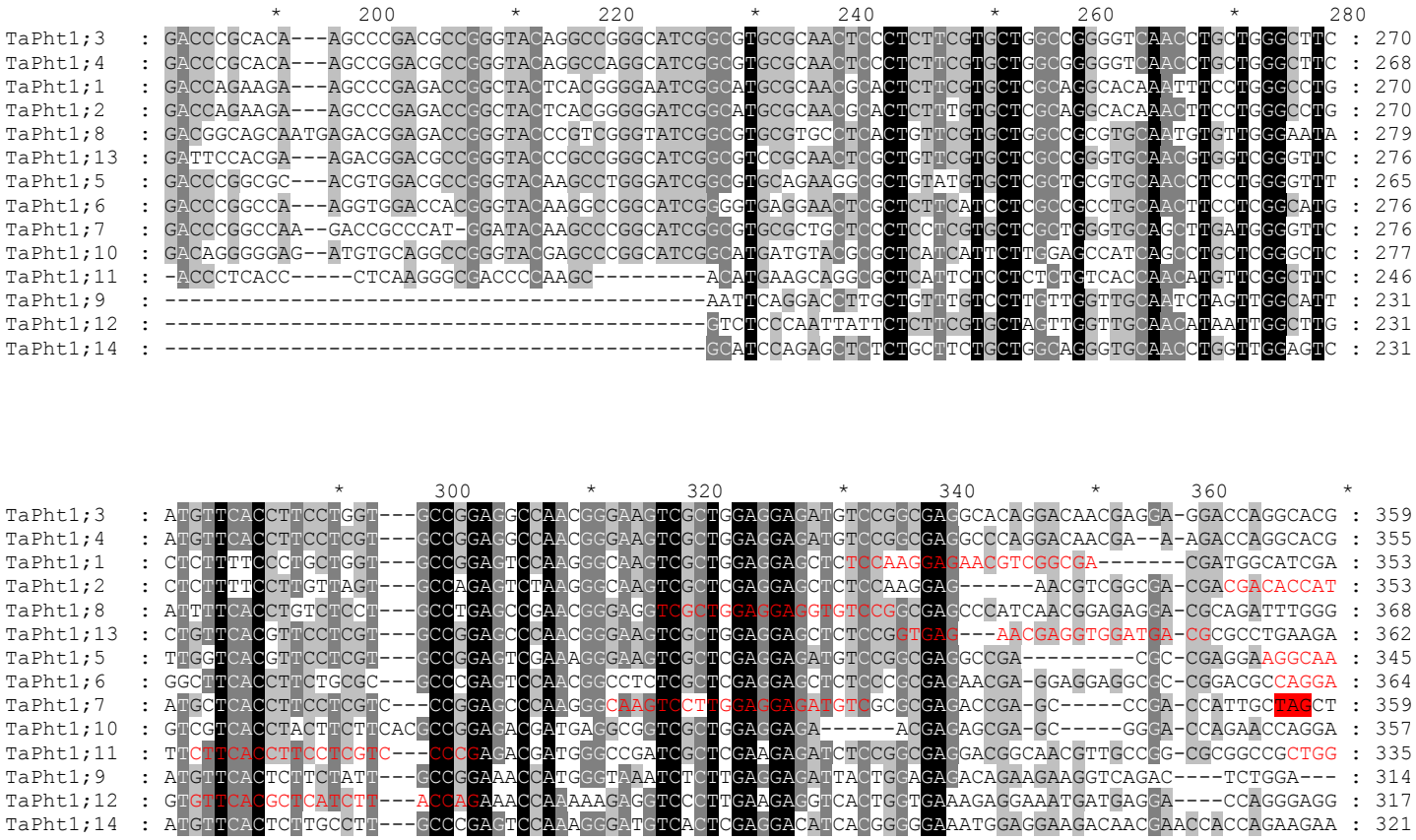

Figure 8 continued.

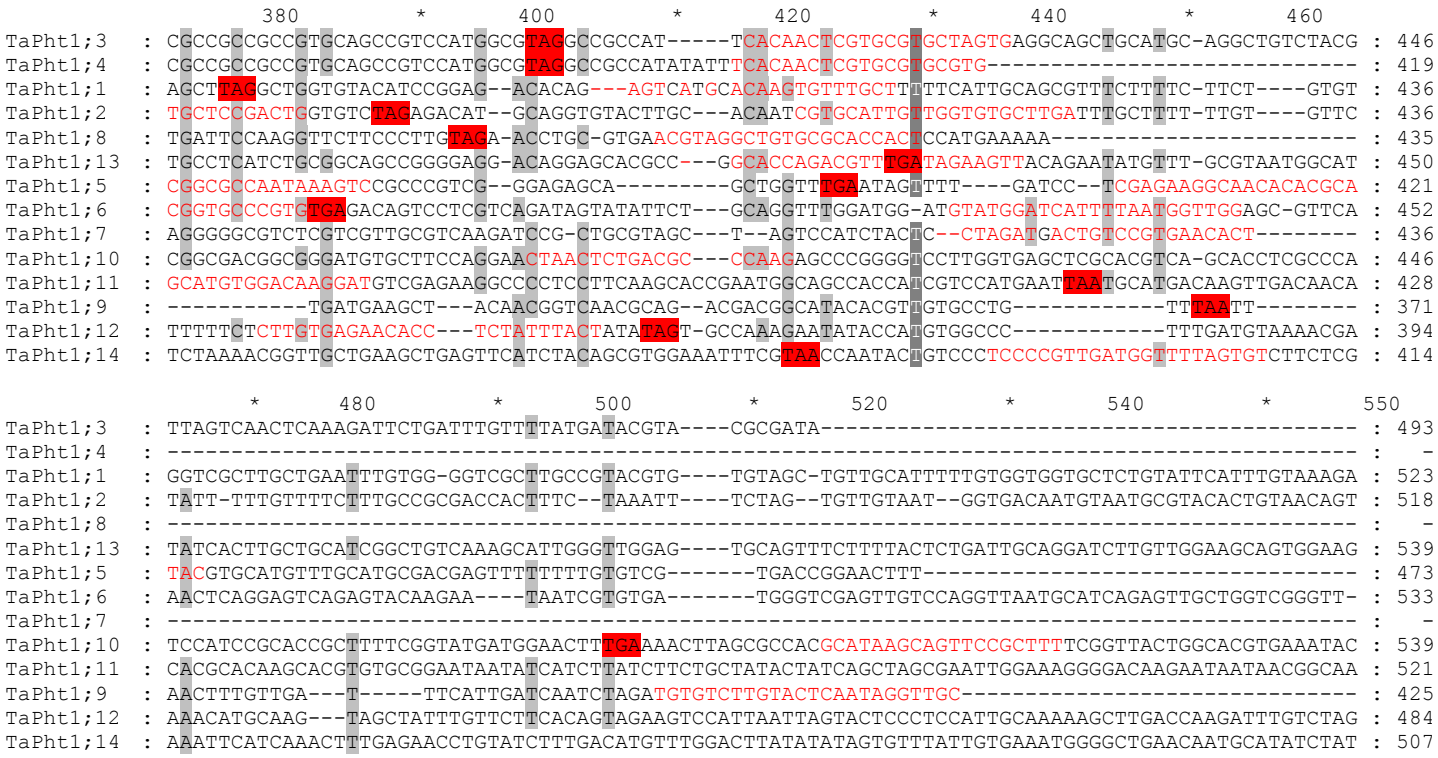

Figure 8 continued.

TaPht1:3 and TaPht1;4 showed > 99 % sequence homology. Therefore no appropriate primers were determined for distiguishing between both genes by real-time PCR analysis. TaPht1;7 was only expressed in field-grown material. However, TaPht1;9 and TaPht1:14 were not expressed in any of the sampled tissues. TaPht1;12 and TaPht1:13 were excluded due to problems with primer dimer formation during the analysis.

2.3.4. In-vitro TaPht1 expression in roots of wheat seedlings

The nutritional status of wheat seedlings was determined in shoots during 3-12 d of P_i starvation (Tables 9 and 10). Total P concentrations decreased with time and were lower in P_i starved plants (Table 9). Average Mo and Na concentrations were 1.8 g^{-1} DM and 446 g^{-1} DM respectively during the entire experimental period. The majority of nutritional elements (Ca, K, S and Mg) decreased during the experimental time (Table 9). Total Zn and P_i concentrations decreased over time, but also significantly as a result of restricted P_i nutrition across all harvest time points (Tables 9 and 10). Fe concentrations were initially higher in P_i starved plants but decreased with time and progressing P_i starvation (Table 10). Trace elements (Al, As, Cd, Co, Se) were not detected in wheat shoot tissues (results not shown), except Ni with 856 g^{-1} DM. Pb and Ti were present at extremely low concentrations and declined over time (results not shown). However, the nutrient solution specification did not contain these trace elements and therefore were likely to be seed or water contamination derived.

Table 9: Macronutrient concentrations in shoots of wheat seedlings exposed to P_i starvation in liquid culture.

Different letters indicate significant differences (P≤0.05) of nutrient concentrations at different time points (capital letters) and during P_i starvation (small letters)* (n = 3).

Treatment factors		Macronutrients (mg g^{-1} DM)				
Harvest	**P_i supply**	**Calcium (Ca)**	**Potassium (K)**	**Magnesium (Mg)**	**Phosphorus (P)**	**Sulfur (S)**
Day 3	high	2.3 **A**	48.4 **a**	1.72 **bcd**	6.8 **Aa**	3.2 **a**
	low	2.9 **A**	47.5 **a**	2.57 **a**	4.7 **Ab**	3.5 **a**
Day 6	high	2.4 **A**	44.8 **a**	2.29 **ab**	7.0 **Aa**	3.3 **a**
	low	2.5 A	49.7 **a**	1.98 **abc**	2.8 **Ab**	3.4 **a**
Day 9	high	2.3 **AB**	40.1 **ab**	1.92 **abc**	5.6 **Ba**	2.7 **ab**
	low	1.5 **AB**	30.8 **bc**	1.13 **cd**	1.3 **Bb**	1.9 **bc**
Day 12	high	1.3 **B**	28.2 **c**	1.08 **d**	3.27 **Ca**	1.7 **bc**
	low	1.3 **B**	24.4 **c**	0.91 **d**	0.84 **Cb**	1.5 **c**
Statistical properties	max SED	0.34	5.1	0.39	0.30 (TF1) 0.47 (TF2)	0.5
	max LSD	0.76	11.2	0.85	0.66 (TF1) 1.21 (TF2)	1.2
	F-statistic	$F_{3,11}$ = 9.14	$F_{3,11}$ = 3.5	$F_{3,11}$ = 4.72	TF1/TF2: $F_{1,11}$ = 143.6 / $F_{3,11}$ = 25.5	$F_{3,11}$ = 23.7
	p-value	0.003	0.053	0.024	< 0.001 (TF1/2)	< 0.001

* F-statistic for the interaction of P_i starvation = treatment factor 1 = TF1; harvest time point = TF2

Table 10: Micronutrient concentrations in shoots of wheat seedlings exposed to P_i starvation in liquid culture.

Different letters indicate significant differences (P≤0.05) of nutrient concentrations at different time points (capital letters) and during P_i starvation (small letters)* (n = 3).

Treatment factors		Micronutrients (µg g^{-1} DM)				Trace element
Harvest	**P_i supply**	**Iron (Fe)**	**Zinc (Zn)**	**Manganese (Mn)**	**Copper (Cu)**	**Cr**
Day 3	high	65.6 **bc**	57.9 **A**	145.2 **A**	12.3 **A**	2.25 **AB**
	low	101.2 **a**				
Day 6	high	59.9 **bc**	65.3 **A**	151 **A**	12.6 **A**	2.86 **A**
	low	85.3 **ab**				
Day 9	high	51.06 **cd**	54.9 **A**	109.2 **B**	9.2 **B**	0.91 **AB**
	low	43.8 **cd**				
Day 12	high	31.3 **d**	30.9 **B**	66.1 **C**	5.7 **C**	0.38 **B**
	low	33.9 **d**				
Mean	high	(48.7)	54.9 **A**	(116.2)	(9.7)	(1.27)
	low	(57.6)	45.4 **B**	(104)	(8.9)	(1.54)
Statistical properties	max SED	11.6	4.0 (TF1) 7.3 (TF2)	7.4 (TF1) 13.5 (TF2)	1.12	1.11
	max LSD	25.6	8.8 (TF1) 16.05 (TF2)	16.4 (TF1) 29.8 (TF2)	2.46	2.45
	F-statistic	$F_{3,11}$ = 5.6	TF1/TF2: $F_{1,11}$ = 7.5 $F_{3,1\,1}$ = 16.5	TF1/TF2: $F_{1,11}$ = 4.9 $F_{3,11}$ = 29.4	$F_{3,11}$ = 28.5	$F_{3,11}$ = 10.2
	p-value	0.014	0.019 (TF1) < 0.001 (TF2)	0.048 (TF1) < 0.001 (TF2)	<0.001	0.002

TaPht1;5 and TaPht1;11 were expressed weakest in hydroponically-grown wheat roots (Figure 9) whereas TaPht1;6, TaPht1;8 and TaPht1;10 expression were intermediate with P_i starvation having an impact at an advanced stage (day 12), especially for TaPht1;6 (Figure 9). No root expression of TaPht1;3, TaPht1;4, Pht1;7; Pht1;9 and Pht1;13 was detectable in in vitro-grown wheat.

TaPht1 transporter expression in roots of wheat seedlings generally increased with progressing P_i starvation (Figure 9, Table 11). TaPht1;1 and TaPht1;2 expression levels rapidly increased in the roots until day 6 but were then reduced at day 12 (Figure 9). Nonetheless, across all TaPht1 transporters, TaPht1;1 and TaPht1;2 were expressed strongest in the control as well as during P_i starvation (Figure 9). In contrast, TaPht1;6 and TaPht1;11 expression was not enhanced before day 12 of P_i starvation (Figure 9). TaPht1;5 and TaPht1;8 expression were mostly influenced by the physiological stage, although TaPht1;8 had a higher transcript level in P_i starved roots at day 12 (Figure 9).

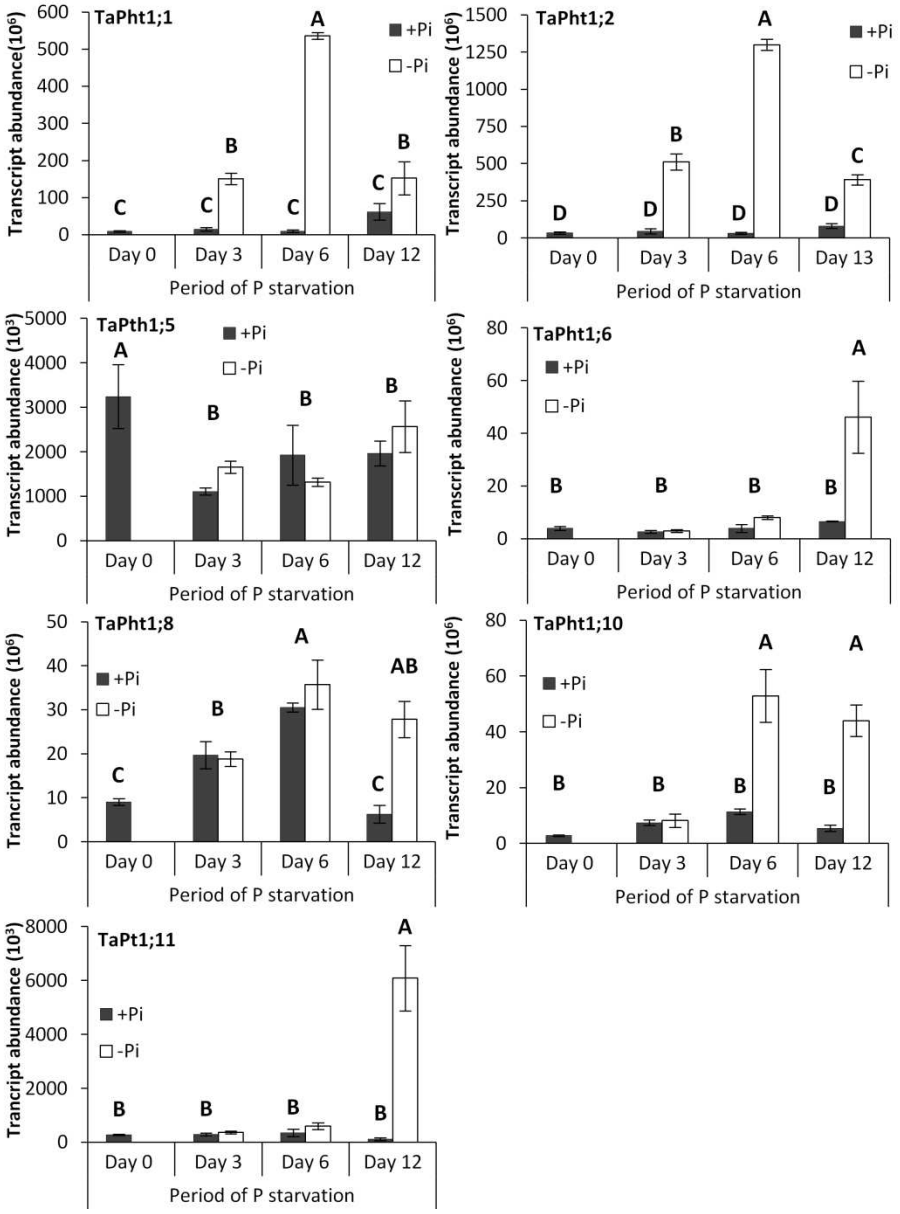

Figure 9: Expression of seven TaPht1 transporters in hydroponically-grown wheat roots exposed to P_i starvation.

Differential TaPht1 expression in roots of wheat (cv. Hereward) grown in liquid culture in a controlled environment at Rothamsted Research, UK and exposed to 12 days of P_i starvation. Means and SE are presented as normalized copy number (x 10^3 or 10^6) in 0.1 µg total RNA from 3 biological replicates (n=3). Statistical properties are displayed in Table 11. Bars sharing the same letter are not statistically different between P_i availability treatments at different time points (P>0.05).

Table 11: Statistical properties of TaPht1 expression analysis in hydroponically-grown wheat roots exposed to P_i starvation (Figure 9).
Predicted mean values, SED, LSD and F-statistic used for each particular comparison. Bars sharing the same letter are not statistically different between P_i availability treatment at day 6 or day 12 (P>0.05).

P_i supply	Time point	Transcript abundance of wheat Pht1 transporters (log_{10} scale)						
		Pht1;1	**Pht1;2**	**Pht1;5**	**Pht1;6**	**Pht1;8**	**Pht1;10**	**Pht1;11**
+P	Day 6	6.94 **E**	7.50 **CD**	6.28 **GH**	6.53 **FG**	7.28 **DE**	7.06 **E**	5.41 **I**
- P		8.59 **B**	9.02 **A**	6.12 **H**	6.90 **EF**	7.54 **CD**	7.72 **C**	5.76 **I**
mean		7.76	8.26	6.20	6.72	7.41	7.39	5.59
+ P	Day 12	7.74 **CD**	7.89 **BC**	6.28 **F**	6.82 **E**	6.75 **E**	6.72 **E**	4.98 **G**
- P		8.13 **B**	8.59 **A**	6.39 **F**	7.63 **CD**	7.43 **D**	7.64 **CD**	6.76 **E**
mean		7.94	8.24	6.34	7.22	7.09	7.18	5.87
Day 6	SED	0.192	LDS	0.395	df	6 (treatm.)	26 (Res.)	$F_{6,26} = 12.3$
Day12		0.165		0.339		6 (treatm.)	28 (Res.)	$F_{6,28} = 9.9$

2.3.5. TaPht1 expression in nutrient starved field-grown wheat roots

Wheat Pht1 transporter expression patterns were analysed in roots of field-grown wheat to identify possible interactions and differential expression patterns during other macronutrient starvations in addition to P_i and at several stages of physiological development, including tillering, booting, elongation, anthesis and post-anthesis.

With regards to the growing conditions, available soil-P_i (Olsen P), exchangeable soil-K and soil-Mg were reduced on plots with no P_i, K and Mg fertilizer applications (Table 2). However, pH or % organic carbon remained consistent (Table 2). With the exception of S, long-term Mg, K, N and P_i soil-starvation in specific plots led to lower shoot Mg, K, N and total P concentrations compared to the control (Table 12) and yields were affected negatively, at least when N, P_i and K availability was limited (Table 2). Apart from Mn, other shoot nutrient concentrations (Fe, Zn), were not affected by P_i starvation (Table 12). Sodium shoot concentrations were higher in K starved, and to a lesser extent in P_i, S and Mg starved plants (Table 12).

Table 12: Nutritional status of wheat shoots sampled from Broadbalk plots at booting in 2011.

Bars sharing the same letter are not statistically different between fertilizer treatments at different time points (P>0.05). This plant material was used for gene expression studies on TaPht1 transporter and microarray analysis.

Fertilizer treatment (no. – Sec.)	Fertilizer	Macronutrients (mg g^{-1} DM)					
		Phosphorus (total P)	Sulfur (S)	Magnesium (Mg)	Potassium (K)	Nitrogen (N)	Calcium (Ca)
Control (BB 0**9** - 1)	N4, (P), KMg	0.88 **B**	0.71 **B**	0.37 **C**	9.8 **A**	17.1 **B**	1.52 **C**
No P_i (BB **19** - 1)	N1+1+1, KMg	0.69 **C**	0.73 **B**	0.38 **C**	8.5 **A**	15.97 **B**	1.69 **BC**
No S (BB **14** - 1)	N4, PK* (Mg*)	0.95 **AB**	0.62 **B**	0.45 **B**	9.38 **A**	16.95 **B**	1.84 **B**
No Mg (BB **13** - 1)	N4, PK	0.90 **B**	0.58 **B**	0.30 **D**	9.40 **A**	15.8 **B**	1.56 **BC**
No K (BB **11** - 1)	N4, P, Mg	1.09 **A**	0.89**A**	0.59 **A**	5.7 **B**	21.1 **A**	3.11 **A**
No N (BB **06** - 1)	N1, (P), KMg	1.03 **AB**	0.69 **B**	0.39 **C**	9.4 **A**	13.6 **B**	1.6 **BC**
Statistical properties	SED	0.07	0.07	0.021	0.84	1.81	0.14
	LSD	0.15	0.16	0.046	1.84	3.95	0.302
	$F_{5,\ 12}$ = , p-value	8.7, 0.001	4.7, 0.018	46.5, <0.001	6.6, 0.04	3.7, 0.03	39.0, <0.001
Treatment Plot (no. – Sec.)	**Fertilizer**	**Micronutrients (µg g^{-1})**					
		Iron (Fe)	**Zinc (Zn)**	**Manganese (Mn)**	**Sodium (Na)**		
Control (BB 0**9** - 1)	N4, (P), KMg	78.8	7.7	19.0 **BC**	10.6 **B**		
No P_i (BB **19** - 1)	N1+1+1, KMg	96.6	7.7	14.7 **C**	32.6 **B**		
No S (BB **14** - 1)	N4, PK* (Mg*)	87.9	6.9	17.3 **C**	31.8 **B**		
No Mg (BB **13** - 1)	N4, PK	109.8	6.9	19.8 **B**	13.7 **B**		
No K (BB **11** - 1)	N4, P, Mg	114.4	7.0	26.1 **A**	85.1 **A**		
No N (BB **06** - 1)	N1, (P), KMg	133.9	8.2	22.9 **AB**	15.6 **B**		
Statistical properties	SED	20	0.76	2.2	11.9		
	LSD	43.6	1.66	4.9	25.9		
	$F_{5,\ 12}$ = , p-value	1.99, 0.15	1.12, 0.40	6.5, 0.004	11.0, <0.001		

TaPht1;1 root expression decreased in P_i and N starved wheat but increased in roots of K starved plants (Figure 10, Table 13). TaPht1;5 root expression was higher in Mg starved plants compared to any onther treatment (Figure 10, Table 13). In contrast to hydroponically-grown roots (Figure 9, Table 11), the most abundantly expressed TaPht1 transporters at booting in field-grown roots, were TaPht1;8, and TaPht1;6 (Figure 10).

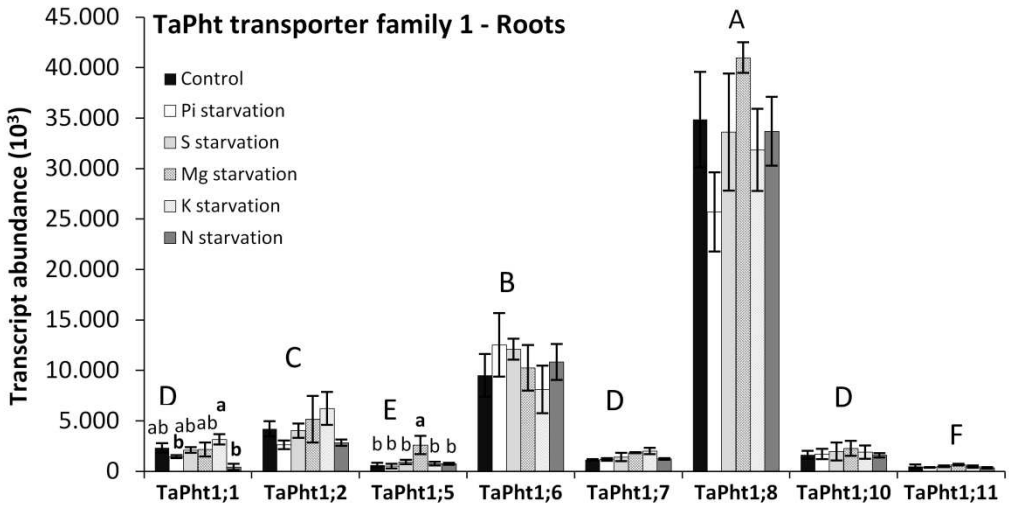

Figure 10: Expression of eight TaPht1 transporters in roots of field-grown wheat at Broadbalk in 2011.
Differential TaPht1 expression in roots of field-grown wheat (cv. Hereward) at booting exposed to nutrient starvation (P_i, S, Mg, K, N) in 2011 at the Broadbalk field site, Rothamsted Research, UK. Means and SE (n=3) are presented as of normalized copy number (x 10^3) in 0.1 µg total RNA from 3 biological replicates. P_i starved plants were sampled from plot 19 (plot treatments; Tab.1). Statistical properties are displayed in Table 13. Bars sharing the same capital letters are not statistically different between the TaPht1 members (P>0.05). Bars sharing the same small letter are not statistically different between P_i, S, Mg, K and N starvation determined for each individual TaPht1 member (P>0.05).

Table 13: Statistical properties of TaPht1 transporter expression analysis in roots of field-grown wheat at Broadbalk in 2011 (Figure 10).
Predicted mean of log_{10}-scale, max SED and max LSD values with the appropriate df for each particular comparison.

Transcript abundance (Log_{10}-value)								Statistical properties		
Main effect: Pht1 transporter								SED	LDS	df
Pht1;1	Pht1;2	Pht1;5	Pht1;6	Pht1;7	Pht1;8	Pht1;10	Pht1;11	0.067	0.13	7
6.26	6.60	5.87	7.05	6.17	7.51	6.22	5.68	$F_{7,35}$ = 164.5,		
D	**C**	**E**	**B**	**D**	**A**	**D**	**F**	p < 0.001		
Main effect: nutrient starvation								SED	LDS	df
Control	No P applied	No S applied	No Mg applied	No K applied	No N applied			0.058	0.12	5
6.37	6.31	6.43	6.64	6.49	6.30			$F_{5,93}$ = 9.43,		
BC	**C**	**B**	**A**	**B**	**C**			p < 0.001		

However, TaPht1;2 was more highly expressed than TaPht1;1, similarly to the patterns in the P_i starved in vitro-grown roots (Figure 9), indicating either a shift in expression over the growing period related to physiological development, environmental conditions or production procedures such as

fertilizer inputs. TaPht1;10, TaPht1;11 and TaPht1;6 transcripts were less abundant in field-grown (Figure 10) compared to in-vitro grown roots (Figure 9). TaPht1;5 and TaPht1;7 had minor transcript abundance (Figure 10) and may have a potential roles in other tissues.

2.3.6. TaPht1 expression in P_i starved field-grown wheat at different physiological stages

In 2012, plant material from Broadbalk was sampled from plot 20, where P_i availability was lower than in plot 19 (used in 2011) (Tables 1 and 2), and likely to trigger a stronger molecular response to soil-P_i depletion.

From tillering until maturity, total P concentrations in shoot and ear tissues of plants grown on non-P_i fertilized plots were lower than in plants grown on the P_i-fertilized control plots (Figure 11, Table 14). Yields were reduced in non-P_i fertilized plots (Table 2). Shoot P_i concentrations generally decreased throughout the season but increased in ear tissues with the developing grains as major P sinks (Figure 11).

Shoot K concentrations were increased in P_i starved plants at booting; Ca concentrations decreased during the season and were only higher in P_i starved plants at booting; Mg concentrations decreased at ripening and maturity but were not altered by P_i availability; S concentrations were lower in P_i starved plants at tillering, anthesis and ripening (Figure 11). Zn and Mo concentrations were lower in P_i starved ear tissues only at maturity, whereas Cu, Fe and Mn concentrations were higher in P_i starved shoots at tillering and declined afterwards (Figure 11). Co, As, Pb and Al accumulated at early stages in P_i starved plants, whereas Cr and Ni concentrations decreased in P_i starved wheat at tillering (Table 15). However, the concentration of all trace elements exhibited a general decline over the growing season; only Cr increased slightly after anthesis (Table 15).

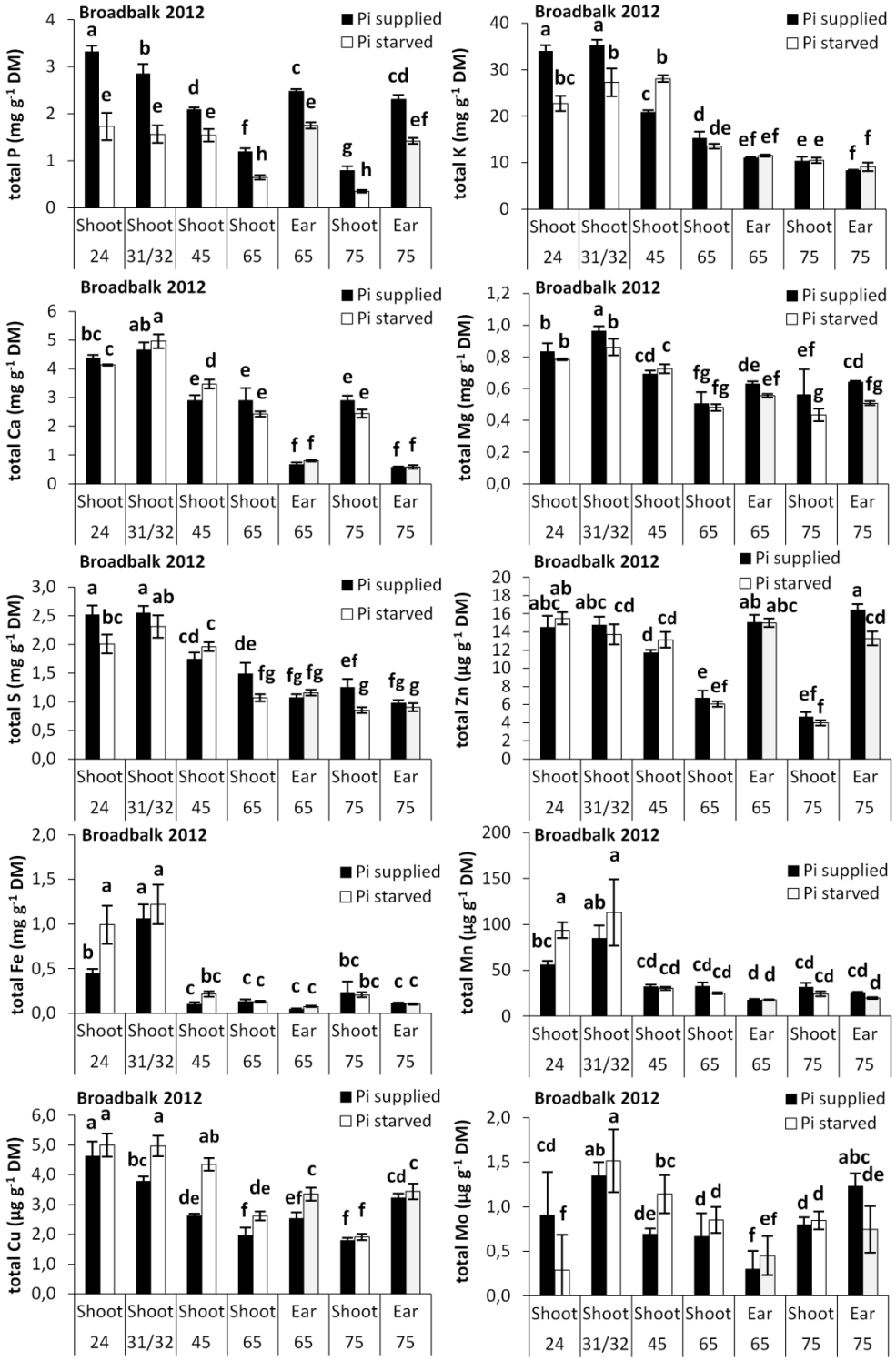

Figure 11: Nutritional status of shoots from field-grown wheat at Broadbalk in 2012.

Macro- and micronutrients in shoot material sampled at each harvest time point (n=3) from P_i fertilized (+P_i: ■) and not P_i fertilized (-P_i: □; plot 20 used) plots at Broadbalk, Rothamsted Research, UK (plot treatments; Tab.1). Material was harvested at tillering (25), stem elongation (32), early booting (41), full booting (45), late booting (48), anthesis (65) and milk ripening (75). Statistical properties are presented in Table 14. Bars sharing the same letter are not statistically different ($P>0.05$) through different P_i availability at different time points.

Table 14: Statistical properties (SED, LSD and F-statistic) of nutritional status of shoots from field-grown wheat at Broadbalk in 2012 (Figure 11).

nutrient	P	K	Ca	Mg	S	Mn	Fe	Zn	Cu	Mo
$F_{10,50}$ =	49.05	57.38	28.18	27.49	23.7	7.59	20.61	34.11	25.51	10.46
p-	<0.001	<0.001	<0.001	<0.001	<0.001	<0.001	<0.001	<0.001	<0.001	<0.001
SED	0.16	1.63	0.24	0.046	0.16	15.8	0.26	1.06	0.34	0.17
LDS	0.32	3.27	0.48	0.092	0.32	31.8	0.13	2.13	0.67	0.35

Table 15: Trace element concentrations in shoots of field-grown wheat at Broadbalk in 2012.

Data was obtained via in oven-dried shoot material sampled at each harvest time point (n=3) from P fertilized (+P_i; plot 9) and non-P fertilized (-P_i; plot 20) plots at Broadbalk, Rothamsted Research, UK (plot treatments; Tab.1). Bars sharing the same value are not statistically different between time points or treatments (P>0.05).

Physiological stage		**Tillering**	**Elongation**	**Booting**	**Anthesis**		**Ripening**		**Statistical properties**	
Zadock scale		**24**	**31/32**	**45**	**65**	**65**	**75**	**75**	**$F_{10,50}$ = ,**	**SED**
Tissue		**Shoot**	**Shoot**	**Shoot**	**Shoot**	**Ear**	**Shoot**	**Ear**	**p-value**	**LSD**
Al (mg g^{-1} DM)	+ P	0.53 **b**	1.31 **a**	0.08 **c**	0.13 **c**	0.02**c**	0.28 **bc**	0.028 **c**	18.9,	0.17,
	- P	1.32 **a**	1.39 **a**	0.19 **c**	0.11 **c**	0.03 **c**	0.22 **bc**	0.039 **c**	<0.001	0.34
Cr (µg g^{-1} DM)	+ P	9.4 **bc**	15.3 **a**	7.0 **cde**	6.5 **de**	4.5 **ef**	6.2 **de**	10.4 **b**	18.02,	1.36,
	- P	2.4 **f**	14.7 **a**	10.5 **b**	7.2 **cd**	5.4 **de**	6.1 **de**	8.1 **bcd**	<0.001	2.72
Na (µg g^{-1} DM)	+ P	93.2 **b**	77.9 **bc**	27.3 **f**	36.2 **ef**	43.1 **ef**	30.9 **ef**	37.7 **ef**	56.5,	9.04,
	- P	179.3 **a**	179.8 **a**	48.2 **de**	63.5 **cd**	66.7 **cd**	48.7 **e**	47.7 **e**	<0.001	18.2
Ni (µg g^{-1} DM)	+ P	5.5 **bc**	8.9 **a**	4.0 **c**	4.1 **cd**	3.01 **d**	4.1 **cd**	8.9 **a**	15.8,	0.83,
	- P	3.2 **d**	8.9 **a**	6.14 **b**	4.9 **bc**	4.6 **bcd**	4 **cd**	5.6 **bc**	<0.001	1.66
Pb (µg g^{-1} DM)	+ P	0.49**c**	1.18 **b**	0 **f**	0.01 **f**	0.19 **cf**	0.31 **cf**	0.16 **cf**	16.8,	0.19,
	- P	1.60 **a**	1.40 **ab**	0.14 **cf**	0.16 **cf**	0.32 **cf**	0.35 **cf**	0.18 **cf**	<0.001	0.38
As (µg g^{-1} DM)	+ P	0.29 **b**	0.63 **a**	0.1 **bc**	neg.	0.01 **c**	0.14 **bc**	neg.	12.45,	0.11,
	- P	0.71 **a**	0.76 **a**	0.15 **bc**	0.07 **c**	0.01 **c**	0.20 **bc**	0.1 **bc**	<0.001	0.21
Cd (ng g^{-1} DM)	+ P	77.7 **a**	60.6 **b**	44.6 **c**	40.3 **c**	neg.	28.5 **c**	11	15.6,	7.79,
	- P	80.4 **a**	48 **b**	21.9 **de**	23.3 **de**	9.6	10.5 **de**	neg.	<0.001	15.7
Co (ng g^{-1} DM)	+ P	335 **bc**	938 **a**	98 **c**	129 **c**	36 **c**	184 **c**	111 **c**	11,	149,
	- P	623 **b**	1137 **a**	199 **c**	151 **c**	50 **c**	167 **c**	75 **c**	<0.001	299

TaPht1 transporters were not exclusively root-expressed but also found in various wheat ear tissues (Figures 12 to 14). A general pattern for TaPht1 transporters was a high level of expression at very early growth stages and at maturity, but a decease in expression during booting and anthesis (Figures 12 to 14).

TaPht1;1, TaPht1;6 and TaPht1;7 expression was determined by all three factors, P_i availability, tissue and developmental stage at any particular time point during the season (Figure 12, Table 16). TaPht1;1 was expressed in roots, ears, glume, grain and rachis and P_i starvation enhanced TaPht1;1 expression at tillering (Figure 12). TaPht1;1 transcript abundance increased in the roots at the beginning of stem elogation, decreased at booting and anthesis and increased again during ripening in P_i supplied and P_i starved plants (Figure 12). TaPht1;1 expression was lower in the glume, even not significantly, when P_i availability was decreased (Figure 12) indicating that P_i translocation into the grain may have also been affected via differentially TaPth1 expression in ear tissues. TaPht1;6 root expression was not altered by P_i starvation at booting in 2012 (Figure 12). However, root TaPht1;6 expression increased through P_i limitation at tillering, stem elongation and anthesis; but not at maturity (Figure 12). TaPht1;6 was the only phosphate transporter in that group with high transcript abundance in the ear tissues, particularly if P_i was limiting and in the rachis (Figure 12). TaPht1;7 expression exhibited a peculiar pattern being induced in P_i starved ear tissues (Figure 12).

TaPht1;2, TaPht1;5 and TaPht1;8 expression in the different tissues was determined by growth stage without showing a response to P_i availability (Figure 13, Table 16). TaPht1;2 root expression was highest at tillering and elongation, decreased significantly at booting and increased again at maturity (Figure 13). TaPht1;2 expression in ear tissues from anthesis to grain ripening was as low as in roots during elongation (Figure 13). TaPht1;8 expression follows the TaPht1;2 expression pattern but was more abundant in the grain at ripening (Figure 13). Root TaPht1;5 expression was highest at tillering and milk ripening, significantly lower at elongation and at an intermediate range in ear tissues (Figure 13).

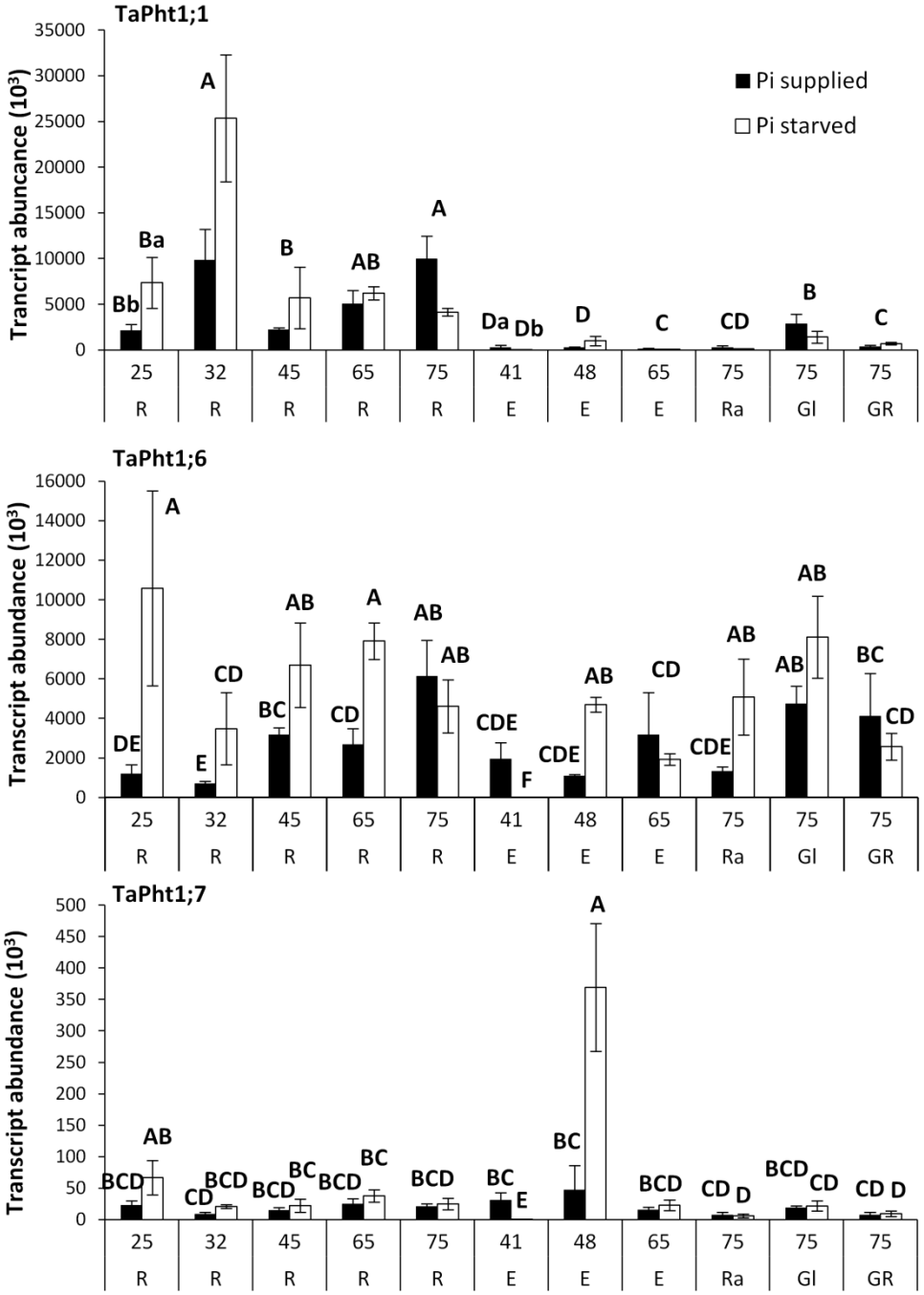

Figure 12: Transcript abundance of TaPht1;1, TaPht1;6 and TaPht1;7 in root and ear tissues of field-grown wheat at Broadbalk in 2012.

The data was log_{10}-transformed for statistical analysis. Therefore, the Figure above displays the back transformed data shown as the predicted means of normalized transcript abundance (10^3) in 0.1 µg of total RNA in root (R) and ear tissues (E=entire ear, Ra=rachis, Gl=glume, GR=grain) at tillering (25), stem elongation (32), early booting (41), full booting (45), late booting (48), anthesis (65) and milk ripening (75). P_i fertilized (+P_i: ■) and non-P_i fertilized (-P_i: □; plot 20 used) plant material was used (plot treatments; Tab.1). Predicted means (log_{10}-scale) were compared using the SED (on the relevant df) and LSD values at the 5 % level of significance. Statistical properties are presented in Table 16. Bars sharing the same letter are not statistically different between tissues across growth stages or soil-P_i availability (P>0.05).

Table 16: Statistical properties for transcript abundance of TaPht1 transporters in root and ear tissues of field-grown wheat at Broadbalk in 2012 (Figures 12 to 15).

Predicted means on log_{10}-scale for statistical comparisons, max SED and max LSD values with the appropriate df for the particular comparison. Growth stage according to Zadoks et al. (1974): tillering (25), stem elongation (32), early booting (41), full booting (45), late booting (48), anthesis (65) and milk ripening (75).

Gene	Tissue	Stage	P_i supply	Log_{10}-value	P_i supply	Log_{10}-value	Max SED	Max LSD	d.f
	Root	25	high	6.26	low	6.81	0.352	0.08	54
	Root	32	high	6.92	low	7.35			
	Root	45	high	6.35	low	6.59			
	Ear	41	high	5.18	low	4.12			
	Ear	48	high	4.91	low	4.57			
TaPht1;1	Root	65	high	6.65	low	6.78			
	Ear		high	5.38	low	5.96			
	Root		high	6.93	low	6.61			
	Rachis	75	high	5.20	low	5.13			
	Glume		high	6.39	low	6.03			
	Grain		high	5.52	low	5.82			
	Root	25	mean	6.58			0.209	0.42	51
	Root	32	mean	6.98					
	Root	45	mean	5.89					
	Ear	41	mean	3.64					
	Ear	48	mean	5.52					
TaPht1;2	Root	65	mean	6.72					
	Ear		mean	4.94					
	Root		mean	6.74					
	Rachis	75	mean	5.82					
	Glume		mean	6.1					
	Grain		mean	5.35					
	Root	25	mean	5.67			0.43	0.86	48
	Root	32	mean	5.36					
	Root	45	mean	5.02					
	Ear	41	mean	3.88					
	Ear	48	mean	5.15					
TaPht1;5	Root	65	mean	5.59					
	Ear		mean	3.96					
	Root		mean	5.08					
	Rachis	75	mean	4.74					
	Glume		mean	4.99					
	Grain		mean	4.93					
	Root	25	high	6.01	low	6.93	0.26	0.52	60
	Root	32	high	5.83	low	6.4			
	Root	45	high	6.49	low	6.73			
	Ear	41	high	6.22	low	3.78			
	Ear	48	high	6.03	low	6.67			
TaPht1;6	Root	65	high	6.39	low	6.89			
	Ear		high	6.25	low	6.27			
	Root		high	6.72	low	6.58			
	Rachis	75	high	6.11	low	6.64			
	Glume		high	6.65	low	6.79			
	Grain		high	6.44	low	6.36			

Table 16 continued.

Gene	Tissue	Stage	P_i supply	Log_{10}-value	P_i supply	Log_{10}-value	Max SED	Max LSD	d.f
TaPht1;7	Root	25	high	4.13	low	4.76	0.49	0.98	55
	Root	32	high	3.82	low	4.30			
	Root	45	high	4.07	low	4.10			
	Ear	41	high	4.38	low	2.55			
	Ear	48	high	3.33	low	5.54			
	Root	65	high	4.19	low	4.33			
	Ear		high	4.06	low	4.18			
	Root	75	high	4.29	low	4.27			
	Rachis		high	3.78	low	3.56			
	Glume		high	4.26	low	3.89			
	Grain		high	3.69	low	3.56			
TaPht1;8	Root	25	mean	7.28			0.28	0.57	56
	Root	32	mean	7.35					
	Root	45	mean	6.84					
	Ear	41	mean	5.42					
	Ear	48	mean	6.22					
	Root	65	mean	7.26					
	Ear		mean	5.98					
	Root	75	mean	6.94					
	Rachis		mean	6.54					
	Glume		mean	6.62					
	Grain		mean	6.58					
TaPht1;10 A: P_i supply	Root	mean	high	5.54	low	6.16	0.303	0.61	38
	Ear	Mean	high	4.03	low	3.83			
	Rachis	75	high	4.49	low	4.68			
	Glume		high	4.83	low	4.85			
	Grain		high	5.02	low	4.66			
TaPht1;10 B: tissues	Root	25	mean	5.76		0.24	0.49	38	
	Root	32	mean	5.76					
	Root	45	mean	5.53					
	Ear	41	mean	3.75					
	Ear	48	mean	4.18					
	Root	65	mean	6.14					
	Ear		mean	3.86					
	Root	75	mean	6.06					
	Rachis		mean	4.58					
	Glume		mean	4.84					
	Grain		mean	4.84					
TaPht1;11 A: P_i supply	Root	mean	high	5.37	low	6.7	0.55	1.12	39
	Ear	mean	high	3.04	low	3.36			
	Rachis	75	high	*	low	3.68			
	Glume		high	4.117	low	3.51			
	Grain		high	5.772	low	*			

Table 16 continued.

Gene	Tissue	Stage	P_i supply	Log_{10}-value	P_i supply	Log_{10}-value	Max SED	Max LSD	d.f
TaPht1;11 B: tissues	Root	25	mean	6.08			0.52	1.05	39
	Root	32	mean	5.88					
	Root	45	mean	5.24					
	Ear	41	mean	2.39					
	Ear	48	mean	3.86					
	Root	65	mean	6.54					
	Ear		mean	3.34					
	Root	75	mean	6.42					
	Rachis		mean	3.68					
	Glume		mean	3.81					
	Grain		mean	5.77					
TaPht1;1	**Root**	**32**	high	6.92	low	7.35	0.20	0.43	13
TaPht1;2			high	6.82	low	7.13			
TaPht1;5			high	5.07	low	5.61			
TaPht1;6			high	5.83	low	6.4			
TaPht1;6			high	3.82	low	4.30			
TaPht1;8			high	7.17	low	7.52			
TaPht1;10			high	5.31	low	6.10			
TaPht1;11			high	5.35	low	6.41			

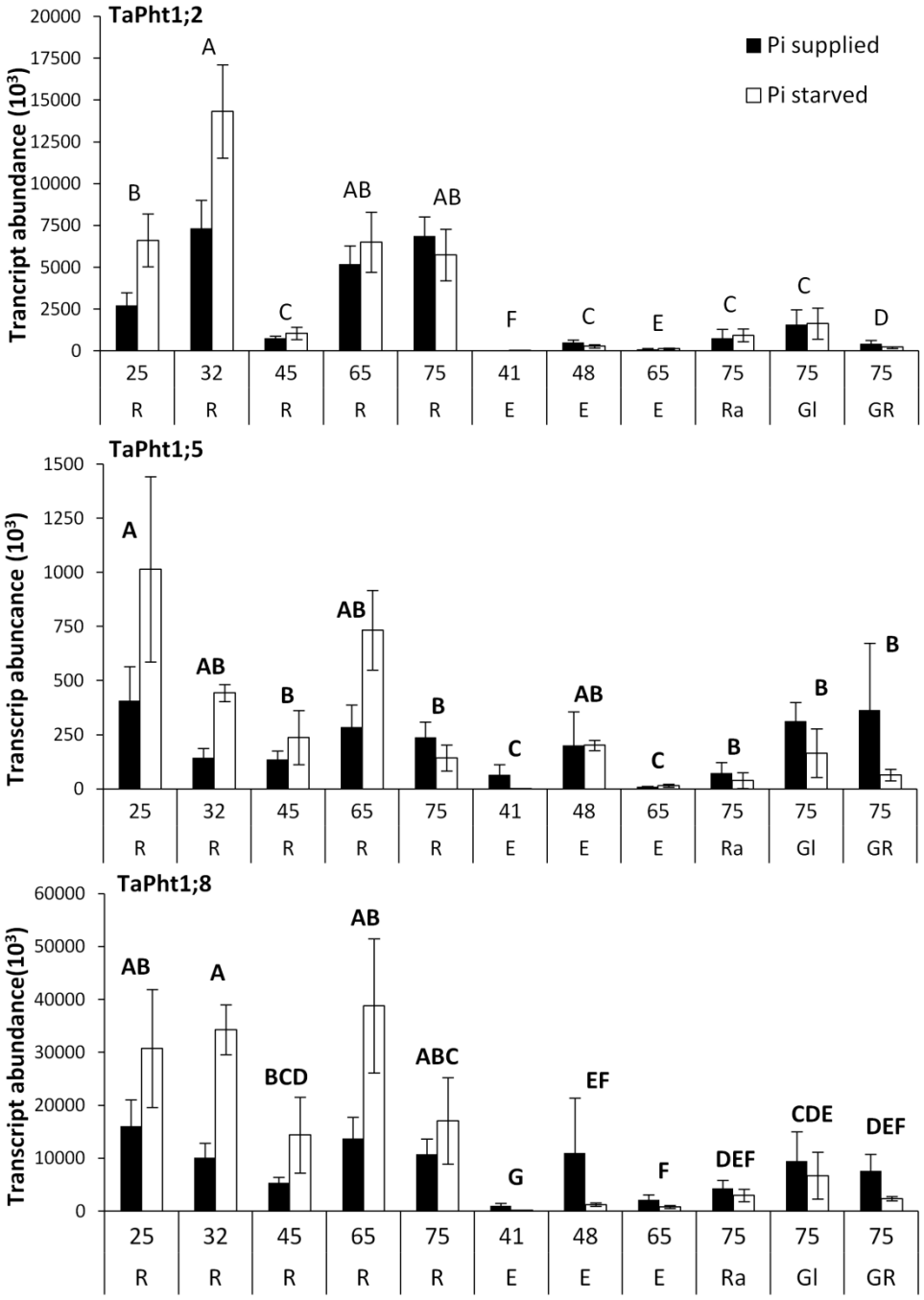

Figure 13: Transcript abundance of TaPht1;2, TaPht1;5 and TaPht1;8 in root and ear tissues of field-grown wheat at Broadbalk in 2012.

The data had to be log_{10}-transformed for statistical analysis. The Figure displays the back transformed data shown as the predicted means of normalized transcript abundance (10^3) in 0.1 µg of total RNA in root (R) and ear tissues (E=entire ear, Ra=rachis, Gl=glume, GR=grain) at tillering (25), stem elongation (32), early booting (41), full booting (45), late booting (48), anthesis (65) and milk ripening (75). There was a stage nested in tissue effect but no P_i by tissue interaction. Predicted means (log_{10}-scale) were compared using the SED (on the relevant df) and LSD values at the 5 % level of significance. Statistical properties are presented in Table 16. Bars sharing the same letter are not statistically different between tissues across growth stages (P>0.05).

TaPht1;10 and TaPht1;11 expression in root and ear tissues was determined by the growth stage and influenced by P_i availability in the roots at all growth stages and in the grain at maturity (Figure 14, Table 16). TaPht1;10 and TaPht1;11 followed a similar expression pattern to other root-expressed TaPht1 transporters (Figures 13 and 14) being highest at tillering, decreasing after elongation and increasing again at milk and grain ripening stages (Figure 14). However, TaPht1;10 and TaPht1;11 expression was highest at maturity (Figure 14). Similarly to TaPht1;6 (Figure 12), TaPht1;10 and TaPht1;11 expression decreased in the grain tissues during limited P_i availability (Figure 14). The expression of TaPht1;10 and TaPht1;11 was much lower in shoot tissues compared to the roots (Figure 14). In contrast to TaPht1;1 and TaPht1;6, for which the time point was relevant for determining an effect of P_i availability on the transcript abundance (Figure 12), reduced P_i availability increased TaPht1;10 and TaPht1;11 root expression during the entire development (Figure 14).

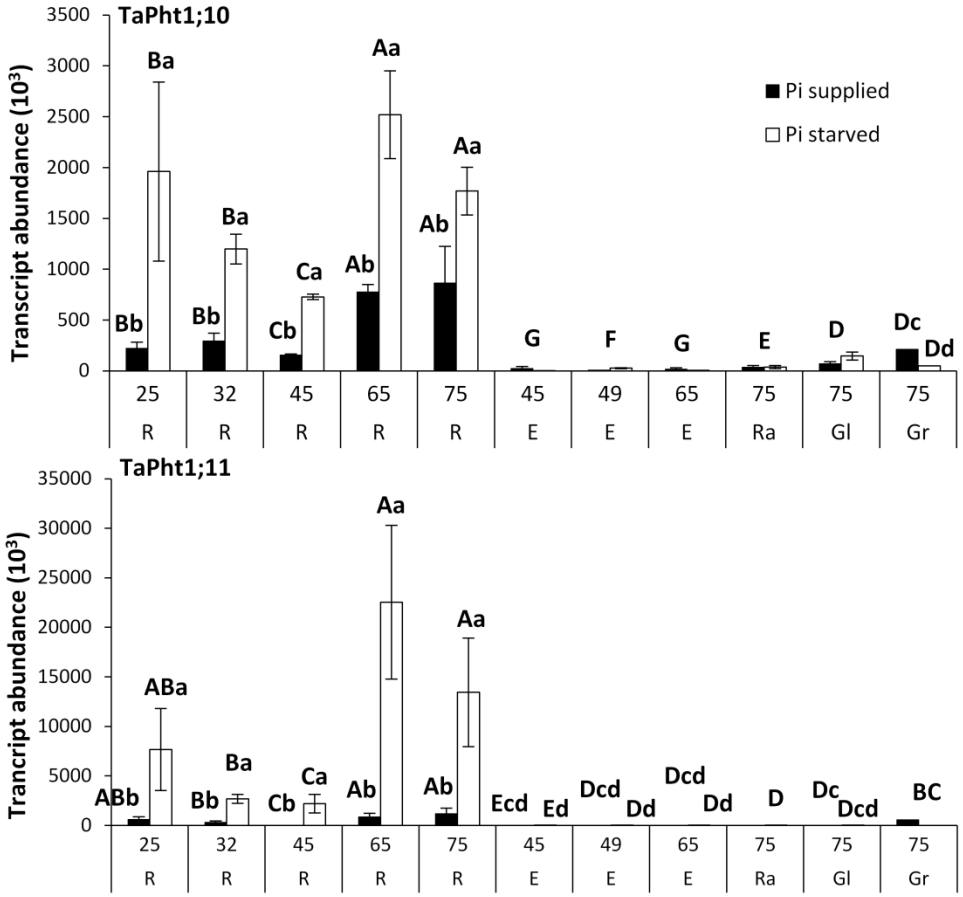

Figure 14: Transcript abundance of TaPht1;10 and TaPht1;11 in root and ear tissues of field-grown wheat at Broadbalk in 2012.

The data had to be log_{10}-transformed for statistical analysis. The Figure displays the back transformed data shown as the predicted means of normalized transcript abundance (10^3) in 0.1 µg of total RNA in root (R) and ear tissues (E=entire ear, Ra=rachis, Gl=glume, GR=grain) at tillering (25), stem elongation (32), early booting (41), full booting (45), late booting (48), anthesis (65) and milk ripening (75). Predicted means (log_{10}-scale) were compared using the SED (on the relevant f) and LSD values at the 5 % level of significance. Statistical properties are presented in Table 16. Bars sharing the same capital letter are not statistically different between tissues across growth stages (P>0.05) and bars sharing the same small letter are not statistically different between P_i supplied or P_i starved tissues.

In order to validate TaPht1 expression data in wheat roots from Broadbalk in 2011 which was sampled at this growth stage (Figure 10), TaPht1 transporter expression in wheat roots from Broadbalk in 2012 was compared for all TaPht1 transporters at elongation (Figure 15, Table 16). Similar expression profiles as in 2011 were revealed (Figure 15): TaPth1;1, TaPht1;2 and particularly TaPht1;8 were the most abundant in the roots in 2012 (Figure 15). However, limited P_i availability increased significantly the expression of TaPht1;6, TaPht1;10 and TaPht1;11 which were all expressed at an

intermediate level (Figure 15). In contrast to 2011 (Figure 10), TaPht1;6 expression was low in 2012 (Figure 15). Furthermore, TaPht1;7, and not TaPht1;11 as in 2011 was the lowest expressed TaPht1 transporter in 2012 (Figure 15).

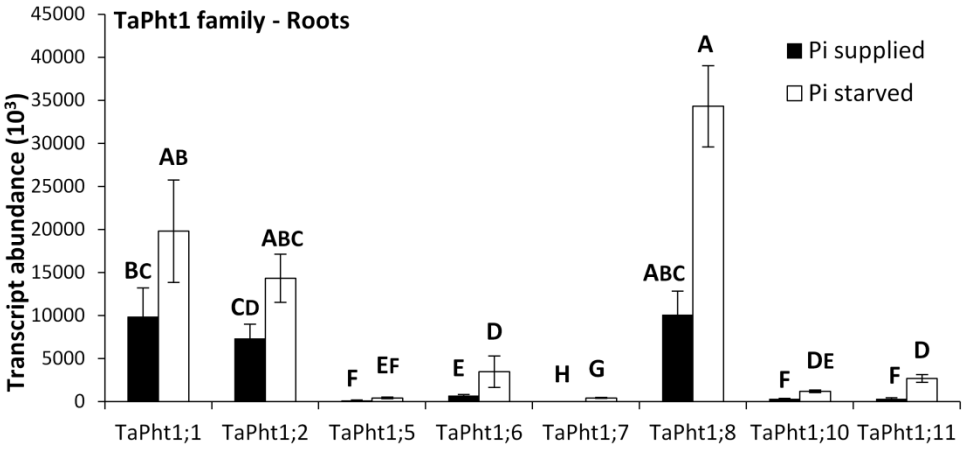

Figure 15: Comparison of transcript abundance of eight TaPht1 transporters in root tissues of field-grown wheat at Broadbalk in 2012 during elongation.

The data had to be log_{10}-transformed for statistical analysis assessing the main effects and interaction between P_i availability and genes. The back transformed data is shown as the predicted means of normalized transcript abundance (10^3) in 0.1 µg of total RNA in the Figure. Means were compared using statistical properties at the 5 % level of significance. Statistical properties are presented in Table 16. Bars sharing the same letter are not statistically different between TaPht1 transporter expression at different soil-P_i availability ($P>0.05$).

2.4. Discussion

2.4.1. TaPht1 transporter sequence identification

Mining of public databases, including the SeqRepository platform (IWGSC) and Chinese spring wheat Cerealsdb BLAST, revealed a total of 14 wheat TaPht1 genes (Table 7). Alignment of TaPht1 sequences with three TaPht1 genes identified by Sisaphaithong et al. (2012) revealed that they are the three homeologues genes of TaPht1;11 from all wheat genomes (ABD), rather than being three different genes (Table 6). However, 14 wheat TaPht1 genes in the wheat genome is the highest gene number for the Pht1 family compared to other cereal species, including barley with 8 HvPht1 genes (Rae et al. 2003), rice with 11 OsPht1 genes (Paszowski et al. 2002) or Brachypodium with 13 BdPht1 genes (Hong et al. 2012) (Figure 7). There are indications of wheat specific gene duplication events including TaPht1;1 and TaPh1;2, TaPht1;3 and TaPh1;4 (Figure 7). There are also specific wheat Pht1 genes, including TaPh1;8, TaPh1;9, TaPh1;12 and TaPh1;14, which had one Brachypodium homologue, respectively, or only one homologue in barley, such as TaPht1;8, and one homologue in rice, such as TaPht1;9 (Figure 7).

In July 2014, the IWGSC published a complete wheat survey sequence[11]. Considering muliple gene duplication events in the wheat genome for members of the Pht1 family, the next step would be to mine the now fully available wheat survey sequence for validating the completeness of the Pht1 transporter family in wheat.

Incomplete IWGSC contig sequences of some TaPht1 genes, such as TaPht1;1 and TaPht1;2, were completed with contig sequences from the Chinese spring database. This may have resulted in an ambiguously nucleotide or amino acid sequence similarity assignment (Table 8, Figure 6). However, cloning and sequence analysis for TaPht1;1 and TaPht1;2 revealed two distinct genes by identifying distict 3′ non-conding region sequences (Figure 8), refusing the previous apprehension. Furthermore, TaPht1;1 and TaPht1;2 exhibited similar,

[11] http://www.wheatgenome.org/Projects/IWGSC-Bread-Wheat-Projects/Sequencing/Whole-Chromosome-Survey-Sequencing

but not entirely identical expression pattern in in vitro studies (Figure 9) or in field grown root studies (Figure 10, 12 and 13).

The nucleotide sequences of two particular TaPht1 genes, including TaPht1;3 and TaPth1;4, differed only in a few bases leading to a > 99 % sequence similarity between the protein sequences of both Pht1 transporter genes (Table 8). Rae et al. (2003) reported similar difficulties in distinguishing HvPht1;3 and HvPht1;4 in barley. Accurate expression studies using real-time qPCR technique is therefore inaccurat and other techniques such as the KBioscience competetive allele-specific PCR genotyping system (KASP) (Allen et al. 2011) would have be required.

2.4.2. Functional assessment of the phylogenetic relationship of TaPht1 genes to other Pht1 members in cereals

The phylogenetic analysis of the identified TaPht1 genes with Pht1 genes in other species revealed five main clusters (Figure 7). The genes from cluster one, including TaPht1;1 and TaPht1;2, and cluster two, including TaPht1;3 and TaPht1;4, are phylogenetically related to homologues in other cereal species which were reported being high-affinity transporters predominantly expressed in roots during P_i starvation (Daram et al. 1998, Rae et al. 2002, Paszkowski et al. 2002, Schünmann et al. 2004, Miao et al. 2009, Huang et al. 2011). Expression of TaPht1;1 even correlated with P_i acquisition efficiency in wheat (Aziz et al. 2013). For the third identified wheat Pht1 gene of cluster one, TaPht1;5, homologues such as HvPht1;5 in barley (Rae et al. 2003, Huang et al. 2011), OsPht1;12 in rice (Paszkowski et al. 2002) or BdPht1;5 in Brachypodium (Hong et al. 2012) (Figure 7) showed only weak or even no expression in root tissues.

The cluster three genes seem to belong to a group of genes which is expressed in aerial tissues functioning as low-affinity Pht1 transporters. The barley TaPht1;6 homologue, HvPht1;6 (Figure 7), was characterized as low-affinity transporter in the epidermis of lateral roots (Ai et al. 200), further localized to the phloem tissue where it may be involved in P_i remobilization from the

leaves (Rae et al. 2003) and correlated with P_i use efficiency in barley (Huang et al. 2011). The TaPht1;7 homologues in rice, OsPht1;7, or Brachyodium, BdPht1;6, were not detectable in roots (Paszkowsi et al. 2002, Hong et al. 2012). However, TaPht1;7 homologues in barley, HvPht1;7, was reported preferentially expressed in green and mature anthers (Druka et al. 2006). The TaPht1;13 homologues, BdPht1;13, was weakly expressed in shoot tissues (Hong et al. 2012), OsPht1;4 was strongly expressed in the flag leave, particulary after the heading stage (Liu et al. 2011) and OsPht1;5 has not investigated in enough detail for a functional assingment (Paszkowski etal. 2002).

Even with low nucleotide sequence similarity (Table 8), TaPht1;8 and TaPht1;11 genes were in phylogenetic proximity to each other in cluster four (Figure 7). The TaPht1;8 and TaPht1;11 homologues genes in Brachypodium (BdPht1;7, BdPht1;3), rice (OsPht1;11), and barley (HvPht1;8, HvPht1;11) (Figure 7) have been associated with AM fungi and were induced during the establishment of an AM symbiosis (Paszkowski et al. 2002, Glassop et al. 2005, Hong et al. 2013). But also TaPht1;8 and TaPht1;11 expression was induced and related to AM infection (Glassop et al. 2005, Sisaphaithong et al. 2012, Teng et al. 2013). TaPht1;10 was in phylogenetic proximity to TaPht1;8 and TaPht1;11. However, the TaPht1;10 homologue in Brachypodium, BdPht1;2 was not expressed in root tissues, and no particular expression pattern or functional localization has been reported for the rice homologues, OsPht1;9 and OsPht1;10, either (Figure 7).

The Pht1 genes which were identified as mainly wheat and Brachypodium genes included TaPht1;9, TaPht1;12 and TaPht1;14 (Figure 7). OsPht1;13, the rice homologue of TaPht1;9, was reported to be induced in AM symbiosis in rice roots (Güimil et al. 2005). Also, BdPht1;12 and BdPht1;13, the homologues to TaPht1;12 and TaPht1;14, were induced specifically during AM infection (Hong et al. 2012). However, even if these TaPht1 transporters were in phylogenetic proximity to the AM associated Pht1 genes, TaPh1;9, TaPh1;12 and TaPh1;14 exhibited either weakly or not expression at all in any of the tissues or growing conditions tested here.

With the exception of genes derived from gene duplication events, such as OsPht1;1 and OsPht1;2, TaPht1;1 and TaPht1;2, OsPht1;4 and OsPht1;5, OsPht1;9 and OsPht1;10 (Figure 7), there is no indication that TaPht1 transporters located on similar or specifc chromosomes are phylogenetically closer related to each other. However, if specific expression patterns are in congruence with the functional assignment based on the phylogenetic grouping will be discussed below.

2.4.3. Responsiveness of TaPht1 expression in roots during in vitro P_i starvation

Most root-expressed TaPht1 transporters in the liquid culture system responded quickly, within a few days, to limited P_i availability (Figures 8 and 9). Pht1 transporters have been reported to be largely dependent on the amount of externally available P_i: Liu et al. (1998) showed that Pht1 expression in tomato increased within 24 h of P_i starvation and decreased after 24 h of P_i resupply suggesting a fine coordination in relation to P_i availability. Nagy et al. (2006) observed a quick induction of some ZmPht1 maize transporters, whereas others exhibited a delayed but equally strong induction over a P_i withdrawal period of 3 to 15 days. Variable responsiveness of TaPht1 transporters was therefore an expected feature.

2.4.4. Responsiveness of TaPht1 expression in nutrient starved field-grown roots

TaPht1 expression was determined for the first time in field-grown wheat roots and ear tissues. However, the regulation of TaPht1 expression in the field appeared to be more complex (Figures 10 to 15) than in a liquid-culture system (Figure 9). Nutrient deficiencies cause unspecific abiotic stress, for instance oxidative stress (Juszczuk et al. 2001). Abiotic stress may interfere with P metabolism and mechanisms initiating the PSR, or simply affecting root growth and epidermal cell differentiation which then alters Pht1 expression. This effect may depend on the specific nutrient but also on the plant species

and its nutritional requirements, the physiological stage and the experimental conditions in which the starvation occurs including if P_i starvation is simultaneously applied or not. This may explain the inconsistent results of other studies which investigated Pht1 expression during nutrient deficiencies additional to P_i (Smith et al. 1999, Liu et al. 1998, Wang et al. 2002, Miao et al. 2009, Qin et al. 2012), and the complex TaPht1 regulation towards nutrient availability in the field.

2.4.5. Influence of N, P_i, K, Mg and S soil-availability on TaPht1 expression

Soil analysis data (Table 2) and the nutritional status of the plants were considered (Table 12) to exclude any treatment ambiguity and revealed that soil-P_i availability (Olsen P) in all Broadbalk field-site plots was above the optimum of 12 to 20 Olsen P for good agricultural practice (Defra 2010). Olsen P concentrations were highest in S, Mg, K and N deplete plots which constantly received P_i fertilizer, medium in the control plot where no P_i fertilizer had been applied since 2001 and lowest in the P_i depleted plot were no P_i fertilizers had been applied since 1843 (Tables 1, 2 and 12). However, total shoot P concentration mirrored the soil Olsen P values (Table 2 and 12). A critical Olsen P value of 9 mg kg^{-1} air-dried soil is considered to be sufficient to reach 95 % of maximum grain yield for winter wheat at Rothamsted (Bollons and Barraclough 1999). In China, the soil-P_i availability of 20 Olsen P was necessary for the maximum yield and coincided with the down-regulation of PSR marker genes (Teng et al. 2013). This suggests, that the wheat plants at the Broadbalk-field site were not likely to have suffered severely from substantial P_i stavation to trigger a strong PRS, including stimulated P_i acquisition via increasing TaPht1 transporter expression at booting stage (Figure 10). It also indicated that high TaPht1;1 expression during K starvation and high TaPht1;5 expression during Mg starvation were presumably a consequence of extremely high P_i availability (Olsen P values) in these plots (Table 2) which resulted in high shoot P concentrations in K and Mg starved wheat (Table 12).

A feed-back mechanism due to the plants internal nutritional P status, in addition to the external P_i availability, seemed unlikely. Schünmann et al. (2004) assumed that the high internal P_i content prior to P_i starvation caused the delayed expressional response of HvPht1;1 and HvPht1;2, which are TaPht1;1 and TaPht1;2 homolgs (Figure 7). However, N and K starvation had no supressing effects on TaPht1 expression patterns (Figure 10) when soil-P_i availablity (Table 2) and shoot P concentrations (Table 12) were higher than in P_i starved plants. In roots of P_i and N starved wheat plants, the expression of TaPht1;1 was significantly decreased even if this was not signifiantly different from the control (Figure 10). In contrast, Qin et al. (2012) observed an increase of expression for the majority of GmPht1 transporters in soybean seedlings during N starvation. However, there is evidence of an influence on the signalling pathways of P_i homeostasis by the nitrogen nutritional status: nitrate application to the growth media stimulated TaPht1 expression in wheat roots (Miao et al. 2009). However, N starvation decreases nitrate assimilation and nitrate reduction (Schlüter et al. 2013), but N acquisition and use are also affected in P_i starved plants (Li et al. 2010). Restricted P_i transporter expression in N starved maize and wheat plants counteracted their enhanced expression during P_i limiting conditions in maize (Schlüter et al. 2013) and wheat (Miao et al. 2009), but not when plants were only N starved (Miao et al. 2009).

In K starved wheat roots, TaPht1;1 and TaPht1;5 expression was significantly higher than in P_i or N starved roots (Figure 10). This was also observed by Smith et al. (1998) for HvPht1 transporters in K starved barley. In tomato roots, K and Fe starvation enhanced LePht1;1 expression even more strongly than P_i starvation, whereas LePht1;2 was only induced by P_i starvation (Wang et al. 2002). However, Liu et al. (1998) could not detect any influence of N, K or Fe deficiencies on LePht1;1 or LePht1;2 expression in tomato. In contrast, Qin et al. (2012) showed that Fe and K starvation altered GmPht1 expression in soybean seedlings in a differentially and Pht-dependent manner. Generally, K starvation increases the amount of soluble sugars and alters enzymes involved in sugar metabolism, TCA cycle and N assimilation, as well as a strong decrease of pyruvate and organic acids in the roots (Amtmann and Armengaud

2009). P_i transporters seem to belong to a group of sugar-modulated genes (Jain et al. 2007, Karthikeyan et al. 2007, Hammond and White 2008) interacting with and stimulating P_i starvation signals, for instance TaPht1;2 (Miao et al. 2009). This coincides with increasing levels of di- and trisaccharides in P_i starved plants (Huang et al. 2008). Furthermore, sucrose and IPS genes are assumed to be involved in the adaptation to low P_i availability by being global regulators of the PSR (Li et al. 2008b). However, sucrose synthesis and transport was reduced in N starved maize leaves (Schlüter et al. 2013) and N starvation strongly repressed TaIPS1 expression in roots and of TaIPS2 in shoots of P_i starved wheat (Li et al. 2008b). Therefore, K and N starvation probably influenced the sugar metabolism and PSR genes, resulting in altered P_i acquisition patterns derived from the up-regulation of specific Pht1 transporters such as TaPht1;1 and TaPht1;5 (Figure 10).

S limitation had no influence on TaPht1 expression in wheat (Figure 10). In previous studies, S starvation enhanced the steady-state expression of root expressed TaPht1 transporters in wheat (TaPht1;2) and barley (HvPht1;3) (Smith et al. 1998, Miao et al. 2009). HvPh1;6 transports not only P_i but also SO_4^{2-} (Preuss et al. 2010). However, it is likely that the plant material was not sufficiently S starved (Table 12) in order to trigger TaPht1 expression changes.

2.4.6. TaPht1 expression patterns in root tissues

Root-expressed TaPht1 transporters exhibited a general pattern of high expression at early vegetative growth stages, which coincides with the growth stages when P_i requirement in wheat is high (Römer and Schilling 1986) and is deceasing during booting and anthesis (Figures 12 to 14). High P_i input during late gowth stages increases the thousand-grain mass (Römer and Schilling 1986). Sun et al. (2012) observed an considerable increase of P_i transport into the shoot during grainfilling through OsPht1;1 over-expression. Therefore, it may be assumed that there is still reasonable P_i acquisition from the soil solution at maturity, coinciding with the increase of transcription of root-

expressed TaPht1 transporters during grainfilling and ripening (Figures 12 to 14).

2.4.7. TaPht1 expression patterns in ear tissues

Root-expressed TaPht1 transporters were also expressed in ear tissues. In contrast to studies on TaPht1;5 homologues such as HvPht1;5 in barley (Rae et al. 2003, Huang et al. 2011) or OsPht1;12 in rice (Paszkowski et al. 2002) (Figure 7), TaPht1;5 was weakly expressed in root and also in shoot tissues (Figure 13). Specific Pht1 transporters are preferentially expressed in green and mature anthers, for instance in Arabidopsis (Mudge et al. 2002) and TaPht1;7 homologues in maize (Nagy et al. 2006) and barley (Druka et al. 2006). Therefore, it may be assumed that TaPht1;7 expression was strong in ear tissues (Figure 12) due to the induced transcript abundance in the anthers or pollen which are developed and formed at booting. The extremely weak TaPth1;7 root-expression is in agreement with Paszkowski et al. (2002) who detected very little root-expression of the rice homologue OsPht1;7 (Figure 7). Therefore, green and mature anthers might also be a target tissue for further investigations in wheat and require consideration in expression profiling studies. In addition, TaPht1;5 and TaPht1;7 are examples, which emphasize how crucial it may be for target gene discovery to dissect the biological function of each TaPht1 gene with its distinct roles for the plants development. Therefore, expression should not be altered, even indirectly, as a result of genetic improvement of PAE or PUE. However, several TaPht1 genes were identified as potential determinants of P_i acquisition mechanism in agronomic conditions and will be discussed further below.

2.4.8. Potential wheat P_i transporter genes determining P_i acquisition

The most abundant and probably most crucial root-expressed TaPht1 transporters were TaPht1;1 and TaPht1;2 (Figures 9, 10 and 15). Both may be promising candidates for investigations in diverse germplasm varying in P_i acquisition efficiency. The increasing P_i acquisition rate during P_i starvation

occurs presumably due to increased V_{max}, rather than increased affinity (K_m), which implies increasing high-affinity P-transporter synthesis with similar kinetic properties (Raghothama 2005). As variability in P_i depletion profiles in the rhizosphere of wheat genotypes suggest genetic variability in root hair formation (Gahoonia et al. 1996, Gahoonia and Nielsen 1997), varietal expression differences with respect to preferentially root expressed TaPht1 seems likely. This is particularly because TaPht1;2 was differentially expressed in genotyped which were either P_i starvation tolerant or not (Davies et al. 2002). Furthermore, high expression levels of root expressed Pht1 transporters, for instance HvPht1;1 and HvPht1;2 which are the TaPht1;1 and TaPht1;2 homologues (Figure 7), occur in trichoblast cells (Daram et al. 1998, Davies et al. 2002, Mudge et al. 2002, Schünmann et al. 2004).

TaPht1;1 and TaPht1;2 exhibited much lower transcript abundance in field-grown roots compared to liquid culture (Figures 8, 10 and 12). The question is, whether the presence or absence of root hairs during sampling had an effect on the TaPht1 expression profiles in different experimental systems. Soil moisture, structure, etc. limits and alters the P_i replenishement via the soil solution constantly leading to the development of many root hairs. However, the excavation of field-grown roots favours older roots in the top soil rather than the young, growing root tips where P_i acquisition proceeds to a much greater extent, especially at later growth stages. As a consequence, TaPht1;1 and TaPht1;2 expression might have been under-estimated in the long-term field studies compared to the in vitro-grown wheat seedling experiment. Nonetheless, in a hydroponic system, the nutrient solution is constantly washed around the roots. Therefore nutrients are always available and no visible root hairs developed. The expression patterns of some maize ZmPht1 transporters, ZmPht1;2 and ZmPht1;3, remained unaltered in a root hairless maize mutant (rth3; Wen and Schnable, 1994) showing that ZmPht1 transporters were not exclusively expressed in root hair cells (Nagy et al. 2006). ZmPht1;2 is closely related to OsPht1;6 and OsPht1;7, homologues of TaPht1; 6 and TaPht1;7 (Figure 7) and ZmPht1;3 to OsPht1;8 and OsPht1;12, homologues of TaPht1;3/4 and TaPht1;5 (Figure 7); but not TaPht1;1 or TaPht1;2. Therefore, these results obtained by Nagy et al (2006) cannot necessarily be applied for

clarifying why TaPht1;1 and TaPht1;2 transcription levels are so different in the two experimental systems. However, AM colonization could also potentially have changed the TaPht1;1 and TaPth1;2 expressional response which will be discussed further below.

TaPht1 expression patterns were analysed in field-grow roots (Figures 10 and 12 to 14). However, there are a lack of studies investigating TaPht1 transporter expression in agronomic systems apart from Teng et al. (2013) who did not provide any information (accession numbers, protein or nucleotide sequences) apart from primer sequence information. The information provided by Teng et al. (2013) is not consistent with primer combinations allocated to different TaPht1. For example Teng_TaPht1;1, Teng_TaPht1;2 and Teng_TaPht1;8, and not Teng_TaPht1;6, could be assigned with the TaPht1 sequences presented here by aligning the primers Teng et al. (2013) (Table 6): Teng_TaPht1;1 primers aligned to the identified TaPht1;1, but Teng_TaPht1;2 and Teng_TaPht1;10 both align to the identified TaPht1;2, which were all more highly up-regulated under high P_i fertilizer inputs. This is consistent with the assumption that there was no down-regulating feedback mechanism for TaPht1;1 and TaPht1;2, for instance in K starved plants (Figure 10). For Teng_TaPht1;8, which seems to be identical to TaPht1;8, expression decreased when P_i availability increased, probably due to reduced mycorrhiza infection under such conditions (Teng et al. 2013).

Differential Pht1 regulation in the PSR cross-talks is another important aspect for determining which TaPht1 transporters may be potential targets for P_i efficiency improvements. Sun et al. (2012) suggested that OsPht1;1, in contrast to OsPh1;2 (Liu et al. 2012), may not be regulated by PHR, as it lacked the P1Bs binding motif. Both of these rice Pht1 transporters are in phylogenetic proximity to TaPht1;1 and TaPht1;2 in wheat (Figure 7). However, Miao et al. (2009) studied the TaPht1;2 promoter region and identified other elements which potentially interact with regulatory PSR genes, including the P1BS motif (GTATATTC), a P1Bs-like motif (GTATATTT) and a conserved W-box (TTGACT). Therefore, the identification and isolation of the promoter regions of TaPht1 transporters and their common motifs for potential binding factors,

as performed by Tittarelli et al (2007) for TaPht1;2, is the next crucial step for understanding the regulation of their expression in the PSR. Especially for putative candidates such as TaPht1;1, TaPht1;2, TaPht1;6 and TaPht1;8.

2.4.9. Potential wheat P_i transporter genes determining P_i translocation

Intermediate TaPht1;6 expression was detected in hydroponically-grown (Figure 9), field-grown root and shoot tissues (Figures 11 and 12) where TaPht1;6 expression was strongly induced by P_i starvation. Furthermore, TaPht1;6 was responsive to external P_i availability during the entire growing season and all three experiments (Figures 9, 10 and 12). TaPht1;6 corresponds to the homologue HvPT1;6 gene in barley (Figure 7), which has been previously described as a low-affinity transporter predominantly expressed only in shoot tissues (Rae et al. 2003, Preuss et al. 2010). Huang et al. (2011) correlated expression of the HvPh1;6, the TaPht1;6 homologue (Figure 7), with P_i use efficiency of different barley genotypes. These results suggest a crucial role for P_i re-translocation or in P_i remobilization. Therefore, TaPht1;6 may be another candidate for P_i efficiency improvement of crops whereas TaPht1;5, TaPht1;7 and Ta1;11 seem to have minor importance.

The expression of TaPht1;10 and TaPht1;11 was much lower in shoot tissues compared to the roots (Figure 14), indicating that both transporters may be particularly crucial for acquisition of P_i from the soil solution via the roots rather than being involved in the subsequent P_i translocation processes within the plant itself.

2.4.10. Expression patterns of AM-associated TaPht1 transporters

A fourth transporter exhibiting a major importance in roots as well as in ear tissues was TaPht1;8. TaPht1;8 expression was particularly high in field-grown wheat (Figures 10 and 13) compared to in vitro growing conditions (Figure 9). TaPht1;8 expression was even higher compared to TaPht1;1 and TaPht1;2 (Figures 10 and 15). TaPht1;8 and TaPht1;11, both share

phylogenetic proximity to AM-induced rice and Brachypodium homologues, OsPht1;11, BdPht1;7 and BdPht1;3 (Figure 7), (Paszkowski et al. 2002, Hong et al. 2013). The establishment of a mycorrhizal symbiosis is a well-known adaptation strategy of plants in a low-P_i environment to increase P_i accessibility (Tarafdar and Marschner 1994, Koide and Kabir 2000, Fitter 2006), and the mycelium and hyphal length density can scavenge P_i to a much larger extent than afforded by the local rhizosphere and the root length density (Jakobsen et al. 1992). Therefore, AM-inducible P_i transporters have been widely studied in plants (Nagy et al. 2006, Qin et al. 2012, Hong et al. 2013).

Interestingly, TaPht1;8 and TaPht1;11 transcripts were abundant in hydroponically-grown roots at a similar level to field-grown roots, a system in which mycorrhiza should have been absent (Figure 9). In a study by Glassop et al. (2005), TaPht1;8 was expressed in the root cortical cells containing mycorrhizal structures aiming to scavenge apoplastic $P_{i.}$ The regulatory nature of some members of the direct P_i acquisition pathway including OsPht1;2, OsPht1;6, OsPht1;8 and OsPht1;11 in root and shoot of rice (Paszkowski et al. 2002, Jia et al. 2011, Yang et al. 2012) or HvPht1;8 on HvPht1;1 and HvPht1;2 in barley (Glassop et al. 2005) is known and suggests an alteration from the direct to the specific mycorrhizal P_i acquisition pathway. However, a weak expression of HvPht1;8 in barley and of ZmPht1;6, another TaPht1;8 homologue (Figure 7) in maize, was observed even if there was no colonization (Glassop et al. 2005, Nagy et al. 2006). Furthermore, the expression was high in AM-colonized barley roots independently from the degree of colonization (Glassop et al. 2005). All these observations indicate a transcriptional response of AM-inducible P_i transporters to P_i starvation occurred regardless of actual infection or a successfully established symbiosis. Furthermore, it is difficult to assume expression exclusively of AM-related P_i transporters in the roots: TaPht1;8 (Figure 7) was not exclusively root-expressed (Figure 13) similarly to AM-related soybean Pht1, which was expressed in aerial tissues and was even up-regulated in P_i-replete plants (Qin et al. 2012). In contrast, the majority of BdPht1 transporters were root induced during AM-symbiosis with G. intraradices, some even exclusively such as BdPht1;3 (Hong et al. 2012), which is the TaPht1;8 homologue (Figure 7).

The TaPht1;11 gene was reported to be AM-induced and to a much higher extent than TaPht1;8 or HvPht1;8 (Sisaphaithong et al. 2012). In contrast to these findings, TaPht1;8 was more strongly expressed than TaPht1;11 in all experiments (Figures 9, 10 and 15). TaPht1;11 orthologues have been identified in rice (OsPht1;11) and Brachypodium (BdPht1;7) (Paszkowski et al. 2002, Hong et al. 2012) (Figure 7). BdPht1;7 was detected in root and shoot (Hong et al. 2012), whereas OsPht1;11 expression seemed to be restricted to the root (Gutjahr et al. 2008). BdPht1;11, BdPht1;12, BdPht1;13 belong to the same clade as BdPht1;7 (Hong et al. 2012). Apart from BdPht1;11, which seems to be constitutively expressed, BdPht1;12 and BdPht1;13 are strongly expressed in mycorrhizal roots (Hong et al. 2012). The homologues to BdPht1;12 and BdPht1;13 in wheat are TaPht1;9, TaPht1;12 and TaPht1;14 (Figure 7). Gene expression for none of these TaPht1 transporters could be verified in any tissue sampled at any time or in any experimental system. OsPht1;13, the rice homologue of TaPht1;9, was reported to be induced in AM-symbiosis in rice roots (Güimil et al. 2005). However, TaPht1;9, TaPht1;12 and TaPht1;14 might be expressed under a specific condition or treatment which was not included in this work here. In conclusion, the expression of AM-associated Pht1s varies largely between plant species and experimental conditions.

Interestingly, phylogenetic analysis revealed a clustering of AM-induced Pht1 genes of monocotyledonous and dicotyledonous species without showing strong evolutionary divergence (Qin et al. 2012). Mycorrhizal symbiosis is an ancient mechanism (Smith and Smith 2012) and factors involved in the core steps of AM symbiosis formation may be conserved in evolution (Paszkowski et al. 2002). Therefore, findings here lead to a model that AM-induced TaPht1 transporters may be generally expressed during P_i starvation. It may be a strategy change signal in order to enhance 'AM-P_i acquisition' additionally to 'soil-P_i acquisition'. It may also be that this transcriptional change of TaPht1;8 and TaPht1;10 is not translated into a metabolic change. Yang and Paszkowski (2011) speculated that the P_i flow across the peri-arbuscular cortex membrane may be among the mechanisms allowing AM-fungi recognition for the plant

rather than other less beneficial microbes. Therefore, Pht1 transporters may have to be expressed before a symbiosis is established in order to allow the fungus to proliferate P_i to the root. Once the AM infection under low P_i availability is successful, Pht1 expression of the direct P_i acquisition pathway may be suppressed (Paszkowski et al. 2002, Glassop et al. 2005). This may occur even if this second mycorrhizal P_i acquisition pathway is not delivering sufficient P_i to raise the internal P_i status (Glassop et al. 2005). Paszkowski et al. (2002) showed that OsPht1;11 activation was independent from the internal nutritional status of the plant or P_i availability in the presence of G. intraradices. Aditionally, OsPht1;11 expression mimicked the AM fungal spread within the mycorrhizal roots which explains the increase of TaPht1;11 transcript abundance throughout the season at maturity (Figure 14). However, in order to prove that hypothesis, it is necessary to determine fungal symbiosis e.g. using markers as proposed by Thonar et al. (2012). However**,** only if this second P_i acquisition pathway via mycorrhizal symbiosis is actually established, may it result in a subsequent down-regulation of TaPht1;1 and TaPht1;2. Nevertheless, in situ hybridization of roots during colonization and non-colonization during P_i starvation as well as promoter-reporter gene fusions would be promising avenues for future studies on TaPht1 transporters to dissect the mechanism and confirm the suggested models.

2.5. Conclusion

The next steps for assessing which TaPht1 transporter may potentially be relevant for improving PUE and PAE in wheat is the dissection of the subcellular localization, the biological functions and the molecular regulation of each member. It is crucial to dissect the complex interaction amongst all family members and reveal varietal variation in TaPht1 expression. However, this study identified several members of the TaPht1 family in wheat, determined their expression profiles during nutrient starvation and physiological development. This expression profiling provided evidence that some members are highly expressed in roots and particularly important for P_i acquisition. Others are relevant in establishing the AM symbiosis during long-term P_i starvation; these were mainly root-expressed but also exhibited weak expression in ear tissues. A third group of TaPht1 family members seem to be relevant for P_i translocation from vegetative to generative growth, and a forth group is either weakly or constitutively expressed without a specific impact on PUE or PAE, even if they may have important biological roles.

Chapter 3: Genome-wide response to macronutrient limitation in field-grown wheat roots

3.1. Introduction

3.1.1. Transcriptome studies as a tool

Amongst the approaches to identify potential targets for genetic improvement of crops in regards to P_i efficiency traits, transcriptome studies are widely used tools (Chapter 1). Transcriptomics help the understanding of the control of a biological system (Lan et al. 2012) or reveal specific gene functions by investigating mutants linked to a trait (Lei et al. 2011, Nilsson et al. 2012). They can also be a starting point to dissect and identify potential candidate genes related to a phenotype, an agricultural trait or a plant response, for instance nutrient starvation (Leader 2005, Nilsson et al. 2010, Dai et al. 2012). Subsequently, transcriptome studies can be exploited as tools in agronomic systems: as functional gene markers in marker assisted-selection (MAS) based breeding (Collard et al. 2005, Vreugdenhil et al. 2005, Bagge et al. 2007, Collard and Mackill 2008) or as diagnostic expression marker genes for predicting e.g. stress tolerance (Coram et al. 2008) which can, when linked with marker fluorescence genes, be used in combination with sensor techniques as "smart plants" (Hammond et al. 2003).

3.1.2. Application of results from transcriptome studies

The application of marker genes may be a future alternative for replacing empiric models which are used for predicting fertilizer application based on soil analysis or plant tissues. Such an application would increase the predicting precision of nutrient requirement before any visible symptoms of P_i starvation and yield damage occur; this has been shown for potato by Hammond et al. (2011). Another study determined the impact of N organic and conventional fertilizer forms on the wheat transcriptome providing potential diagnostic genes for "production system authentication" and a more targeted breeding under organic conditions (Lu et al. 2005, Tenea et al. 2012). However, practical application of transcriptomics remains a future prospect. Furthermore,

most candidate genes have not been tested further for exploitability in a broader range of scenarios.

3.1.3. Different transcriptome study techniques

Many experimental transcriptome approaches have used microarrays, a widely used high-throughput technique which assesses transcriptional changes via the hybridization between a labelled probe and a gene of interest (cDNA or RNA). This technique reveals differential gene expression and co-expression dynamics for thousands of genes within a single experiment assuming that there is congruency between transcriptional, protein or metabolic changes (Maathuis and Amtmann 2005, Morcuende et al. 2007). However, this may not always be the case (Calderón-Vázquez et al. 2008, Torabi et al. 2009, Lan et al. 2012). Other approaches, SAGE (Serial Analysis of Gene Expression), MPSS (Massive Parallel Signature Sequencing), the Roche 545 pyrosequencing technology and RNA seq (Illumina), are sequencing-based and have the advantage of calculating absolute gene expression rather than only determining relative expression changes (Maathuis and Amtmann 2005, Coram et al. 2008). However, all these methods are still very costly and therefore, they have only recently been used more commonly. Even array studies are mostly restricted to a single or a very specific question (Maathuis and Amtmann 2005, Coram et al. 2008) and experimental set-ups are biologically very simple (Nilsson et al. 2010). Transcriptomes are, in contrast to genomes, very variable depending on the particular conditions of the investigated organism implying they have to be assigned and annotated to it (Brazma et al. 2001). Therefore, transcriptome analyses usually face the problem that data sets are complex and have to be disentangled in order to allow an interpretation. Therefore, clustering and integrating transcriptome results from multiple studies to build gene-co-expression networks or integrating genomic, proteomic, metabolomics and phenotypic data from other experiments may help to improve the ability of identifying key genes and pathways (Morcuende et al. 2007, Coram et al. 2008, Plaxton and Tran 2011, Lan et al. 2012, Shewry et al. 2012, Liang et al. 2013, Schlüter et al. 2013). However, in many cases the lack of gene annotation

restricts the interpretation of array data (Maathuis and Amtmann 2005, Lan et al. 2012, Liang et al. 2013) or the lack of (array) annotation restricts integrating additional data from other studies (Brazma et al. 2001), particularly in crops (Leader 2005).

3.1.4. Validation of transcriptome studies

PCR methods which are transcriptomic analysis methods themselves access a more limited number of genes but quantify expression changes more accurately which allows addressing very specific biological questions rather than just being descriptive. Furthermore, it is possible to determine absolute transcript abundance of genes, even when they are very low expressed (Brazma et al. 2001, Maathuis and Amtmann 2005, Coram et al. 2008, Morcuende et al. 2007). Therefore, array results are usually validated using real-time PCR (Leader 2005, Lu et al. 2005, Poole et al. 2007, Dai et al. 2012, Oono et al. 2013).

3.1.5. Transcriptome studies related to phosphate nutrition

Transcriptome studies are useful tools to study regulatory mechanisms with regards to adaptation to nutrient stresses (Hammond et al. 2004, Nilsson et al. 2010) and have identified numerous genes related to P_i starvation (Wang et al. 2002, Hammond et al. 2003, Wasaki et al. 2003, Wu et al. 2003, Hammond et al. 2005, Misson et al. 2005, Morcuende et al. 2007, Calderón-Vázquez et al. 2008, Pariasca-Tanaka et al. 2009, Hammond et al. 2011ab, Lan et al. 2012, Oono et al. 2012, Oono et al. 2013). Genes responding to P_i starvation can be grouped into “early” and “late”; “early” genes respond rapidly and are often general stress-related genes, whereas later induced genes alter the morphology, physiology or metabolism and might therefore promote P_i acquisition or P_i use efficiency within the plant (Hammond et al. 2003). Using this technique has revealed that sugars seem to modulate PSI gene expression (Jain et al. 2007, Karthikeyan et al. 2007, Müller et al. 2007, Hammond and White 2011), which is consistent with increasing levels of di- and trisaccharides in P_i starved plants

(Huang et al. 2008). Observed changes in transcriptional profiling include signalling cascades (MYB-TF, Zn-finger-TF, microRNA, IPS genes), hormone-related genes (ABA, ethlyene, auxin), genes related to alterations in carbon metabolism (e.g. organic acid synthesis through glycolysis), lipid metabolism (rearrangement of cell wall compounds and lipid composition of the plasma membranes), by-passes of respiration, P_i acquisition via enhanced P_i transporter expression, P_i recycling via increasing expression of phosphatases and SPX-domain encoding proteins involved in P_i homeostasis (Wang et al. 2002, Hammond et al. 2003, Wasaki et al. 2003, Müller et al. 2004, Morcuende et al. 2007, Calderón-Vázquez et al. 2008, Lan et al. 2012).

Unfortunately, there are only few studies (Calderón-Vázquez et al. 2008, Pariasca-Tanaka, Oono et al. 2011, Dai et al. 2012, Oon et al. 2013, Aziz et al. 2014) looking at regulatory systems in economically important crops where a vast amount of gene functions and their gene products are still unknown or not well defined. Furthermore, the majority of transcriptional profiling studies were based on hydroponically grown plant material exposed to short-term P_i starvation rather than on soil-grown or field-grown crops (Hammond et al. 2003, Misson et al. 2005, Hammond et al. 2007, Calderón-Vázquez et al. 2008, Dai et al. 2012, Woo et al. 2012, Cai et al. 2013). However, these model plant or in vitro systems studies provide useful data for approaching complex data such as wheat transcriptomics and are useful for applying more generalised models to complex networks such as PAE and PUE in wheat. Furthermore, the lack of annotation or functional characterization of wheat genes may often be overcome by identifying orthologues of genes in rice or Arabidopsis which have already been investigated in more detail (Leader 2005).

3.1.6. Studying genome-wide responses in wheat using the microarray technique

Studies investigating differential gene expression responses in wheat via microarrays have focused on grain development (Lu et al. 2005, Wan et al. 2008, Xu et al. 2013), defence mechanisms during pathogen and pest infection (Lysøe et al. 2011, Reddy et al. 2013, Wang et al. 2013b), germination (Yu et

al. 2014) and different abiotic stresses such as drought stress (Krugman et al. 2011).

The application of transcriptomics to wheat faces various challenges and is far more complex compared to their use in model plants (Leader 2005). However, microarrays have been widely used in wheat research since the commercial Affymetrix Wheat Chip® genome array (Santa Clara, USA) (named Affymetrix Genechip® in the following) was released (2006); however, they may soon be replaced by the new generation sequencing techniques (Coram et al. 2008). This microarray contains around 61,000 probe sets representing around 55,000 unique transcripts from the three genomes (A, B and D) covering all 42 wheat chromosomes. It also includes around 1760 probes from wheat ancestors comprising Triticum monococcum which is a near A genome relative, Triticum turgidum and Triticum turdigum ssp. durum which contain ancestral A and B genomes and Aegilops tauschii which is a near D genome relative[12].

Unfortunately, the trancriptome coverage of the Affymetrix Genechip® for wheat is limited and covers only around two thirds of the total number of currently known genes in wheat which probably exceeds 100,000 putatively coding genes (Brenchley et al. 2012). The Affymetrix Genechip® annotation covers around 200 UniGene counts (Affymetrix Genechip® data sheet[13]), but without a fully sequenced wheat genome, rare transcripts may not be represented in the analysis (Leader 2005). Furthermore, Poole et al. (2007) revealed a weak reproducibly between results from the Affymetrix Genechip®, quantitative reverse PCR results and an in-house custom-spotted DNA array which are arrays enriched with target sequences according to the focus of the experimental setup e.g. testing genes in a varying genetic background (Coram et al. 2008). This discrepancy occurred due to the allohexaploid nature of the wheat genome and the inability of the different methods to discriminate between related transcripts (homeologues and paralogues genes) (Poole et al.

[12] http://www.affymetrix.com/estore/browse/products.jsp?productId=131517&navMode=34000&navAction=jump&aId=productsNav#1_1

[13] http://www.affymetrix.com/catalog/131517/AFFY/Wheat-Genome-Array#1_1

2007). However, to differentiate between expression of homeologues genes might be crucial in wheat as they may influence certain traits individually (Leader 2005). Therefore it is crucial to use homoelog-specific transcriptomic approaches and to validate results obtained using the Affymetrix Genechip®.

3.1.7. Studying genome-wide responses in wheat related to nutrition

Apart from N, there are no microarray studies to date investigating the effect of specific macronutrient stresses such as P_i or K on the wheat transcriptome. This is particularly the case for roots, in contrast to many model plants (rice, maize, Arabidopsis). One transcriptome study using de novo assembly for wheat root and shoot tissues exposed to P_i starvation has been reported (Oono et al. 2013). However, gene ontology could be assigned to only 40 % of the root and 34 % of the shoot transcripts showing transcript regulation in the oxidation-reduction (cytochrome P450), the protein phosphorylation (kinases) and the lipid metabolism process category (lipases) (Oono et al. 2013). TaIPS genes were strongly up-regulated, particularly in the roots which suggested a functioning PHR1-IPS1-miRNA399-UBC24/Pho2 signalling cascade in wheat similarly to rice or Arabidopsis.

Other investigations were assessing the role of particular genes as transcriptional responses in wheat suffering from P_i limitation via other expression methods (real-time PCR techniques or reporter genes) comprising studies by Aziz et al. (2014) and Tittarelli et al. (2007) rather than studying the genome-wide response for identifying new wheat specific candidates. Therefore, this study will fill the gap between the many and extensive transcriptome studies on model plants investigating P_i starvation responses and the lack of studies investigating transcriptional responses in wheat. Field-grown root material exposed to limited P_i availability will be assessed in relation to other macronutrient deficiencies combining the commercially available Affymetrix Genechip® and real-time PCR techniques.

3.2. Material and Methods

3.2.1. Plant material

Root material from T. aestivum cv. Hereward were sampled at growth stage 45 (Zadoks et al. 1974) from plots representing continuous wheat plots of the "Broadbalk" field experiment (Rothamsted Research 2006 , Watts et al. 2006) where the plants were exposed to multiple long-term nutrient deficiencies through the omission of N, P_i, K, Mg and S fertilizers (Table 1). In May 2011, roots were excavated between 9 to 12 am with a fork-like spade in triplicates (n = 3) from plots in section 0 and 1 (Tables 1 and 2). The P_i starved material was sampled from plot 19 (Tables 1 and 2). However, the experimental design and the treatments as well as the sampling method for excavating the roots have been described previously in Chapter 2, Section 2.3. Futhermore, meteorological data was requested from the electronic Rothamsted Archive (eRA data) and weather conditions during the sampling season in 2011 have been presented in Chapter 2 (Figure 5). Total RNA was extracted according to the procedures described in Chapter 2, Section 2.6. In order to get highly-purified RNA free of ethanol, each sample was cleaned additionally using a silica-gel-membrane technology (RNeasy Plant Mini Kit, Qiagen, Maryland, USA). 15 µl of each RNA sample with concentrations from 0.3 to 1 µg μl^{-1} were then sent on dry ice to the University of Bristol Transcriptomics Facility to conduct the hybridization to the Affymetrix Genechip® Wheat Genome Array (Santa Clara, USA).

3.2.2. Hybridization to the Affymetrix Genechip® Wheat Genome Array

The Affymetrix Genechip® is a short oligonucleotide microarray (~25 bp per probe) and probes are synthesised using photolithographic technology and combinatory chemistry. Each probe contains hundreds of thousands of a given oligonucleotide. Hybridized probe arrays are scanned by a gene array scanner which captures the amount of emitted light at 570 nm which is proportional to the bound target at each probe array location[14].

[14] http://media.affymetrix.com/support/downloads/manuals/expression_analysis_technical_manual.pdf

cDNA synthesis and biotin-modified cRNA were prepared from 500 ng total RNA using the Affymetrix 3' IVT Express kit (Affymetrix User Manual P/N 702646 rev.7). GeneChip® Hybridization, Wash, and Stain Kits were used for cRNA hybridization according to the manufactures instructions (Affymetrix P/N 702731 Rev.3). Gene chips were washed in the Affymetrix GeneChip fluidics station 450 (fluidics script EukGE-WS2v5).

Arrays were scanned using the Affymetrix® GeneChip® Scanner 3000; default settings in GeneChip Command Console Software (AGCC) for 3' arrays. Probe cell intensity data are analysed in the Affymetrix GeneChip Expression Console software using the MAS 5 algorithm and Affymetrix default analysis settings and global scaling as normalization (3' Expression Array Analysis: User Manual P/N 702387 Rev. 3). All probes were scaled to target intensity (TGT) of 500 and MAS5.0 signal intensity used for value definition. CEL and CHP files were generated and together with MAS5.TXT files which contain the normalized raw data, will be released 1st April 2015 in the GEO database[15]: Accession GSE61679.

3.2.3. Data analysis and validation

Results were analysed with GeneSpring GX (version 12.6, Agilent Technologies, Santa Clara, USA). All data (18 .CEL files) were imported into GeneSpring and normalized using the RMA normalisation algorithm (Bolstad et al. 2003, Irizarry et al. 2003a; b).

Normalized signal values for individual probe-sets were standardized to the median signal value for the probe across all microarrays. In order to verify the variation among biological replicates, a principal component analysis (PCA) was performed and correlation coefficients between all samples determined.

Probe-sets which were differentially expressed under nutrient limitation treatment compared to the control were determined using multiple t-tests with

[15] http://www.ncbi.nlm.nih.gov/geo/

Benjamini-Hochberg multiple testing correction. This approach allowed a dissection of genome–wide responses associated with macronutrient starvations. A $\log_2$-fold change threshold was applied to determine genes which were significantly ≥ 2 fold up- or down-regulated as a response to each nutrient limitation. In order to confirm the reliability of the microarray results, the data was validated for selected candidates using real-time qPCR in Chapter 4.

3.2.4. Cluster analysis

A cluster analysis was conducted for dissecting specific expression patterns of significantly altered genes across multiple nutrient deficiencies. The expression of each probe was classified into the most appropriate cluster defined by the k-means algorithm. Probes included in the analysis were determined using a one-way ANOVA ($P \leq 0.05$) which compared each nutrient limitation-treatment to the control. This method was less restrictive on the selection of probes which were included into the analysis compared to the multiple t-tests (with a defined $\log_2$-fold threshold). Therefore, it resulted in more probe-sets available for clustering into 6 clusters using 200 iterations and Euclidean similarity measure.

3.2.5. Cross-comparison study

A cross-comparison of the gene expression data with results from similar studies investigating the PSR of rice, maize and Arabidopsis was performed by uploading downloaded genes lists from the GEO database or online publications (Table 17) into the GeneSpring 12.6 (Agilent Technologies) software and comparing these data to results from the multiple t-test and the cluster analysis. Rice, maize and Arabidopsis gene could be assigned to wheat probes using the 'HarvEST annotation' mentioned below.

Table 17: References used for cross-comparison study.

Cai H., Xie, W.B., Lian and X.M. (2013) Comparative analysis of differentially expressed genes in rice under nitrogen and phosphorus starvation stress conditions. Plant Mol. Biol. Rep. 31: 160-173.
Calderón-Vázquez, C., Ilbarra-Laclette, E., Caballero-Perez, J. and Herrera-Estrella, L. (2008) Transcrip profiling of Zea mays roots reveals responses to phosphate deficiency and the plant-species-specific level. J. Exp. Bot. 59: 2479-2497.
Dai, X., Wang, Y., Yang, A. and Zhang, W. (2012) OsPYB2P-1, an R2R3 MYB transcription factor, is involved in the regulation of phosphate-starvation responses and root architecture in rice. Plant Physiol. 159: 169-183.
Misson, J., Raghothama, K.G., Jain, A., Jouhet, J., Block, M.A., Bligny, R., Ortet, P., Creff, A., Somerville, S., Rolland, N., Doumas, P., Nacry, P., Herrerra-Estrella, L., Nussaume, L. and Thibaud, M.C. (2005) A genome-wide transcriptional analysis using Arabidopsis thaliana Affymetrix gene chips determined plant responses to phosphate deprivation. PNAS 102: 11934-11939.
Morcuende, R., Bari, R., Gibon, Y., Zhen, W., Pant, B.D., Bläsing, O., Usadel, B., Czechowski, T., Udvardi, M.K., Stitt, M. and Scheible, W. R. (2007) Genome-wide reprogramming of metabolism and regulatory networks of Arabidopsis in response to phosphorus. Plant Cell Environ. 30: 85-112.
Müller, R., Morant, M., Jarmer, H., Nilsson, L. and Nielsen, T.H. (2007) Genome-wide analysis of the Arabidopsis leaf transcriptome reveals interaction of phosphate and sugar metabolism. Plant Physiol. 143: 156-171.
Hammond, J.P. (2007); GEO acc number GSE5611: Differential gene expression patterns in the phosphate deficient mutant, pho 1 (Arabidopsis thaliana).
Woo, J., MacPherson, C.R., Liu, J., Wang, H., Kiba, T., Hannah, M.A., Wang, X.J., Bajic, V.B. and Chua, N.H. (2012) The response and recovery of the Arabidopsis thaliana transcriptome to phosphate starvation. BMC Plant Biol. 12: 62 (http://www.biomedcentral.com/1471-2229/12/62).
Wu, P., Ma, L.G., Hou, X.L., Wang, M.Y., Wu, Y.R., Liu, F.Y. and Deng, X.W. (2003) Phosphate starvation triggers distinct alterations of genome expression in Arabidopsis roots and leaves. Plant Physiol. 132: 1260-1271.

3.2.6. Gene annotation

For wheat, the Affymetrix Genechip® probes are poorly annotated. Therefore, additional wheat probe-set annotation with rice, Brachypodium and Arabidopsis was imported from the HarvEST web page[16] using a minimum of one perfect-match probes. Sequences of significant probes were extracted using the GrainGenes 2.0 database[17] and putative gene annotation was done using the NCBI BLAST(x/n)[18] or PLEXdb database[19]. The best hit with the lowest e-

[16] http://www.harvest-web.org/
[17] http://wheat.pw.usda.gov/GG3/
[18] http://blast.ncbi.nlm.nih.gov/Blast.cgi
[19] http://www.plexdb.org/modules/PD_probeset/annotation.php

value and the highest percentage of sequence similarity and query coverage (%) was selected for as putative annotation. A selection of putatively annotated transcripts allowed deriving comprehensive conclusions. However, the Affymetrix Genechip® contains more probe sets than transcript which are different sequences for the same gene transcript. They show nearly identical log_2-fold change values and were therefore used as internal quality controls.

3.2.7. Ionomic data

Ionomic data was obtained through chemical analysis for oven-dried wheat shoot sampled as previously described (Chapter 2, Section 2.3. and 2.5.). Wheat shoot mineral nutrition data and the root transcriptome data was loaded into the Genespring software. Similarly to the previously method, an ANOVA was performed. Graphs show concentration profiles between treatments for each macronutrient concentration and gene expression profiles that have been selected following a similar pattern than the nutrient concentration across treatments using a Euclidean metric (maximal value: 1 = identical).

3.3. Results

3.3.1. Sample analysis

The PCA analysis revealed that the first three principal components could only describe ~40 % of the variance in the data: PC1 = 22. 09 %, PC2 = 11 % and PC3 = 9.2 % . The high variation in the biological replicates (n=3) is not surprising when analysing field-derived material. Samples derived from the K starvation plot were most similar to those from the control plot (Figure not shown). Samples derived from the P_i and N starvation plots were most different from the control. The correlation coefficients of all biological replicates were between 0.97 and 0.99 (data not shown).

3.3.2. Genome–wide responses associated with nutrient limitation

N, P_i, K, Mg and S starved field-grown wheat roots exhibited 198 significantly down regulated (≥ 2 fold change) (Figure 16 A) and 99 significantly up-regulated (Figure 16 B) and. The strongest impact on the root transcriptome was related to P_i starvation (Figure 16) and down-regulated genes exceeded the number of up-regulated genes (Figure 16). Several transcripts were up-regulated or down-regulated under multiple deficiencies (Figure 16). Others were significantly up-regulated (≥ 2 fold change) under one specific starvation (Table 18 A, C and D) but significantly down-regulated under another (Figures 15 and 18, Table 18 B and E).

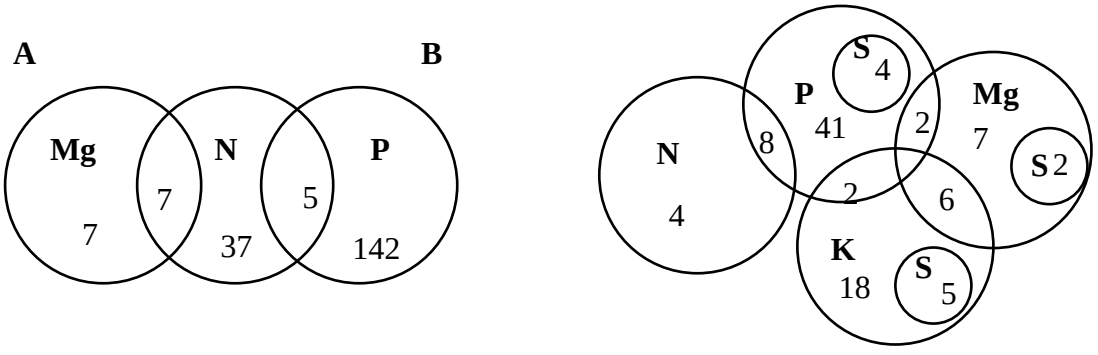

Figure 16: Venn diagrams showing wheat gene probes significantly (P≤0.05) (A) ≤ 2 fold down-regulated and (B) ≥ 2 fold up-regulated in wheat roots from Broadbalk at booting in 2011 as a response to long-term phosphate (P_i), nitrogen (N), magnesium (Mg), potassium (K) and sulphate (S) starvation.

The majority of significant expression changes were in a range of ± 1.2 to ± 2.5 log_2-fold (Table 18). Some differentially regulated transcripts which were P_i specific were also associated with other nutrient deficiencies (Table 18 B and E). Furthermore, some which were significantly repressed under N starvation but implicated with P_i starvation in the literature (Table 18 C). Several general stress or hormone related genes were differentially, e.g. late embryogenesis abundant (LEA) proteins, abscisic acid (ABA), jasmonate and ethylene responsive/inducible proteins, glutathione-S-transferase and peroxidases, cytochrome P450 proteins, and genes involved in signal transduction and P_i homeostasis, e.g. MYB transcription factors, SPX proteins, Pho-like transporter and IPS genes (Table 18). Other genes coding for phosphatases, phosphodiesterases, sugar transporter, expansins and lipid transfer proteins involved in P_i remobilization and P_i acquisition were also differentially expressed (Table 18). In order to select potential candidates for validation and further expression studies, the cluster-, cross-comparison and ionome analysis were used to dissect the data from three different angles rather than just arrange the data according to the level of alteration (Table 18).

Table 18: A subset of wheat gene probes significantly (P≤0.05) induced (+) or down-regulated (-) in field-grown wheat roots from Broadbalk in 2011 at booting as a response of long-term P_i, N, Mg, K and S fertilizer withdrawal (Table 18 A, B, C, D and E).

Change of expression is shown as a significant log_2-fold change value either specific for P_i starvation or associated with other nutrient deficiencies which are significantly changed in their expression level.

Wheat probe ID	Specificity, log_{2fold} change		Putative annotation; Accession No.	Cluster
Table 18 (A): Subset of significantly up-regulated probes during P_i fertilizer withdrawal				
Ta.25744.1.S1_at	+P	2.06	MYB-like; EMT17444 A. tauschii // MYB related; AEV91181; T. aestivum	**5**
Ta.5843.1.S1_x_at	+P	1.83	Late embryogenesis abundant protein (LEA); XM_003562004; B. distachyon	**5**
Ta.26997.1.S1_at	+P	1.76	Early light-inducible protein (HV58); XM_003561306; B. distachyon	**5**
Ta.9600.1.S1_x_at	+P	1.61	Cold-regulated for early light-inducible protein; AB019617; T. aestivum	**5**
Ta.5945.1.S1_at	+P	1.51	Oleosin; NM_001159239; Z. mays	**5**
Ta.4826.2.S1_at	+P	1.51	Late embryogenesis abundant protein (LEA); ABA54793; Picea glauca	**5**
Ta.13396.1.S1_at	+P	1.45	LEA protein group 1; ACV91870; H. vulgare	**5**
Ta.28848.1.S1_at	+P	1.43	LEA protein 12; AAT99310; O. sativa	**5**
Ta.29375.1.S1_at	+P	1.42	Putative ABA induced; TA71731_4565; O. sativa//LEA protein; XP_003575514; B. distachyon	**5**
Ta.9063.1.S1_x_at	+P	1.39	S-adenosylmethionine decarboxylase; GU016570; T. aestivum	**5**
Ta.23659.1.S1_at	+P	1.26	LEA2 protein inducible by ABA; AY148491; T. aestivum	**5**
Ta.28555.2.S1_at	+P	1.24	ABA induced plasma membrane protein; U80037; T. aestivum	**5**
Ta.303.2.S1_at	+P	1.24	Glutathione-S-transferase; AAL47688; T. aestivum	**3**
TaAffx.52861.1.S1_at	+P	1.22	Zinc finger protein DOF3.3-like; XM_003565574; B. distachyon	**5**
TaAffx.6447.1.S1_x_at	+P	1.22	B-Box zinc finger family protein; NP_001147455; Z. mays	**2**
Ta.27094.1.S1_at	+P	1.19	B-Box putative zinc finger protein; ADG85706; T. aestivum	**5**
Ta.11849.1.S1_at	+P	1.17	TaMYB59/TaMYB43, MYB-related protein; JF951942/JF951926; T. aestivum	**2**
TaAffx.53797.1.S1_s_at	+P	1.15	TaMYB58, MYB-related protein; JF951941; T. aestivum	**5**
Ta.14269.1.A1_at	+P	1.14	Glutathione S-transferase gene; AY013754; A. tauschii	**5**
Ta.5734.1.S1_at	+P	1.13	Serine/threonine phospatase; family 2C; NP_001234500; Solanum lycopersicum	**5**
Ta.28838.1.S1_x_at	+P	1.13	Putative late embryogenesis abundant (LEA) protein; EF535810; H. vulgare	**5**
TaAffx.34778.1.S1_at	+P	1.06	Heat stress transcription factor C-1b-like; XM_003569688; B. distachyon	**5**
Ta.9564.1.S1_at	+P	1.06	Ethylene-responsive protein; NM_001158174; Z. mays	**5**
Ta.226.1.S1_at	+P	1.02	ABA-inducible WRAB1; Cor/Lea gene group 3; BAF79928; T. aestivum	**5**
Ta.7973.1.S1_at	+P	1.02	LURP-one-related 8-like; XM_003567174; B. distachyon	**5**
Ta.5915.2.S1_at	+P	1.01	ABA inducible LEA1 (group 3) protein; AAN74637; T. aestivum	**5**

Wheat probe ID	Specificity, log_{2fold} change		Putative annotation; Accession No.	Cluster
Table 18 (B): Subset of significantly up-regulated probes during P_i, N. Mg, and S fertilizer withdrawal				
Ta.9063.2.A1_at	+P +S	1.85	S-adenosylmethionine decarboxylase; GU016570; T. aestivum	**5**
Ta.9063.3.S1_at	+P +S	1.55	S-adenosylmethionine decarboxylase; GU016570; T. aestivum	**5**
Ta.28838.2.S1_at	+P +N	1.85	Putative late embryogenesis abundant protein; EF535810; H. vulgare	**5**
Ta.23812.1.S1_a_at	+P + N	1.75	ABA induced plasma membrane protein (WTABAPM); U80037; T. aestivum	**5**
Ta.27001.2.S1_at	+P +N	1.69	Chloroplast-targeted COR protein (Wcor15); BAC56935; T. aestivum	**5**
Ta.20483.1.S1_at	+P +N	1.68	Dehydrin 6; AF181456; H. vulgare	**5**
Ta.20483.3.A1_a_at	+P +N	1.50	Dehydrin 6; AF043091; H. vulgare	**5**
Ta.64.1.S1_at	+P +N	1.23	Zn^{2+} metallothionein gene (embryogenesis); X68288; T. aestivum	**5**
Ta.6831.1.S1_at	+P -Mg -N	1.49	SPX, N-terminal domain containing protein; NP_001064515; O. sativa	**3**
Ta.13989.1.S1_at	+P -Mg -N	1.17	TaIPS1.3; EU753152; T. aestivum	**3**
Ta.12413.1.S1_at	+P -Mg -N	1.35	Pyrophosphatase 1-like; DQ912176; B. distachyon	**3**
Ta.6770.1.S1_s_at	+P -N	1.16	Glycerophosphodiester phosphodiesterase; XM_003579607; B. distachyon	**3**
TaAffx.9237.1.S1_at	+P -N	1.13	TaIPS2.2; EU753154; T. aestivum	**3**

Wheat probe ID	Specificity, log_{2fold} change		Putative annotation; Accession No.	Cluster
Table 18 (C): Subset of significantly down-regulated probes during N fertilizer withdrawal				
Ta.4399.1.S1_x_at/ Ta.6744.2.S1_s_at	-N	-4.32	Ta IPS1.2; EU753151; T. aestivum	**3**
Ta.22712.1.S1_at	-N	-2.23	Ta IPS2.1; EU753153; T. aestivum	**3**
Ta.18257.1.A1_x_at	-N	-1.69	Ta IPS2.2; EU753154; T. aestivum	**3**
Ta.9492.1.S1_at	-N	-2.66	Glycerophosphodiester phosphodiesterase GDE1-like; XM_003574983; B. distachyon	**3**
Ta.13993.1.S1_x_at	-N	-2.23	SPX domain containing protein 6-like; XM_003559915; B distachyon	**3**
Ta.14013.1.S1_at	-N	-1.23	SPX domain containing protein 5-like; XP_003557742; B. distachyon	**3**
Ta.19715.1.S1_at	-N	-1.92	PHO1-3-like transporter (LOC100831716); XM_003563831; B. distachyon	**3**
Ta.24434.1.S1_at	-N	-1.50	Glycerophosphodiester phosphodiesterase GDE1-like; XM_003579607; B. distachyon	**3**
Ta.3186.1.A1_at	-N	-1.25	Purple acid phosphatase (AtPAP16); AY630355; A. thaliana	**3**
TaAffx.53053.1.S1_at	-N	-1.24	Sugar phosphate exchanger 2; EMT17209; A. tauschii	**3**

Wheat probe ID	Specificity, log_{2fold} change		Putative annotation; Accession No.	Cluster
Table 18 (D): Subset of significantly down-regulated probes during P_i fertilizer withdrawal				
Ta.5426.2.A1_a_at	-P	-2.46	CypX superfamiliy; cytochrome P450; ABU54407; T. aestivum	**6**
Ta.1807.1.S1_at	-P	-2.16	Class III secretory peroxidase 66 precursor; CBH32576; T. aestivum	**6**
Ta.14580.2.S1_x_at	-P	-2.05	Class III peroxidase Prx109-B; EU725468; T. aestivum	**6**
Ta.19176.1.S1_at	-P	-1.94	Class III peroxidase 66 precursor; CBH32576; T. aestivum	**6**
TaAffx.12181.1.S1_at	-P	-1.94	Bidirectional sugar transporter sweet17-like; XP_003565716; B. distachyon	**6**
Ta.994.1.S1_at	-P	-1.93	Cortical cell-delineating protein, NM_001153893; Z. mays	**6**
Ta.5435.1.S1_x_at	-P	-1.87	Cortical cell-delineating protein; NM_001159115; Z. mays	**6**
Ta.13950.1.S1_x_at	-P	-1.86	Cortical cell-delineating protein-like (LOC102699756); XM_006649164 ; O. brachyantha	**6**
Ta.14010.3.S1_x_at	-P	-1.86	Secretory peroxidase; AAG46133; O. sativa	**6**
TaAffx.84394.1.S1_at	-P	-1.85	Jasmonate induced protein; AAR20919; H. vulgare	**6**
Ta.1840.1.S1_at	-P	-1.81	Protease inhibitor-like protein; EU293132; T. aestivum	**6**
Ta.952.2.S1_a_at	-P	-1.57	Heme-dependent peroxidase class III (Prx110-C); EU725472; T. aestivum	**6**
Ta.29534.1.S1_x_at	-P	-1.53	Cysteine proteinase (Peptidase C1A subfamily); CAB09698; H. vulgare	**6**
Ta.14580.1.S1_at	-P	-1.55	Class III peroxidase; ACI00835; T. aestivum	**6**
Ta.14492.1.S1_at	-P	-1.51	Cortical cell-delineating protein; EMS64339; T.urartu	**6**
Ta.24423.1.S1_s_at	-P	-1.43	Beta-expansin EXPB6 Expansin; AAW32215; T. aestivum	**6**
Ta.30668.1.S1_at	-P	-1.40	Expansin EXPB10; AY543544; T. aestivum	**6**
TaAffx.86321.1.S1_at	-P	-1.40	Alpha-expansin 25; AAY63557; O. sativa	**6**
Ta.18703.1.S1_at	-P	-1.38	Expansin EXPA6; AY543532; T. aestivum	**6**
TaAffx.82031.1.S1_s_at	-P	-1.61	Peroxidase 54-like; XM_003563078; B. distachyon	**6**
Ta.1840.2.S1_x_at	-P	-1.28	Protease inhibitor-like protein; ABX84383; T. aestivum	**6**
Ta.2870.1.S1_at	-P	-1.27	Glutamine synthetase isoform GSr2; AY491969; T. aestivum	**6**
Ta.25703.2.A1_s_at	-P	-1.27	Flavonol synthase/flavanone 3-hydroxylase; EMS54532.1; T. urartu	**6**
TaAffx.111573.2.S1_at	-P	-1.24	Vegetative cell wall protein gp1 precursor; ACG29807; Z. mays	**6**
Ta.5388.1.S1_a_at	-P	-1.23	N-methyltransferase jasmonate induced; AAC18643; H. vulgare	**6**
TaAffx.9025.1.S1_at	-P	-1.22	Auxin-induced protein PCNT115-like; XP_003575317; B. distachyon	**6**
TaAffx.33689.1.S1_s_at	-P	-1.15	Leucine-rich repeat extensin-like protein; XP_003581687; B .distachyon	**6**
TaAffx.59372.1.S1_at	-P	-1.15	Beta-D-glucan exohydrolase; AY586531; S. cereale	**6**
Ta.22998.1.S1_at	-P	-1.19	Cytochrome P450; AAK38084; Lolium rigidum	**6**
Ta.6538.2.S1_at	-P	-1.13	Histone H2A; ACG32226; Z. mays	**6**

Wheat probe ID	Specificity, log_{2fold} change		Putative annotation; Accession No.	Cluster
Table 18 (E): Subset of significantly down-regulated probes during P_i fertilizer withdrawal, but up- or down-regulated in through K or N fertilizer withdrawal				
Ta.5145.1.S1_at	-P -N +K +S	-2.70	Nicotianamine synthase 3; AB011264; H. vulgare	**4**
Ta.26144.1.A1_at	-P +K	-1.29	Fatty acid-CoA reductase 1-like; XM_003566967; B. distachyon	**4**
Ta.21108.1.S1_at	-P +K	-1.27	CypX superfamiliy; cytochrome P450; ACG28703; Z. mays	**4**
TaAffx.106421.1.S1_at	-P +K	-1.35	Zn-Transporter; AY864924; T. aestivum	**4**
TaAffx.91995.1.A1_at	-P -N +K	-1.58	Prolyl endopeptidase-like; XM_003580272; B. distachyon	**4**

3.3.3. Gene response patterns across nutrient limitations

For determining a specific assignment of gene expression patterns across all macronutrient starvations, a cluster analysis was performed which resulted in the determination of 6 clusters (Figure 17). Mg and S starvation had the lowest impact on the wheat root transcriptome at booting stage in 2011 and there were not any particular expression pattern associated with these two nutrients (Figure 17). Therefore, the subsequent focus was on the interaction of N, K and P_i on the wheat root transcriptome. N and P_i starvation exhibited either contrasting (cluster 3) or similar (cluster 4 and 5) expression profiles (Figure 17) whereas K starvation exhibited a contrasting effect on transcript abundance compared to P_i and N limitation (cluster 4 and 5) (Figure 17).

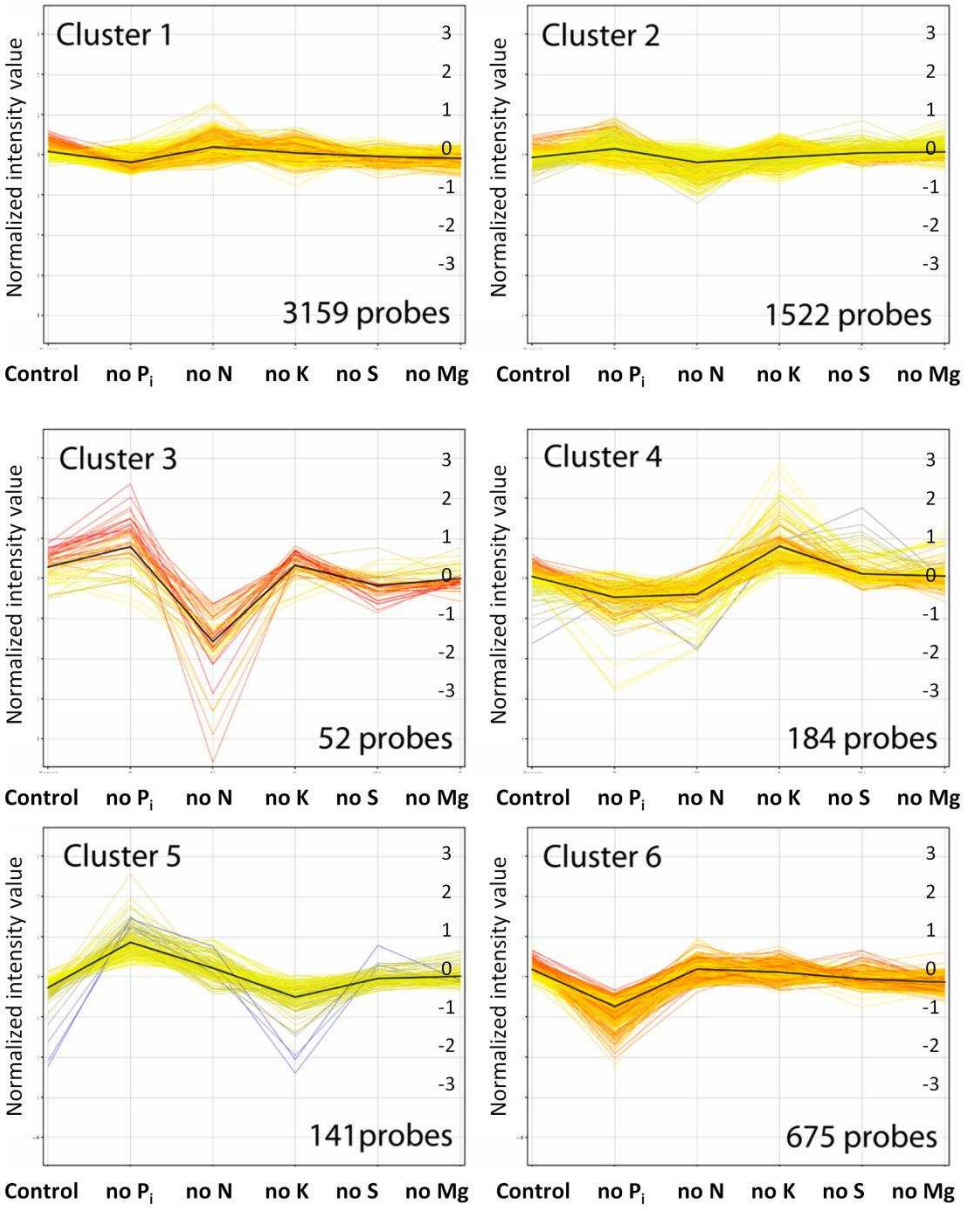

Figure 17: Cluster analysis of wheat gene probes significantly up-or down-regulated (P≤0.05) in wheat roots from Broadbalk at booting in 2011 as a response of long-term P_i, N, Mg, K and S starvation.
Normalized expression data was analysed using GeneSpring GX v. 12.6 (Agilent Technologies). Significantly altered gene probes were determined using a one-way ANOVA (P≤0.05) which compared each nutrient limitation-treatment to the control. 6 clusters were determined using 200 iterations and Euclidean similarity measure. Gene probe annotation is displayed in Table 19 (cluster 3), 20 (cluster 4), 21 (cluster 5) and 22 (cluster 6).

The majority of significantly up- and down-regulated transcripts were in cluster 1 and 2 and 6 (Figure 17). Cluster 1 contained probes with a tendency of down-regulation and cluster 2 contained probes with a tendency of up-regulation (Figure 17). However, cluster 1 and 2 were of little interest as they did not

reveal strongly responsive expression patterns across treatments. Cluster 3 contained the minimum of significantly up- or down-regulated transcripts which were up-regulated under P_i starvation but strongly down-regulated under N starvation (Figure 17, Table 19): TaIPS genes and genes coding for SPX domain containing proteins and glycerophosphodiester phosphodiesterases or other phosphatases like a purple acid phosphatases or an inorganic pyrophosphatase. Cluster 4 contained transcripts which are down-regulated in P_i and N starvation but up-regulated in K starvation (Figure 17, Table 20): Nicotianamine synthase, a nitrate and Zn transporter and cytochrome P450. Cluster 5 exhibited up-regulated probes during P_i starvation of which some are strongly down-regulated in K starved plants such as LEA proteins, dehydrins which are ABA responsive, defensins and membrane associated proteins (Figure 17, Table 21). Interestingly, several probe sequences on the Affymetrix Genechip® originate from wheat leaf samples infected with Septoria tritici[20]. Several of these probes were identified in cluster 5 (Table 21). A BLAST using these sequences revealed a high identity with fungal genes, especially from Mycospharella graminicola, the asexual form of S. tritici, but no sequence identity with plant or wheat genes (Table 21). Therefore, it is likely that these probes were not wheat genes and were not considered further. Cluster 6 contained exclusively down-regulated transcripts under P_i starvation (Figure 17, Table 22), coding for proteins comprising cytochrome P450, jasmonate inducible proteins, a bidirectional sugar transporter, aquaporins, nitrate transporters and many lipid transfer proteins/cell delineating proteins and peroxidases (Table 22). These probes were previously determined through multiple t-tests as being significantly altered (Table 18).

It can be concluded that cluster 3, 5 and 6 are key clusters for understanding the P_i starvation responses in wheat roots and the interaction of these genes when other macronutrients become limiting. The probes in these particular four clusters were also the gene probes significantly differentially regulated in the multiple-t test (Table 18).

[20] Example:
http://wheat.pw.usda.gov/cgi-bin/graingenes/report.cgi?class=sequence;name=CA743242

Table 19: Annotation for a subset of wheat gene probes in cluster 3 derived from transcriptome study on field-grown wheat roots from Broadbalk in 2011 at booting (Figure 17).

Wheat probe ID	Species	Annotation
Ta.13989.1.S1_at	T. aestivum	**Ta IPS** 1.3 miRNA; EU753152
Ta.4399.1.S1_x_at	T. aestivum	**Ta IPS** 1.2 miRNA; EU753151
Ta.6744.1.S1_at / Ta.6744.2.S1_s_at	T. aestivum	**Ta IPS** 1.1 miRNA; EU753150
Ta.6831.1.S1_at	B. distachyon	**SPX** protein 5-like; XP_003557742/LOC100836898
	S. italica	**SPX** protein; XM_004983053 / LOC101754863
TaAffx.64258.1.A1_at	H. vulgare	**Chloroplast purple acid phosphatase** isoform c; FJ974006.1
	Z. mays	**Chloroplast purple acid phosphatase** isoform precursor; NP_001130354
Ta.9492.1.S1_at	B. distachyon	**Glycerophosphodiester phosphodiesterase** GDE1-like; XM_003574982/XM_003574983; LOC100832479
	O. sativa	**Glycerophosphoryl diester phosphodiesterase** family protein; LOC_Os02g31030.2
	A. thaliana	**Glycerophosphodiester phosphodiesterase**/ phosphoric diester hydrolase; senescence-related; AT3G02040
TaAffx.111546.1.S1_s_at	B. distachyon	**Glycerophosphodiester phosphodiesterase**; Bradi3g44290
	O. sativa	**Glycerophosphoryl diester phosphodiesterase** family protein; LOC_Os02g31030.2
	A .thaliana	**Glycerophosphodiester phosphodiesterase**/ phosphoric diester hydrolase; senescence-related; AT3G02040
TaAffx.9237.1.S1_at	T. aestivum	**Ta IPS** 2.2 miRNA; EU753154
TaAffx.11942.1.A1_at	H. vulgare	Uncharacterized protein; AK358914
Ta.24785.1.A1_at	T. urartu	**GDP-mannose-dependent alpha-mannosyltransferase**; EMS60261
	B. distachyon	**GDP-mannose-dependent alpha-mannosyltransferase**-like; XP_003568443
Ta.13993.1.S1_x_at	B. distachyon	**SPX** protein 6-like (Bradi1g21510); XM_003559915
	A. thaliana	**SPX** 3 gene; AT2G45130
Ta.22712.1.S1_at	T. aestivum	**Ta IPS** 2.1 miRNA; EU753153//**Ta IPS** 2.2 miRNA; EU753154
TaAffx.115546.1.S1_at	B. distachyon	**SPX** domain; protein involved in vacuolar polyphosphate accumulation; Bradi1g21510
	O. sativa	**SPX** protein; LOC_Os03g29250.1
	A. thaliana	**SPX** SPX domain gene 3; AT2G45130

Table 19 continued.

Wheat probe ID	Species	Annotation
Ta.6770.1.S1_s_at	B. distachyon	**Glycerophosphodiester phosphodiesterase**; XM_003579607; Bradi5g08710
	O. sativa	**Glycerophosphoryl diester phosphodiesterase** family protein; LOC_Os02g31030.1
	A. thaliana	**Glycerophosphoryl diester phosphodiesterase** family protein; AT5G41080
Ta.12413.1.S1_at	B. distachyon	**Inorganic pyrophosphatase 1**-like, transcript variant 2; LOC100828291; XM_003569652; Bradi2g48420
	O. sativa	**Phosphoethanolamine/phosphocholine phosphatase**; LOC_Os01g52230.1
	A. thaliana	**Phosphatase**; XM_003569652; AT1G73010
TaAffx.104994.1.S1_at	B. distachyon	**SPX** protein 1-like; LOC100840599; XM_003563615
	O. sativa	**SPX** domain containing protein, LOC_Os06g40120.1
	A. thaliana	**SPX** SPX domain gene 2; AT2G26660
Ta.5957.1.S1_at*	H. vulgare	**Ethylene-responsive transcription factor**; putative iron-deficiency specific 4 protein; AP009567.1
	B. distachyon	Protein involved in **vacuolar polyphosphate accumulation**, contains **SPX domain;** Bradi1g36610
	O. sativa	**SPX** domain containing protein; LOC_Os06g40120.1
	A. thaliana	**SPX** SPX domain gene 2; AT2G26660
Ta.24434.1.S1_at	B. distachyon	**Glycerophosphodiester phosphodiesterase** GDE1-like; XM_003579607.1; LOC100823116
TaAffx.114235.1.S1_at	H. vulgare	Predicted, uncharacterized protein; AK358914
Ta.14013.1.S1_at	B. distachyon	**SPX** protein 5-like; vacuolar polyphosphate accumulation, XP_003557742; Bradi1g60250
	O. sativa	**SPX** domain containing protein, putative, expressed LOC_Os10g25310.1
	A. thaliana	**SPX** SPX domain gene 3; AT2G45130

Table 20: Annotation for a subset of wheat gene probes in cluster 4 derived from transcriptome study on field-grown wheat roots from Broadbalk in 2011 at booting (Figure 17).

Wheat probe ID	Species	Annotation
Ta.5549.2.A1_at	H. vulgare	**Nicotianamine synthase** 1; AB010086; 97 % query coverage, 0.0 e-value, 86 % identities
Ta.5549.3.S1_at	H. vulgare	**Nicotianamine synthase** 1; AB010086; 67 % query coverage, 2e-105 value, 83 % identities
Ta.5549.1.S1_a_at / Ta.5549.1.S1_x_at	H. vulgare	**Nicotianamine synthase** 1; AB010086; 83 % query coverage, 0.0value, 92 % identities
	O. sativa	**Nicotianamine synthase** 2; cv. Dongjin-byeo; JQ002674
Ta.21108.1.S1_at	A. tauschii	**Isoflavone 2'-hydroxylase**; EMT05047
	Z. mays	**Cytochrome P450**; CYP81L6; ACG28703
	O. sativa	**Cytochrome P450**; putative ; NP_001046906; Os02g0503700
	B. distachyon	**Isoflavone 2'-hydroxylase-like**; XP_003571092 /XM_003571044
Ta.5145.1.S1_x_at / Ta.5145.1.S1_at	H. vulgare	**Nicochianamine synthase** 3; AB011264
	O. sativa	**Nicotianamine synthase;** LOC_Os03g19427.1
	A. thaliana	**Nicotianamine synthase** 3 (NAS3); AT1G09240
Ta.26144.1.A1_at	H. vulgare	**Nicochianamine synthase** 3 (hvnas3); AB011264
Ta.21127.1.S1_at	T. aestivum	**Low affinity nitrate transporter** (NRT1.1B); NRT1.1C (HF544987); NRT1.1A (HF544985); cv. Paragon
	B. distachyon	**Nitrate transporter** 1.1-like mRNA; LOC100841051; XM_003574264
Ta.5145.4.S1_at / Ta.5145.1.S1_x_at	H. vulgare	**Nicochianamine synthase 3** (hvnas3); AB011264
	O. sativa	**Nicotianamine synthase**; LOC_Os03g19427.1
	A. thaliana	**Nicotianamine synthase 3 (**NAS3); AT1G09240
TaAffx.91995.1.A1_at	T. urartu	**Prolyl endopeptidase**; EMS49886.1
	B. distachyon	**Prolyl endopeptidase**-like (LOC100820865), mRNA; XM_003580272
	S. italica	**Prolyl endopeptidase**-like (LOC101755076), transcript variant X1; XM_004976436
Ta.26144.1.A1_s_at	B. distachyon	**Fatty acyl-CoA reductase 1-like** LOC100838987; XM_003566967 // LOC100822349; XM_003573625
	O. sativa	**Protein male sterility protein**; LOC_Os08g20200.1
	A. thaliana	**FAR1 (fatty acid reductase 1)**; fatty acyl-CoA reductase (alcohol-forming)/ oxidoreductase, acting on the CH-CH group of donors; AT5G22500

Table 20 continued.

Wheat probe ID	Species	Annotation
Ta.12673.1.S1_at	O. sativa	**Protein transposon protein**, putative, CACTA, En/Spm sub-class; LOC_Os12g11330.1
	B. distachyon	**Rho GTPase binding**, formin related, uncharacterized protein; Bradi5g02480
	A. thaliana	Unknown protein; AT3G28840
TaAffx.106421.1.S1_at	T. aestivum	**Zinc transporter** putative zinc transporter (ZIP3); AY864924; Affymetrix LOC606346/606346; metal ion transport, transmembrane transport, zinc ion transmembrane transport
Ta.13134.1.A1_at	H. vulgare	Predicted protein
	O. sativa	Protein UP-9A; LOC_Os02g03710.1
	A. thaliana	Unknown protein; AT2G28671
TaAffx.143995.24.S1_at	T. aestivum	S-responsive protein; EU908729.1
Ta.22548.1.S1_a_at	T. aestivum	**Zinc transporter** (ZIP7); putative
	O. sativa	Protein metal cation transporter; LOC_Os05g10940.1
	A. thaliana	**Zinc transporter** 4 precursor; AT1G10970 ZIP4

Table 21: Annotation for a subset of wheat gene probes in cluster 5 derived from transcriptome study on field-grown wheat roots from Broadbalk in 2011 at booting (Figure 17).

Wheat probe ID	Species	Annotation
Ta.23260.1.S1_at*	M. graminicola	**Phosphate-repressible phosphate permease** (IPO323); hypothetical protein; (MYCGRDRAFT_104538)
Ta.22453.1.S1_at*	M. graminicola	IPO323 hypothetical protein; (MYCGRDRAFT_109517)
TaAffx.77682.1.S1_at*	M. graminicola	NAD-dependent formate dehydrogenase; AF123482
TaAffx.50141.3.S1_s_at*	M. graminicola	Mitochondrion mRNA; EU090238
TaAffx.104595.1.S1_at*	M. graminicola	Mitochondrion mRNA; EU090238
Ta.22406.1.S1_at *	M. graminicola	IPO323 (MgPHO4); XM_003849164
Ta.20930.1.S1_at	T. turgidum ssp. durum	**Defensin** precursor (PRPI-7); GQ449377
Ta.23812.1.S1_a_at	T. aestivum	**ABA induced plasma membrane protein PM-19** (WTABAPM); U80037
	H. vulgare	**Plasma membrane associated protein** (pm19); AF218627
	O. sativa	AWPM-19-like **membrane family protein**; LOC_Os07g24000.1
Ta.13396.1.S1_at	H. vulgare	**Late embryogenesis abundant** group 1**, LEA;** ACV91870
	B. distachyon	**Late embryogenesis abundant** group 1(**LEA**); Bradi1g51800
	O. sativa	**Late embryogenesis abundant** group **1 (LEA),** LOC_Os06g02040.1
	A. thaliana	**LEA** group 1 domain-containing protein; AT1G32560
Ta.22049.1.S1_at	H. vulgare	mRNA for predicted protein; AK362981
Ta.28848.1.S1_at	T. aestivum	clone WT006_L01, cv.Chinese Spring; AK333528
	O. sativa	Heat shock protein; LOC_Os09g30439.1
	B. distachyon	**Late embryogenesis abundant protein** 18; Bradi4g33400
Ta.23659.1.S1_at	T. aestivum	**LEA2** protein (LEA2); AY148491; Affymetrix LEA2 (543396)
Ta.12787.1.S1_at	H. vulgare	mRNA for predicted protein, clone: NIASHv1010M05; AK354749
Ta.4826.2.S1_at	T. aestivum	UFG2 (=unknown function gene); EF675610
Ta.226.1.S1_at	T. aestivum	**Cold-responsive LEA/RAB-related COR protein** (Wrab19); Affymetrix Wrab19 (542854)
Ta.23797.1.S1_x_at	Affymetrix	LOC543476 (543476); response to stress (0006950)

Table 21 continued.

Wheat probe ID	Species	Annotation
Ta.20483.1.S1_at	H. vulgare	**Dehydrin** 6 (dhn6) gene; DQ885460
	O. sativa	**Dehydrin**, LOC_Os11g26570.1
	B. distachyon	**Dehydrin**; response to water; response to stress; Bradi1g37410
	A. thaliana	RAB18 (**responsive to aba** 18); AT5G66400
Ta.20483.2.S1_x_at	H. vulgare	**Dehydrin** 6 (dhn6) gene,; AF043091
	B. distachyon	**Dehydrin**; response to water; response to stress; Bradi2g47580
	O. sativa	**Dehydrin**, putative, expressed; LOC_Os11g26570.1
	A. thaliana	RAB18 (**responsive to aba** 18); AT5G66400
TaAffx.50285.1.S1_at*	M. graminicola	IPO323 phosphate-repressible phosphate permease (MgPHO4)
Ta.8629.1.A1_at	Affymetrix	**Lipid transport** (0006869); lipid binding (0008289) ; WLTP1 (100125701)
	A. tauschii	Hypothetical protein; EMT01750
Ta.28052.1.S1_at	H. vulgare / A.tauschii	Hypothetical proteins; BAJ85823.1, EMT02151.1; Affymetrix LOC543273 (543273); photorespiration , carbon fixation , photosynthesis, chloroplast, plastid, monooxygenase activity, oxidoreductase activity, lyase activity, ribulose-bisPhosphate carboxylase activity
Ta.14281.1.S1_at	T. aestivum	**Defensin**; AB089942; Affymetrix Tad1 (542796); defense response
Ta.5899.1.S1_at*	Affymetrix	wheatpab (543264); **protein serine/threonine phosphatase** [Micromonospora sp. L5)
Ta.9063.3.S1_x_at	T. aestivum	**S-adenosylmethionine decarboxylase** (SAMDC); cv. NR1121; GU016570 Affymetix SAMDC (100682430); polyamine and spermine biosynthetic process; adenosylmethionine decarboxylase activity; lyase and carboxy-lyase activity
	B. distachyon	**Adenosylmethionine decarboxylase** ; Bradi3g48490
	O. sativa	**S-adenosyl-l-methionine decarboxylase** leader peptide; LOC_Os04g42095.1
	A. thaliana	**Adenosylmethionine decarboxylase** family protein; AT3G25570

*Probe sequence extracted from S. tritici infected wheat leaves

Table 22: Annotation for a subset of wheat gene probes in cluster 6 derived from transcriptome study on field-grown wheat roots from Broadbalk in 2011 at booting (Figure 17).

Wheat probe ID	Species	Gene Annotation
Ta.14580.3.S1_x_at	T. aestivum	**Peroxidase** (Prx109-B) gene, class III ; Prx109-B-5 allele; response to oxidative stress, oxidation-reduction process
Ta.5426.2.A1_a_at	T. aestivum	**Cytochrome P450**; CypX superfamiliy**;** ABU54407
	B. distachyon	**Cytochrome P450** CYP2 subfamily; beta-carotene 15,15'-monooxygenase; Bradi1g22340
	O. sativa	**Cytochrome P450**; LOC_Os12g32850.1
	A. thaliana	**Cytochrome P450** 71B2; CYP71B2; electron carrier/ heme binding / iron ion binding / monooxygenase/ oxygen binding; AT1G13080
Ta.19473.1.S1_at	T. aestivum	No annotation available; similar to (Ta.19473.1.S1_x_at, (Ta.19473.1.S1_at)
TaAffx.79196.1.S1_at	T. aestivum	**Jasmonate-induced** protein; AAR20919
TaAffx.84394.1.S1_at	H. vulgare	**Jasmonate-induced** protein; BAK00621
Ta.14580.2.S1_x_at/ Ta.14580.3.S1_x_at	T. aestivum	**Peroxidase** (Prx109-B) gene, class III; Prx109-B-5 allele, complete cds; EU725468; Affymetrix Prx109-C; response to oxidative stress; oxidation-reduction process; peroxidase activity; oxidoreductase activity; heme binding; metal ion binding
	B. distachyon	**Peroxidase** (oxidation reduction/heme binding/response to oxidative stress/peroxidase activity); Bradi2g20850
	O. sativa	**Peroxidase** precursor; LOC_Os05g41990.1
	A. thaliana	**Peroxidase** ; RCI3 (rare cold inducible gene 3); AT1G05260
TaAffx.111581.1.S1_at	T. aestivum	T. aestivum clone; wr1.pk0136.c2fis; BT009535
Ta.1807.1.S1_at	A. tauschii	**Peroxidase** 2; EMT07517
	O. sativa	**Peroxidase**; LOC_Os07g44600.1
	B. distachyon	**Peroxidase** (oxidation reduction/heme binding/response to oxidative stress/peroxidase activity); Bradi1g19980
Ta.19176.1.S1_at	A. tauschii	**Peroxidase** 2; EMT25063
TaAffx.113831.1.S1_at	H. vulgare	Predicted, uncharacterized protein; AK357789
TaAffx.82031.1.S1_s_at	B. distachyon	**Peroxidase** 54-like (oxidation reduction/heme binding/response to oxidative stress/peroxidase activity); XM_003563078; Bradi1g27920
	O. sativa	**Peroxidase** precursor; LOC_Os10g02040.1
	A. thaliana	**Peroxidase** 22 (PER22) (P22) (PRXEA) / basic peroxidase E; AT2G38380

Table 22 continued.

Wheat probe ID	Species	Gene Annotation
Ta.16683.1.A1_at	B. distachyon	BURP domain-containing protein 13-like (LOC100821750);XM_003577522
TaAffx.12181.1.S1_at	T. urartu	**Bidirectional sugar transporter** SWEET17; EMS58275
	S. italica	**Bidirectional sugar transporter**; SWEET17-like; LOC101779488; XM_004967460
Ta.1840.1.S1_at	T. aestivum	**Proteolysis; lipid transport**; Affymetrix wheat annotation LOC100136980 (100136980)
	B. distachyon	**Protease inhibitor**/seed storage/LTP family; Bradi3g50900
	O. sativa	**Protease inhibitor**/seed storage/LTP family protein precursor; LOC_Os04g46820.1
	A. thaliana	**Protease inhibitor/seed storage/lipid transfer protein (LTP) family protein**; AT4G12510
Ta.13950.1.S1_x_at	A.tauschii	**Cortical cell-delineating protein**; EMT02055
	O. sativa	**Protease inhibitor/seed storage**/LTP family protein precursor; protein LTPL114; LOC_Os03g01300.1
	B. distachyon	**Protease inhibitor/seed storage**/LTP family; Bradi1g78260
Ta.952.2.S1_a_at	T. aestivum	**Peroxidase**; class II; EU725468; Affymetrix Prx110-A (100415850); response to oxidative stress; oxidation-reduction process
	B. distachyon	**Peroxidase** (oxidation reduction/heme binding/response to oxidative stress/peroxidase activity); Bradi1g32870
	O. sativa	**Peroxidase** precursor; LOC_Os06g46799.1
	A. thaliana	**Extensin-like protein**; lipid binding; AT1G12090
Ta.18487.1.S1_x_at	T. aestivum	**Cold-responsive** protein; AF271260.1
Ta.25187.1.A1_at	H. vulgare	Predicted uncharacterized protein; AK248326
	B. distachyon	Domain of unknown function (DUF588); Bradi4g11420:
	O. sativa	Protein integral membrane protein TIGR01569 containing protein; LOC_Os11g42960.1
	A. thaliana	**Splicing factor** PWI domain-containing protein; AT2G29210
Ta.19183.2.S1_at	H. vulgare	Predicted, uncharacterized protein
Ta.994.1.S1_at (Ta.994.1.S1_x_at)	Z. mays	**Cortical cell-delineating protein** (LOC100280973); NM_001153893
	B. distachyon	**Protease inhibitor/seed storage/LTP family**; Bradi1g78260
	O. sativa	**Protease inhibitor/seed storage/LTP** family protein precursor; LTPL114 protein; LOC_Os03g01300.1
	A. thaliana	**Protease inhibitor/seed storage/lipid transfer protein (LTP) family protein**; AT4G12470

Table 22 continued.

Wheat probe ID	Species	Gene Annotation
Ta.23377.1.S1_x_at	T. urartu	**Cortical cell-delineating protein**; EMS68038
TaAffx.138472.1.S1_s_at	T. aestivum	clone; SET3_D17; AK336100
Ta.5435.1.S1_x_at	Z. mays	**Cortical cell-delineating protein** (LOC100286227); NM_001159115
	B. distachyon	**Protease inhibitor/seed storage/LTP** family; Bradi1g78260
	O. sativa	**Protease inhibitor/seed storage/LTP** family protein precursor; lipid binding; LOC_Os03g01300.1
	A. thaliana	**Extensin-like protein**; lipid binding; AT1G12090
Ta.8805.1.A1_at	H. vulgare	**Peroxidase** (PRX2) gene; Class III; cv. Karat; JQ649324
	B. distachyon	**Peroxidase**; oxidation reduction; heme binding; response to oxidative stress Bradi1g26870
	O. sativa	**Peroxidase** precursor; LOC_Os07g31610.1
	A. thaliana	**peroxidase**; cationic; AT1G30870
Ta.5406.1.S1_at	B. distachyon	**Peroxidase** 2-like; (LOC100841701), mRNA; XM_003561555
Ta.1840.1.S1_x_at (Ta.1840.1.S1_a_at)	T. aestivum	**Protease inhibitor**-like protein (PI-3); EU293132
	B. distachyon	**Protease inhibitor/seed storage/LTP** family; Bradi3g50900
	O. sativa	**Protease inhibitor/seed storage/LTP** family protein precursor; protein LTPL121; LOC_Os04g46820.1
	A. thaliana	**Protease inhibitor/seed storage/lipid transfer protein** (**LTP**) family protein; AT4G12510
Ta.14010.3.S1_x_at	T. urartu	**Peroxidase** 2; EMS58804
	B. distachyon	**Peroxidase**; oxidation reduction; heme binding; response to oxidative stress; Bradi1g61540
	O. sativa	**Peroxidase** precursor; LOC_Os03g25330.1
	A. thaliana	**Peroxidase**; rare cold inducible gene 3 (RCI3); AT1G05260
Ta.2870.1.S1_at	T. aestivum	**Glutamine synthetase** isoform GSr2 (GS) gene; AY491969
	B. distachyon	**Glutamate-ammonia ligase** activity, ATP binding; glutamine synthetase; Bradi1g69530
	O. sativa	**Glutamine synthetase**, catalytic domain containing protein; LOC_Os03g12290.1
	A. thaliana	**Copper ion binding / glutamate-ammonia ligase**; ATGSR1; AT5G37600
Ta.29534.1.S1_x_at/ Ta.29534.1.S1_at	H. vulgare	**Cysteine proteinase**; Z97022

Table 22 continued.

Wheat probe ID	Species	Gene Annotation
Ta.5652.1.S1_at	T. aestivum	**Tonoplast intrinsic protein** (AQP5); DQ867079
	B. distachyon	**Nitrate transmembrane transporter** activity, cation channel activity; aquaporin (major intrinsic protein family); Bradi3g50690
	O. sativa	**Aquaporin protein**; LOC_Os02g44080.1
	A. thaliana	**Ammonia transporter**/methylammonium transmembrane transporter/ water channel (AtTIP2); AT5G47450
Ta.28162.1.S1_at	T. urartu	**Cortical cell-delineating protein**; EMS64339; ; 48% query coverage, 6e-32value; 95% identities
	B. distachyon	**Protease inhibitor/seed storage/LTP family**; Bradi1g78260
	O. sativa	**Protease inhibitor/seed storage/LTP** family protein precursor; (**LTP**L114); LOC_Os03g01300.1
	A. thaliana	**Extensin-like protein**; lipid binding; AT1G12090
Ta.9396.1.S1_x_at	Z. mays	**Xyloglucan endotransglycosylase**/hydrolase; protein 8 precursor; clone 291197; EU966049
	B. distachyon	**Glycosyl hydrolase** (GH), subfamily GH16; hydrolase activity, hydrolyzing O-glycosyl compounds; carbohydrate metabolism; glucan metabolism; apoplast; Bradi3g18590
	O. sativa	**Glycosyl hydrolases** family 16; LOC_Os08g13920.1
	A. thaliana	**Xyloglucan endotransglucosylase/hydrolase** 20 (XTH20); AT5G48070

3.3.4. Cross-comparison study

There are many genes regulated similarly during P_i starvation in model plants, other crops and wheat which could be assigned to the previously defined clusters (Tables 23). There was no particular difference between root and the shoot responses (Table 23).

Table 23: Wheat gene probes induced or down-regulated in field-grown wheat roots from Broadbalk in 2011 at booting as a response of long-term P_i fertilizer withdrawal (Figure 17, Table 18) overlapping with data from studies on gene responses to P_i starvation in model plant tissues and other cereal crops sorted according to the wheat cluster assignment.

Reference (treatment)	Tissue	Species	Cluster					
			1	2	3	4	5	6
Calderón-Vázquez et al. 2008	Root	Z. mays	14	13	4	3	*	12
Cai et al. 2013_N_def_1 h up	Root	O. sativa	*	2	*	*	*	1
Cai et al. 2013_N_def_24 h up			*	*	1	*	1	1
Cai et al. 2013_N_def_7 d up			9	4	1	*	*	12
Cai et al. 2013_P_i_def_1 h up								
Cai et al. 2013_P_i_def_24 h up			*	4	*	*	1	3
Cai et al. 2013_P_i_def_7 d up			3	2	5	*	*	4
Dai et al. 2012_6 to 72 h up	Seedlings	O. sativa	7	6	*	2	1	6
Dai et al. 2012_6 to 72 h down			3	5	*	1	*	1
Dai et al. 2012_6 h up	Seedlings	O. sativa	121	40	3	10	4	56
Dai et al. 2012_6 h down			45	28	*	5	2	7
Dai et al. 2012_24 h up			78	69	1	11	7	29
Dai et al. 2012_24 h down			98	36	1	14	2	28
Dai et al. 2012_48 h up			90	25	2	6	1	69
Dai et al. 2012_48 h down			19	22	*	3	4	10
Dai et al. 2012_72 h up			16	14	2	4	2	16
Dai et al. 2012_72 h down			188	83	2	11	10	30
Morcuende et al. 2007_ 30min_3 h of P_i re-supply	Seedlings	Arabidopsis	*	*	3	*	*	*
Hammond et al. 2007_ Pho1 mutant	Leaves		32	15	3	*	2	10
Mission et al. 2005_ 3,6 and 12 h_ 1_2 days_ pooled_ P_i stavation	Root and leaves		30	14	3	*	*	4
Wu et al. 2003_ 6_24_48_72_h P_i starvation	Root and leaves		40	11	*	1	2	7
Woo et al. 2012_10 days depletion_3 days P_i re-suppy	Root		9	11	3	5	1	9
Müller et al. 2007_ 1 week P_i starvation_4 h sucrose addition	Leaves		1	4	*	1	*	*

However, overlapping transcript responses could only be detected when wheat genes were assigned to a corresponding gene in rice or Arabidopsis (Table 24 to 29). Therefore, wheat genes which still lack functional annotation or lack homologues genes in other species are not taken into account. This has to be considered when using this comparative approach. Examples are the MYB-related transcription factor (Ta.25744.1.S1_at) (Table 18 A) or the TaIPS genes (Table 18 C).

Table 24: Subset of wheat gene probes assigned to cluster 1 (Figure 17) overlapping with other model plants and crops gene probes with altered gene expression in responses to P_i starvation (Table 23).

The annotation for a subset of T. aeastivum or other wheat ancestor probe-sets (Affymetrix Genechip® Wheat Genome Array) was done using the NCBI BLAST(x)[21] database. Rice, maize and Arabidopsis gene were assigned in GeneSpring v. 12.6. to wheat probes using the 'HarvEST annotation' [22] database using the threshold of a minimum of one perfect-match probes.

Wheat probe ID	References	Gene annotation			
		Wheat/ancestors/barley/ maize/ other species	**B. distachyon**	**O. sativa**	**A. thaliana**
Ta.3031.2.S1_at	Dai et al. 2012_6 to 72 h up	**MYB 75**; JN857310; T. aestivum cv. Shannong 0431	**MYB**-related transcription factor; DNA-binding domain; Bradi2g36730	**MYB family transcription factor** LOC_Os05g04820.1	**MYB domain protein** 61; transcription factor; AT1G09540
Ta.23848.2.A1_a_at	Dai et al. 2012_6_48 h down	**Potassium transporter** 7; EMT06515; A. tauschii	**Potassium transmembrane transporter**; Bradi1g18600	**Potassium transporter**; LOC_Os07g47350.2	**K^+ uptake transporter 3**; AT3G02050
Ta.25770.2.S1_at	Hammond et al. 2007	**Extensin-like protein** (LOC100384424); NM_001176961; Z. mays	No functional annotation; Bradi2g01060	No functional annotation; LOC_Os01g02160.1	**Hydroxyproline-rich glycoprotein** family protein; AT1G70985
Ta.19603.1.S1_s_at	Calderón-Vázquez et al. 2008	**CYP51**; Obtusifoliol 14-alpha-demethylase; Y09291; T. aestivum	**Cytochrome P450, family 51 (sterol 14-demethylase)**;Bradi4g25930	**Cytochrome P450** (51); LOC_Os11g32240.1	**Cytochrome P450** (51G1); oxygen binding/sterol 14-demethylase; AT1G11680
Ta.2641.1.S1_at	Hammond et al. 2007	**Glutamate synthase** (NADH-GOGAT-3B) gene; NADH-dependent; KC960544; T. turgidum	**Glutamate synthase** (NADPH) activity, glutamate synthase Bradi2g46670	**Glutamate synthase**, chloroplast precursor; LOC_Os01g48960.1	**Glutamate synthase** (NADH); AT5G53460
Ta.28728.1.S1_x_at / Ta.28728.1.S1_at	Dai et al. 2012_24_48 h up	**Plasma membrane intrinsic protein 2**; / aquaporin 7 (AQP7); HQ650109; T. aestivum	**Nitrate transmembrane transporter; aquaporin transporter;** Bradi3g49360	**Aquaporin protein** LOC_Os02g41860.2	**Plasma membrane intrinsic protein** 2A; **water channe**l; AT3G53420

[21] http://blast.ncbi.nlm.nih.gov/Blast.cgi
[22] http://www.harvest-web.org/

Table 24 continued.

Wheat probe ID	References	Gene annotation			
		Wheat/ancestors/barley/ maize/ other species	**B. distachyon**	**O. sativa**	**A. thaliana**
Ta.1666.1.S1_a_at	Dai et al. 2012_6 to 72 h up	Protein without annotation; AK366067; H. vulgare	No functional annotation; Bradi1g00920	**Receptor protein kinase**; LOC_Os03g64030.1	**Hydrolase**; AT4G34215
Ta.10107.2.S1_a_at	Mission et al. 2005, Wu et al. 2003	**Fructokinase 1** (frk1); NM_001111740; Z. mays	**pfkB** family carbohydrate kinase;sugar kinase related; ribokinase-related; **fructokinase**; Bradi2g57500	**Protein kinase**, pfkB family; LOC_Os01g66940.1	**Carbohydrate kinase** family protein; **pfkB**-type; AT2G31390
Ta.1580.1.A1_a_at	Mission et al. 2005	**Glycerol-3-phosphate dehydrogenase**; (TaGPDH3), KC953027; T. aestivum	**NAD-dependent glycerol-3-phosphate dehydrogenase**/dihydroxyacetone 3-phosphate reductase; Bradi2g62020	**Glycerol-3-phosphate dehydrogenase**; LOC_Os01g74000.1	**Glycerol-3-phosphate dehydrogenase** (NAD+)/ GPDH; AT5G40610
Ta.3504.1.A1_at (**+N**: 1.27)	Dai et al. 2012 _24 h down	**Asparaginase gene**; AF308474; H. vulgare	No functional annotation; Bradi5g24230	**Transposon protein**; LOC_Os04g55710.1	**L-asparaginase/ asparagine amidohydrolase**; AT3G16150
Ta.5396.2.S1_a_at	Dai et al. 2012_6 to 72 h up	Bowman-Birk type **trypsin inhibitor**; EMS35637; T. urartu	Bowman-Birk **serine protease inhibitor family**; **serine protease** inhibitor activity; Bradi2g01920	protein BBTI8 - Bowman-Birk type bran **trypsin inhibitor precursor;** LOC_Os01g03680.1	

Table 25: Subset of wheat gene probes assigned to cluster 2 (Figure 17) overlapping with other model plants and crops gene probes with altered gene expression in responses to P_i starvation (Table 23).

The annotation for a subset of T. aeastivum or other wheat ancestor probe-sets (Affymetrix Genechip® Wheat Genome Array) was done using the NCBI BLAST(x)[23] database. Rice, maize and Arabidopsis gene were assigned in GeneSpring v. 12.6. to wheat probes using the 'HarvEST annotation' [24] database using the threshold of a minimum of one perfect-match probes.

Wheat probe ID	References	Gene annotation			
		Wheat/ancestors/barley/ maize/other species	**B. distachyon**	**O. sativa**	**A. thaliana**
Ta.11849.1.S1_at (**+P**: 1.17)	Dai et al 2012_72 h up	**TaMYB59 MYB-related protein**; JF951942; T. aestivum	**MYB-related transcription factor**; Bradi1g29680	**MYB family transcription factor** LOC_Os06g51260.2	
Ta.7524.2.A1_x_at / Ta.7524.3.S1_at / TaAffx.28555.1.S1_s_at	Dai et al. 2012_6 to 72 h up	**Late elongated hypocotyl**; HQ222606; T. aestivum	No functional annotation; Bradi3g16510	**MYB family transcription factor**; LOC_Os08g06110.5	**Late elongated hypocotyl;** DNA binding/ transcription factor; AT1G01060
Ta.10772.1.A1_at	Calderón-Vázquez et al. 2008	**Auxin-induced protein** 5NG4; EMS56196; T. urartu	**EamA-like transporter family**; Bradi1g25930	**Integral membrane protein** DUF6 containing; LOC_Os07g34110.1	**Nodulin** MtN21 family protein; AT5G64700:
Ta.11166.1.A1_at	Calderón-Vázquez et al. 2008, Hammond et al. 2007, Mission et al. 2005, Woo et al. 2012, Müller et al. 2007, Dai et al. 2012_24_48 h up	**Glycerol-3-phosphate transporter** 1; EMS66165; T. urartu// **sugar phosphate exchanger 2**; EMT30609; A. tauschii	**Sugar:hydrogen symporter activity, organophosphate:inorganic phosphate antiporter activity**; Bradi3g16640	**Transporter, major facilitator family**; LOC_Os08g06010.1	**Glycerol-3-phosphate transporter;** glycerol 3-phosphate permease; AT3G47420
Ta.13285.2.S1_s_at	Mission et al. 2005		**Serine-threonine protein kinase**;Tyrosine kinase specific for activated (GTP-bound); Bradi3g60210	**Protein kinase** domain containing protein; LOC_Os02g54510.3	**Protein kinase** family; AT5G57610
Ta.12436.1.S1_at	Dai et al. 2012_24 h up, Woo et al. 2012	**Purple acid phosphatase** 22-like isoform X2; XP_004977563; S. italica	No functional annotation; Bradi4g42520	**Ser/thr protein phosphatase** protein; LOC_Os11g05400.1	**Purple acid phosphatase** 22; protein serine/threonine phosphatase; AT3G52820

[23] http://blast.ncbi.nlm.nih.gov/Blast.cgi
[24] http://www.harvest-web.org/

Table 25 continued.

Wheat probe ID	References	Gene annotation			
		Wheat/ancestors/barley/ maize/other species	**B. distachyon**	**O. sativa**	**A. thaliana**
Ta.14152.3.S1_at	Hammond et al. 2007		**Dual-specificity kinase**; Bradi4g38310	**Serine/threonine-protein kinase** AFC3; LOC_Os01g40840.1	**ATP binding, kinase/ protein serine/threonine kinase**; AT3G53570
Ta.1780.3.S1_x_at / Ta.1780.1.S1_at	Cai et al. 2013_N_def_7 d up	**6-phosphogluconate dehydrogenase**; EMS56831; T. urartu A.tauschii	**Phosphogluconate dehydrogenase**; pentose-phosphate shunt; Bradi1g54350	**Protein 6-phosphogluconate dehydrogenase**; LOC_Os11g29400.1	**6-phosphogluconate dehydrogenase** family protein; AT1G64190

Table 26: Subset of wheat gene probes assigned to cluster 3 (Figure 17) overlapping with other model plants and crops gene probes with altered gene expression in responses to P_i starvation (Table 23).

The annotation for a subset of T. aeastivum or other wheat ancestor probe-sets (Affymetrix Genechip® Wheat Genome Array) was done using the NCBI BLAST(x)[25] database. Rice, maize and Arabidopsis gene were assigned in GeneSpring v. 12.6. to wheat probes using the 'HarvEST annotation' [26] database using the threshold of a minimum of one perfect-match probes.

Wheat probe ID	**References**	**Gene annotation**			
		Wheat/ancestors/barley/ maize/other species	**B. distachyon**	**O. sativa**	**A. thaliana**
Ta.12413.1.S1_at (**-N**: 2.01 / **+P**: 1.35 / **-Mg**: 1.22)	Calderón-Vázquez et al. 2008, Hammond et al. 2007, Mission et al. 2005, Woo et al. 2012, Müller et al. 2007, Morcuende et al. 2007	**Phosphatase**; putative EMT33032.1; A. tauschii // **Inorganic pyrophosphatase** 1-like, transcript variant 2 XM_003569652; Bradi2g48420	**Phosphatase**; putative; phosphoric monoester hydrolase activity; Bradi2g48420	**Phosphoethanolamine/ phosphocholine phosphatase**; LOC_Os01g52230.1	**Phosphatase**; AT1G73010
Ta.13993.1.S1_x_at (**-N**: 2.23 / **+P**: 0.90)	Calderón-Vázquez et al. 2008, Dai et al. 2012_6_48_72 h up, Hammond et al. 2007, Mission et al. 2005, Woo et al. 2012, Morcuende et al. 2007	Protein without annotation; AK375927.1; H. vulgare	**SPX domain containing protein 6-like;** vacuolar polyphosphate accumulation; Bradi1g21510	**SPX domain-containing protein;** LOC_Os03g29250.1	**SPX domain gene** 3; AT2G45130
Ta.14013.1.S1_at (**-N**: 1.23 / **+P**: 0.90)	Calderón-Vázquez et al. 2008, Hammond et al. 2007, Mission et al. 2005, Woo et al. 2012, Morcuende et al. 2007	**SPX domain containing protein**; predicted; XM_004983053.1; S. italica	**SPX domain containing protein 5-like;** vacuolar polyphosphate accumulation; Bradi1g60250	**SPX domain-containing protein;** LOC_Os03g29250.1	**SPX domain gene** 3; AT2G45130

[25] http://blast.ncbi.nlm.nih.gov/Blast.cgi
[26] http://www.harvest-web.org/

Table 26 continued.

Wheat probe ID	References	Gene annotation			
		Wheat/ancestors/barley/ maize/other species	**B. distachyon**	**O. sativa**	**A. thaliana**
TaAffx.115546.1.S1_at /TaAffx.111546.1.S1_x_at (**-N**: -2.09, +**P**: 0.47 / **-N**: -1.26, +**P**: 0.25)	Dai et al 2012_6_48_72 h up		**SPX domain containing protein 6-like**; vacuolar polyphosphate accumulation; Bradi1g21510	**SPX domain-containing protein;** LOC_Os03g29250.1	**SPX domain gene** 3; AT2G45130
Ta.9492.1.S1_at (**-N**: 2.66 / **+P**: 0.79)	Cai et al. 2013_P_def_7 d up	**Glycerophosphodiester phosphodiesterase** GDE1; A. tauschii	**Glycerophosphodiester phosphodiesterase activity;** predicted starch-binding; Bradi3g44290	**Glycerophosphoryl diester phosphodiesterase family protein**; LOC_Os02g31030.2	**Senescence-related gene** 3; **glycerophosphodiester phosphodiesterase**/ phosphoric diester hydrolase; AT3G02040
Ta.6770.1.S1_s_at (**+P**: 1.16 / **-N**: 1.99)	Cai et al. 2013_P_def_7 d up	**Glycerophosphodiester PhosPhodiesterase**; XM_003579607; B. distachyon	**Glycerophosphodiester PhosPhodiesterase activity;** predicted starch-binding protein; Bradi3g44290	**Glycerophosphodiester phosphodiesterase**; starch binding; LOC_Os02g31030.2	**Glycerophosphodiester phosphodiesterase**/ phosphoric diester hydrolase; senescence-related gene 3; AT3G02040
TaAffx.111546.1.S1_s_at (**+P**:1.01 / **-N**: 1.26)	Cai et al. 2013_P_def_7 d up, Cai et al. 2013 _P_def_7 d up,		No functional annotation; Bradi5g08710	**Glycerophosphodiester PhosPhodiesterase**; starch binding; LOC_Os02g31030.2	**Glycerophosphoryl diester phosphodiesterase** family protein; AT5G41080
TaAffx.57156.1.S1_x_at (**-N**: 1.25 / **+P**: 0.54)	Cai et al.2013 _N_def_24 h_7 d up, Cai et al.2013 _P_def_7 d up, Dai et al. 2012_24_72 h_down_6 h up	**Abscisic stress-ripening protein** 2; EMT26478/EMS47440; A. tauschii/T. urartu	No functional annotation; Bradi5g10030	**Abscisic stress-ripening;** LOC_Os04g34600.1	
Ta.27098.1.S1_at (**+K**: 1.53 / **-P**: 0.66)	Dai et al 2012_24 h down	**Defensin** Tk-AMP-D1.1; EMS52277; T. urartu	**Defense response;** gamma-thionin family; Bradi1g76420	**Defensin and Defensin-like DEFL** family protein**;** LOC_Os03g03810.1	**Peptidase inhibitor**; low-molecular-weight cysteine-rich 68; AT2G02130

Table 27: Subset of wheat gene probes assigned to cluster 4 (Figure 17) overlapping with other model plants and crops gene probes with altered gene expression in responses to P_i starvation (Table 23).

The annotation for a subset of T. aeastivum or other wheat ancestor probe-sets (Affymetrix Genechip® Wheat Genome Array) was done using the NCBI BLAST(x)[27] database. Rice, maize and Arabidopsis gene were assigned in GeneSpring v. 12.6. to wheat probes using the 'HarvEST annotation' [28] database using the threshold of a minimum of one perfect-match probes.

Wheat probe ID	References	Gene annotation			
		Wheat/ancestors/barley/ maize/other species	**B. distachyon**	**O. sativa**	**A. thaliana**
Ta.26144.1.A1_at / Ta.26144.1.A1_s_at (+**K**: 1.25 / **–P**: -1.29)	Calderón-Vázquez et al. 2008, Woo et al. 2012	**Nicochianamine synthase 3**; AB011264; H .vulgare	**Male sterility protein;** 2-related; acyl-CoA reductase; steroid biosynthesis; Bradi3g20000	**Male sterility protein**; LOC_Os08g20200.1	**Fatty acid reductase** 1; fatty acyl-CoA reductase; AT5G22500
Ta.975.1.S1_a_at / Ta.975.2.S1_x_at (**+K**: 1.83)	Dai et al 2012_24 h_72 h up	Protein without annotation; AK252724; H. vulgare	No functional annotation; Bradi2g44950	Expressed protein; LOC_Os01g45470.1	**Prenylcysteine methylesterase**; AT5G15860
Ta.27744.2.S1_a_at / Ta.27744.1.S1_x_at	Dai et al 2012_24_72 h up	**Nucleoside-triphosphatase**; EMT30219 /EMS57965; Aegilops tauschii/T. urartu	**Adenosine/guanosine diphosphatase**; GDA1/CD39 nucleoside phosphatase family; Bradi3g06420	**Nucleoside-triphosphatase**; LOC_Os11g03290.1	**Nucleotide diphosphatase**; Apyrase 2; ATPase/ AT5G18280
Ta.1574.1.S1_s_at	Wu et al. 2003	**Copper chaperone**; CAE51321; H. vulgare	Heavy-metal-associated domain; **copper transport protein** ATOX1-RELATED; Bradi3g44820	Protein heavy metal-associated domain containing protein; LOC_Os02g32814.1	**Copper chaperone**; AT3G56240
Ta.22548.1.S1_a_at	Woo et al. 2012	**Zinc transporter (ZIP7)**; DQ490134; T. aestivum //Affymetrix: 100136969	**ZIP Zinc transporter**; Fe2+/Zn2+ regulated transporter; Bradi2g33110	Metal cation transporter; LOC_Os05g10940.1	**Zinc transporter 4 precursor**; AT1G10970
Ta.25114.1.S1_at / Ta.25114.1.S1_at	Cai et al. 2013 _24 h up	**Nicotianamine aminotransferase B**; AB005788; H. vulgare	**HPP family;** Bradi1g12280	**Integral membrane HPP family protein**; LOC_Os03g48030.1	**Integral membrane HPP family protein**; AT5G62720

[27] http://blast.ncbi.nlm.nih.gov/Blast.cgi
[28] http://www.harvest-web.org/

Table 27 continued.

Wheat probe ID	References	Gene annotation			
		Wheat/ancestors/barley/ maize/other species	**B. distachyon**	**O. sativa**	**A. thaliana**
Ta.14087.1.S1_at (**+Mg**: 2.01 / **+K**: 1.65)	Dai et al. 2012_24 h_up	**Gibberellin 20 oxidase 1**; EMT01311; A. tauschii	**Iron/ascorbate family oxidoreductases;** 2OG-Fe(II) oxygenase superfamily; Bradi1g14580	**Gibberellin 20 oxidase** 2; LOC_Os03g42130.1	**Oxidoreductase**, 2OG-Fe(II) oxygenase family; AT3G19000
Ta.25385.1.S1_at	Dai et al. 2012_6_24 h_ up	**Indole-3-acetate beta-glucosyltransferase** 1; EMT04529; A. tauschii	**UDP-glucoronosyl and UDP-glucosyl transferase**; transferring hexosyl groups; Bradi2g05050	**UDP-glucoronosyl and UDP-glucosyl transferase** domain containing protein; LOC_Os01g08440.1	**UDP-glucosyltransferase** 75B1; AT1G05560
Ta.667.1.A1_at / Ta.667.2.S1_a_at (**-N:** -1.69 / **-P**: -1.11)	Dai et al. 2012_48 h up-regul.	Protein without annotation; AK336149; T. aestivum	**HPP family;** Bradi1g12280	**Integral membrane HPP family protein**; LOC_Os03g48030.1	**Integral membrane HPP family protein**; AT5G62720
Ta.27744.2.S1_a_at / Ta.27744.1.S1_x_at	Cai et al. 2013_24 h up, Dai et al. 2012_24 h up	**Nucleoside-triPhosphatase**; EMT30219 /EMS57965; A.s tauschii/T. urartu	**Cellulose synthase**; N-**acetylglucosaminyltransferase-related**; UDP-forming activity; Bradi1g50170	**Cellulose synthase**-like family F; CSLF6 - ; beta1,3;1,4 glucan synthase; LOC_Os08g06380.2	**Cellulose-synthase** like D2; transferring glycosyl groups; AT5G16910
Ta.975.2.S1_x_at	Dai et al. 2012_72 h up-regul.		**Chlorophyll A-B binding protein**; Bradi1g55560	**Early light-induced protein**, chloroplast precursor; LOC_Os01g14410.1	**Early light-inducable protein**; chlorophyll binding; AT3G22840

Table 28: Subset of wheat gene probes assigned to cluster 5 (Figure 17) overlapping with other model plants and crops gene probes with altered gene expression in responses to P_i starvation (Table 23).

The annotation for a subset of T. aeastivum or other wheat ancestor probe-sets (Affymetrix Genechip® Wheat Genome Array) was done using the NCBI BLAST(x)[29] database. Rice, maize and Arabidopsis gene were assigned in GeneSpring v. 12.6. to wheat probes using the 'HarvEST annotation' [30] database using the threshold of a minimum of one perfect-match probes.

Wheat probe ID	References	Gene annotation			
		Wheat/ancestors/barley/ maize/other species	**B. distachyon**	**O. sativa**	**A. thaliana**
Ta.30113.1.S1_at	Cai et al. 2013_P_def_24 h up	**Galactinol synthase** (TaGolS2); AB250357; T. aestivum //Affymetrix: TaGolS2	**Glycosyl transferase** family 8; glycogenin; Bradi1g64120	**Glycosyl transferase** 8 domain containing protein; LOC_Os07g48830.1	**Galactinol synthase** 3; AT1G09350
Ta.10909.1.S1_s_at / (Ta.10909.1.S1_x_at)	Dai et al. 2013_24 h up		No functional annotation; Bradi1g42710	Putative C-terminal processing **peptidase**; LOC_Os06g21380.1	**Peptidase** S41 family protein; AT3G57680
Ta.23797.1.S1_x_at	Dai et al. 2013_24 h up	**Late embryogenesis abundant protein** (**LEA**); Group 3 ; X56882; T. aestivum	**Late embryogenesis abundant protein** (LEA); Bradi2g18100	**Late embryogenesis abundant protein**, group 3; LOC_Os05g46480.2	**Late embryogenesis abundant protein (LEA)**; AT3G15670
TaAffx.53797.1.S1_s_at (**+P**: 1.15)	Dai et al. 2013_24 h up	**TaMYB58** MYB-related protein; JF951941; T. aestivum	**MYB-related transcription factor**; SWI/SNF complex-related; Bradi3g51960	**MYB family transcription factor**; LOC_Os02g46030.1	
Ta.13811.1.S1_at **(+P: 1.97)**	Dai et al. 2013_24 h up	**TaMYB58** MYB-related protein; JF951941; T. aestivum	**MYB-related transcription factor**; SWI/SNF complex-related; Bradi3g51960	**MYB family transcription factor**; LOC_Os02g46030.1	
Ta.26997.1.S1_at (**+P**: 1.76)	Dai et al. 2012_6_24_48 h up	**LEA1 protein**; AAN74637; T. aestivum	**Chlorophyll A-B binding protein**; Bradi1g55560	**Early light-induced protein**, chloroplast precursor; LOC_Os01g14410.1	**Early light-inducable protein**; chlorophyll binding; AT3G22840

[29] http://blast.ncbi.nlm.nih.gov/Blast.cgi
[30] http://www.harvest-web.org/

Table 29: Subset of wheat gene probes assigned to cluster 6 (Figure 17) overlapping with other model plants and crops gene probes with altered gene expression in responses to P_i starvation (Table 23).

The annotation for a subset of T. aeastivum or other wheat ancestor probe-sets (Affymetrix Genechip® Wheat Genome Array) was done using the NCBI BLAST(x)[31] database. Rice, maize and Arabidopsis gene were assigned in GeneSpring v. 12.6. to wheat probes using the 'HarvEST annotation' [32] database using the threshold of a minimum of one perfect-match probes.

Wheat probe ID	References	Gene annotation			
		Wheat/ancestors/barley/ maize/other species	**B. distachyon**	**O. sativa**	**A. thaliana**
Ta.24120.1.S1_at	Calderón-Vázquez et al. 2008	**Expansin** EXPB7; AY543541; T. aestivum; Affymetrix: LOC543145	**Pollen allergen**; rare lipoprotein A (RlpA)-like; Bradi3g33110	**Expansin precursor;** LOC_Os10g40700.1	**Expansin** (ATEXPB2); AT1G65680
Ta.24423.1.S1_s_at (**-P**: -1.43)	Calderón-Vázquez et al. 2008, Dai et al 2012_all genes_up	**Expansin EXPB6**, AY692478; T. aestivum; Affymetrix: TaEXPB6	**Pollen allergen**; Rare lipoprotein A (RlpA)-like; Bradi3g33110	**Expansin precursor;** LOC_Os10g40700.1	**Expansin** (ATEXPB2); AT1G65680
Ta.25636.1.S1_at	Calderón-Vázquez et al. 2008, Cai et al. _N_def_1 h	Beta-**expansin 1 precursor** (EXPB1); AY351786; H. vulgare	**Protease inhibitor/seed storage/LTP family**; Bradi1g78260	**Expansin precursor**; LOC_Os04g46650.1	**Expansin** (ATEXPB2); AT1G65680
Ta.1840.1.S1_at / Ta.1840.1.S1_x_at	Calderón-Vázquez et al. 2008	PI-3 **protease inhibitor**-like; EU293132; T. aestivum; Affymetrix: LOC100136980//	**Protease inhibitor**/seed storage/LTP family; Bradi3g50900	**Protease inhibitor**/seed storage/LTP family protein precursor; LTPL121; LOC_Os04g46820.1	**Protease inhibitor/seed storage/lipid transfer protein (LTP)** family protein; AT4G12510
Ta.13950.1.S1_x_at	Calderón-Vázquez et al. 2008, Dai et al. 2012_48 h up	**Cortical cell-delineating protein**; EMT02055; A. tauschii		**Protease inhibitor**/seed storage/LTP family protein precursor; LTPL114; LOC_Os03g01300.1	**Extensin-like protein;** lipid binding; AT1G12090

[31] http://blast.ncbi.nlm.nih.gov/Blast.cgi
[32] http://www.harvest-web.org/

Table 29 continued.

Wheat probe ID	References	Gene annotation			
		Wheat/ancestors/barley/ maize/other species	**B. distachyon**	**O. sativa**	**A. thaliana**
Ta.14492.1.S1_at (Ta.994.1.S1_at / Ta.994.1.S1_x_at / **Ta.5435.1.S1_x_at** / **Ta.13950.1.S1_x_at** / **Ta.28162.1.S1_at**) (**-P**: - 1.87 to -1.84)	Calderón-Vázquez et al. 2008, Dai et al. 2012_6_24_48 h up	**Cortical cell-delineating protein** (LOC100280973/ LOC100286227); Z. mays	**Protease inhibitor**/seed storage/LTP family; Bradi1g78260	LTPL114 - **Protease inhibitor**/seed storage/LTP family protein precursor; LOC_Os03g01300.1	**Extensin-like protein;** lipid binding; AT1G12090
TaAffx.83885.1.S1_at / (Ta.24015.1.A1_at)	Cai et al. 2013_N_def_ 7 d up, Cai et al. 2013_P_def_ 24 h_7 d up, Dai et al. 2012_6 h down	**Peroxidase** 11; T.urartu	**Peroxidase**; Bradi1g43680	**Peroxidase precursor**; LOC_Os06g16350.1	**Peroxidase**; AT1G68850
Ta.10186.1.S1_at	Dai et al. 2012_all genes_up	**Expansin EXPB6**, AY692478; T. aestivum	**Pollen allergen;** rare lipoprotein A (RlpA)-like; Bradi1g78340	**Expansin precursor**; LOC_Os03g12290.1	**Expansin** (ATEXPB2); AT1G65680
Ta.14580.1.S1_at / (Ta.14580.2.S1_x_at) (**-P**: -2.05)	Calderón-Vázquez et al. 2008, Dai et al. 2012_6_48_72 h up, Woo et al. 2012	**Peroxidase (Prx109-B) class III**, Prx109-B-5 allele; EU725468; T. aestivum	**Peroxidase**; Bradi2g20850	**Peroxidase precursor**; LOC_Os05g41990.1	**Peroxidase**; rare cold inducible gene 3; AT1G05260
Ta.1842.1.S1_a_at	Calderón-Vázquez et al. 2008, Hammond et al. 2007, Wu et al. 2003	**Phosphoethanolamine methyltransferase**; AY065971; T. aestivum	**SAM-dependent methyltransferases; phosphoethanolamine N-methyltransferase** Bradi2g1768	Conserved peptide uORF-containing transcript; CPuORF26; LOC_Os05g47540.2	**Phosphoethanolamine N-methyltransferase** 2, putative (NMT2); AT1G48600
Ta.5652.1.S1_at (**-P**: -1.35)	Dai et al 2012; all genes_up	**Tonoplast intrinsic protein** (AQP5); T. aestivum	**Aquaporin-7**; aquaporin TIP; transporter activity Bradi3g50690	**Aquaporin**; LOC_Os02g44080.1	**Ammonia transporter transporter** 2;3; AT5G47450
Ta.1082.1.S1_a_at / (Ta.1082.2.S1_x_at)	Wu et al. 2003, Woo et al. 2012	delta **tonoplast intrinsic protein** TIP2;3; AY525641; T. aestivum	**Aquaporin** (major intrinsic protein family); Bradi5g17690	**Aquaporin** protein; LOC_Os06g22960.1	Ammonia transmembrane transporter/ **water channel**; AT3G16240
Ta.12823.1.S1_at / (Ta.12823.1.S1_s_at)	Dai et al. 2012_6_24_48 h up, Cai et al. 2013_N_def_7 d up, Woo et al. 2012	**Ammonium transporter** 1;1; AY525637; T. aestivum	**Ammonium transporter** 1; Bradi3g48950	**Ammonium transporter**; LOC_Os02g40730.1	**Ammonium transporter** 1;2; AT1G64780

Table 29 continued.

Wheat probe ID	References	Gene annotation			
		Wheat/ancestors/barley/ maize/other species	**B. distachyon**	**O. sativa**	**A. thaliana**
TaAffx.143995.3.S1_s_at	Dai et al. 2012_all genes_up	**Glutamine synthetase** (isoform GSr1/GSr2); AY491968/ AY491969; T. aestivum	**Glutamine synthetase** catalytic domain; Bradi1g69530	**Glutamine synthetase**; LOC_Os03g12290.1	**Glutamate-ammonia ligase** GLN1;4; AT5G16570
Ta.2870.1.S1_at **(-P**: -1.27)	Dai et al. 2012_all genes up, Dai et al. 2012_ 24_48_72 h up	**Glutamine synthetase** isoform GSr2 (GS) gene; AY491969; T. aestivum	**Glutamine synthetase**; Bradi1g69530		ATGSR1; copper ion binding / glutamate-ammonia ligase; AT5G37600
Ta.10381.1.S1_x_at / (Ta.10381.1.S1_at)	Mission et al. 2005, Wu et al. 2003, Hammond et al. 2007	Protein without annotation; AK374737; H. vulgare	**Glycosyl hydrolases** family 35; Bradi1g37450	**Beta-galactosidase precursor**; LOC_Os06g37560.1	**Beta galactosidase** 1; AT3G13750
Ta.25277.1.A1_at	Calderón-Vázquez et al. 2008, Hammond et al. 2007, Mission et al. 2005, Dai et al. 2012_72 h down	**Fructan 6-exohydrolase** (6FEH1SM); AB196524; T. aestivum	**Glycosyl hydrolases** family 32 N-terminal domain; Beta-fructofuranosidase (invertase); Bradi5g25270	**Glycosyl hydrolases**; LOC_Os09g08072.1	**Beta-fructofuranosidase 5; hydrolyzing O-glycosyl compounds**; AT1G55120
Ta.7871.2.S1_a_at (**-P**: 1.26)	Cai et al._N_def_7 d up	**Glycerol-3-phosphate dehydrogenase** (TaGPDH1); KC953025; T. aestivum	NAD-**dependent glycerol-3-phosphate dehydrogenase;** Bradi2g60390	**Glycerol-3-phosphate dehydrogenase**; LOC_Os01g71280.1	GPDHC1; NAD or NADH binding / **glycerol-3-phosphate dehydrogenase** (NAD+); AT2G41540
Ta.1688.1.S1_at	Mission et al. 2005, Hammond et al. 2007	Benzoxazinone:**UDP-Glc glucosyltransferase** (TaGTb), AB547238; T. aestivum	**UDP-glucuronosyl /UDP-glucosyl transferase**; cytokinin-N-glucosyltransferase; Bradi1g53550	**Protein cytokinin-N-glucosyltransferase** 1; LOC_Os11g25454.1	**UDP-glucoronosyl/UDP-glucosyl transferase** family; AT3G55710
TaAffx.84154.1.S1_at	Cai et al. 2013_ N_def_24 h up	**Phenylalanine ammonia-lyase**, EMS62198; T. urartu	**Phenylalanine and histidine ammonia-lyase**; Bradi5g15830	**Phenylalanine ammonia-lyase**; LOC_Os04g43800.1	**Phenyl alanine ammonia-lyase** 3; phenylalanine ammonia-lyase; AT5G04230

Table 29 continued.

Wheat probe ID	References	Gene annotation			
		Wheat/ancestors/barley/ maize/other species	**B. distachyon**	**O. sativa**	**A. thaliana**
Ta.3628.1.S1_a_at	Dai et al. 2012_24 h up	**Glutathione S-transferase** 6, chloroplastic, EMS65229; T. urartu	**Glutathione S-transferase**; Bradi1g76080	**Glutathione S-transferase**, LOC_Os03g04240.1	**Glutathione s-transferase** PHI 8); AT2G47730
Ta.7592.1.S1_at	Dai et al. 2012_24_48 h_up	Putative mixed beta **glucan synthase** (cslf6 gene); AM743080; T. aestivum	**Cellulose synthase**; N-acetylglucosaminyltransferase-related; Bradi1g50170	**Cellulose synthase**-like family F; beta1,3;1,4 glucan synthase,; LOC_Os08g06380.2	**Cellulose-synthase** like D2; transferring glycosyl groups; AT5G16910
Ta.25454.1.S1_at	Dai et al. 2012_24_48 h up	**Transcription factor RF2a**; EMT20411.1; A. tauschii	**bZIP** transcription factor; X-box; Bradi3g09340	**bZIP** transcription factor family protein; LOC_Os02g14910.1	**bZIP** transcription factor family protein; AT2G42380:
TaAffx.107617.2.S1_x_at **(-P**: -1.37)	Dai et al. 2012_6_48 h down	Soluble **inorganic pyrophosphatase**; EMT22354/EMT22352; A. tauschi	**Inorganic pyroPhosphatase**/Nucleosome remodeling factor, NURF38; Bradi2g62470	Soluble **inorganic pyrophosphatase**; LOC_Os01g74350.1	**Pyrophosphorylase** 4; inorganic diPhosphatase; AT3G53620
Ta.254.1.S1_s_at	Cai et al. 2013_N_def_ 7 d up	**Cytochrome P450** (CYP86), AF123609; T. aestivum	**Cytochrome P450** CYP4/CYP19/CYP26; Bradi3g51370	**Cytochrome P450**; LOC_Os04g47250.1	**Cytochrome P450** 86 A2; fatty acid (omega-1)-hydroxylase/ oxygen binding; AT4G00360
TaAffx.37361.1.A1_at	Cai et al. 2013_N_def_ 7 d up	Non-lysosomal **glucosylceramidase**; EMT33716; A. tauschii		**Cytochrome P450**; LOC_Os04g47250.1	
TaAffx.56748.1.S1_at	Cai et al. 2013_N_def_7 d up	**Cytochrome P450** 86A1, EMT13769; A. tauschii	**Cytochrome P450** CYP4/CYP19/CYP26; Bradi2g55280	**Cytochrome P450**; LOC_Os01g63540.1	**Cytochrome P450** (86 A1); AT5G58860

Both genes, TaMYBrel and TaIPS, were significantly up-regulated during P_i starvation in wheat roots (Table 18 A and C) but lack a corresponding annotation in other plants or crops. Nonetheless, cross-comparison studies help to identify potential key targets.

The majority of differentially regulated genes during P_i starvation in model plants or other crops species belonged mainly to cluster 1 and 2 (Table 23). This observation coincided with the fact that the majority of transcript level alterations in wheat also occurred for genes in cluster 1 and 2 (Figure 17). However, these two clusters were of low importance for the long-term PSR in wheat roots. Genes in these two clusters may play a crucial role in the immediate stress response directly after onset of P_i stavation and may be more related to general nutritional stress. Cluster 1 genes which were altered in other P_i starvation studies (Table 24) with a decrease in expression and a slight increase during N starvation belong to similar gene families to cluster 6 genes (Table 24). For instance, they code for aquaporins, glycerol-3-phosphate dehydrogenases, cytochome P450 or protease inhibitor proteins, which are all related to N and carbohydrate metabolism. In cluster 2, a gene coding for a putative glycerol-3-phosphate transporter with sugar:hydrogen symporter activity, was up-regulated in five other studies investigating the PSR (Table 25). TaMYB59, which was up-regulated during long-term P_i starvation in wheat roots (Table 18 A), was already up-regulated after 72 h of P_i starvation in rice seedlings (Dai et al. 2013; Table 25).

Cluster 3, 4 and 5 genes (Figure 17) which were similarly regulated in other studies were not numerous (Table 23) but were very similar in all studies investigated (Tables 26 to 28), indicating a role as key regulators in the P_i stress response. Cluster 3 genes such as genes containing an SPX domain, an inorganic pyrophosphatase (PP_iase) gene and an abscisic stress-ripening protein coding gene, were significantly up-regulated in the majority of other studies (Table 26). Interestingly, except for the PP_iase, all genes that were up-regulated through P_i starvation in other studies were down-regulated in N starved wheat (Table 26). Cluster 4 genes which were altered similarly in other P_i starved plants comprised coding for a nicotiamine synthase, nicotiamine

aminotransferase, several glycosyltransferases and a Zn-transporter (Table 27). Some cluster 5 genes overlapped with at least one study for two putative LEA proteins, MYB58 and a galactinolsynthase/glycosyltransferase (Table 28). Several candidates were determined among cluster 6 genes which may reveal whether varieties exhibiting a higher P_i starvation tolerance are also exhibiting a less strong stress response via these genes (Table 29). Expansins and cell-delineating proteins involved in lipid transfer processes were among those significantly down-regulated cluster 6 transcripts in wheat roots and other plant tissue in many of the other studies (Table 29). In addition, class III peroxidase genes may be of particular interest (Table 29).

Many of the overlapping genes assigned to cluster 1 and 6 comprising genes coding for ammonium transporters with nitrate transporter activity, aquaporins, a glutamine and glutamate synthase, kinases as well as enzymes involved in glycosyl/glycerol phosphate transfer processes (transferases, hydrolases, dehydrogenase) (Tables 24 and 29), give evidence that N and P metabolism are linked. This indicates that N and P_i starvation impacts similar gene regulation networks and that N starvation represses genes which are upregulated as the transcriptional response of P_i starvation. Nonetheless, one gene being up-regulated under P_i starvation was similarly influenced in their transcript level by N starvation (24 h and 7 d) (TaAffx.57156.1.S1_x_at). There was a lot of overlap in differentially regulated cluster 6 genes of different plants species (Table 23). However, these genes were either up- or down-regulated rather than being all strongly down-regulated during P_i starvation as in wheat roots (Table 23). This indicates that many of these transcriptional responses may be related to other experimental conditions in addition to the P_i limitation.

3.4.5. Impact of the shoot ionome on the root transcription of wheat

In order to reveal a potential linkage of transcriptional responses to specific nutrient concentrations rather than just to a specific nutrient starvation, a second cluster analysis was performed using the nutritional profiles as criteria (Figures 18 and 19). The gene selection (Table 30) was based on the available

annotation of each gene, a high similarity value and linkage to a nutrient specific pathway rather than just abiotic stress responses.

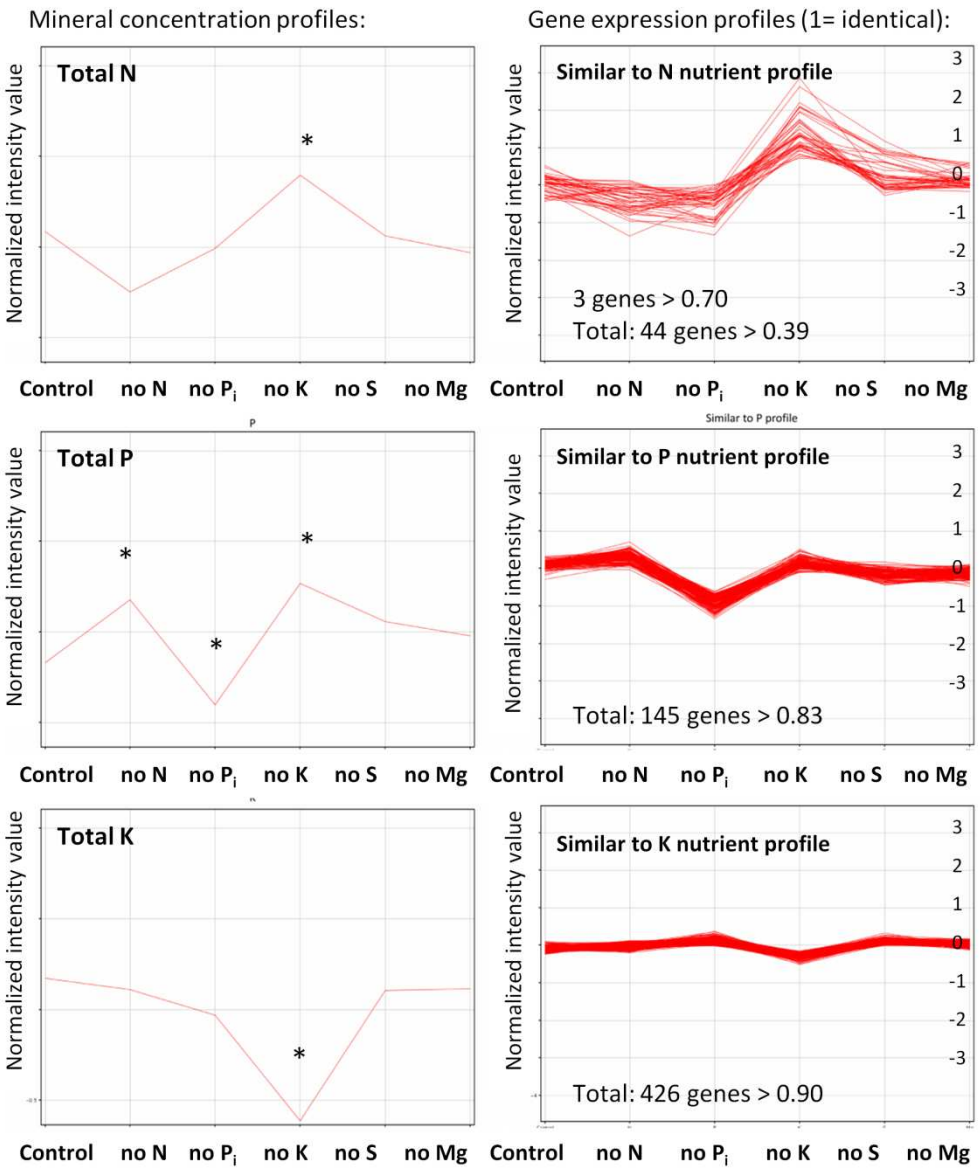

Figure 18: Impact of long-term N, P_i and K fertilizer omission on total N, P and K shoot concentrations (mg g^{-1} DM) and root transcription in wheat from Broadbalk 2011 at booting following a similar pattern.
Graphs show the profile of concentration changes between the treatments for each macronutrient and similar transcriptional changes of wheat probes. The similarity value is the similarity measure (max value = 1 i.e. identical) using a Euclidean metric. The normalized intensity value 0 = nutrient concentration in the shoots of the control plants. Statistical properties for significant changes (*) are displayed in Table 12.

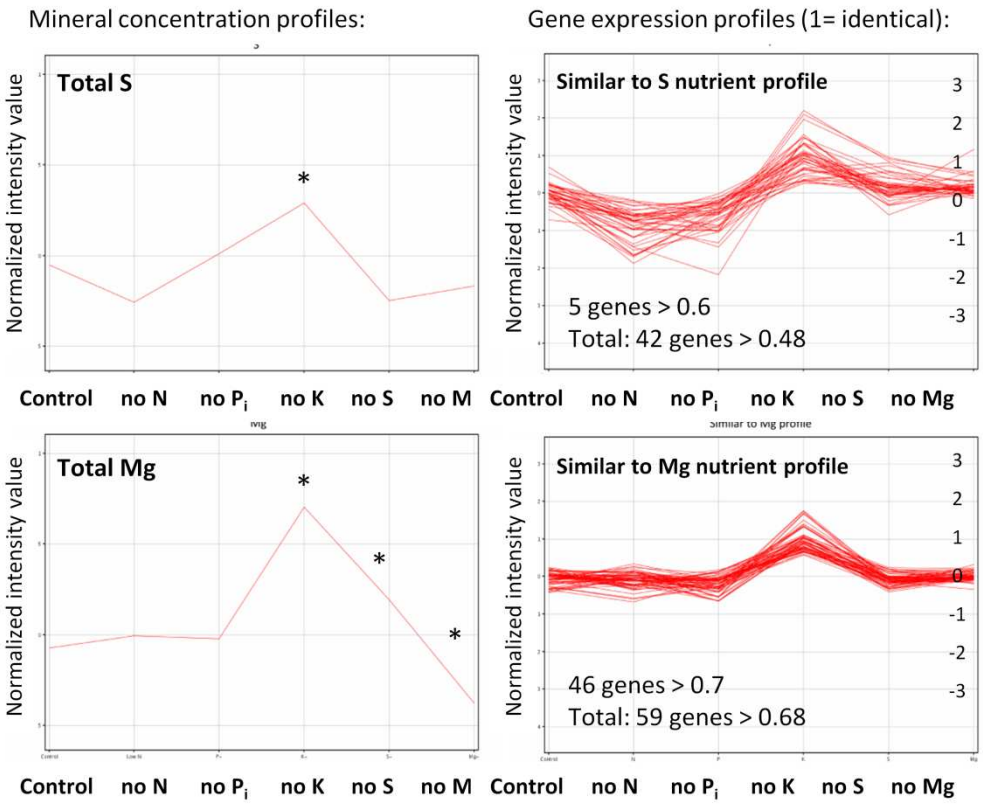

Figure 19: Impact of long-term S and Mg fertilizer omission on Mg and S shoot concentrations (mg g^{-1} DM) and root transcription in wheat from Broadbalk 2011 at booting following a similar pattern.
Graphs show the profile of concentration changes between the treatments for each macronutrient and similar transcriptional changes of wheat probes. The similarity value is the similarity measure (max value =1 i.e. identical) using a Euclidean metric. The normalized intensity value 0 = nutrient concentration in the shoots of the control plants. Statistical properties for significant changes (*) are displayed in Table 12.

N concentrations were only altered in K starved wheat plants (Figure 18, Table 12) following a profile across treatments very similar to cluster 4 (Figure 17). Only a few genes were related to N shoot concentrations which were actually cluster 4 genes (Figure 17, Table 30 A). Annotation of those revealed different isoforms of a nicotiamine synthase (Table 30 A), which was previously discovered as a gene being down-regulated during P_i- and N-deficient and up-regulated during K starvation (Table 18 E).

Table 30: Annotation for a subset of wheat gene probes induced or down-regulated in field-grown wheat roots from Broadbalk in 2011 at booting with linkage to mineral concentrations in the wheat shoot (Figures 18 and 19).

Gene were selected following a similar pattern than the nutrient concentration across treatments using a Euclidean metric (maximal similarity value: 1 = identical). Values in the colums represent log_2-fold changes of gene expressions during nutrient starvation treatments determined by using a one-way ANOVA ($P \leq 0.05$) on the normalized expression data in GeneSpring v. 12.6. (Agilent Technologies).

Probe	Similarity value	Nutrient starvation					Annotation
		N	P_i	K	S	Mg	
Table 30 (A): Similar gene expression profile to N concentrations							
TaAffx.6284.1.S1_at	1	-0.7	-0.3	**2.6**	1,2	0.1	No annotation; cluster 4
Ta.5549.2.A1_at	0.74	-0.8	-0.9	**2.2**	0.8	0.5	H. vulgare: **Nicotianamine synthase 1**; AB010086; cluster 4
Ta.5549.2.A1_x_at	0.72	-0.6	-0.9	**2.1**	0.9	0.5	H. vulgare: **Nicotianamine synthase 1** ; AB010086; cluster 4
Ta.5549.3.S1_at	0.71	-1.0	-1.0	**2.1**	1.0	0.5	H. vulgare: **Nicotianamine synthase 1**; AB010086; cluster 4
Table 30 (B): Similar gene expression profile to P concentrations							
TaAffx.111224.1.S1_at	0.81	**0.57**	**-1.27**	**0.49**	-0.31	-0.41	A.tauschii: **Peroxidase** 2; EMT07517; cluster 6
Ta.13327.1.S1_x_at	0.85	**0.34**	**-1.23**	**0.26**	-0.36	-0.25	A. tauschii: **Prolamin** gene locus 1DS; JX295577; cluster 6
Ta.12823.1.S1_s_at / Ta.12823.1.S1_at	0.90	**0.58**	**-1.13**	**0.11**	0.11	0.03	T. aestivum: **Ammonium transporter** Amt1;1 AY525637; cluster 6
Ta.27477.1.S1_at	0.89	**0.42**	**-1.08**	**0.31**	0.04	-0.38	T. aestivum cv.Yumai 13 **germin-like protein** 2; FJ815171
Ta.25856.1.S1_s_at / Ta.25856.1.S1_x_at	0.81	**0.40**	**-1.06**	**0.09**	-0.27	-0.11	T. urartu: **B_zip1 transcription factor** VIP1; EMS61681; cluster 6
Ta.9396.1.S1_a_at	0.81	**0.09**	**-1.06**	**-0.08**	-0.06	-0.08	T. urartu: Xyloglucan **endotransglycosylase/hydrolase** protein 8; EMS47876; Cluster 6
Ta.5388.1.S1_a_at	0.82	**0.61**	**-1.04**	**0.33**	-0.06	0.11	A. tauschi: **Caffeic acid 3-O-methyltransferase**; EMT15952; cluster 6
Ta.11367.1.A1_at	0.83	**0.30**	**-0.90**	**0.14**	-0.33	-0.24	A. tauschii: **Putative serine/threonine-protein kinase**; EMT08274; cluster 6
Ta.25277.1.A1_at	0.83	**0.44**	**-0.86**	**0.20**	-0.18	0.01	T. aestivum: **Fructan 6-exohydrolase**; BAM74039; cluster 6
TaAffx.93308.1.S1_at	0.82	**0.46**	**-0.77**	**0.14**	-0.08	-0.01	A. tauschii: Putative **xyloglucan endotransglucosylase/hydrolase** protein 16; EMT20095; cluster 6
Ta.28092.1.S1_s_at	0.82	**0.15**	**-0.83**	**0.08**	-0.18	-0.08	T. aestivum cv. Shannong0431 **MYB75**; JN857310
Table 30 (C): Similar gene expression profile to S concentrations							
Ta.21127.1.S1_at	1	-1.64	-0.87	**1.57**	-0.3	0.37	T. aestivum cv. Paragon: **low affinity nitrate transporter** (TaNPF6.2 gene; HF544986; cluster 4
Ta.12673.1.S1_at	0.79	-1.36	-0.39	**1.29**	-0.21	0.18	Uncharacterized protein; cluster 4
Ta.21039.1.S1_at	0.68	-0.87	-0.52	**1.33**	-0.58	0.24	Uncharacterized protein; cluster 4
Ta.22711.1.S1_at	0.63	-0.72	-0.25	**1.50**	-0.10	0.60	Uncharacterized protein; cluster 4

Table 30 continued.

Table 30 (D): Similar gene expression profile to Mg concentrations							
Ta.975.1.S1_a_at	1	-0.04	-0.20	**1.40**	**-0.14**	**-0.02**	Uncharacterized protein; cluster 4
Ta.975.2.S1_at / Ta.975.2.S1_at	0.96	-0.04	-0.13	**1.35**	**-0.08**	**-0.03**	Uncharacterized protein; cluster 4
Ta.26981.2.S1_a_at	0.90	-0.05	-0.08	**1.34**	**-0.07**	**0.18**	B. distachyon: Znf_RBZ superfamily: **RNA-binding protein**, XP_003557200; cluster 4
Ta.18871.1.S1_x_at	0.80	0.05	-0.40	**1.38**	**0.07**	**0.02**	A.tauschii: **Cytochrome P450**, EMT03552

Phosphate starvation had no consequences on macronutrients other than P_i in this experiment (Figures 18 and 19, Table 12). There is large numbers of genes exhibiting a linkage to changing P concentrations across nutrient starvation treatments (Figure 17). Changes in nutrient concentrations partly reflect fertilizer application regimes on soil-P_i availability (Olsen P). Particularly the control plot, which did not receive any P_i fertilizer since the year 2000 (Tables 1 and 2). Therefore, it was likely that plants growing at K and N deplete plots exhibited higher shoot P concentrations compared to plants growing on P_i deplete plots (Figure 18). In plots in without Mg and S fertilization, the P_i fertilizer supply was similar like in the N and K starvation plots (Table 1), which resulted in high amounts of available soil-P_i in all these plots (Table 2). In contrast to the N and K starved plant material, total P concentrations did not increase in S and Mg starved material (Figure 18). This indicates that there may be a stronger linkage between N and K metabolism to P metabolism, than between P, S and Mg metabolism. Among the genes linked to P concentrations were an ammonium-transporter, a bZIP–TF, serine/threonine kinases, a MYB-TF and glycosyl hydrolases (Table 30 B). The profile of the P concentrations across nutrient treatments (Figure 18) exhibited an inverse pattern to cluster 3 (Figure 17), with the majority of linked genes being in cluster 6 (Table 30 B). This indicates that these genes are not up-regulated due to higher P concentrations in N starved tissues and that N starvation may have a down-regulating effect, similarly to the down-regulating effect through N starvation on genes which are usually up-regulated in P_i starved plants material (cluster 3) (Figure 17).

K concentrations were altered in plants growing in plots without receiving K fertilizers; other nutrient starvations had no effect of K concentrations when receiving similar and sufficient amounts of K fertilizers (Figure 18, Table 1, 2 and 12). A high number of genes were regulated similarly to K concentrations without exhibiting significant expression differences or being assigned to cluster 5 (results not shown).

There are a very few genes for which the expression follows the trend of S concentrations across the different nutrient treatments (Figure 19). The lowest S concentrations were found in N and S starved plant material (Figure 19, Table 12). The peak in S concentrations was found in plants growing at plots which did not receive K fertilizers and were K starved as a result of that (Figure 19, Tables 3 and 12). Therefore, the genes which may be linked to S concentrations belonged to cluster 4 but were, unfortunately, mostly uncharacterized proteins with unknown functions except a nitrate transporter (Table 30 C).

Mg concentrations increased in plants growing on plots where no K and S fertilizers were applied (Figure 19, Table 12). However, genes with a transcriptional response profile similar to the Mg concentrations were not strongly down-regulated in Mg or S starvation treatments but mainly up-regulated through increased Mg concentrations belonging to cluster 4 (Figure 19, Table 30 D).

In conclusion, there is an apparent linkage of P, N and K metabolism with the transcriptome in a differentially manner. Most macronutrient concentrations increased during K limited growing conditions (Figures 18 and 19, Table 12). Furthermore, P_i was the nutrient with the highest number of genes exhibiting expression profiles similar to shoot P concentrations (Figures 19 and 20).

3.4.6. Candidate gene selection

Based on the four approaches for interpreting the transcriptome data from wheat roots at booting exposed to limited macronutrient availability, several candidate genes were selected coding for MYB-TFs, pyrophosphatases, glycerol-3-phosphate permeases, SPX proteins, Pho-like transporters, extensins (expansin-like) and a peroxidase (Table 31). This list emphasises genes which were regulated in P_i starved wheat plants and may have putative key functions in the P_i starvation response (Table 18). They are related to the specificity of expression during a particular nutrient limitation in addition to P_i and their classification into clusters which are potentially crucial for PAE/PUE traits (Figure 17). Moreover, target probes have been selected based on their frequency of overlap with results from other expression studies (Table 23). Some genes are homologues or potential members of the same gene family as the chosen candidates (Table 31) and are included in the data validation (Chapter 4).

Table 31: Candidate genes derived from transcriptome study on field-grown wheat roots from Broadbalk in 2011 at booting.
* = homologues genes or potential members of the same gene family as the chosen candidates

Cluster	Gene annotation	Gene name	Functional annotation	Wheat chip probe
2	MYB related protein; transcription factor	TaMYB 59*	P_i signalling cascades; hormone-related	Ta.11849.1.S1_at
2	Glycerol-3-phosphate transporter 1; sugar exchanger	TaG3Pp1	P_i signalling, P_i starvation responses	Ta.11166.1.A1_at
3		TaG3Pp2*		TaAffx.53053.1.S1_at
3	Pyrophosphatase 1-like A	PP_iase3*	P_i recycling	Ta.12413.1.S1_at
	Pyrophosphatase 1-like B	PP_iase 7		TaAffx.96414.1.S1_s_at
3	SPX domain containing protein 6-like	TaSPX1	P_i signalling and P_i homeostasis	Ta.13993.1.S1_x_at / TaAffx.115546.1.S1_at / TaAffx.115546.1.S1_x_at
3	SPX domain containing protein 5-like	TaSPX2	P_i signalling and P_i homeostasis	Ta.14013.1.S1_at
3	Pho1;3	TaPho1;3	P transport and allocation, P_i sensing	Ta.19715.1.S1_at
	Pho1;2	TaPho1;2		TaAffx.84359.1.S1_at / Ta.1006.1.S1_at
4	TaMYB related; transcription factor	MYBrel	P_i signalling cascades	Ta.25744.1.S1_at
5	MYB related protein; transcription factor	TaMYB 58*	P_i signalling cascades; hormone-related	TaAffx.53797.1.S1_s_at / Ta.13811.1.S1_at
6	Cortical cell-delineating protein // Extensin	TaExt (a)	Stress and hormone-related	Ta.14492.1.S1_at / Ta.994.1.S1_at / Ta.994.1.S1_x_at / Ta.28162.1.S1_at
6		TaExt (b)		Ta.5435.1.S1_x_at / Ta.13950.1.S1_x_at,
6	Peroxidase class III (Prx 109-B)	Ta109B	Stress and hormone-related	Ta.14580.1.S1_at / Ta.14580.2.S1_x_at

3.4. Discussion

3.4.1. Transcriptional responses in field-grown roots to nutrient limitations

Particular gene expression patterns and putative gene functions were derived from the microarray analysis and related to different metabolic and transcriptomic network changes in nutrient limited conditions in wheat roots using different approaches. However, log_2-fold changes of transcripts were lower than usually reported such as the 340-fold change in TaIPS gene expression (Oono et al. 2013) compared to a maximum of 16-fold here (Table 18 C). Pariasca-Tanaka et al. (2009), who also investigated soil-grown rice, reported much lower relative expression changes to P_i starvation. Soil-P_i availability is influenced by many factors (Chapter 1, Section 2.5.). Growing conditions are not as uniform as in a hydroponic culture which was used in so many other studies. Therefore, the field-grown plant material was not exposed to a consistent extent of P_i starvation explaining the high variation between replicates and lower log_2-fold changes.

3.4.2. Transcriptional responses in field-grown roots to N, P_i and K starvation

Nitrogen and P_i availability had the strongest impact on the wheat transcriptome, particularly on gene down-regulation (Figure 16). The majority of these genes are potentially involved in cell wall restructuring and root growth (Table 18 D). In most other studies on maize, rice or wheat (Calderón-Vázquez et al. 2008, Pariasca-Tanaka et al. 2009, Oono et al. 2013), the number of up-regulated genes exceeded the number of down-regulated transcripts, and N starvation triggered a stronger transcriptional response than P_i limitation (Cai et al. 2013, Schlüter et al. 2013). Long-term limitation of soil-P_i availability and its distribution in the root-soil interface affects root growth patterns strongly (Gahoonia et al. 1997, Lynch and Brown 2001, Niu et al. 2012, Teng et al. 2013); probably more so than short term P_i or N stress applied in hydroponics explaining why it had the biggest impact on the root transcriptome. However, this crucial phenotypic data was not acquired here nor

in other studies investigating transcriptional responses to N and P_i limitation (Cai et al. 2013, Schlüter et al. 2013).

Many genes with altered expression in response to P_i limitation were also influenced by N (cluster 3) and K nutrition (cluster 5) (Figure 17). Both aspects may be largely related to the different amounts of P_i fertilizers applied in each of the treatments (Table 1) resulting in differences of available soil-P_i (Table 2) as previously discussed (Chapter 2, Section 4.5.). As a consequence, shoot P concentrations changed the most across treatments and had the strongest impact on transcription associated with it (Figure 18) comprising mainly cluster 6 genes (Table 30 B). Nonetheless, the majority of up-regulated genes in N starved plant material (Table 23; Cai et al. 2013) could be assigned as cluster 6 genes indicating that N and P metabolism are regulating similar transcription pathways contrastingly when their availability becomes limiting.

Schlüter et al. (2013) reported a significant increase in P concentrations in N starved maize plants, whereas P_i deplete growing conditions did not influence N concentrations. Similar observations were made for N and P_i starved wheat (Figure 17) which may be related to the effect of lower biomass in N starved wheat (Table 2) which increases indirectly the shoot P concentrations (Table 12). Schlüter et al. (2012 and 2013) speculated that a down-regulation of phosphatases increased the P bound in organic compounds leading to higher P levels in N starved plants. The authors further identified a transcript cluster in maize containing genes coding for SPX domain proteins, P_i transporters and phosphoesterases which correlated negatively with P concentrations (Schlüter et al. 2013), similar to transcript cluster 3 in wheat (Figure 17, Table 19). In maize leaves, N and nitrate assimilation was down-regulated in P_i and N limitation depending on the growth demand (Schlüter et al. 2013). In P_i starved maize roots, genes involved in amino acid synthesis and degradation, for instance glutamine synthase and nitrate reductase, were similarly repressed (Calderón-Vázquez et al. 2008). This is in congruency with results for cluster 4 showing an equal down-regulation of a wheat nitrate transporter in N and P_i starved wheat roots (Table 22).

Some of the P_i starvation regulated genes in wheat roots were actually related to sugar metabolism and sugar transport, such as a down-regulated sugar transporter (Table 22) and a sugar kinase related gene/fructokinase (Table 24) or an up-regulated sugar:phosphate exchange antiporter (Table 25). This is not surprising, considering a trend of preserving N containing metabolites and simultaneously increasing ammonium related metabolites and di-and tri-saccharides in P_i starved barley (Huang et al. 2008). In N and P starved maize leaves, starch accumulated (Marchner 2012, Schlüter et al. 2012). However, during P_i starvation, genes related to carbon transport, particularly sucrose synthesis and sugar transport, are induced (Wu et al. 2003, Schlüter et al. 2013, Huang et al. 2008). Sucrose transport into the roots is promoted during P_i starvation stimulating genes related to P_i acquisition, transport and excretion (Liu et al. 2005, Tesfaye et al. 2007). Many other P signalling genes like SPX genes are also sugar regulated (Müller et al. 2007, Karthikeyan et al. 2007, Hammond and White 2008). However, in regards to the determined regulated wheat transcripts, further validation is required to investigate whether most genes which were only detected due to their down-regulation in N starved wheat roots are also putative key regulators of the PSR (Tables 18 B and C, 19, 20 and 22), exhibiting stronger regulation in more P_i starved plant material than the one which had been used here.

3.4.3. Transcriptional responses in roots of P_i starved wheat

In soil-grown wheat, long-term P_i starvation had the largest impact on root transcripts related to P signalling, P recycling and improved P_i acquisition. Many of these transcriptional changes have been reported previously in studies on model plants grown hydroponically (Chapter 3, Section 1.1 and 1.5.). For instance, the repression of genes related to starch biosynthesis, proteins, fatty acids and lipids, photosynthesis and nitrogen assimilation in P_i starved Arabidopsis resulted in carbon starvation and the up-regulation of genes with roles in carbon transport, sucrose synthesis and glycolytic by-pass reactions (Wu et al. 2003). Other studies with Arabidopsis, rice or maize reported similar changes in transport processes and carbohydrate fluxes (ions, amino acids,

lipids, organic acids, sugars), plant growth (cell wall, root architecture, membrane remodelling), responses to oxidative stress and genes involved in modification of transduction pathways, P_i acquisition and P_i recycling (Lan et al. 2012). Calderón-Vázquez et al. (2008) referred to the P_i transport and P_i recycling related genes as the most constant responses in maize roots towards P_i limitation. Such transcriptional alterations occurred similarly in field-grown wheat roots and will be discussed in more detail in the following sections focussing on expression changes related to general stress or plant hormones, to root restructuring, P_i homeostasis and P_i acquisition and regulatory factors in the plant-AM interaction.

3.4.4. General stress or hormone related genes

Genes related to cell defence, cell rescue and secondary metabolism were up-regulated in many array studies including peroxidases, cytochrome P450, glutathione-transferases or UDP-glucosyl-transferases (Hammond et al. 2003, Uhde-Stone et al. 2003, Calderón-Vázquez et al. 2008, Woo et al. 2012). However, oxidative stress in P_i starved bean roots also caused membrane lipid peroxidation and restricted the electron flow through the cytochrome pathway (Juszczuk et al. 2001) which may explain why cytochrome P450 genes in field-grown wheat roots were down and not up-regulated (Table 18 D). Furthermore, peroxidase activity was enhanced in P_i starved bean roots (Juszczuk et al. 2001), but again, wheat peroxidase genes were down-regulated (Table 18 D).

Many differentially regulated wheat gene probes are responsive to abscisic acid (ABA) (Table 18 A). ABA is a plant hormone which appears to be a regulator of P responsive genes (Woo et al. 2012). Putative serine/threonine phosphatases were amongst the significantly up-regulated genes in wheat roots (Table 18 A) which code for an abundant and very diverse group of phosphor protein phosphatases PP2C and are involved in stress signal transduction (Luan 2003). Putative serine/threonine phosphatases of type PP2C were also found in Arabidopsis as a component involved in ABA signalling pathways (Luan 2003). They have also been found in the soluble fraction of wheat leaves

(MacKintosh et al. 1991) and in barley roots (Panara et al. 1990) without revealing a precise function. However, a putative serine/threonine kinase was more highly expressed in a rice line (NIL6-4) containing Pup1, a major QTL for P_i starvation tolerance, compared to a susceptible rice (Nipponbare) variety (Pariasca-Tanaka et al. 2009). These findings suggest an involvement of serine/threonine phosphatases in the ABA signalling pathway and the adaptation to P limited conditions. Among ABA responsive genes were MYB-TF and LEA genes and dehydrins (Table 18 A). LEA genes encode for proteins with unknown function or proteins which are expressed at different stages of late embryogenesis in plant seed embryos. Dehydrins also belong to the LEA family. Hammond et al. (2003) also identified up-regulated LEA proteins or dehydrins in P_i starved shoots of Arabidopsis. Usually, these ABA responsive LEA proteins respond to conditions of drought, osmotic or salt stress (Zhu et al. 2000, Rampino et al. 2006). Dehydrins are also involved in drought tolerance of wheat (Lopez et al. 2003), although, their precise roles or mechanism of adaptation is unknown. However, the results here and in the literature indicate that they may have an additional role in P limited conditions.

3.4.5. Genes related to restructuring the root system

Although root growth is less inhibited under P_i starvation, cell growth might have been affected as indicated by the reduction of expansin/extensin transcripts in wheat roots (Table 18 D). A strong decrease of leaf expansion and epidermal cell expansion has also been reported in other P_i starved plants (Marschner 2012, Schlüter et al. 2013) and changes in root morphology are common response to P_i starvation (Chapter 1, Section 6). Expansins are involved in cell wall extension (Zhao et al. 2012), including ABA stimulated root- hair formation (Yu et al. 2011, Zhao et al. 2012). In rice, genes coding for proteins which are involved in cell wall loosening and root hair extension such as a root-specific cell-delineating proteins had higher expression in the Pup1 QTL containing rice line (NIL6-4) compared to a susceptible rice (Nipponbare) variety (Pariasca-Tanka et al. 2009). In contrast to rice, many of putative wheat cell-delineating proteins/expansins/extensins (Table 18 D) or cellulose

synthase genes (Table 29) were down-regulated in P_i starved wheat roots. Teng et al. (2013) showed that the stimulated expression of two expansin genes in field-grown wheat roots with P_i fertilizer rates below the optimum declined again with either increased or further reduced fertilizer rates. This effect coincided with the effect on root development at low or high P_i fertilizer rates (Teng et al. 2013). Therefore, cell-wall restructuring and root architectural changes seem too be actually inhibited in wheat rather than being enhanced by severe P_i starvation. However, the data requires further validation by screening transcriptional responses in plants exposed to a wider range of soil-P_i availability.

3.4.6. Genes involved in P_i homeostasis and P_i signalling

Among the altered root transcripts in wheat during nutrient starvation were putative SPX domain proteins (Tables 19 and 26). Proteins containing a SPX domain (SYG1, PHO81, XPR1) are essential for maintaining P_i homeostasis and P_i signalling in plants (Rouached et al. 2010, Nilsson et al. 2012, Secco et al. 2012). Members of the SPX protein family in rice (OsSPX3) have been shown to be highly induced (preferentially) in rice roots and shoots where they are involved in the regulation of PSI and OsIPS1 genes (Duan et al. 2008, Wang et al. 2009b, Liu et al. 2010, Oono et al. 2011). The putative wheat SPX genes were also predominantly down-regulated in N starved roots of plants with higher shoot P concentrations (Tables 12 and 26). These results suggest that wheat SPX homologues are involved in the P signalling response which should be investigated further. The expression of another SPX-EXS domain containing protein, the putative wheat homologue of OsPho1;3, was significantly repressed in N starved wheat roots similar to observations in N starved maize (Schlüter et al. 2012) but was not up-regulated in P_i starved roots (Table 18 C). N starvation affects long-distance P_i distribution and remobilization within the plant (Schlüter et al. 2012, Schlüter et al. 2013). Unfortunately, this putative TaPho1 transcript was not annotated and therefore not recognised in the cross-comparison study (Tables 23 to 29). However, OsPho1;3 clusters with Arabidopsis Pho1 proteins which are involved in long-

distance P_i transfer and P_i acquisition into cells (Wang et al. 2004, Secco et al. 2012) and have been reported as P regulated (Woo et al. 2012). Therefore, the involvement of TaPho1 transporters in P_i translocation in wheat should be validated and investigated further (Table 31).

In wheat roots, TaIPS genes were also among the significantly up-regulated transcripts in P_i starved roots (Table 18 B) and significantly down-regulated transcripts in N starved roots with higher shoot P concentrations (Tables12, 18 C, and 26). IPS genes are involved in the miR399-PHO2 regulatory loop as negative regulators of PHO2 at the post-transcriptional level (Franco-Zorrilla et al. 2007, Doerner 2008), putatively to stabilize the initial decrease of PHO2 transcript to prevent P_i toxicity via P_i accumulation in the shoots (Chitwood and Timmermans 2007). Rapid TaIPS gene induction in wheat might therefore not be exclusively a rapid response to P-starvation with very high expression levels (Oono et al. 2013) but also be an adaptation mechanism to long-term P_i starvation. Consistent with the results (Table 18 C), Li et al. (2008) observed strongly repressed TaIPS1 transcript abundance in roots and TaIPS2 transcript abundance in shoots of P_i starved wheat by N starvation. These findings provide evidence of an influence on the signalling pathways of P_i homeostasis by the N nutritional status. Furthermore, HvIPS1 expression in barley correlated with the expression two HvPht1 transporters related to P_i use efficiency (Huang et al. 2011).

Four MYB-TF members were up-regulated in P deprived field-grown wheat roots (Tables 18 A, 24, 25 and 28) consistent with results from other studies (Morcuende et al. 2007, Calderón-Vázquez et al. 2008, Dai et al. 2012). The MYB-TFs belong to a large gene family in plants (Chen et al. 2006, Ahuja et al. 2010). Some of these are involved in signalling cascades initiated by P-starvation and bind to the promoter of several P-responsive genes including secreted acid phosphatase (Miller et al. 2011). At4 and AtIPS4 in Arabidopsis are involved in P_i allocation between roots and shoot and enhance lateral root development (Shin et al. 2006, Franco-Zorrilla et al. 2007). AtIPS1 further modulates PHR expression, which is a MYB-TF involved in P-starvation responses (Rubio et al. 2001). Other MYB-TF family members, for instance

AtMYB96, are involved in the ABA and auxin signalling pathways during lateral root growth (Seo et al. 2009). Interestingly, AthMYB96 clustered on sequence level with TaMYB59 and TaMYB58 MYB-related proteins (Zhang et al. 2012) which were identified here (Table 18 A) suggesting that they may be promising candidates for validation (Table 31).

3.4.7. Genes involved in P_i recycling and P_i acquisition

Several genes which encode putative acid phosphatases (APases) comprising serine/threonine phosphatases, glycerophosphodiester phosphodiesterases and purple acid phosphatases were induced in field-grown wheat roots (Table 18 B and C). Uhde-Stode et al. (2003) and Calderón-Vázquez et al. (2008) made similar observations in white lupin and maize roots. APases are enzymes which hydrolyse P_i from orthophosphate monoesters without absolute substrate specificity and occur in a wide range of species where they are presumed to contribute to hydrolysis of internal P_i to restore the P_i pool (Duff et al. 1994). Extracellular APases are localized in the cell wall and secreted by the root (Lee 1988, Goldstein et al. 1989, Lefebvre et al. 1990). They play a further important role in P_i acquisition from organic P sources (Helal 1990). Intracellular APases occur in a larger set of tissues and are involved in P_i acquisition, P_i recycling or P_i scavenging (Duff et al. 1994). However, the underlying genetic mechanisms have been investigated only recently (Vance et al. 2003). The first secreted phosphatase (sATPase) was reported in cluster roots of white lupins by Miller et al. (2001) and reporter gene fusion detected sATPases in root exudates of Arabidopsis (Haran et al. 2000).

Phosphate starvation had an impact on the lipid metabolism in wheat roots, as lipid transfer proteins were strongly down-regulated (Tables 18 D, 22 and 29). P_i limitation generally has a large impact on the metabolism affecting the expression of genes involved in lipid transfer activities, fatty acid synthesis, lipases and hydrolases (Wasaki et al. 2003, Morcuende et al. 2007, Calderón-Vázques et al. 2008). Furthermore, glycerophosphodiester phosphodiesterases (GPX-PDE) expression was induced in P_i starved wheat roots (Table 18 B).

Morcuende et al. (2006) and Calderón-Vázquez et al. (2008) also observed increasing induction of phospholipases and glycerophosphodiesterases (GPDEs) as a response to P_i starvation. GPX-PDEs were also highly expressed in cluster roots of white lupin under P_i starvation (Uhde-Stone et al. 2003, Cheng et al. 2011). However, P_i starvation alters membrane lipid composition by replacing phospholipids by galactolipids or sulpholipids (Andersson et al. 2003, Byrne et al. 2011). In this process, GPX-PDEs catalyse the hydrolysis of phospholipids to glycerol-3-phosphate and the corresponding alcohol. Therefore, GPX-PDEs were suggested to play a role in root hair development as well as in phospholipid turnover.

Puple acid phosphatises (PAPs) transcription increased in P_i starved wheat roots (Figure 17, Tables 18 C and 19). Purple acid phosphatases (PAP) are intracellular and secreted non-specific enzymes that belong to a metallophosphoesterase superfamily typically containing a Fe(III)-X(II) with Zn^{2+} or Mn^{2+} as active site and catalyse P_i hydrolysis from a broad spectrum of P_i-esters (Tran et al. 2010). PAPs have been isolated and characterized in tomato and Arabidopsis and both seem to be involved in internal P_i remobilization (delPozo et al. 1999, Baldwin et al. 2001).

3.4.8. Genes involved in the plant-AM fungus interaction

The S-adenosylmethionine decarboxylase (SAMD) gene was highly responsive and strongly up-regulated in P_i- and S-deficient wheat roots (Table 18 B). SAMD is a key enzyme of the polyamine biosynthesis pathway (Hussain et al. 2011): Spermidine (Spd) and spermine (Spm) are formed by the sequential addition of aminopropyl groups to putrescine and spermidine from decarboxylated S-adenosylmethionine (SAM) by SAMD. Polyamines are involved in a wide range of biotic or abiotic stresses and in a large set of developmental processes, but their precise biological and molecular function is still elusive (Walters 2000, Hussain et al. 2011). Putrescine might be a relevant factor inhibiting cell growth during P_i starvation (Shih and Kao 1996). It is conclusive that P_i limitation induced the expression of a key enzyme of the

secondary metabolism which is suggested to act as regulatory factors in the plant-AM fungus interaction which is one strategy to cope with P_i limited conditions (Chapter 1, Section 2.7.). However, it is poorly understood how (Walters 2000). However, the presence of polyamines stimulates hyphal growth (Chen et al. 2012) as well as mycorrhizal colonization frequency (El-Ghachtouli et al. 1996). Furthermore, higher concentrations of polyamines were found in mycorrhiza infected roots (Kytoviita and Sarajala 1997).

The nicotianamine synthase (NAS) gene was significantly down-regulated in P and N starved wheat roots (Tables 18 E and 30). NAS is a key enzyme in the biosynthetic pathway for the mugineic acid family of phytosiderphores which are secreted as Fe-chelators in Fe-deficient roots (Higuchi et al. 1999). Interestingly, NAS was strongly up-regulated in tomato roots after 3 h to 24 h of P-starvation (Wang et al. 2002). NAS catalyses the trimerization of three S-adenosylmethionine molecules to form one molecule of nicotianamine which is then converted to members of the mugineic acid family (Higuchi et al. 1999). Since both enzymes, NAS and SAMD require S-adenosylmethionine to form either phytosiderphores (Higuchi et al. 1999) or polyamines (Hussain et al. 2011), a pathway shift during P_i starvation must have occurred favouring polyamine synthesis. This shift might contribute to stimulated mycorrhizal infection in order to cope with P starvation. Therefore, both genes should be investigated further in future experiments but their crucial roles remain currently unclear.

3.4.9. Data ambiguity and possible caveats

Transcript numbers and putative annotations only approximate the extent of alterations on the wheat transcriptome in roots related to nutritional availability. The insufficient Affymetrix Genechip® annotation required other tools for overcoming the poor functional gene characterization. Gene ontology references were therefore omitted from the analysis in order to prevent false conclusions. Affymetrix Genechip® contamination detected due to the additional screening of significant probes via BLAST caused additional data

ambiguity. Furthermore, distinguishing between orthologues, paralogues or homeologues genes for each annotated wheat transcript on the Affymetrix Genechip® is difficult due to the lack of a fully sequenced reference genome. Examples are Ta.13993.1.S1_x_at, TaAffx.115546.1.S1_at and TaAffx.111546.1.S1_x_at which showed sequence similarities to a SPX domain containing protein (6-like) in model plant species (Table 26). All three probes represent the expression of one gene but had different log_2-fold values (Table 26). Another example is the expression of a putative transcription factor TaMYB58 for which the log_2 –fold values of the two probes, TaAffx.53797.1.S1_s_at and Ta.13811.1.S1_at exhibited a discrepancy (Table 28). However, many probes were assigned to just one gene in a model plant, but represented several wheat genes due to putative gene duplication which was revealed through sequence screening in the IWGSC database (Chapter 4). Furthermore, it is important to consider the incomplete coverage of the Affymetrix Genechip® for many genes which have not been identified. For instance, apart from TaPht1;1 (Ta.2758.1.S1_at), TaPht1;6 (Ta.10084.1.S1_at) and TaPht1;4 (Ta.18863.1.S1_a_at), other TaPht1 ESTs are missing. This explains why no TaPht1 expression changes could be reported in P_i starved wheat roots via microarray analysis although several other array studies revealed the induction of Pht1 family members (Wang et al. 2002, Wasaki et al. 2003, Calderón-Vázquez et al. 2008). The wheat microarray data needed validation using real-time qPCR technique considering homeologues and paralogues gene sequences. This allows assessment of transcriptional changes more accurately and has been done for TaPht1 transporters in Chapter 2 and for selected candidates based on the microarray results in Chapter 4.

3.5. Conclusion

The transcriptome study on nutrient starved wheat roots revealed expression patterns related to structural, metabolic and signalling changes predominantly induced through soil N and P_i availability, which have been reported similarly in model plants and other cereal crops. However, due to several factors causing data ambiguity, further replication and validation with more precise methods such as real-time qPCR is required. It is difficult to draw conclusions on which transcripts are only regulated as a response to immediate abiotic stress and which are actually relevant to increase the ability of tolerating P_i limiting conditions. Therefore, the subsequent step was to screen candidates for a potential linkage of their expression patterns to P_i efficiency traits in order to determine their exploitability as targets in crop improvement.

Chapter 4: Transcriptional response screen of target genes to the nutritional status and to PAE and PUE properties of wheat genotypes

4.1. Introduction

This chapter is a study on genotypic variation of P_i efficiency traits (PAE, PUE) in wheat. At the same time, it is a study on candidate genes which are potentially involved in these traits and validates the global transcriptional responses defined previously (Chapter 3). The selected candidates were TaSPX, TaG3Pp, TaPho1, TaMYB-TF, TaPP$_i$ase and TaExt genes (Table 31). Gene expression changes were determined by real-time qPCR using plant material from two different field trials: Firstly, root material which was already used for the transcriptome study. Secondly, root and ear tissues from a broader wheat germplasm selection at a range of soil-P_i availability concentations and growth stages.

4.1.1. Definition of P_i efficiency in crops

Phosphate efficiency traits of crops have been described in the literature as P_i acquisition efficiency (PAE) and P_i use efficiency (PUE) (Wang et al. 2010). Both traits and the bottlenecks for their improvement were characterized previously in the introduction (Chapter 1, Section 3). The definition of agronomic P_i efficiency, which is used to provide fertilizer recommendations, is relatively consistent across the literature (Table 32 A). Unfortunately, fertilizer applications in the P_i trial at Sawyers were applied in variable amounts according to the requirements to hold the target soil-P_i concentration. Therefore, agronomic P_i efficiency measures (Table 32 A) could not be determined.

Table 32: Definitions of P efficiency ratios used the literature including definitions from (A) agronomic P efficiency, (B) general P efficiency, (C) P use efficiency and (D) P acquisition efficiency.

Abbreviations: Y= Yield (t ha^{-1}), GY = Grain yield (t ha^{-1}), DM = dry matter, +P/-P = P_i fertilized/P_i depleted growing conditions, P_iFA = P_i fertilizer applied (kg ha^{-1}); NaHCO3-P_i determined by the method of Murphy and Riley (1962), P = P or P_i (used interchangeably in the different references). Studies comprise field studies and pot experiments in glasshouses and growth chambers studying genotypic variation, Qtl analysis or gene expression between cultivars showing variability in P_i starvation tolerance in T. aestivum, T. durum, H. vulgare, O.sativa, B. oleracea and Brassica napus.

(A) Agronomic P efficiency:		
Fertilizer efficiency	kg GY kg^{-1} P_iFA	Batten et al. 1992
P fertilizer recovery (%)	[(Total P in biomass$_{+P}$ - Total P in biomass$_{-P}$) kg^{-1} P_iFA] x100	Manske et al. 2001
P fertilizer response (%)	[($GY_{+P} - GY_{-P}$) / GY_{-P}] x 100	
Fertilizer use efficiency (kg DM kg^{-1} $_{fertilzer}$P)	($Y_{+P} - Y_{-P}$) / Δ P_iFA	Hammond et al. 2009
(B) General P efficiency:		
P harvest index (%)	(g grain-P g^{-1} shoot-P) x 100	Batten et al. 1992
Relative shoot growth	(g DM_{-P} g^{-1} DM_{+P}) x 100	Ozturk et al. 2005
P efficiency ratio	GY kg^{-1} shoot P	Batten et al. 1992
	Y_{+P} / (P conc.$_{+P}$ x Y_{+P})	Hammond et al. 2009
	Y_{-P} / (P conc.$_{-P}$ x Y_{+P})	
P efficiency coefficient (PEC)	(g shoot or grain DM_{-P} g^{-1} shoot or grain DM_{+P}) x 100	Ding et al. 2012
(C) P_i acquisition/uptake efficiency:		
Root efficiency ratio	mg shoot P g^{-1} root DM	Batten et al. 1992
Acquisition efficiency for rhizosphere P_i (%)	(Quantity of NaHCO3-P_i depleted / total of NaHCO3 extractable P_i) x 100	Gahoonia and Nielsen 1997
P_i acquisition efficiency	Total P in biomass / available P_i; available P_i not defined	Manske et al. 2001
P uptake efficiency (PUpE)	[(P conc.$_{+P}$ x Y_{+P}) - (P conc.$_{-P}$ x Y_{-P})]/ Δ P_iFA	Hammond et al. 2009
(D) P_i use efficiency:		
P use efficiency	g shoot DM mg^{-1} shoot P_i	Su et al. 2006, Rose et al. 2011, Huang et al. 2011, Yang et al. 2011
	kg GY kg^{-1} total P in biomass	Manske et al. 2001

Table 32 continued

P utilization efficiency (PUpE)	$(Y_{+P}-Y_{-P})/ [(P\ conc._{+P} \times Y_{+P}) \times (P\ conc._{-P} \times Y_{-P})]$	Hammond et al. 2009
Physiological P use efficiency	$(Y_{+P} / (P\ conc._{+P})$ or $(Y_{-P}) / (P\ conc._{-P})$	Hammond et al. 2009

For PAE and PUE in P_i efficiency screenings, many different measures have been used for PAE and PUE in P_i efficiency screenings (Table 32 B to C) and there is a lack of a consistent definition for P_i efficiency measures (Rose and Wissuwa 2012). Therfore, the majority of studies investigating the diversity of PAE/PUE in contrasting cultivar use specific traits rather than P_i efficiency ratios.

P_i efficiency traits include root characteristics such as root-to-shoot ratios, root length, root exudation (e.g. phosphatases) or the ability to extract rhizosphere P_i from the soil solution due to root hair formation (Gahoonia and Nielsen 1996, Davies et al. 2002, Zhu et al. 2005, George et al. 2008). Other studies use the above ground plant material, such as plant dry matter, shoot biomass, grain yield, P concentrations or P content, total grain P at maturity, P harvest index, etc. (Batten 1992, Manske et al. 2001, Davies et al. 2002, Hayes et al. 2004, Huang et al. 2011, Ding et al. 2012, Aziz et al. 2014).

Estimating the genotypic variability using P_i efficiency parameters determines if breeding for P_i efficiency using the available gene pools would be worthwhile (Rose et al 2011). However, assessing the genotypic variability in the field is difficult without including ambiguous and confounding effects of soil-interactions (Hayes et al. 2004). Furthermore, it is impractical to compare a large number of genotypes at many soil-P_i concentrations (Batten 1992). In practice, selecting for yield at latent P_i starvation may increase P_i efficiency without distinct quantification of P_i uptake and P_i use efficiency (Batten 1992). The variation of genotypic variability for P efficiency has been reported and ranges largely, for instance from 50 to 70 % for relative shoot growth in wheat and durum wheat (Ozturk et al. 2005), 37 to 47 % for P_i acquisition efficiency

in winter wheat, 26 to 41 % in spring wheat and 22 to 35 % in winter barley (Gahoonia and Nielsen 1997). However, P_i acquistion efficiency for wheat cultivars growing in the P_i trial at Sawyers could not be assessed. Olsen P (mg extractable P_i kg_{-1} soil) as determinant for soil-P_i availability is a ration itself, which does not fully determine the total amount of available P_i to the plant. Furthermore, the total soil-P_i availability for each genotype depends on the soil volume accessed by the root, which was not determined either. Therefore, PUE (kg yield kg^{-1} P_i taken up) was the only measure used for comparing the P_i efficiency of wheat cultivars in the P_i field trial at Sawyers. Considering the inconsistency of definitions (Table 32), this work is focused on specific growth traits between cultivars, rather than determining P_i efficiency ratios.

Usually, response curves are used to make fertilizer recommendations (Chapter 1, Section 2.3.) and have also be used to describe P_i efficiency or P_i starvation tolerance. For instance, the "critical K_m value" determining the P_i concentration in the rooting medium for achieving at least 90 % maximal yield (Hayes et al. 2004, Hammond et al. 2009) or a similar concept, based on shoot P concentrations in relation to yield (Bollons and Barraclough 1997, Bollons and Barraclough 1999, Sanchez 2007), were used for measuring the potential of a genotype to cope with minimal P_i fertilizer input. However, there is a lack of studies linking P_i efficiency measures to critical Olsen P or shoot P concentration in agronomic systems and the expression of P_i starvation induced genes (Figure 4). Nontheless, this may be crucial when investigating P_i starvation tolerance mechanisms in field-grown crops. Therefore, contributing to fill this gap is one aims of this thesis.

4.1.2. Determinants of phenotypic and genotypic variation

'Phosphate efficiency' is a complex trait which can be differentiated into several physiological responses to P_i availability including growth development, P_i acquisition and P_i translocation pattern rather than exclusively yield or biomass development (Batten 1992, Wang et al. 2010, Rose and Wissuwa 2012, Veneklaas et al. 2012). This has to be considered in screening

approaches when comparing heterogeneous plant material (Rose and Wissuwa 2012). Genotypic variation related to P_i starvation tolerance and P_i acquisition and P_i use efficiency does exist. In Brassica species P_i efficiency properties could be allocated to P partitioning and root trait QTLs (Hammond et al. 2009, Zhang et al. 2009) similar to studies on maize (Zhu et al. 2005 a; b, Zhu et al. 2006); among cereal species, differences in P_i efficiency have been assessed in wheat by Manske et al. (2001), Osborne and Rengel (2002), Ozturk et al. (2005) and Gunes et al. (2006). However, whether specific target gene expression is correlated with P_i efficiency traits and responsible for genetic variability is poorly understood. Some studies on rice and Brassica species have looked at genotypic differences using the array technique (Pariasca-Tanaka et al. 2009, Li et al. 2010). In contrast, Aziz et al. (2014) focused on a panel of potential key regulator genes. The authors related them to P partitioning in wheat tissues aiming to identify molecular differences between the two wheat varieties, which had been previously described as contrasting in their P_i efficiency (Osborne and Rengel 2002). However, these were very young plants grown hydroponically (Aziz et al. 2014). Hence, phenotypic differences based on genotypic P_i acquisition and translocation patterns will be linked to transcriptional responses of selected candidate genes in field-grown wheat material over three growing seasons.

4.1.3. Candidate genes involved in P_i starvation signalling cascades: Pho1 genes (TaPho1;3)

The TaPho1 genes belong to the Pho1 family which have been widely studied in rice and Arabidopsis (Hamburger et al. 2002, Wang et al. 2004, Secco et al. 2012). None of the Pho1 members in Arabidopsis show homology to the AtPht1 family (Hamburger et al. 2002, Wang et al. 2004), as found for the putative TaPho1 and the TaPht1 transporters. However, Pho1 genes in rice and Brassica were related to P_i starvation tolerance QTLs (Ni et al. 1998, Shi et al. 2013). Only two AtPho1 genes, AtPho1 and AtPho1:H1, rescued the defects of the pho1 mutation in Arabidopsis (Stevanovic et al. 2007). Their regulation through AtPHR1, sucrose or other phytohormomes (Stevanovic et al. 2007, Ribot et al. 2008) suggested a distinct regulatory pathway during P_i limitation

(Secco et al. 2010). AtPho1 and AtPho1:H1 cluster with rice Pho1 proteins which have been reported to be up-regulated under P_i starvation (Secco et al. 2010, Secco et al. 2012) and for which wheat orthologues were found. Oono et al. (2013) showed a weak up-regulation of a putative TaPho1 gene and the microarray data implied that TaPho1;3 was up-regulated in N starved wheat roots (Table 18 C). However, TaPho1;3 was assigned to cluster 3 suggesting an up-regulation in P_i starved plants (Figure 17, Table 19). Therefore, the regulation of these putative TaPho1 genes in response to P_i nutrition will be reassessed.

4.1.4. Candidate genes involved in P_i starvation signalling cascades: SPX protein coding genes (TaSPX2)

SPX proteins are key players in the P_i homeostasis controlling network (Hamburger et al. 2002, Duan et al. 2008, Wang et al. 2009a;b, Secco et al. 2010) (Chapter 1, Section 4.5.). In wheat, two potential orthologues, TaSPX1 and TaSPX2, were identified by sequence similarity and cross comparison studies (Chapter 3, Table 31). OsSPX4 (Os03g29250) is a membrane-localized protein (Wang et al. 2009b) and a potential rice orthologue of TaSPX1. The two TaSPX2 orthologues genes in rice and Arabidosis, OsSPX3 and AtSPX3, were localized to the cytoplasm (Duan et al. 2008, Wang et al. 2009b). GUS staining indicated expression of OsSPX1, OsSPX2 and OsSPX5 in lateral roots and were enhanced during P_i starvation (Wang et al. 2009b). Furthermore, expression of OsSPX3, OsSPX5 and OsSPX6 was reduced in the phr2 mutant (Shi et al. 2014). OsSPX3 and OsSXP5 are actually paralogues genes which both negatively regulated P_i translocation from root to shoot by supressing OsPHR2 (Shi et al. 2014). In rice, P_i starvation inducible genes are mainly OsPHR2 rather than OsPHR1 regulated and OsPHR2 is promoting root architectural changes, P_i acquisition mechanisms and other PSR (Zhou et al. 2008). The over-expression of OsSPX3 restricted plant growth (Wang et al. 2009a, Shi et al. 2014). Therefore, the authors assumed that OsSPX3 and OsSPX5 are important for post P_i-starvation P_i homeostasis, avoiding long-term P_i starvation signalling. Both genes may restore the P balance after the immediate P_i starvation (Shi et al. 2014). The microarray analysis did not

reveal a strong up-regulation of TaSPX genes during low soil-P_i availability. However, due to their previously suggested crucial roles in P_i starvation signalling and P_i starvation tolerance, their expression patterns will be re-assessed here.

4.1.5. Candidate genes involved in P_i starvation signalling cascades: MYB-TF (MYBrel)

MYB-TFs belong to a large gene family in plants with multiple key functions in developmental processes and defence responses (Chen et al. 2006, Ahuja et al. 2010). In wheat, 60 MYB-TFs genes have been identified (Zhang et al. 2012). Over-expression of P_i starvation responsive MYB-TFs in rice seedlings increased root branching during P_i starvation and altered the expression of many P_i responsive genes e.g. OsIPS1, OsmiRNA399, OsPAP and phosphate transporters (Dai et al. 2012). In Arabidopsis, the over-expression of another MYB-TF, AthMYB 62, which is specifically induced during P_i starvation in the leaves, had an impact on root architecture, P_i acquisition and acid phosphatase activity via interfering with gibberellic acid metabolism (Devaiah et al. 2009). Aziz et al. (2014) showed that TaMYB75 is co-expressed in a tissue-specific manner with other genotypic marker genes, for instance TaPht2;1, TaPht3;1, a plastid and mitochondrial P_i transporter, a plasma-membrane H^+-ATPase or a malate dehydrogenase. However, TaMYB75 was repressed in the fine roots and enhanced in the stem of the more efficient wheat cultivar (Aziz et al. 2014). However, in the microarray analysis, TaMYB75 was not significantly altered by limited soil-P_i (Figure 17, Table 24). Nonetheless, these findings reveal that MYB-TFs have various functions and are regulated in a tissue and genotypic differentiated manner, which is relevant for adapting to a low-P_i environment. Therefore, TaMYB-TFs transcripts which were significantly regulated in the microarray analysis, TaMYB58 and MYB43/59, will be validated using real-time PCR to confirm their P specific regulation.

4.1.6. Candidate genes involved in P_i recycling and P_i stress response: Glycerol-3-phosphate-sugar-exchanger (G3Pp1/2)

A putative wheat glycerol-3-phosphate (G3P) permease (G3Pp) or transporter (Ta.11166.1.A1.at) was not up-regulated when soil-P_i availability was limited. However, differential regulation of G3Pp in P_i starved plants and a role in the adaptation to P_i starvation were suggested by results of the cross-comparison study (Table 26). G3Pps are organic P_i/inorganic P_i antiporters for which a broad role P_i homeostasis and P_i recycling was suggested (Ramaiah et al. 2011). G3Pps are members of the major facilitator superfamily (MFS), transporting G3P into the cytoplasm and P_i into the periplasm (Huang et al. 2003). Functional characterization and spatiotemporal regulation of members of the G3Pp family in Arabidopsis was reported: AtG3Pps were induced specifically during P_i starvation and not by any of the applied other nutrient starvations (K, N, Fe) in root and shoot tissues (Ramaiah et al. 2011). The TaG3Pp probe on the Affymetix Genechip® showed high sequence similarity with the AtG3Pp1 gene. AtG3Pp1 and AtG3Pp2 exhibited an early, sustained and high induction in the roots and a specific involvement of these genes in P_i acquisition mechanisms by facilitating the release of P_i from organic P sources has been suggested (Mission et al. 2005, Ramaiah et al. 2011). However, the actual mechanism of how G3Pp up-regulation enhances the responsiveness and the capability to cope with limited P_i availability is elusive.

Phosphorylated C3 and C6 compounds are important for the metabolic adaption to P_i starvation. G3P is such a C3 compound and concentrations were reduced in P_i starved barley plants (Huang et al. 2008). G3P is an essential intermediate and precursor in the biosynthesis of phospholipids (Misson et al. 2005, Ramaiah et al. 2011) but also is generated during phospholipid breakdown in P_i starved plants. A large fraction of organic P_i in plants is distributed in membrane phospholipids (Poirier et al. 1991). During P_i starvation, phospholipid hydrolysis is induced for using them as an additional internal P_i source (Andersson et al. 2003, Pariasca-Tanaka et al. 2009, Nakamura 2013). Therefore, G3Pp may regulate the organellar P_i homeostasis in the same way as P_i transporters regulate inorganic P_i homeostasis. Whether

TaG3Pp regulation is present in P_i starved wheat roots at a particular growth stage or genotype will be verified in the following analysis.

4.1.7. Candidate genes involved in P_i recycling and P_i stress response: Pyrophosphatase (TaPP$_i$ase3)

A putative wheat pyrophosphatase (PP$_i$ase) gene, TaPP$_i$ase, was significantly up-regulated in P_i starved wheat roots (Table 18 B). This gene shows sequence similarity to the haloacid dehalogenase-like hydrolase superfamily (HAD) in Brachypodium and Arabidopsis (Table 26), particularly to AtPP$_i$ase1 (At1g73010). AtPP$_i$ase uses pyrophosphate (PP_i) as substrate, was strongly up-regulated during P_i starvation in other studies (Morcuende et al. 2007, Müller et al. 2007, Lan et al. 2012), and was characterized as a novel type of cytoplasmic HAD enzyme (May et al. 2011).

Phosphate starved plants recover P_i from small phosphorylated metabolites including nucleic acids, phospholipids and other metabolites which are important for glycolysis, phospholipid and polysaccharide synthesis (Huang et al. 2008). Therefore, PP$_i$ases seem to be involved in these P_i scavenging systems (May et al. 2011). PP_i seems to be important for sucrose translocation, which acts as signalling metabolite for the P_i scavenging and signalling system. Huang et al. (2008) showed that di-and tri-saccharides accumulated in P_i starved barley plants. Phosphohydrolases are involved in the regulation of cytosolic P_i homeostasis via cleavage of PP_i from phosphorylated substrates in the cell (May et al. 2011). Cytoplasmic PP_i concentrations do not change significantly during P_i starvation despite a decline in cytosolic P_i concentrations or other inorganic storage pools in the plant (Duff et al. 1989, Huang et al. 2008). However, PP_i is a “by-product” of many reactions of plant metabolism (Plaxton and Tran 2011) and is generated during alternative glycolysis pathways to replace ATP as energy resource or altered lipid composition. Consequently, P_i starvation results in a deplete ATP-pool and favours PP_i dependent pathways and PP_i glycolytic reactions. The strategy of promoting the sucrose synthase pathway, the PP_i: fructose-6-P 1-phosphotansferase pathway or up-regulating the abundance and activity of

vacuolar H^+PP_iases on the tonoplast membrane (Stitt 1998, Palma et al. 2000) ATP is conserved and PP_i used as an energy donor (Palma et al. 2000). Increased PP_iase expression and activity would increase and stabilize intracellular P_i levels (May et al. 2011). This means that TaPP_iases may be involved in the metabolic adaptation capability to P in wheat which will be investigated here.

4.1.8. Candidate genes involved in root system restructuring: Extensins (TaExt (a) and TaExt (b))

There were a number of extensin-like genes coding for cell delineating proteins significantly down-regulated in the transcriptome analysis (Tables 18 D, 22 and 29). This observation revealed several contradictions with other studies and raised the question as to what extent these genes play a role in root restructuring during limited soil-P_i. Additionally, there is not much known about the involvement of specific extensins in the response to P_i starvation.

Extensins are hydroxyproline-rich glycoproteins which are important components for cell wall biosynthesis and root hair elongation (Ito et al. 1998, Kwasniewski et al. 2010, Velasquez et al. 2011). At the same time, extensins have also been suggested to play a role in PERK4 (proline-rich extensine-like receptor kinase) mediated ABA signalling to inhibit root growth and root cell elongation (Bai et al. 2009). However, these findings exhibit similarities with expansin genes, which seem to be involved in the root development and for which the responses to P_i availability have been more extensively investigated. For instance, the over-expression of an expansin gene, GmEXPB2, in soybean improved P_i acquisition and growth (Guo et al. 2011). However, in wheat, the majority of expansins were strongly responsive at excess P_i and down-regulated at P_i starvation (Han et al. 2014). Furthermore, in a field situation the expression patterns seem to be determined by root growth patterns and therefore only indirectly linked to the internal P_i status of the plant or soil-P_i availability (Teng et al. 2013). This hypothesis will be evaluated here using two extensin-like proteins for gene expression studies in wheat.

4.2. Material and Methods

4.2.1. The P_i trial at Sawyers field

The P_i field trial at Sawyers was in grass/clover since 1980, and then ploughed and sown with spring oats in 1993. Afterwards, it was used for P_i acquisition assessments in wheat (Bollons and Barraclough 1999) and spring oat cultivation in 2011. The soil is a silty loam with flints and a clay content of 25 %. The first winter wheat for the season 2011/12 was drilled on 17th October 2011 and for the season 2012/13 on 15th October 2012. The sowing density was 350 seeds m^2. Combine-harvest was performed on 20th/21th August 2012 and 19th August 2013, respectively. The experimental design is two main blocks which were used in consecutive years (Figure 20). Each main block contained a range of 12 randomly arranged non-replicated plots of different plant-available soil-P_i (Figure 20). These 12 plots are equilibrated to a specific soil Olsen P availability level by appropriate P_i fertilizer application.

Each of the 12 plots contains 27 sub-plots with nine different wheat genotypes (Figure 20, Table 33), in triplicates, randomly arranged within the three columns of each plot. The 27 plots comprised an area of 2 m^2 in 2011/12 and 2.5 m^2 in 2012/13 (in order to separate the sampling and measuring area from the yield assessment and grain quality monitoring area at harvest in 2013). P_i fertilizer was applied as triple superphosphate in the autumn, pre-cultivations, and incorporated. P_i fertilizer requirement was monitored in the autumn before drilling since 2010, by measurement of 12 bulked top-soil (0-23 cm) core samples taken by Andrew Riche from each of the 12 plots within each main block (Figure 20)**.** The soil samples were analysed by the "Analytical Unit of the Sustainable Soil and Grassland Systems Department" at Rothamsted using the Olsen method (mg P_i kg^{-1} air dried soil; Olsen et al. 1954; Skalar Continouse Flow Analysis, SAN^{PLUS} System, Skalar Ltd, Breda House, Wheldrake, York, UK). All other fertilizer applications, pesticide treatments or cultivations were performed according to common practices by the farm management.

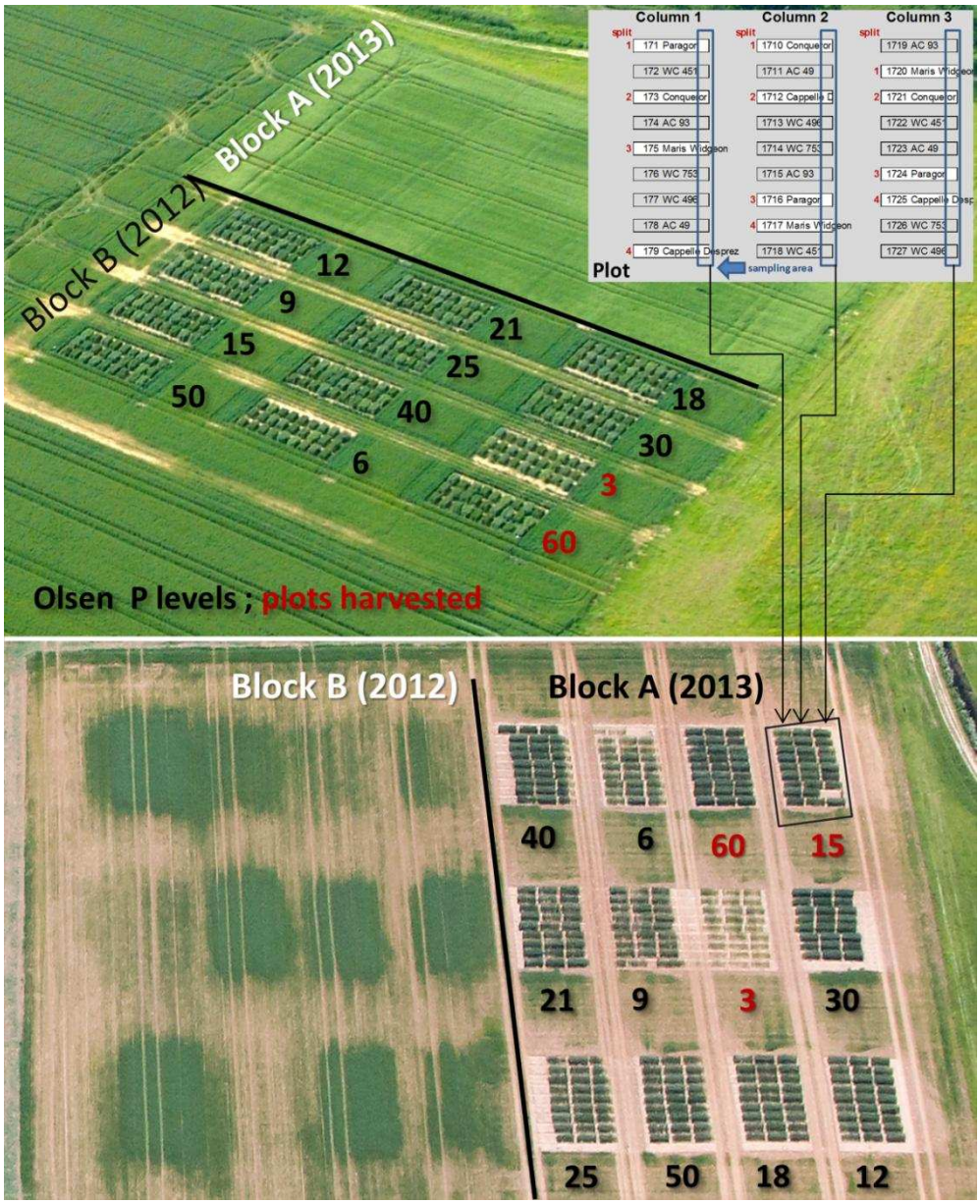

Figure 20: The experimental design of the P_i field trial at Sawyers in 2012 and 2013.

The available soil-P_i concentration in each plot is indicated as Olsen P concentration (mg P_i kg^{-1} air dried soil; Olsen et al. 1954) in the aerial photographs which display the entire experiment. The wheat germplasm are randomized within columns of each plot. Sampled plots are indicated in red. Statistical notions are displayed in the grey scatter: plot, column, split (= the spatial position of each variety in a column), soil-P_i concentrations and varieties. Plants were sampled from the plots where the soil-P_i concentration is colored in red.

Table 33: Wheat genotypes growing in the 1st (2011/12) and 2nd year (2012/13) in the P_i field trial at Sawyers.

Cultivar	Description	Year
Commercially available varieties:		
Hereward	high quality winter bread wheat	1st
Cappelle Desprez	high quality winter bread wheat	1st and 2nd
Paragon	spring milling wheat, WISP mapping population parent	1st and 2nd
Maris Widgeon	heritage wheat used for thatching, tall stemmed	1st and 2nd
Conqueror	high yielding winter wheat used for animal feeding	1st and 2nd
Avalon x Cadenza lines*[1]:		
AxC 149	long major root, long fine roots	1st
AxC 88	average major root, long fine root	1st
AxC 49	short major root, short fine root	1st and 2nd
AxC 93	average major root, average fine roots	1st and 2nd
Watkins collection*[2]:		
Wat 753	average yield, low grain P content	2nd
Wat 451	highest yield, high grain P content	2nd
Wat 496	high yield, high grain P content	2nd

***[1]** Chosen from a paper-roll pre-study conducted by Chaihong Bai; growing conditions see Bai et al. (2013)
*[2]: choice based on pre-experimental study (WISP donor experiment) at Rothamsted Research, Harpenden, UK

4.2.2. Wheat varieties

All wheat genotypes in the P_i trial at Sawyers were selected to contrast root and shoot architecture traits as well as P_i acquisition capability (Table 33). However, wheat genotypes were regularly replaced in each consecutive year by the main researchers working with this trial, Malcolm Hawkesford and Andrew Riche. Both focused on pre-selecting interesting wheat genotypes for the BBSRC founded Wheat Improvement Strategic Programme (WISP)[33].

In the frist year of the P_i trial at Sawyers, in 2011/12, the commercial wheat varieties growing in this trial were simply selected based on their shoot characteristics (Table 33), which are described in the HGCA (home grown cereals authority) recommended lists for winter and spring wheat[34]. Different

[33] http://www.wheatisp.org/
[34] http://www.hgca.com/varieties/hgca-recommended-lists.aspx

shoot characteristics were assumed to represent different root characteristic. The double-haploid (DH) wheat lines Avalon and Candenza (AxC) have been selected based on their different root characteristics determined in paper-roll pre studies by Caihong Bai (for growing conditions see Bai et al. 2013). The double-haploid (DH) lines in the trial derived from F_1 progeny of a cross between cvs. Avalon and Candenza (AxC) developed by Clare Ellerbrook, Liz Sayers and Tony Worland (JIC) as part of a Defra funded project led by ADAS. The parents were originally chosen to contrast for canopy architecture traits by Steve Parker (CSL), Tony Worland and Darren Lovell (Rothamsted) (Table 33).

In the second year of the P_i field trial at Sawyers, 2012/13, some of the commercial varieties and AxC lines were replaced by wheat lines derived from the Watkins landraces wheat collection (Wingen et al. 2014) (Table 33). These lines have been screened in another field experiment at Rothamsted, the WISP donor experiment in 2011/12. In this screening, two varieties had high yield combined with a high capability for P_i translocation into the grain and another had low yield with low capability for P_i translocation into the grain. High biomass with a low dilution effect was considered a desired trait of pre-breeding material by Hawkesford and Riche. Therefore, these three lines were additionally screened at different soil-P_i availability concentrations at Sawyers in 2012/13.

Therefore, the focus for using the P_i field trial at Sawyers was different from that of this thesis which used plant material from it. However, the first aim of this thesis was to screen all genotypes used in the first year of the experiment for potential differences in terms of P_i acquisition, P_i translocation capability and potentially gene expression. The second aim was to screen promising genotypes in at least two consecutive years. However, this was only feasible when using the commercial varieties. The AxC lines 49 and 149 were included in the expression studies for 2011/12 due to their reported root characteristics. However, they could not be investigated further due to their replacement by other varieties in the trial. Finally, only two phenotypically most contrasting commercial wheat varieties were used for gene expression studies in both years

assuming that they would be the most likely to show expressional differences between the selected candidate genes (Table 31).

4.2.3. Plant sampling

Samples were taken from the P_i field trial at Sawyers in 2011/12 (block B) and 2012/13 (block A) from specific plots (Figure 20). Sampling was always done between 9 to 12 am. In order to determine phenotypic and transcriptional differences between the wheat germplasm, root tissues from all nine wheat cultivars (Table 33) were sampled in triplicates (n=3) 21th to 23th May 2012 at growth stage 39/41 (Zadoks et al. 1974) from two main plots with low (3 mg Olsen P_i kg^{-1} air dried soil) and high soil-P_i availability (60 mg Olsen P_i kg^{-1} air dried soil) (Figure 20). In 2012/13, root and shoot samples were taken from four wheat cultivars at three growth stages (Tables 33 and 34) from three main plots with low (3 mg Olsen P_i kg^{-1} air dried soil), average (21 mg Olsen P_i kg^{-1} air-dried soil) and high soil-P_i availability (60 mg Olsen P_i kg^{-1} air-dried soil). P_i acquisition capabilities were the crucial determinants for reducing the number of investigated wheat genotypes in 2012/13 (Table 34).

Table 34: Wheat genotypes and tissues sampled from the P_i-trial at Sawyers in 2013.

Abbreviations for the growth stages were used according to Zadoks et al. (1974). Abbreviations for the cultivars: Conqueror = Con, Paragon = Pa, Maris Widgeon = MW, Cappelle Desprez = CaDe.

Growth stage	Sampling date	Soil-P_i (Olsen P)	Cultivar	Tissues
Late tillering (29/30)	9th May	60	all	Root, shoot
	10th May	15, 3	all	
Booting /heading (49/51)	14th June	60, 15	Con, Pa	Root, leaves, ears
	17th June	60	CaDe, MW	
		15	MW	
		3	Con, Pa	
	19th June	15	CaDe	
		3	CaDe, MW	
Ripening (75); ~30 days post-anthesis	16th July	60, 15	Con, Pa	Root, leaves, rachis, glume, grain
	17th July	60	MW, CaDe	
		15	MW	
		3	Con	
	19th July	15	CaDe	
		3	MW, CaDe, Pa	

Plants were excavated and processed according to previously described procedures for field-derived material sampled at the Broadbalk site (Chapter 2, Section 2.3.). Samples were taken within plot core rows on the plot edge without impairing canopy and yield assessments (Figure 20). Sampling from specific plots made the experimental design a split-plot containing two or three main plots (soil-P_i) and 27 completely randomized sub-plots (genotypes). This arrangement was applied in the statistical analysis for main and interacting effects of genotype and P_i availability (Chapter 4, Section 2.10.). The remaining shoot material from each independent sampling point was bulked for assessing phenotypic traits e.g. tiller weights. The fresh and dry matter (DM) was assessed by subsequent weighing after oven-drying at 80 ˚C for 72 h. The remaining shoot material was further used for chemical analysis (Chapter 4, Section 2.5.).

4.2.4. On-site weather data

On-site meteorological records from 2011 to 2013 were provided by the long-term experiments national capability and data sets requested from the electronic Rothamsted Archive (eRA data) (Figure 21). In 2011, it was dry before the root sampling for the transcriptome analysis at Broadbalk with only 39 mm of rain from March to May and 156 mm pre-harvest from April to July (Figure 21). In 2012, it was very wet before the sampling at Sawyers for the first target gene screening with 250 mm of rain from March to May and 516 mm pre-harvest April to July (Figure 21). In 2013, rainfall was actually within average with 170 mm of rain from March to May and 160 mm April to July pre-harvest (Figure 21).

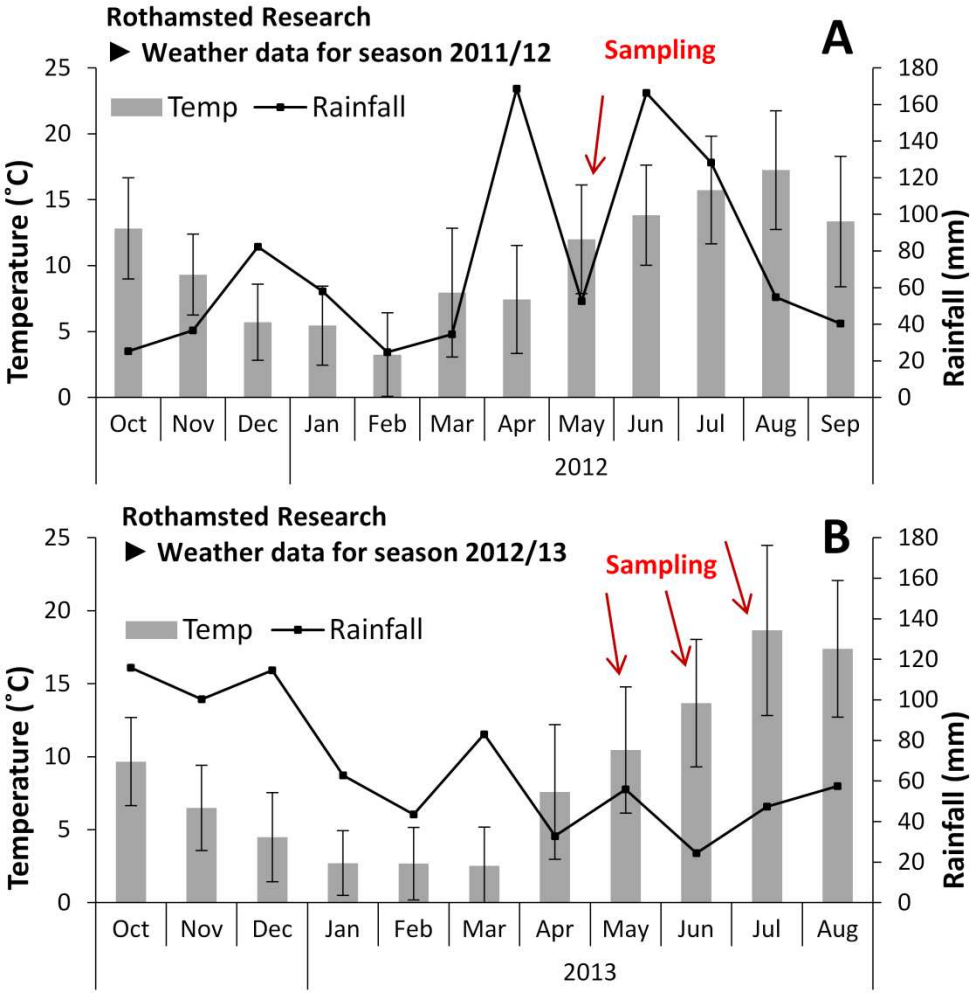

Figure 21: Meteorological data (eRA) from the growing season (A) autumn 2011 to autumn 2012 and (B) autumn 2012 to autumn 2013 at Rothamsted Research, Harpenden, UK.

Temperature and rainfall are presented as average monthly values. Monthly maximal and minimal temperatures are represented as bars with SE. Sampling of plant material from the P_i field trial was done (A) 21th to 23th May in 2012 at early booting (GS 41) (B), 9th and 10th May (GS 29/30), 14th to 19th June (GS 49/50) and 16th to 19th July (GS 75) in 2013; GS = growth stage according to Zadoks et al. 1974 (see also Table 34). The average temperature and rainfall at Rothamsted is 10 °C and 704 mm (Rothamsted 2006).

4.2.5. Chemical analysis

Shoot material was analysed using ICP-AES (Chapter 2, Section 2.5.). Additionally, PO_4-P concentrations were determined in 2012. 100 mg aliquots of ground wheat shoot material was incubated in 2 ml of de-ionised water in a shaking heating block at 80 ˚C for 3 h, followed by 20 min of centrifugation by the maximal speed of 15,000 rpm (HeraeusBiofuge primo R, Kendro, Hanau, Gemany). The supernatant was transferred to a fresh 2 mL Eppendorf tube and

frozen at -20 ˚C over night. After thawing and centrifuging 20 min at a speed of 15,000 rpm (HeraeusBiofuge primo R), the supernatant was filtered using 0.2 µm membrane syringe filter and transferred to a fresh 2 mL Eppendorf tube. Subsequently, samples were diluted 10-fold using 200 µL of filtered extract by adding 1800 µL of deionised water. The concentration of ions was measured using a Skalar SanPlus Colourimetric Continuous Flow Analyser (Skalar SANPLUS System, Skalar Ltd, Breda House, Wheldrake, York, UK) based on the molybdate-blue method (Biltz et al. 1948, Walinga et al. 1989), including blanks and in-house standards every 10th sample.

4.2.6. Phenotyping

Phenotypic data and the nutritional status were determined in both experimental years 2011/12 and 2012/13. Dry matter (DM) and total concentrations of macro- and micronutrients (mg g^{-1} DM) in wheat shoots during the growing season were determined as described previously (Chapter 4, Section 2.3. and 2.5.). Some of the processing steps including samples from tillering and heading in 2012 were performed by a summer student, Adèle Lautrou[35] who was under my supervision. Andrew Riche and Saroj Parmar supervised several more summer students (2013: Adèle Lautrou, Estelle Bancourt, Juliette Hezeques and Pauline Grimonpont, 2012: Nicolas Dien, Theophile Sollet and Xiaochang Dong) who determined tiller density at anthesis (ears numbers per m^2), total P content in grain and straw as well as yield parameters using the core plot area. Raw grain, straw and yield data was also provided by Andrew Riche and Saroj Parmar and calculations and statistical analysis performed. Thousand grain weights (g) were assessed by weighing two 500 grain counts (n=2). These were determined after 16 h of additional oven-drying at 105 ˚C over night in order to avoid any imprecision due to re-moistening during post-harvest storage. Through acquiring all this data, phenotyping during the growing season and at harvest was focused on

[35] Internship 3rd June 2013 to 23rd August 2013; first year undergraduate student (arable and vegetable production) at Campus de Poullié, Angers, France

several aspects for assessing growth development (biomass m^{-2}) and nutrient acquisition. For all these measures except for the response curves to increasing soil-P_i availability, a statistical analysis was performed:

- **Tiller weight** (g DM):
  Average of weighing a bulk of 10 tillers after oven-drying

- **Biomass per area** (g DM m^{-2}):
  Tiller dry weight (g DM) x tiller number per area (number m^{-2})

- **Mineral concentration** (mg g^{-1} DM) determining the nutritional status:
  ICP-AES measurement (ppm) x (sample volume / amount measured)

- **P_i removal per area** (mg m^{-2} or kg ha^{-1}) and other nutritional ions:

  Mineral concentration in shoot tissues (mg g^{-1} DM) x above-ground biomass (g DM m^{-2}) / 100 = P_i acquisition during the growing season

  Mineral concentration in grain or straw (kg t^{-1} DM) x grain or straw yield (t DM ha^{-1}) = P_i removal at harvest

- **P_i efficiency measures**:
  P_i use efficiency (PUE);
  total PUE = grain+ straw yield (kg ha^{-1}) / P_i taken up (kg ha^{-1});
  grain PUE = grain yield (kg ha^{-1}) / P_i taken up (kg ha^{-1})

- **Response curves to increasing soil-P_i availability**:
  Yield response curve (YRC);
  Applying a fitting procedure in Excel v. 2010 (MS Office using the model equation $y = a \ln x + b$ and the natural log of x;

  Critical Olsen P (%) = relative yield ≥ 95 %; corresponds to the critical soil-P_i availability for reaching 95 % of maximal yield
  Relative yield = plot yield / maximal yield plot yield) x 100

4.2.7. Sequence analysis

Homeologue sequence coverage of probes on the Affymetrix Genechip® for the selected candidate genes (Table 31) was partly incomplete. However, this information is indispensable for appropriate primer design and accurate real-time qPCR in order to amplify a putative gene rather than the probe of interest which was hybridized on the microarray. Therefore, each probe sequence was downloaded from the GrainGenes[36] sequence report database and the IWGSC[37] platform using the SeqRepository platform with the basic default BLAST parameter settings "blastn" and "wheat survey sequence / chromosome 1, 2, 3, 4, 5, 6 and 7 ABD genome" for identifying the corresponding contig sequences (Table 35). The best contig with the lowest e-value and the highest percentage of sequence similarity and query coverage (%) was selected and the sequences used for designing primers for gene expression studies.

[36] http://wheat.pw.usda.gov/GG2/index.shtml
[37] http://www.wheatgenome.org/Tools-and-Resources/Sequences, http://wheat-urgi.versailles.inra.fr/Seq-Repository

Table 35: Wheat gene probes and contig sequences of putative candidate genes available in the IWGSC database.

Probe sequences for genes of interest (GOI) were downloaded from the GrainGene sequence report [38] and used as query in the IWGSC SeqRepository platform[39] in order to identify contigs of the wheat survey sequence.

GOI	Probe	IWGSC_ chomosome localization_contig name
TaMYB43/59	Ta.11849.1.S1_at	**chr7AL**_ab_k71_contigs_longerthan_200_4553177 **chr7BL**_ab_k71_contigs_longerthan_200_6737499 **chr7D**L_ab_k71_contigs_longerthan_200_3315689
TaMYB rel	Ta.25744.1.S1_at	**chr2AL**_ab_k71_contigs_longerthan_200_6429953 **chr2BL**_ab_k71_contigs_longerthan_200_8042424 **chr2DL**_ab_k71_contigs_longerthan_200_9898136
TaG3Pp1	Ta.11166.1.A1_at	**chr7AL**_ab_k71_contigs_longerthan_200_4461170 **chr7BL**_ab_k71_contigs_longerthan_200_6714249 **chr7BL**_ab_k71_contigs_longerthan_200_6750285 **chr7DL**_ab_k71_contigs_longerthan_200_3315661
TaG3Pp2	TaAffx.53053.1.S1_at	**chr2AL**_ab_k71_contigs_longerthan_200_6426396 **chr2BL**_ab_k71_contigs_longerthan_200_8052785 **chr2DL**_ab_k71_contigs_longerthan_200_8649713 **chr2DL**_ab_k71_contigs_longerthan_200_4728291
TaPP$_i$ase3	Ta.12413.1.S1_at	**chr3AL**_ab_k71_contigs_longerthan_200_39955 **chr3B**_ab_k71_contigs_longerthan_200_10653973 **chr3B**_ab_k71_contigs_longerthan_200_10653974 **chr3B**_ab_k71_contigs_longerthan_200_9036296 **chr3DL**_ab_k71_contigs_longerthan_200_4995734*1 **chr3DL**_ab_k71_contigs_longerthan_200_1786496*1 **chr3DL**_ab_k71_contigs_longerthan_200_680387*1
TaExt (a)	Ta.5435.1.S1_x_at Ta.13950.1.S1_x_at	**chr7AL**_ab_k71_contigs_longerthan_200_4460067 **chr7DL**_ab_k71_contigs_longerthan_200_3328055
TaExt (b)*[2]	Ta.14492.1.S1_at	c**hr7AL**_ab_k71_contigs_longerthan_200_**4514201**
	Ta.994.1.S1_at	**chr7DL**_ab_k71_contigs_longerthan_200_3392395 **chr7DL**_ab_k71_contigs_longerthan_200_3393013
	Ta.28162.1.S1_at	**chr7AL**_ab_k71_contigs_longerthan_200_**4514201** **chr7BL**_ab_k71_contigs_longerthan_200_6662759 **chr7DL**_ab_k71_contigs_longerthan_200_3392395 **chr7DL**_ab_k71_contigs_longerthan_200_3393013
TaPho1;2	Ta.1006.1.S1_at, TaAffx.84359.1.S1_at	**chr6AL**_ab_k71_contigs_longerthan_200_5832668 **chr6BL**_ab_k71_contigs_longerthan_200_4337586 **chr6DL**_ab_k71_contigs_longerthan_200_3324933
TaPho1;3*[3]	Ta.19715.1.S1_at	**chr7AS**_ab_k71_contigs_longerthan_200_4237829 **chr7BS**_ab_k71_contigs_longerthan_200_3165824 **chr7DS**_ab_k71_contigs_longerthan_200_3869929
TaSPX2	Ta.14013.1.S1_at	**chr7AL**_ab_k71_contigs_longerthan_200_4544238 **chr7AL**_ab_k71_contigs_longerthan_200_4554925 **chr7AL**_ab_k71_contigs_longerthan_200_4490212 **chr7AL**_ab_k71_contigs_longerthan_200_4544237 **chr7BL**_ab_k71_contigs_longerthan_200_2323145 **chr7DL**_ab_k71_contigs_longerthan_200_3348189 **chr7DL**_ab_k71_contigs_longerthan_200_3371969 **chr2DL**_ab_k71_contigs_longerthan_200_9736658

*[1] unclear which contig corresponds to probe sequence (see Figure 22)
*[2] similar contigs for different probes (see Figure 23)
*[3] two probe sequences for the same gene transcript

[38] http://wheat.pw.usda.gov/GG2/index.shtml
[39] http://wheat-urgi.versailles.inra.fr/Seq-Repository/BLAST

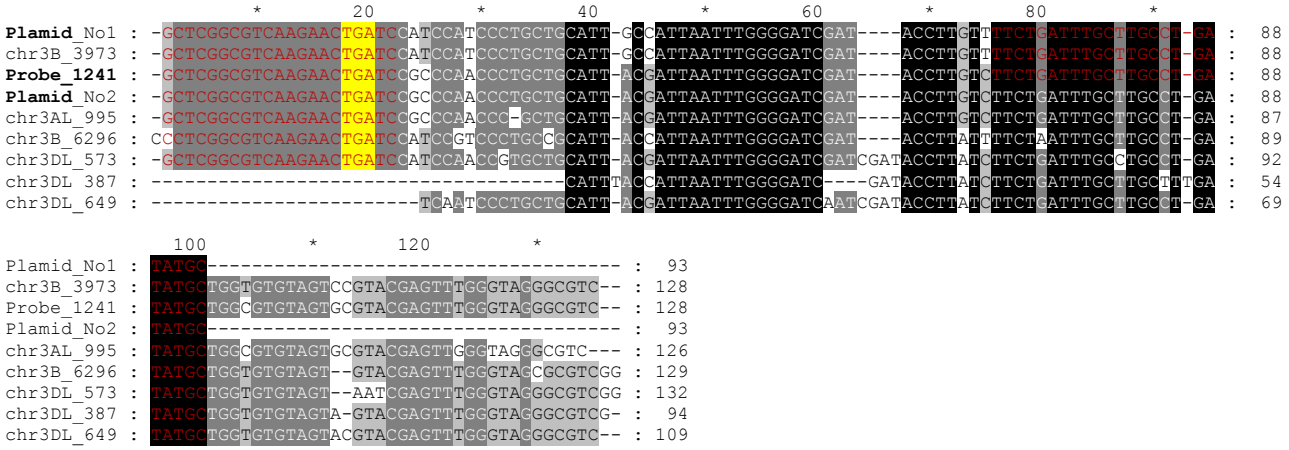

Figure 22: Multiple alignments of IWGSC contig sequences for the TaPP$_i$ase3 gene; in red: primer sequences, in yellow: stop codon.
Alignment generated with the ClustalX v. 1.81 software using the nucleotide sequences of the TaPP$_i$ase3 gene probe on the Affymetrix Genechip® Wheat Genome Array (Ta.12413.1.S1_at), the nucleotide sequences of the two sequenced plasmids containing TaPP$_i$ase3 nucleotide sequences as well as the contigs extracted from the IWGSC SeqRepository wheat survey sequence database (Table 35). The section of the alignment shown contains the nucleotide sequences flanked by the primer sequences used for gene expression studies (Table 37) and the non-coding, untranslated 3` region of the probe Affymetrix probe sequence and the corresponding IWGSC contigs. Primer sequences are displayed in red and the stop-codon positions are indicated in yellow for each nucleotide sequence, respectively.

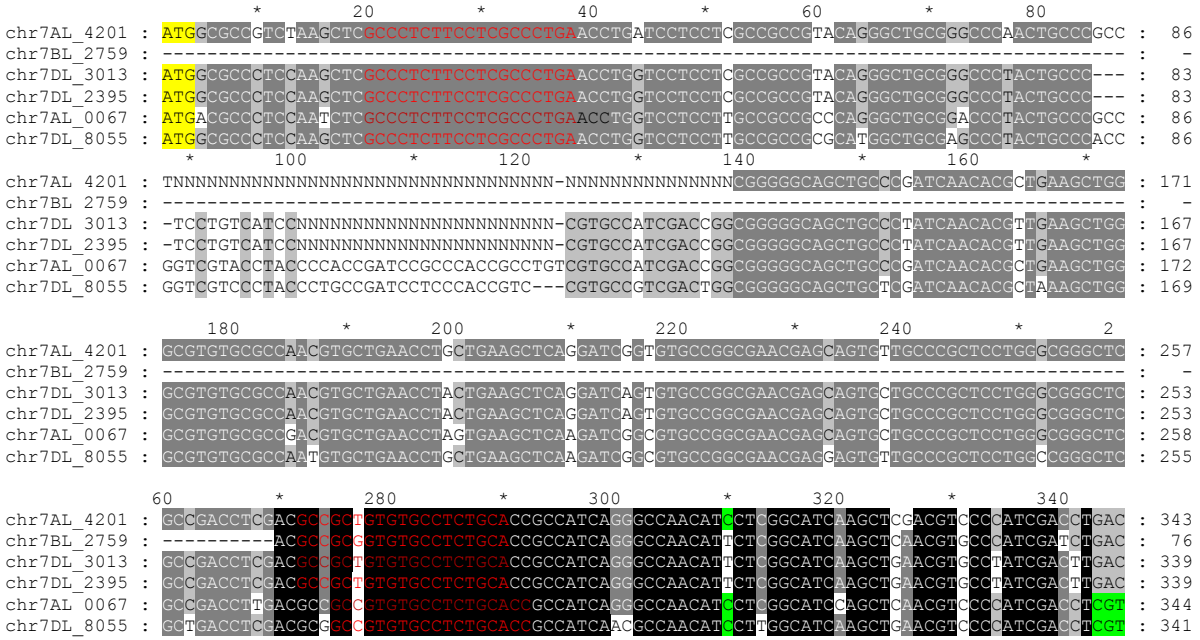

Figure 23: Multiple alignments of IWGSC contig sequences for the TaExt (a) (0067, 8055) and TaExt (b) (4201, 2759, 3013, 2395) genes; in red: primer sequences, in yellow: stop codon.

Alignment generated with the ClustalX v. 1.81 software using the nucleotide sequences of the contigs from the IWGSC SeqRepository wheat survey sequence database (Table 35) for the putative TaExt (a) and TaExt (b) gene probes from the Affymetrix Genechip® Wheat Genome Array (TaExt (a): Ta.5435.1.S1_x_at, Ta.13950.1.S1_x_at; TaExt (b): Ta.14492.1.S1_at, Ta.994.1.S1_at, Ta.28162.1.S1_at). The section of the alignment shown contains the nucleotide sequences flanked by the primer sequences used for cloning and sequencing (Table 36) or for gene expression studies (Table 37) and a part of the non-coding, untranslated 3` region which showed that five probes may represent two different TaExt genes (indicated in green). Primer sequences are displayed in red and the start- and stop-codon positions are indicated in yellow for each nucleotide sequence, respectively.

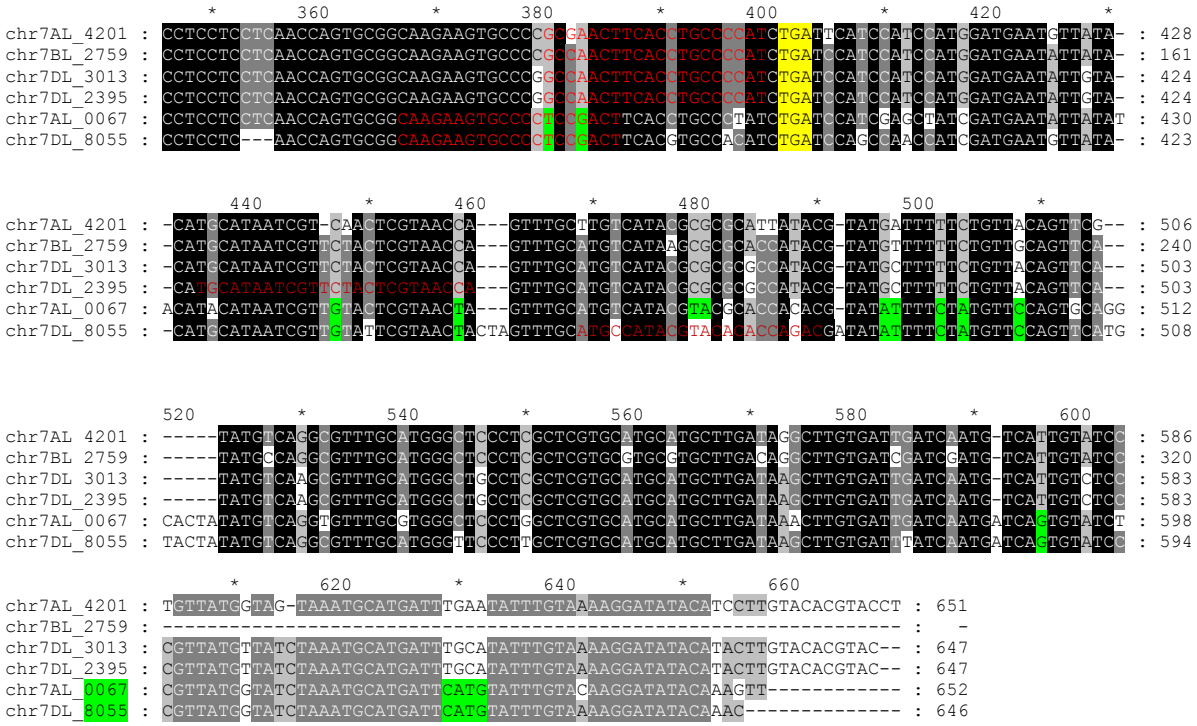

Figure 23 continued.

An additional BLAST in the GrainGenes[40] database was performed using these IWGSC contigs which identified probe sequences as part of the same gene (e.g. TaPho1;2) or putative paralogues of the same gene family (e.g. TaG3Pp1, TaG3Pp2) (Tables 31 and 35). Multiple sequence alignments of the contig and probe sequences were done using the ClustalX v 2.0 (Larkin et al. 2007) and visualized with GeneDoc v. 2.7.000 (Nicholas and Nicholas 1997). For instance, several D genome contigs could be identified for TaPP$_i$ase3 making it difficult to assign them to the specific probe sequence (Figure 22). All probes annotated for putative wheat extensins, TaExts, were used for contig search and the assignment of them to two genes was suggested (Figure 23, Table 35).

4.2.8. RNA isolation, cDNA synthesis and sequence analysis

For validating the expression data from the Affymetrix Genechip®, the identical RNA samples derived from the Broadbalk field trial (Chapter 3, Section 2.1.) were used for cDNA synthesis. Total RNA isolation was extracted from samples derived from the P_i field trial at Sawyers described in Chapter 4, Section 2.8. cDNA synthesis was also performed as described in Chapter 2, Section 2.8. For cloning and sequencing, PCR was performed according to the described procedures in Chapter 2, Section 2.8. and 2.9. using specific primers (Table 36). The purified plasmids were used for determining standard curves in real-time qPCR studies to quantify gene expression on an absolute scale.

[40] http://wheat.pw.usda.gov/GG2/blast.shtml

Table 36: Primer sequences used for cloning and sequencing of wheat candidate genes: Amplicon size (bp), primer concentration (mM), appropriate annealing temperature (˚C) and primer efficiency (%).

Gene	Forward primer, reverse primer	bp	mM	˚C	%
TaMYB 43/59	TGCTTGAGTCGCTTGGAACAGC, ACCGGCTCATCTCCGCTGC	121 ABD	250	59	103
TaMYB rel	GCHGAGACCAAGGCGATGC, GACCTCTGAACCTCCRCCAAT	149 D 150 AB	250	58	101
TaG3Pp1	TTGGCAACGAGTACCTCTCTGA, AGCAGGTAGTTTGTGCATTGGC	546 ABD	250	58	102
TaG3Pp2	GAGATCGACTTGGCTTTCCTTGG, CTCGTAGTCCTTCACATGGCGA	480 ABD	250	58	96
TaPPiase3	GCTCGGCGTCAAGAACTGATC, GCATATCAGGCAAGCAAATCAGAA	93 AB	250	58	97
TaExt-like (a)	GCCCTCTTCCTCGCCCTGA, AGTCGGAGGGGCACTTCTTG	364 AD	250	59	95
TaExt-like (b)	GCCCTCTTCCTCGCCCTGA, ATGGGGCAGGTGAAGTTSGC	379 A	250	59	98
TaPho1;2	CAGTACAAACACCTGGCCTATGT , ATCAATCCGTTTCGAGTTCACGA	565 A	250	59	101
TaPho1;3	GTGTTCTTATTAGTATTGGTCTGC, CAGGCTTCCAATGTTAGGGTG	648 ABD	250	58	97
TaSPX2	GTTCGCCTCCGACAACAGTG, CGCCGGTAAGTAGCCATSGA	320 AD	250	59	85

4.2.9. Expression analysis

Expression analysis via real-time qPCR analysis was described previously (Chapter 2, Section 2.7.). Samples were prepared using gene-specific primers at specific concentrations and appropriate annealing temperatures for 20 sec before extension for 40 sec at 60 ˚C (Table 37). Two reference genes were used for transcript normalization (Long et al. 2010) which code for a heterogeneous nuclear ribonucleoprotein Q (hn RNP)/Ta.10105.1.S1_at for samples derived from Broadbalk (Chapter 3, Section 2.1.) and a cyclin family protein/Ta.27922.1.S1_x_at for samples derived from the P_i field trial at Sawyers (Chapter 4, Section 2.3.) (Table 37). Both primers were stable on the array and not significantly altered by any of the treatments applied. For each primer pair, the amplification efficiency ($E = 10^{(-1/slope)}-1$) was also determined via $\log_{10}$ dilutions dilution series in triplicates (n=3) for different tissues and treatments and considered acceptable within a range of ≥ 85 % to ≤ 115 %. The average efficiencies of each primer pair are presented for plasmid and

standardized root samples in Table 36. However, individual PCR reaction efficiencies for each run will not be shown in the thesis.

Table 37: Primer sequences used for expression analysis of wheat candidate genes via real-time qPCR: Amplicon size (bp), primer concentration (mM) and appropriate annealing temperature (˚C) and primer efficiency (%).
The optimal concentrations with the corresponding annealing temperatures and average efficiencies were determined for each primer pair by $\log_{10}$ dilutions dilution series in triplicates (n=3) using the equation: ($E = 10^{(-1/slope)}-1$).

Gene	Forward primer, reverse primer	bp	mM	˚C	%
TaMYB 43/59	TGCTTGAGTCGCTTGGAACAGC, ACCGGCTCATCTCCGCTGC	121 ABD	200	59	103
TaMYB rel	GCHGAGACCAAGGCGATGC, GACCTCTGAACCTCCRCCAAT	149 D 150AB	150	58	101
TaG3Pp1	GCTCCTCTTGACACATCTTGTC, AGCAGGTAGTTTGTGCATTGGC	92 ABD	150	58	102
TaG3Pp2	GTGGAGCTGGTCGTTTGCAGT, CTCGTAGTCCTTCACATGGCGA	127 ABD	150	58	96
TaPP$_i$ase3	GCTCGGCGTCAAGAACTGATC, GCATATCAGGCAAGCAAATCAGAA	93 AB	150	58	97
TaExt-like (a)	GCCGTGTGCCTCTGCACC, AGTCGGAGGGGCACTTCTTG	112 AB 109 D	200	59	95
TaExt-like (b)	GCCGCTGTGTGCCTCTGCA, ATGGGGCAGGTGAAGTTSGC	128 ABD	150	59	98
TaPho1;2	TTGCBTCCTTGGAGATAATCCG, ATCAATCCGTTTCGAGTTCACGA	135	150	59	101
TaPho1;3	CTTGGCTTCGTAACGATCTGAT, CAGGCTTCCAATGTTAGGGTG	122 ABD	200	58	97
TaSPX2	CATCCAGGTTGCCGATCTCG, GWCGCCGGTAAGTAGCCATS	114 AD	150	58	85
Reference genes					
Ta.10105.1.S1_at	TTGAACTTGCCCGAAACATGCC, CACCTTCGCCAAGCTCAGAAC	123	200	59	110
Ta.27922.1.S1_x_at	TACAGGTGCTTGTTTGCCTATG, GCAGCCTCTTTCCTATCGTTCC	148	200	58	105

4.2.10. Statistical analysis

Phenotypic traits and candidate gene expression data

All phenotypic (Chapter 4, Section 2.6.) and expression data (Chapter 4, Section 2.9.) were statistically analysed using GenStat (2013, 16th edition, (c) VSN International Ltd, Hemel Hempstead, UK). The impact of soil-P$_i$ availability and cultivar on phenotypic traits or candidate gene expression was

determined for each harvest time point in 2012, 2013 and 2014, respectively, by performing a two-way ANOA ($P \leq 0.05$). Sampling in 2012 was performed for two and in 2013 for three (2012/13 and 2013/14) main plots and different numbers of subplots. Therefore, the blocking structure was a non-replicated split plot design [(Plot.Col)/split] and the treatment structure multi factorial [P availability * wheat cultivar] taking into account that columns, not the main plots, are replicated and devoting the varieties spatially within each column (Figure 20).

Correlation of candidate gene expression with mineral concentrations

For determining a correlation of target gene expression in roots (copy number in 0.1 μg of total RNA) vs. total P concentrations (mg g^{-1} DM) in the shoots of wheat grown in two field trials, Broadbalk and Sawyers, at Rothamsted Research and samples at different physiological stages in 2012 and 2013, the method of nonlinear least squares was used to fit an exponential decline model. The model included the gene expression of five target genes (TaPP$_i$ase3, TaExt-like B, TaG3Pp2, TaPho1;3, TaSPX2, TaMYBrel) in terms of nutritional status from five experiments by wheat growth stage combinations and was of the form:

$$\mathbf{y = a + A\exp^{(-B(P+c))}}$$

y = target gene expression,

a = theoretical lower minimal asymptotic gene expression as shoot P concentration increases,

A = maximal possible gene expression above a,

B = exponential rate of decline in gene expression with increasing shoot P concentration,

c = minimal level of shoot P concentration.

F-tests were used to test whether separate a, A, B or c parameters were required for each combination, using the regression method of forward selection of most statistically significant expansion of the model. The parameters a and c were dropped from the model when not significant ($p < 0.05$, F-test). The GenStat

package was used to fit the models by the FITNONLINEAR procedure, which provided the least squares optimisation, estimated parameters and standard errors. Further outputs were the residual variance (s^2), standard error of observations (SE), degrees of freedom (df) and percentage variance explained (R^2) for the best models respectively.

Individual linear relationships may be seen between target gene expression and P_i use efficiency parameters for certain experiment-growth stage combinations. However, both variables were ratios and with underlying variation from two sources, which is unaccounted for applying fitting models such as regression. However, it was possible to look at correlations coefficients, r (lying between -1 and 1) and their p-values in order to show association between gene expression and P_i efficiency ratios. Values greater than -0.5 and 0.5 indicated a strong relationship which is more linear as when r approached -1 or 1.

4.3. Results

4.3.1. Phosphate acquisition determined by growth and yield parameters

Phenotypic variation of growth was determined by assessing tiller density (Figure 24 A, B) and tiller weights (Figure 24 C to G), biomass development (Figure 25) and total P_i removal per area (Figure 26) in 2012 and 2013.

Tiller density was reduced when soil-P_i availability was limiting in both years, but only varied significantly between cultivars in 2012 (Figure 24 A), and not in 2013 (Figure 24 B). In 2012, Conqueror had the highest tiller density at high soil-P_i availability and the lowest tiller density at low soil-P_i availability whereas Capelle Desprez behaved in the opposite manner; however, this observation was not statistically significant (Figure 24 A). Amongst the AxC lines in 2012, AxC 88 had the highest tiller density and AxC 93 had the lowest tiller density (Figure 24 A).

Tiller weights only varied significantly between varieties at booting in 2012 (Figure 24 C). However, they always decreased significantly when soil-P_i availability was limiting in 2012 (Figure 24 C) and at all growth stages in 2013 (Figure 24 D to G). At booting in 2012, the AxC lines all had higher tiller weights compared to the commercial varieties in the trial and amongst the AxC lines, AxC 93 and AxC 149 had the highest and AxC 88 the lowest tiller weights (Figure 24 C). Amongst the commercial varieties, Conqueror had the highest tiller weights at booting in 2012 (Figure 24 C). However, this observation was not significant (Figure 24 C). In 2013, varietal variation in tiller weights occurred at the generative, not the vegetative, stage with Capelle Desprez having the highest tiller weights and Conqueror having the lowest tiller weights (Figure 24 E and F). However, ear weights were not significantly altered by soil-P_i availability at ripening in 2012 (p-value = 0.064; F-statistic not shown) and not significantly different between Conqueror and Capelle Desprez (Figure 24 G). However, Paragon had the highest ear weight at ripening in 2013 and Maris Widgeon had the lowest (Figure 24 G).

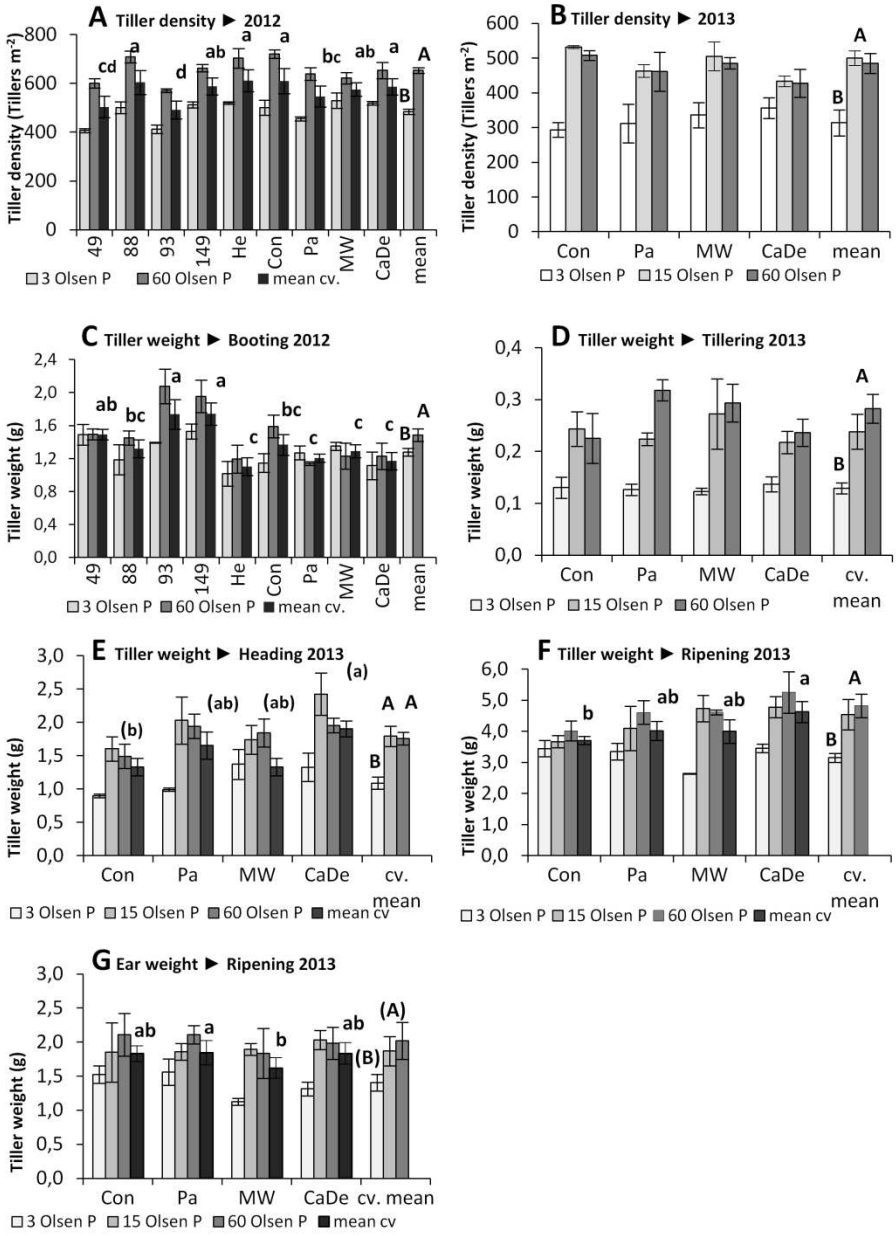

Figure 24: Tiller density in 2012 (A) and 2013 (B) and tiller weights of nine or four wheat genotypes exposed to low (3 Olsen P), medium (15 Olsen P) and high (60 Olsen P) soil-P_i availability (Olsen P; mg P_i kg^{-1} soil) in 2012 at booting (C) and 2013 at tillering (D), heading (E) and ripening (F: shoot, G: ear) at the P_i field trial at Sawyers.

Each bar represents the mean ± SE (n=3) which were compared using statistical properties at the 5% level of significance which are displayed in Table 38. (Abbreviations: Avalon x Cadenza mapping population lines: 49, 88, 93, 149; commercial varieties: Hereward = He, Conqueror = Con, Paragon = Pa, Maris Widgeon = MW (heritage wheat), Capelle Desprez = CaDe). Bars sharing the same capital letter are not statistically different (P>0.05) between canopy parameters and bars sharing the same small letters are not statistically different (P>0.05) between wheat genotype. Figure 25 E: The P-value for the statistical significant influence of cultivars on tiller weight at heading was 0.06. Figure 25 G: The P-value for the statistical significant influence of soil P_i availability on ear weigth was 0.064

Table 38: Statistical properties of phenotypic trait analysis of nine wheat genotypes exposed to different soil-P_i availability (Olsen P) in 2012 and 2013 at the P_i field trial at Sawyers (Figures 25 to 30).*

Sawyers 2012; booting stage (41) Zadoks et al. (1974)				
Trait, growth stage	**F-statistic**	**p-value**	**SED**	**LSD**
Tiller density (no. m^{-2})	$F_{1,4}$ = 418.5 (TF1) $F_{8,32}$ = 8.03 (TF2)	< 0.001 (TF1,TF2)	8.3 (TF1) 22.5 (TF2)	22.9 (TF1) 45.8 (TF2)
Tiller weight (g)	$F_{1,4}$ = 11.7 (TF1) $F_{8,32}$ = 5.9 (TF2)	0.027 (TF1), < 0.001 (TF2)	0.06 (TF1) 0.13 (TF2)	0.168 (TF1) 0.275 (TF2)
Biomass (g m^{-2})	$F_{8,32}$ = 5.2	0.008	109.8	222.8
P_i acquisition (g m^{-2})	$F_{8,30}$ = 4.1	0.041	3.371	6.889
P_i removal at harvest (kg ha^{-1}); straw	$F_{8,31}$ = 13.4	< 0.001	1.431	2.92
P_i removal at harvest (kg ha^{-1}); grain	$F_{8,29}$ = 18.4	< 0.001	1.887	4.032
P_i removal (kg ha^{-1}) ; straw + grain	$F_{8,29}$ = 38.2	< 0.001	2.177	4.794
PO_4-P (mg g^{-1} DM)	$F_{1,4}$ = 108.9	< 0.001	0.0921	0.2557
Total P (mg g^{-1} DM)	$F_{8,30}$ = 4.5	0.006	0.2343	0.4907
Total P (mg g^{-1} DM) at harvest; grain	$F_{1,4}$ = 134.0 (TF1) $F_{8,32}$ = 6.9 (TF2)	< 0.001 (TF1,2)	0.090 (TF1), 0.112 (TF2)	0.251 (TF1) 0.228 (TF2)
Total P (mg g^{-1} DM) at harvest;straw	$F_{8,31}$ = 13.4	< 0.001	1.431	2.92
TGW (g)	$F_{8,32}$ = 2.75	0.020	0.913	1.851
PAE (kg yield per Olsen P); log_2 scale	$F_{1,4}$ = 7301.1 (TF1) $F_{8,32}$ = 32.5 (TF2)	< 0.001 (TF1,2)	0.012 (TF1) 0.017 (TF2)	0.033 (TF1) 0.034 (TF2)
PUE (kg yield per kg P taken up); log_2 scale	$F_{8,29}$ = 6.16	< 0.001	0.035	0.077
Sawyers 2013; growth stages Zadoks et al. (1974)				
Trait , growth stage	**F-statistic**	**p-value**	**SED**	**LSD**
Tiller density (no. m^{-2})	$F_{2,6}$ = 17.2 (TF1)	0.003	30.2	73.8
Tiller weight (g) 29	$F_{2,6}$ = 18.4 (TF1)	0.003	0.024	0.06
Tiller weigth (g) 51	$F_{2,6}$ = 9.1 (TF1)	0.015	0.18	0.442
Tiller weigth (g) 75	$F_{2,6}$ = 7.9 (TF1) $F_{3,17}$ = 3.3 (TF2)	0.021 (TF1) 0.047 (TF2)	0.27 (TF1) 0.36 (TF2)	0.58 (TF1) 0.88 (TF2)
Ear weigth (g) 75	$F_{3,17}$ = 4.4 (TF2)	0.019	0.10	0.21
Biomass (g m^{-2}) 29	$F_{6,12}$ = 8.5 (TF1)	0.018 (TF1)	21.111 (TF1)	51.7 (TF1)
Biomass (g m^{-2}) 51	$F_{2,6}$ = 32.6 (TF1)	<0.001 (TF1)	73.6 (TF1)	180.1 (TF1)
Biomass (g m^{-2}) 75	$F_{2,6}$ = 35.4 (TF1)	<0.001 (TF1)	335.8 (TF1)	137.2 (TF1)
P_i acquisition (kg ha^{-1}) 29	$F_{2,6}$ = 17.6 (TF1)	0.003 (TF1)	0.65 (TF1)	1.59 (TF1)
P_i acquisition (kg ha^{-1}) 51	$F_{2,6}$ = 80.4 (TF1)	< 0.001 (TF1)	1.04 (TF1)	2.55 (TF1)
P_i acquisition (kg ha^{-1}) 75	$F_{2,6}$ = 39.9 (TF1)	< 0.001 (TF1)	2.47 (TF1)	6.05 (TF1)
P concentrations (mg g^{-1} DM) 29	$F_{2,6}$ = 33.23 (TF1)	< 0.001 (TF1)	0.24 (TF1)	0.59 (TF1)
P concentrations (mg g^{-1} DM) 51	$F_{6,18}$ = 3.66	0.015	0.0035	0.19
P concentrations (mg g^{-1} DM) 75; shoot	$F_{2,6}$ = 4.95 (TF1) $F_{3,16}$ = 3.4 (TF2)	0.054 (TF1) 0.044 (TF2)	0.1817 (TF1) 0.082 (TF2)	0.45 (TF1) 0.17 (TF2)
P concentrations (mg g^{-1} DM) 75; ears	$F_{2,6}$ = 5.82 (TF1)	0.039	0.122 (TF1)	0.23 (TF1)
TGW (g) 85	$F_{6,16}$ = 8.46	<0.001	1.014	2.12
P_i removal 85 (kg ha^{-1}); straw	$F_{2,6}$ = 15.4 (TF1)	0.004 (TF1)	0.43 (TF1)	1.05 (TF1)

Table 38 continued.

P_i removal 85 (kg ha^{-1}); grain	$F_{2,6}$ = 48.3	(TF1)	< 0.001	(TF1)	1.43	(TF1)	3.50	(TF1)
P_i removal 85 (kg ha^{-1}); total	$F_{2,6}$ = 111.04	(TF1)	< 0.001	(TF1)	1.07	(TF1)	2.61	(TF1)
PUE (kg yield per kg P taken up); log_2 scale	$F_{2,6}$ = 41.17	(TF1)	< 0.001	(TF1)	0.03		0.07	

* F-statistic; TF = Treatment factors: TF1 = P_i supply, TF2 = cultivar; interaction when no 'TF' indicated; yield @ 100 % DM; 29 = tillering, 51 = heading, 75 = ripening, 85 = harvest; TGW = thousand grain weight; PUE = P_i use efficiency

Shoot biomass was reduced across all cultivars at limited soil-P_i availability in 2012 at booting (Figure 25 A). The varieties growing in the trial in 2012 responded differently to high soil-P_i availability at booting; AxC line 93 and 149 as well as Conqueror had the highest shoot biomass and Paragon, Maris Widgeon and Capelle Desprez had the lowest shoot biomass (Figure 25 A). AxC line 49 and 88 as well as Hereward had intermediate shoot biomasses (Figure 25 A). AxC line 93 and Conqueror increased their shoot biomass by the greatest margin in response to soil-P_i availability whereas Paragon, Maris Widgeon and Capelle Desprez did not respond significantly to increasing soil-P_i availability (Figure 25 A). In 2013, soil-P_i availability had no impact on varietal variation on shoot biomass at any physiological stage (Figure 25 B to D). In 2013, the wheat variety had no significant impact on shoot biomass at any of the growth stages (Figure 25 B to D). However, limited soil-P_i availability decreased shoot biomass of all varieties at all growth stages from booting to ripening (Figure 25 B to D). In contrast to 2012 at booting (Figure 25 A), Paragon, Maris Widgeon and Capelle Desprez increased their shoot biomass in response to increasing soil-P_i availability in 2013 at booting stage (Figure 25 B), heading (Figure 25 C) and ripening (Figure 25 D).

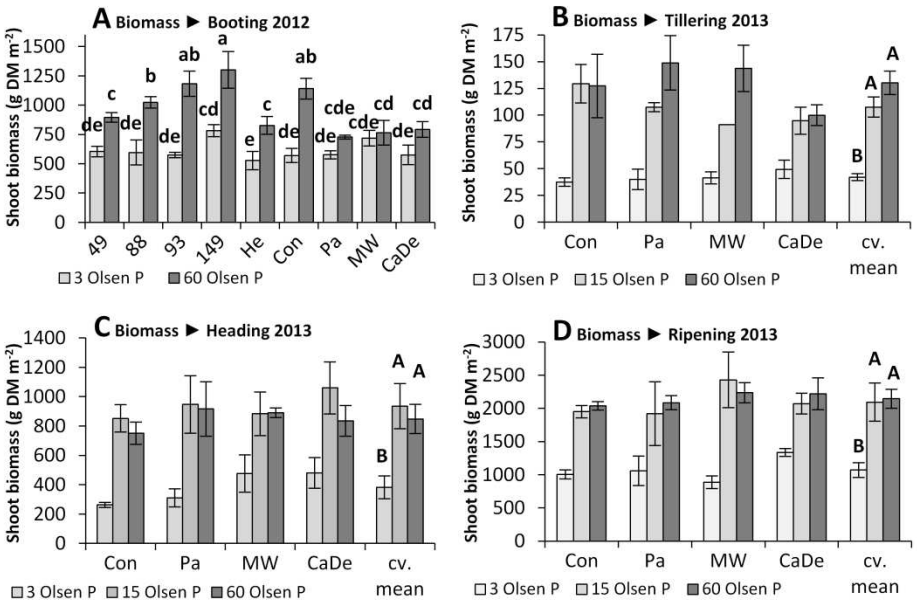

Figure 25: Shoot biomass (g DM m^{-2}) of nine or four wheat genotypes exposed to low (3 Olsen P), medium (15 Olsen P) and high (60 Olsen P) soil-P_i availability (Olsen P; mg P_i kg^{-1} soil) in 2012 at booting (A) and 2013 at tillering (B), heading (C) and ripening (D) at the P_i field trial at Sawyers.

Each bar represents the mean ± SE (n=3) which were compared using statistical properties at the 5% level of significance which are displayed in Table 38. (Abbreviations: Avalon x Cadenza mapping population lines: 49, 88, 93, 149; commercial varieties: Hereward = He, Conqueror = Con, Paragon = Pa, Maris Widgeon = MW (heritage wheat), Capelle Desprez = CaDe). Bars sharing the same capital letter are not statistically different (P>0.05) between biomass and bars sharing the same small letters are not statistically different (P>0.05) between wheat genotype.

In 2012, P removal at booting at low Olsen P concentration was independent from the genotypes whereas at high soil-P_i availability P_i acquisition was highest for AxC lines 88, 93, 149, and Conqueror and lowest for Hereward, Paragon and Maris Widgeon (Figure 26 A). The AxC line 49 and Capelle Desprez had intermediate P removal rates at high soil-P_i availability at booting in 2012 (Figure 26 A). In 2013, P removal rates at booting, heading and ripening were lowest at the lowest Olsen P concentration, intermedium at the medium Olsen P concentration and highest at the highest Olsen P concentration (Figure 26 A to D).

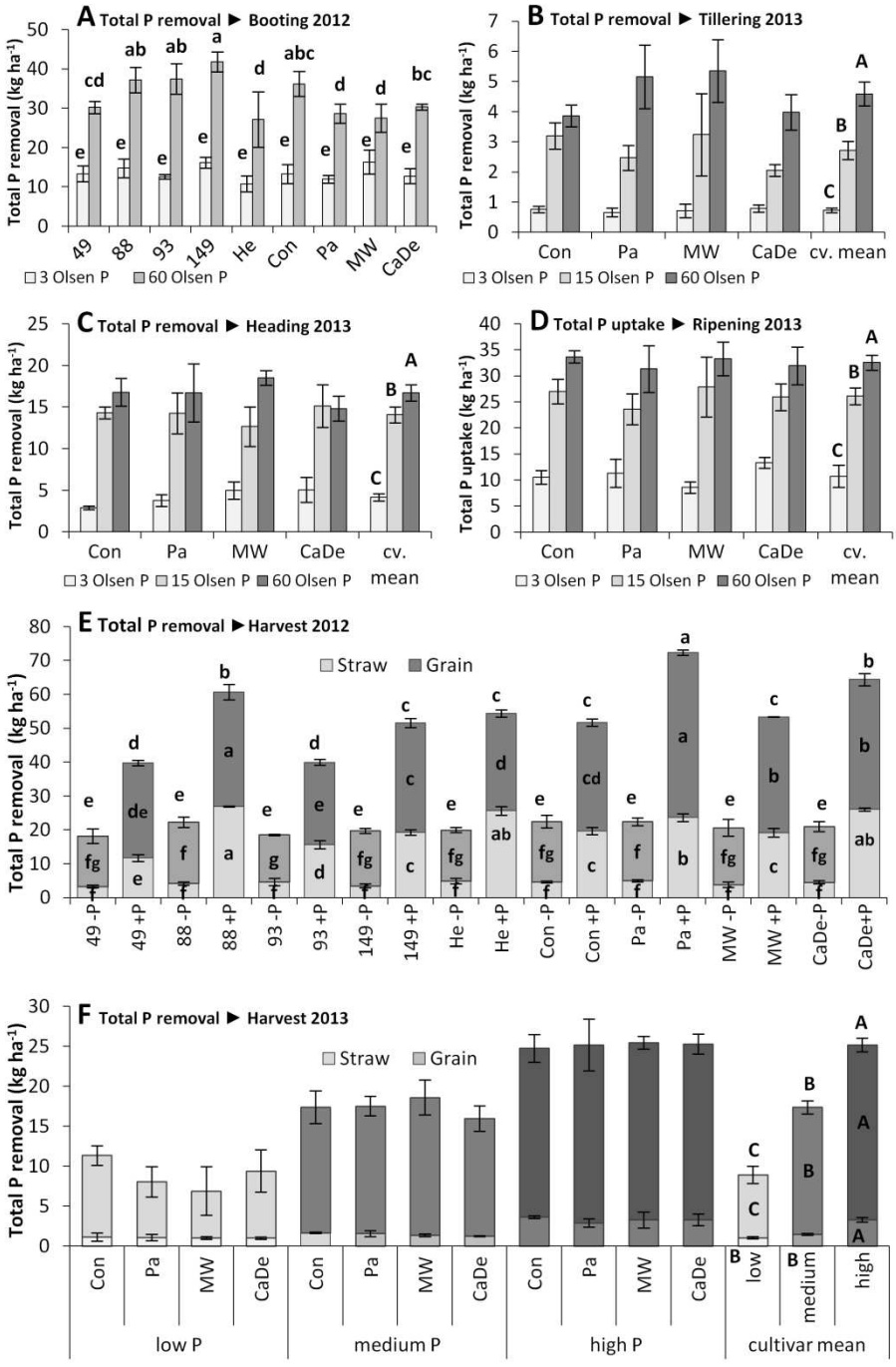

Figure 26: Total P removal (kg P_i ha^{-1}) of nine wheat genotypes exposed to low (3 Olsen P), medium (15 Olsen P) and high (60 Olsen P) soil-P_i availability (Olsen P; mg P_i kg^{-1} soil) in 2012 at booting (A) and harvest (E) and in 2013 at tillering (B), heading (C), ripening (D) and harvest (F) at the P_i field trial at Sawyers.

Each bar represents the mean ± SE (n=3) which were compared using statistical properties at the 5% level of significance which are displayed in Table 38. (Abbreviations: Avalon x Cadenza mapping population lines: 49, 88, 93, 149; commercial varieties: Hereward = He, Conqueror = Con, Paragon = Pa, Maris Widgeon = MW (heritage wheat), Capelle Desprez = CaDe). Bars sharing the same capital letter are not statistically different (P>0.05) between P_i removal and acquisition rates and bars sharing the same small letters are not statistically different (P>0.05) between wheat genotype.

Even at high Olsen P concentrations, the variety had no significant influence on P removal rates in 2013 at any of the growth stages (Figure 26 A to D) including heading (Figure 26 B). Therefore, compared to 2012 at booting (Figure 26 A), Conqueror did not have the highest P removal rates in 2012 at tillering (Figure 26 B), heading (Figure 26 C) or ripening (Figure 26 D).

In 2012, all varieties removed around 20.6 kg P ha^{-1} at harvest; 4.3 P ha^{-1} via straw and 16.3 kg P ha^{-1} via grain at low soil-P_i availability (Figure 26 E). At high soil-P_i availability, P_i removal at harvest was high with 52.9 kg P ha^{-1} across all varieties; 20.6 kg P ha^{-1} via straw and 32.5 kg P ha^{-1} via grain (Figure 26 E). At low Olsen P concentrations, P removal rates via the straw were not significantly different between cultivars (Figure 26 E). Significant differences for P removal rates via the grain were highest for AxC line 88 and Paragon and lowest for AxC line 93 (Figure 26 E). At high soil-P_i at harvest in 2012, Paragon removed the most soil-P_i via grain and straw at high Olsen P concentrations, whereas AxC line 49 and AxC line 93 removed the lowest amounts of soil-P_i via grain and straw (Figure 26 E). AxC line 88, Hereward and Capelle Desprez removed the most soil-P_i through the straw at high Olsen P concentrations. Maris Widgeon and Capelle Desprez removed high amounts of P via the grain in 2012 at high Olsen P concentrations (Figure 26 E). However, AxC line 88 and Paragon removed the highest amounts of P via the grain in 2012 at high Olsen P concentrations (Figure 26 E).

In 2013, only soil-P_i availability, not the cultivar, had a significant effect on P removal rates at harvest (Figure 26 F). Across varieties, the wheat plants removed around 8.05 kg P ha^{-1} at low soil-P_i availability at harvest; 1.05 P ha^{-1} via straw and 7.9 kg P ha^{-1} via grain, 17.36 kg P ha^{-1} at intermedium soil-P_i availability at harvest; 1.46 P ha^{-1} via straw and 15.9 kg P ha^{-1} via grain and 25.2 kg P ha^{-1} at high soil-P_i availability at harvest; 3.28 P ha^{-1} via straw and 21.9 kg P ha^{-1} via grain (Figure 26 F). Therefore, P removal rates at harvest via the straw were highest at high Olsen P concentrations and lower at intermedium and low Olsen P concentrations (Figure 26 F). However, P removal rates at harvest via the grain were highest at high Olsen P

concentrations, intermedium at intermedium Olsen P concentrations and low at low Olsen P concentrations in 2013 (Figure 26 F)

4.3.2. Shoot phosphate concentrations during the growing season

In contrast to shoot P_i concentrations at booting in 2012 (Figure 27 A), total shoot or ear P concentrations varied significantly between genotypes at booting in 2012 (Figure 27 B). However, the cultivar only had a significant effect on shoot P concentrations at booting at high soil-P_i availability (Figure 27 B). At high soil-P_i availability, P shoot concentration was highest in AxC line 88, Paragon and Capelle Desprez, and lowest in AxC lines 49, 93 and 149, Hereward and Conqueror (Figure 27 B).

In 2013, total shoot P concentrations were determined by soil-P_i availability across all cultivars, being low at the lowest Olsen P concentration, intermedium at the medium Olsen P concentration and high at the highest Olsen P concentration (Figure 27 C to F). At tillering in 2012, shoot P concentrations were not significant different between varieties (Figure 27 C). However, significant varietal differences in shoot P concentrations occurred 2013 across all three Olsen P concentrations at heading (Figure 27 D) and ripening in the shoot tissues at medium and high soil-P_i availability (Figure 27 E). Conqueror and Maris Widgeon exhibited the highest shoot P concentrations at high soil-P_i availability at heading (Figure 27 D). However, Conqueror exhibited the highest shoot P concentrations and Maris Widgeon the lowest across all Olsen P concentrations at ripening (Figure 27 E). Paragon and Capelle Desprez had low shoot P concentrations at heading in 2013 (Figure 27 D) but intermedium shoot P concentrations across all Olsen P concentrations at ripening in 2013 (Figure 27 E). P concentrations in the ears at ripening were not significantly different between cultivars (Figure 27 F).

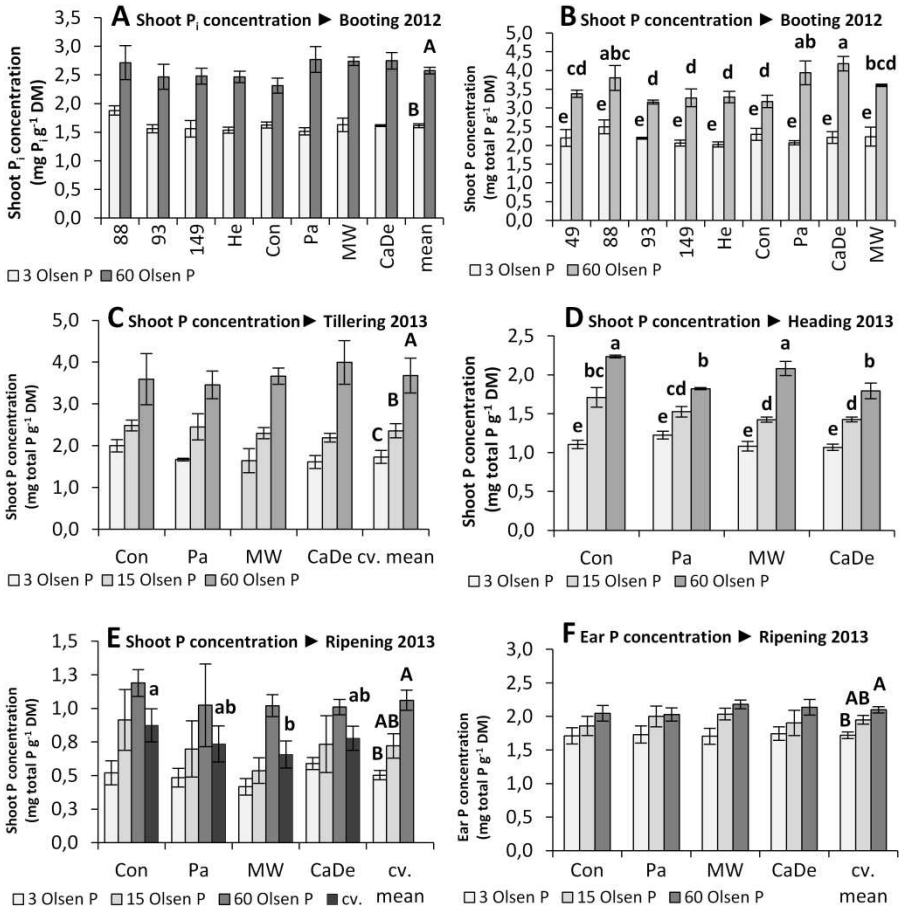

Figure 27: Shoot P_i concentrations (A) and total P concentrations (mg g^{-1} DM) (B to F) in tissues of nine or four wheat genotypes exposed to low (3 Olsen P), medium (15 Olsen P) and high (60 Olsen P) soil-P_i availability (Olsen P; mg P_i kg^{-1} soil) in 2012 (A and B) at booting and in 2013 at tillering (C), heading (D), ripening (E) and in the ears at ripeing (F) at the P_i field trial at Sawyers.

Each bar represents the mean ± SE (n=3) which were compared using statistical properties at the 5% level of significance which are displayed in Table 38. (Abbreviations: Avalon x Cadenza mapping population lines: 49, 88, 93, 149; commercial varieties: Hereward = He, Conqueror = Con, Paragon = Pa, Maris Widgeon = MW (heritage wheat), Capelle Desprez = CaDe). Bars sharing the same capital letter are not statistically different (P>0.05) between shoot P concentrations and bars sharing the same small letters are not statistically different (P>0.05) between wheat genotype.

4.3.3. Phosphate concentrations at harvest

In 2012, P concentrations in the straw decreased at low Olsen P concentrations across all varieties (Figure 28 A). However, P concentrations in the straw were only significantly different between cultivars at high, not at low, Olsen P concentrations (Figure 28 A). AxC line s 88, 93 and Hereward had the highest

P concentrations in the straw and AxC line 149 the lowest (Figure 28 A). In 2013 at harvest, straw P concentrations were not significantly different between the varieties ($p=0.056$), but the straw P concentrations decreased in all varieties at low and intermedium Olsen P concentrations (Figure 28 B). Grain P concentrations at harvest were significantly different between cultivars across Olsen P concentrations in 2012 (Figure 28 C). Again, AxC line 88 had the highest grain P concentrations and AxC line 93 and 149 had lower P concentrations than AxC line 88 (Figure 28 C). Among the commercial varieties, Capelle Desprez and Maris Widgeon had the highest grain P concentrations (Figure 28 C). Hereward, Conqueror and Paragon had the lowest grain P concentrations of all cultivars investigated (Figure 28 C). In 2013, Maris Widgeon and Capelle Desprez had again the highest grain P concentrations (Figure 28 D). Paragon and Conqueror the lowest grain P concentrations (Figure 28 D). Except for AxC line 49 and Maris Widgeon, the TGW decreased with increasing Olsen P concentrations at harvest in 2012 (Figure 28 E). Across cultivars, the TGW was highest for AxC line 149 and lowest for Hereward and Conqueror (Figure 28 E). In 2013, the effect of increasing Olsen P on the TGW was less evident (Figure 28 F); increasing Olsen P concentrations decreased the TGW of Conqueror, had no effect on the TGW of Paragon but increased the TGW of Maris Widgeon and Capelle Desprez.

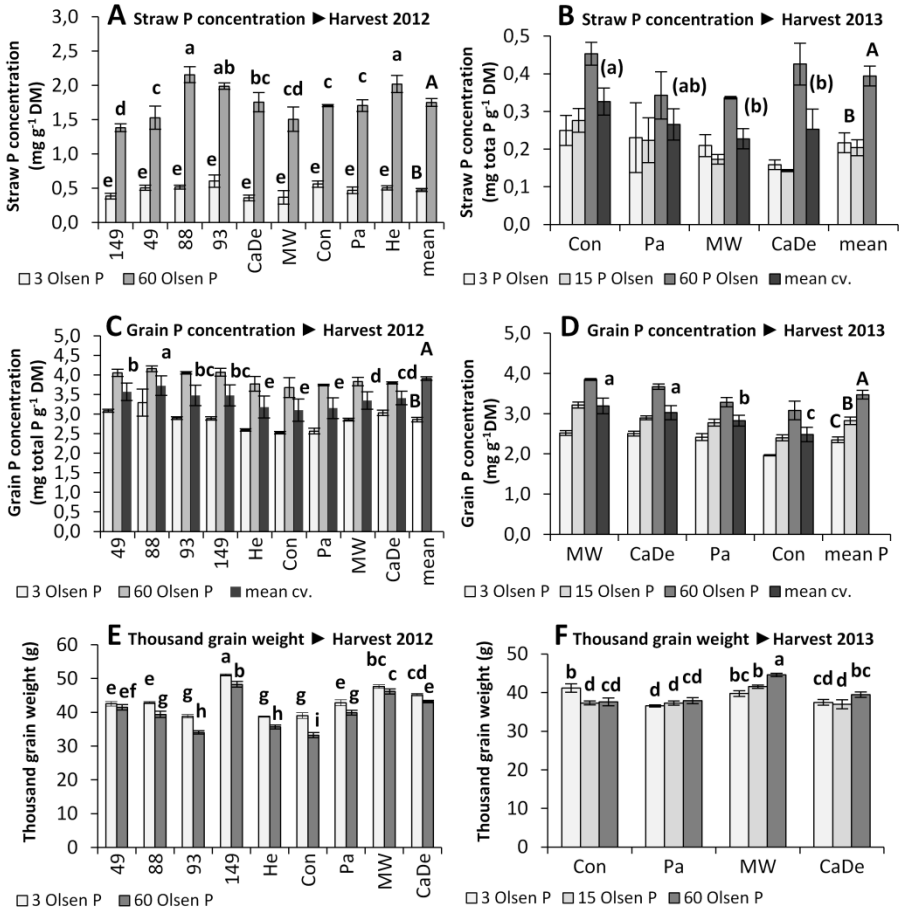

Figure 28: Total P concentrations (mg g^{-1} DM) in straw (A and B) and grain (C and D) and thousand grain weight (g) (E and F) at harvest of nine or four wheat genotypes exposed to low (3 Olsen P), medium (15 Olsen P) and high (60 Olsen P) soil-P_i availability (Olsen P; mg P_i kg^{-1} soil) in 2012 (A, C and E) and 2013 (B, D and F) at the P_i field trial at Sawyers.

Each bar represents the mean ± SE (n=3) which were compared using statistical properties at the 5% level of significance which are displayed in Table 38. (Abbreviations: Avalon x Cadenza mapping population lines: 49, 88, 93, 149; commercial varieties: Hereward = He, Conqueror = Con, Paragon = Pa, Maris Widgeon = MW (heritage wheat), Capelle Desprez = CaDe). Bars sharing the same capital letter are not statistically different (P>0.05) between grain and straw P concentrations and TGW. Bars sharing the same small letters are not statistically different (P>0.05) between wheat genotype. The P-value for significant differences due to cultivar on P concentrations in straw at harvest 2013 was 0,056. Grain and straw data (total P concentration at harvest) are provided and used for analysis with permission of Andrew Riche.

4.3.4. Phosphate acquisition and P_i acquisition efficiency

In 2012, PUE was higher at low soil-P_i and decreased with increasing soil-P_i (Figure 29 A and B). In 2012, PUE was significantly different between

genotypes at high Olsen P availability (Figure 29 A). Capelle Desprez and Maris Widgeon had the highest PUE and AxC 49, 88, 93 and Hereward had the lowest PUE in 2012 (Figure 29 A). However, in 2013, PUE was statistically similar between all genotypes and decreased with increasing soil-P_i availability (Figure 29 A).

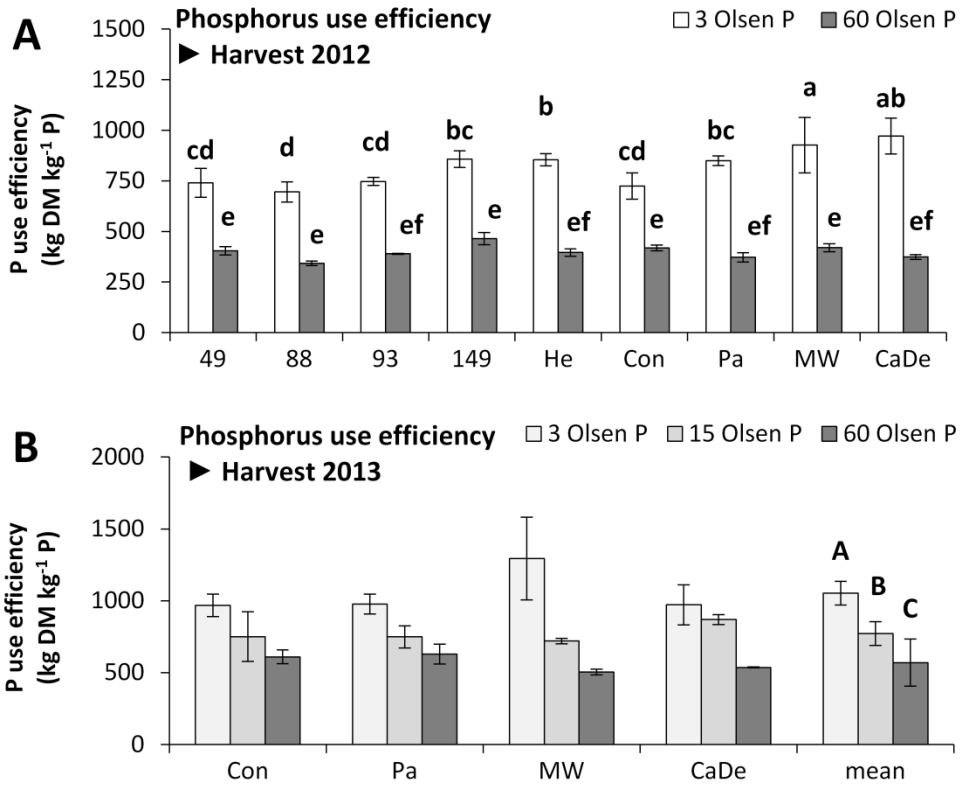

Figure 29: P_i use efficiency (PUE) of nine or four wheat genotypes exposed to low (3 Olsen P), medium (15 Olsen P) and high (60 Olsen P) soil-P_i availability (Olsen P; mg P_i kg^{-1} soil) in 2012 (A) and 2013 (B) at the P_i field trial at Sawyers.

Each bar represents the mean ± SE (n=3) which were compared using statistical properties at the 5 % level of significance which are displayed in Table 38. Yield = grain + straw = total biomass (Abbreviations: Avalon x Cadenza mapping population lines: 49, 88, 93, 149; commercial varieties: Hereward = He, Conqueror = Con, Paragon = Pa, Maris Widgeon = MW (heritage wheat), Capelle Desprez = CaDe). Bars sharing the same capital letter are not statistically different (P>0.05) between P_i efficiency and bars sharing the same small letters are not statistically different (P>0.05) between wheat genotype.

4.3.5. Response curves of the investigated wheat genotypes to increasing soil-P_i availability

In general, the goodness or fit for the yield response curves in 2012 (Figure 30) and in 2013 (Figure 31) was only average (Table 39). The yield reponse curve for 2012 revealed that Conqueror and Paragon had the strongest reponse to increasing soil-P_i availability in 2012 (Figure 30) with Conqueror having the best goodness of fit (Table 39 A). AxC line 49, 88 and Maris Widgeon had a good response to soil-P_i availability in 2012, whereas AxC line 149, Hereward and Capelle Desprez showed nearly no increase in yield as a response to increasing soil-P_i availability (Table 39 A). These three varieties also exhibited the lowest goodness of fit for the determined yield response curve equations in 2012 (Tabel 39 A).

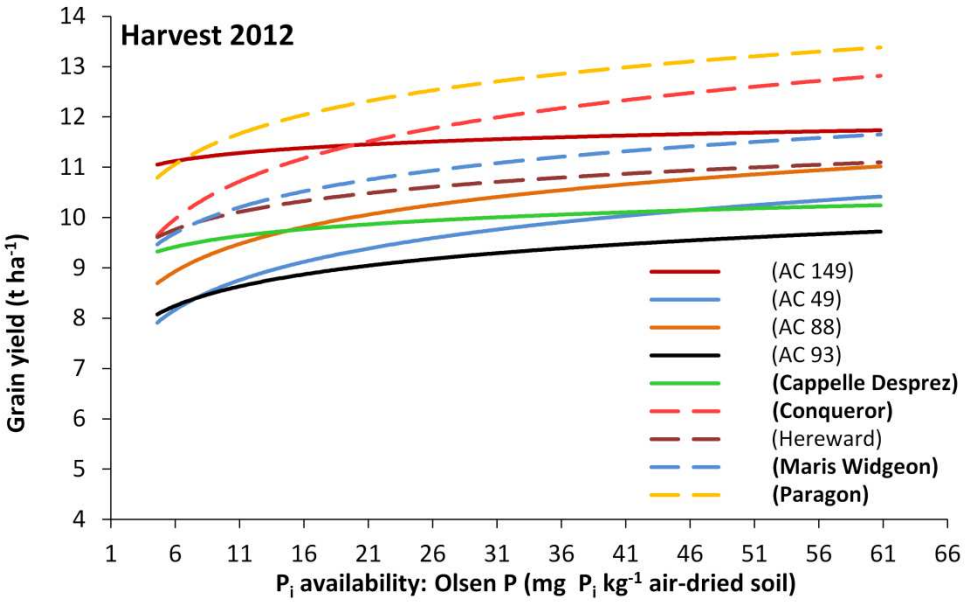

Figure 30: Yield response curve of the nine investigated wheat genotypes exposed to different soil-P_i availability (Olsen P; mg P_i kg^{-1} soil) in 2012 at the P_i field trial at Sawyers.

Abbreviations: Avalon x Cadenza mapping population lines: 49, 88, 93, 149; commercial varieties: Hereward = He, Conqueror = Con, Paragon = Pa, Maris Widgeon = MW (heritage wheat), Capelle Desprez = CaDe The fitting procedure for yield data applied the model equation "y = a ln(x) + b" using the natural log of x (Table 39 A).The data are provided and used with permission of Andrew Riche.

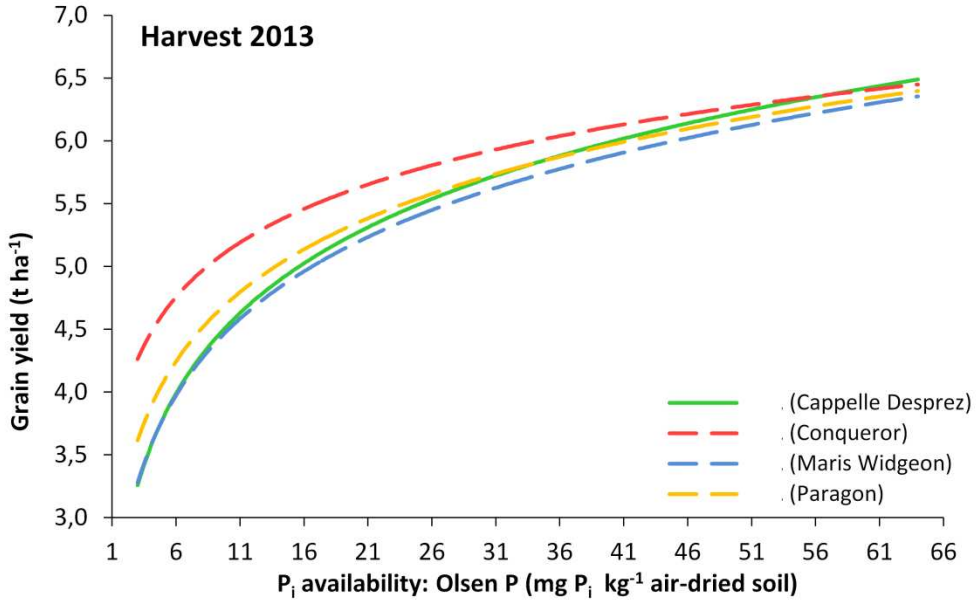

Figure 31: Yield response curve of the four investigated wheat genotypes exposed to different soil-P_i availability (Olsen P; mg P_i kg^{-1} soil) in 2013 at the P_i field trial at Sawyers.

Abbreviations: Conqueror = Con, Paragon = Pa, Maris Widgeon = MW, Capelle Desprez = CaDe. The fitting procedure for yield data applied the model equation "y = a ln(x) + b" using the natural log of x (Table 39 B). The data are provided and used with permission of Andrew Riche.

Table 39: Statistical properties of the fitted yield response curves for the nine investigated wheat genotypes exposed to different soil-P_i availability (Olsen P; mg P_i kg^{-1} soil) at the P_i field trial at Sawyers in 2012 (A) and 2013 (B).

The variables in the model equation "y = a ln(x) + b" are listed for each year and cultivar according to their goodness of fit. The data are provided and used with permission of Andrew Riche.

A: Harvest 2012		
Wheat genotype	**Fitted equation**	**Goodness of fit**
Conqueror	y = 1.2284 ln(x) + 7.7723	R^2 = 0.72
Maris Widgeon	y = 0.846 ln(x) + 8.1767	R^2 = 0.72
AC 49	y = 0.9714 ln(x) + 6.4271	R^2 = 0.71
AC 88	y = 0.9005 ln(x) + 7.3165	R^2 = 0.68
Paragon	y = 1.0027 ln(x) + 9.2619	R^2 = 0.53
AC 93	y = 0.6372 ln(x) + 7.1047	R^2 = 0.49
Hereward	y = 0.5763 ln(x) + 8.7303	R^2 = 0.28
Capelle Desprez	y = 0.3578 ln(x) + 8.7761	R^2 = 0.23
AC 149	y = 0.2639 ln(x) + 10.65	R^2 = 0.05
B: Harvest 2013		
Wheat genotype	**Fitted equation**	**Goodness of fit**
Capelle Desprez	y = 1.0558 ln(x) + 2.0977	R^2 = 0.50
Maris Widgeon	y = 1.0054 ln(x) + 2.1734	R^2 = 0.44
Paragon	y = 0.9091 ln(x) + 2.1734	R^2 = 0.29
Conqueror	y = 0.7149 ln(x) + 3.4765	R^2 = 0.22

In 2013, the yield response curve, Paragon, Maris Widgeon and Capelle Desprez showed the best response to increasing soil-P_i availability (Figure 31, Table 38 B). Conqueror had the lowest response and a very low goodness of fit for the determined yield response curve equations in 2012 (Table 39 B).

The average critical Olsen P (COP) ranged from 12 to 20 mg Olsen P kg^{-1} air-dried soil in 2012 (Table 40) and from 27 to 32 mg Olsen P kg^{-1} air-dried soil in 2013 (Table 41). In 2012, the COP was particularly high for Hereward, Conqueror and AxC lines 49 and 88 compared to other cultivars, whereas it was lower for Paragon, Maris Widgeon and Capelle Desprez (Table 40).

Table 40: Relative yield of nine wheat genotypes exposed to different soil-P_i availability (Olsen P; mg P_i kg^{-1} soil) in 2012 at the P_i field trial at Sawyers.
Abbreviations: Avalon x Cadenza mapping population lines: 49, 88, 93, 149; commercial varieties: Hereward = He, Conqueror = Con, Paragon = Pa, Maris Widgeon = MW (heritage wheat), Capelle Desprez = CaDe. For more information about the varieties: Table 33. The actual Olsen P values were determined before the growing season in 2011/12 and are indicated in brackets ( ) within the table. The yield data provided with permission of Andrew Riche. The relative yield was calculated according to this formula: Relative yield (%) = (yield of each plot / max. plot yield) x 100; yield t ha^{-1}

Olsen P	Cultivar								
	AC 49	AC 88	AC 93	AC 149	He	**Con**	**Pa**	**MW**	**CaDe**
4.6 (3)	73	78	77	72	75	72	74	76	82
6.8 (6)	77	77	86	86	88	82	91	84	**99**
8 (9)	85	85	89	89	90	83	85	88	88
10.8 (12)	81	87	80	90	81	80	78	93	89
12.4 (15)	**95**	92	**97**	**100**	90	82	**96**	**95**	**97**
14.2 (18)	91	84	**94**	94	91	85	90	87	85
22.2 (21)	86	**100**	**99**	**88**	89	**98**	**95**	**97**	90
22.2 (25)	89	**98**	94	**96**	**100**	90	86	92	93
24.2 (30)	**98**	91	**100**	**90**	81	**98**	**98**	**95**	89
32.6 (40)	**98**	**96**	**95**	**90**	93	**100**	93	**96**	**95**
43.8 (50)	**100**	**96**	**96**	78	**99**	94	**96**	**100**	93
60.8 (60)	**95**	**95**	93	91	88	93	**100**	**97**	**100**
max. yield (t ha^{-1})	10.29	10.96	9.72	9.72	11.66	12.75	13.39	11.50	10.67
Critical Olsen P values for 95% yield: 14-22									

Generally the COP values in 2013 were higher (Table 41) compared to 2012 (Table 40). Additionally, yield was around 4 t h^{-1} lower in 2013 (Table 41) than in 2012 (Table 40). Conqueror still required higher soil-P_i availability to reach maximal yield compared to Paragon, Maris Widgeon and Capelle Desprez in 2013 (Table 41). However, for the majority of the varieties, yield decreased when P_i availability exceeded > 32 Olsen P exhibiting a very variable COP response (Table 41). The AxC lines 49 and 93 as well as the three Watkins lines were only considered in order to make a general statement about the average COP in 2013 across varieties growing in the trial. They were not considered in the further analysis.

Table 41: Relative yield of nine wheat genotypes exposed to different soil-P_i availability (Olsen P; mg P_i kg^{-1} soil) in 2013 at the P_i field trial at Sawyers.

Abbreviations: Avalon x Cadenza mapping population lines: 49, 93, commercial varieties: Conqueror = Con, Paragon = Pa, Maris Widgeon = MW (heritage wheat), Capelle Desprez = CaDe, WC = Watkins lines. For more information about the varieties: Table 33. The actual Olsen P values were determined before the growing season in 2012/13 and are indicated in brackets ( ) within the table. The yield data provided with permission of Andrew Riche. The relative yield was calculated according to this formula: Relative yield (%) = (yield of each plot / max. plot yield) x 100; yield t ha^{-1}

	Cultivar								
Olsen P	AC 49	AC 93	**Con**	**Pa**	**MW**	**CaDe**	WC 451	WC 496	WC 753
3 (3)	34	28	61	37	29	46	39	31	60
6 (6)	67	76	51	79	68	64	65	69	51
7 (12)	43	55	45	45	49	51	48	44	53
9 (9)	56	58	77	58	67	72	71	65	**94**
15.2 (18)	42	49	47	48	45	48	46	36	60
15.4 (25)	45	45	50	46	55	53	55	44	63
24 (15)	75	99	76	72	67	70	69	48	87
27 (21)	60	84	76	**91**	64	85	**100**	76	92
32 (30)	**100**	**100**	60	**100**	**100**	**100**	74	**100**	79
51.8 (50)	48	50	50	50	63	69	55	54	73
58 (40)	**87**	**102**	**100**	75	**87**	**106**	**92**	69	**98**
64 (60)	76	86	80	85	73	**82**	84	85	**100**
max. yield (t ha^{-1})	7.21	5.73	8.60	7.98	7.91	7.29	7.08	6.99	6.45
Critical Olsen P values for 95% yield: 27-32									

4.3.6. Validation of results from the transcriptome study in Chapter 3

Generally, gene expression determined via microarray analysis (using the Affymetrix Genechip®) correlated well with those using real-time qPCR (Figure 32, Table 42).

In the microarray analysis, the cluster 2 gene, TaG3Pp1, was weakly up-regulated in P_i starved wheat roots (Figure 17) but differentially regulated in many other studies (Table 25). Real-time qPCR analysis confirmed these expression patterns (Figure 32 A). TaG3Pp2 expression patterns were similar to TaG3Pp1 (Figure 32 A and B); TaG3Pp2 belongs to the same gene family (Table 31), was down-regulated during N starvation and assigned to cluster 3 (Table 18 C). However, TaG3Pp2 was higher expressed than TaG3Pp1, was more up-regulated in P_i starved roots (absolute values not shown; Figure 32 A and B), real-time qPCR and microarray results correlated better (Table 42) and TaG3Pp2 was therefore used in the candidate gene screen in a wider germplasm.

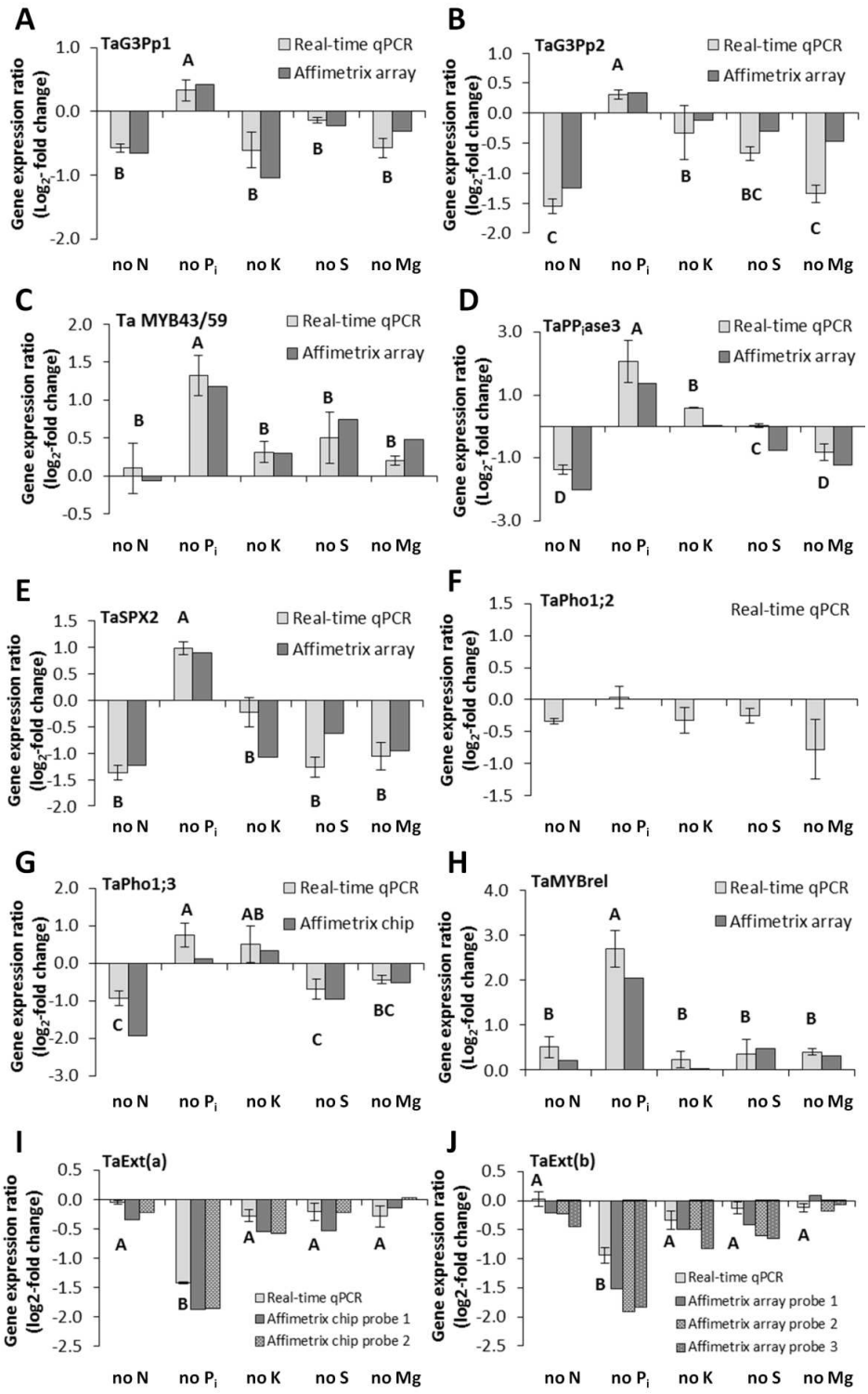

Figure 32: Comparison of candidate gene expression in transcriptome study on field-grown wheat roots from Broadbalk in 2011 (shown as log_2-fold ratio; treatment vs. control) determined via microarray analysis (Affymetrix Genechip®) and real-time qPCR for (A) TaG3Pp1, (B) G3Pp2 and (C) MYB-TF 43/59 (cluster 2), (D) TaPP$_i$ase3, (E) TaSPX2, (F) TaPho1;2 and (G) TaPho1;3 (cluster 3), (H) MYBrel (cluster 5) and (I) TaExt (a) and (J) TaExt (b) (cluster 6).

Figure 32 continued.
The statistical analysis was done using GenStat (2013, 16th edition) on an absolute scale (copy numbers) using real-time qPCR expression data (Table 42) enabling to present SE bars for the data. The microarray data was already statistically analysed using GeneSpring GX v. 12.6 (Agilent Technologies). Therefore, no SE bars are presented for the array data.

Table 42: Statistical properties of comparison of candidate gene expression in transcriptome study on field-grown wheat roots from Broadbalk in 2011 determined via microarray analysis (Affymetrix Genechip®) and real-time qPCR (Figure 32 A to J).

Gene	ANOVA analysis:	Linear regression model:	Correlation: $R^2 \pm$ SE (%)
(A) TaG3Pp1	P = 0.016	y = 0.667x - 0.071; p = 0.043	72.2 ± 0.22
(B) TaG3Pp2	P = 0.004	y = 1.205x - 0.285; p = 0.025	80.5 ± 0.33
(C) TaMYB43/59	P = 0.018	y = 0.951x - 0.011; p = 0.035	75.7 ± 0.24
(D) TaPP$_i$ase3	P ≤ 0.001	y = 1.0355x + 0.6402; p = <0.001	98.5 ± 0.16
(E) TaSPX2	P = 0.002	y = 0.957x - 0.021; p = 0.076	60.6 ± 0.62
(F) TaPho1;2	not significant	no model	no correlation
(G) TaPho1;3	P = 0.040	y = 0.752x + 0.286; p = 0.03	78.2 ± 0.35
(H) TaMYB rel	P ≤ 0.001	y = 1.248x + 0.069; p = 0.003	95.2 ± 0.23
(I) TaExt (a)	P = 0.008	y = 0.7229x + 0.0075; p = <0.001	88 ± 0.18
(J) TaExt (b)	P = 0.021	y = 0.5224x + 0.0408; p = <0.001	85.4 ± 0.14
All genes		y = 0.8405x + 0.1231; p = <0.001	79 ± 0.36

The cluster 2 gene MYB43/59 was up-regulated in P_i starved wheat roots (Table 18 A, Figure 32 C) showing high correlation between both transcriptome analysis methods (Table 42).

The cluster 3 gene TaPP$_i$ase3 was up-regulated under P_i starvation, down-regulated under Mg and N starvation (Table 18 B) and was differentially regulated under P_i starvation in many other studies (Figure 17, Table 26). Validation of the microarray data via real-time qPCR showed similar results (Figure 31 D) and a good correlation (Table 42).

In the microarray analysis, TaSPX2 was only down-regulated in N starved wheat (Figure 17, Tables 18 C, 19 and 26) but was additionally down-regulated in K starved plants when using real-time PCR (Figure 32 E) which reduced the correlation between methods (Table 42). Unfortunately, TaSPX1, another SPX gene (Tables 31 and 35), could not be assessed via real-time qPCR due to a very low expression level and primer-related problems.

TaPho1;2 was not differentially regulated by any macronutrient starvation in wheat roots and was therefore used as a negative control exhibiting comparability between real-time qPCR and microarray analysis (Figure 32 F). The expression of another TaPho1 gene, TaPho1;3 was down-regulated in N starved, but not up-regulated in P_i starved field-grown wheat roots (Table 18 C) in the microarray analysis (log_2fold change: + 0.11). However, TaPho1;3 expression was higher in P_i starved compared to N starved roots when using real-time qPCR (Figure 32 G) resulting in a low correlation between both methods (Table 42).

Amongst the MYB-TFs, the cluster 5 gene TaMYBrel was strongly up-regulated in P_i starved wheat roots (Table 18 A). The microarray TaMYBrel expression analysis was successfully validated via real-time qPCR showing high correlation between both methods (Figure 32 H, Table 42).

TaExt (a) and TaExt (b) were assigned to cluster 6 and down-regulated in P_i starved wheat roots (Table 18 D). The cross-comparison revealed an overlap of five wheat probes with maize and Brachypodium extension genes (Table 29). However, these probes were actually two distinct gene sequences, TaExt (a) and TaExt (b) (Table 31), which was confirmed by cloning and sequencing the real-time qPCR amplicons. Microarray expression data highly correlated with real-time qPCR data and confirmed the P_i specific down-regulation of both TaExts (Figure 32 I). However, TaExt (b) was selected for the candidate gene screen due to higher copy numbers (results not shown).

4.3.7. Candidate gene expression screen in distinct wheat germplasm

Plant material collected in two consecutive years, 2012 and 2013, has been analysed individually in order to investigate if the selected candidates responded similarly to changes in available soil-P_i in a different germplasm and at different growth stages (Figures 33 to 33, Tables 43 and 44).

In 2012, four of the six candidates genes were influenced by soil-P_i availability in the roots at booting stage with increasing expression with limited soil-P_i availability: TaPho1;3 (Figure 33 A), TaG3Pp2 (Figure 33 B), TaSPX2 (Figure 33 C), and TaPP$_i$ase3 (Figure 33 E) (Table 43). Furthermore, the expression of two of the six candidates genes were significantly influenced by wheat cutlivar including TaSPX2 (Figure 33 C) and TaExt (b) (Figure 33 F) (Table 43). TaExt (b) and TaSPX2 transcript abuncance was determined by variety in a contrasting manner (Figure 33 D and F); TaSPX2 expression could only be detected in P_i limited growing conditions and was therefore assumed to be up-regulated at low soil-P_i availability (Figure 33 C). TaExt (b) expression was higher in AxC line 49 and Conqueror compared with Capelle Desprez and AxC line 149 (Figure 33 F). TaSPX2 was lower expressed in AxC line 49 and Conqueror compared with Capelle Desprez and AxC line 149 (Figure 33 F). TaMYBrel expression was the only gene for which the gene expression was not influenced by soil-P_i availability or wheat variety (Figure 33 D, Table 43).

These results confirm partly the observations made in the transcriptome study on plant material from Broadbalk in 2011 (Figure 32 B, D, E and G): TaPho1;3, TaG3Pp2, TaSPX2 and TaPP$_i$ase3 are up-regulated during limited soil-P_i availability (Figure 33 A, B, C and E). However, two genes exhibited contrasting expression patterns to those in P_i starved and control roots from Broadbalk (Figure 32 H and I): TaMYBrel was not up-regulated by soil-P_i availability or influenced by the genotype (Figure 33 D) and TaExt (b) was not down-regulated by limited soil-P_i availability (Figure 33 F).

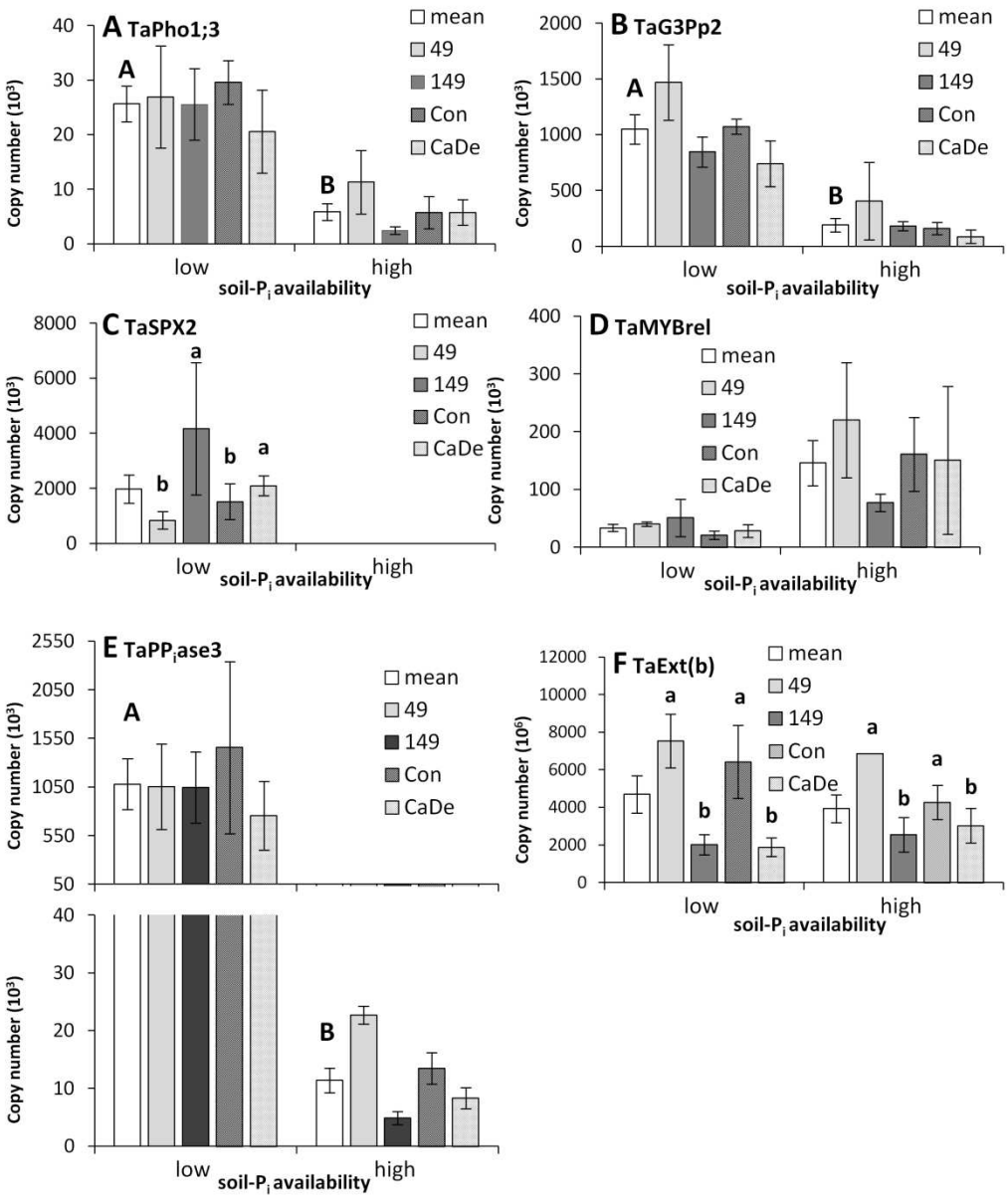

Figure 33: Candidate gene expression (copy number in 0.1 μg of total RNA) in root tissues from the P_i-trial at Sawyers field at booting stage in 2012 which were exposed to three different soil-P_i availability concentrations (Olsen P). Candidate genes include TaPho1;3, (A) TaG3Pp2 (B), TaSPX2 (C), TaMYBrel (D), TaPPiase3 (E) and TaExt(b) (F).

Means were compared for expression differences through available soil-P_i (low: 3 Olsen P, high: 60 Olsen P; mg P_i kg^{-1} soil; Olsen et al. 1954) and wheat genotype (AxC mapping population lines: 49 and 149; commercial varieties: Con = Conqueror; CaDe= Capelle Desprez), using the SED and the LSD at 5 % level of significance from 3 biological replicates (n = 3) which are displayed in Table 43. Bars sharing the same letter are not statistically different (P>0.05) between transcript abundance influenced by soil-P_i availability (capital letters) or wheat genotype (small letters).

Table 43: Statistical properties used for comparing the expression values of candidate genes in root tissues samples from the P_i- trial at Sawyers field in 2012 (Figure 33).

Gene	TaExt(b)*[1]	TaPP$_i$ase3*[1]	TaG3Pp2	TaMYBrel	TaPho1;3	TaSPX2[*2]
Significant	cultivar	available P	available P	not sign.	available P	cultivar
F-test	$F_{3,9} = 11.86$	$F_{1,4} = 14.19$	$F_{1,4} = 76.23$		$F_{1,4} = 17.14$	$F_{3,5} = 5.53$
p-value	p = 0.002	p = < 0.001	p = < 0.001	p = 0.095	p = 0.014	p = 0.048
SED	0.295	0.376	92.67		4.53	0.2608
LSD	0.668	1.045	257.28		12.56	0.6704

*[1]ANOVA was performed using log_2-scale; *[2]ANOVA was performed using square root transformed values

In 2013 gene expression was assessed in plant material sampled at three different growth stages, including roots and ears tissues, and using two varieties of the same wheat germplasm investigated in 2012 (Figures 33 to 39).

TaPP$_i$ase3 was up-regulated in the roots during low or medium soil-P_i availability at tillering, heading and ripening (Figure 34 A, B and C) similar to the results in 2012 (Figure 33 E) and 2011 (Figure 32 D). At heading TaPP$_i$ase3 root transcription was higher in Capelle Desprez compared to Conqueror revealing that the genotype influenced TaPP$_i$ase3 expression at low soil-P_i availability (Figure 34 B). Neither soil-P_i availability nor genotype altered TaPP$_i$ase3 expression in ear tissues such as rachis (Figure 34 D) and glume (Figure 34 E), except in the grain where TaPP$_i$ase3 was more highly expressed in Conqueror compared to Capelle Desprez (Figure 34 F). However, TaPP$_i$ase3 expression was high in the rachis and glume at ripening compared to its expression in the roots (Figure 34 D and E

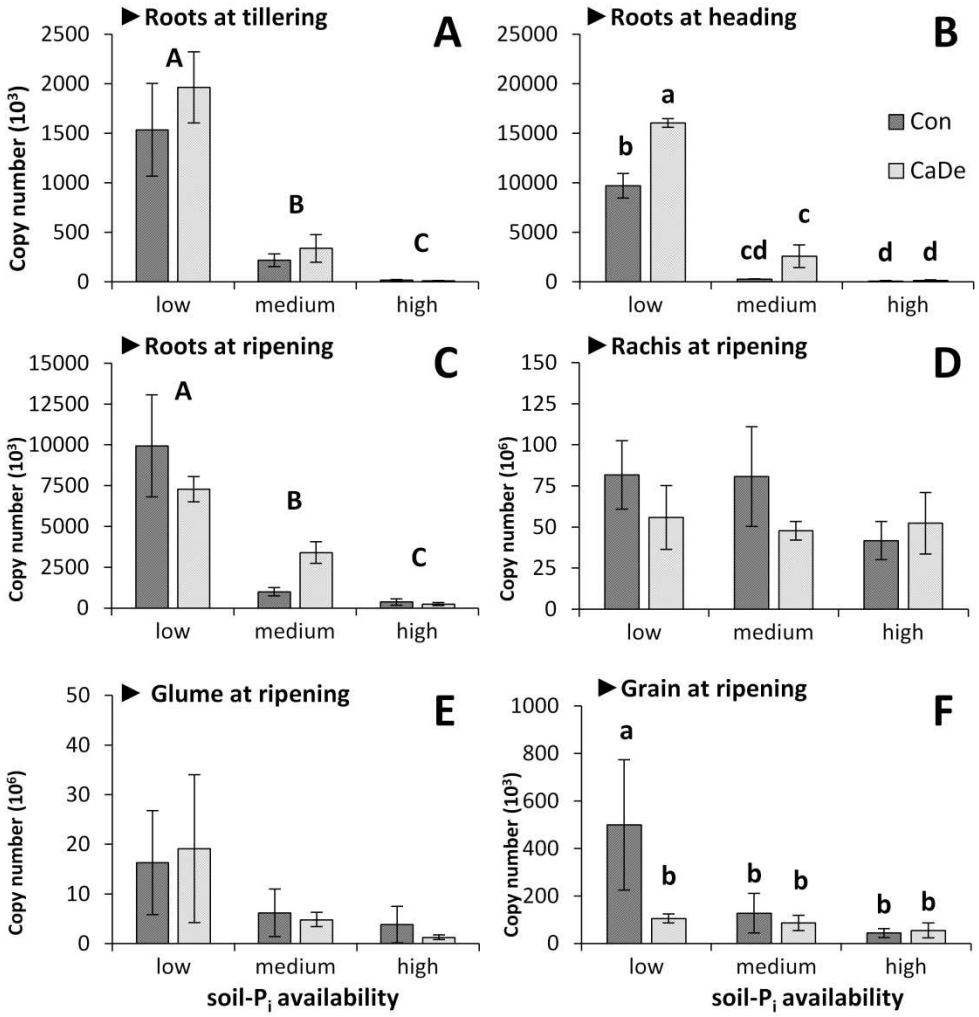

Figure 34: TaPP$_i$ase expression (copy number in 0.1 µg of total RNA) in roots at tillering (A), heading (B) and ripening (C) and in ear tissues at ripening including rachis (D), glume (E) and grain (F) which are derived from two different wheat genotypes from the P$_i$ field trial at Sawyers in 2013 and were exposed to three different soil-P$_i$ availability concentrations (Olsen P).

Means were compared for expression differences through available soil-P_i (low: 3 Olsen P, medium: 15 Olsen P, high: 60 Olsen P; mg P_i kg^{-1} soil; Olsen et al. 1954) and wheat genotype (Con = Conqueror; CaDe= Capelle Desprez), using the SED and the LSD at 5 % level of significance from 3 biological replicates (n = 3) which are displayed in Table 44. Bars sharing the same letter are not statistically different (P>0.05) between transcript abundance influenced by soil-P_i availability (capital letters) or wheat genotype (small letters).

TaExt (b) expression could only be determined at tillering (Figure 35 A) and heading (Figure 35 B) in wheat roots indicative for an importance only at the vegetative growth stage rather than at the generative growth and during maturation. TaExt (b) expression was influenced by soil-P_i availability in 2013

(Figure 35). However, transcription was highest at medium soil-P_i availability at tillering (Figure 35 A) and lowest at heading (Figure 35 B). In contrast, TaExt (b) expression decreased at low and high soil-P_i availability at tillering (Figure 35 A) and increased at heading in low and high P_i availability (Figure 35 B). However, there was no significant genotypic effect (Figure 35).

Table 44: Statistical properties of candidate gene expression analysis in root and ear tissues from two different wheat genotypes at three physiological stages from the P_i field trial at Sawyers in 2013.*

Genes	Statistical properties	Tissue and growth stage					
		Roots			Ripening		
		Tillering	Heading	Ripening	Rachis	Glume	Grain
Ta PP$_i$ase	F-test	$_{2,6}$ = 50.4*	$_{2,4}$ = 10.6	$_{2,6}$ = 35.6	n.sig.	n.sig.	$_{2,3}$ = 89.3
	p-value	<0.001 (1)	0.025 (3)	< 0.001 (1)	n.sig.	n.sig.	n.sig.
	SED	0.72*	1093.4	0.18	n.sig.	n.sig.	165.9
	LSD	1.77*	2440.0	0.45	n.sig.	n.sig.	124.8
Ta Ext(b)	F-test	$_{2,6}$ = 7.17*	$_{2,6}$ = 7.38	n.e.	n.e.	n.e.	n.e.
	p-value	0.026 (1)	0.024 (1)	n.e.	n.e.	n.e.	n.e.
	SED	0.41*	682.9	n.e.	n.e.	n.e.	n.e.
	LSD	0.99*	1671.1	n.e.	n.e.	n.e.	n.e.
Ta G3Pp2	F-test	$_{2,6}$ = 5.3*	$_{2,6}$= 75.1(1) $_{1,2}$= 12.2(2)	$_{2,6}$ = 5.07	n.sig.	n.sig.	n.sig.
	p-value	0.047 (1)	< 0.001 (1) 0.04 (2)	0.051 (1)	n.sig.	n.sig.	n.sig.
	SED	0.904*	58.5 (1) 90.8 (2)	0.153	n.sig.	n.sig.	n.sig.
	LSD	2.211*	143.2(1) 289.1 (2)	0.375	n.sig.	n.sig.	n.sig.
Ta Pho1;3	F-test	$_{2,6}$= 7.4 (1) $_{1,2}$=27.3 (2)	$_{2,6}$ = 15.0	$_{2,6}$= 11.3*	n.sig.	$_{1,2}$=7.26	n.sig.
	p-value	0.024 (1) 0.035 (2)	0.005 (1)	0.009 (1)*	0.88(1), 0.54(2)	0.074 (3)	n.sig.
	SED	15.6 (1) 3.8 (2)	37.17	0.196*	n.sig.	0.257	n.sig.
	LSD	38.1 (1) 16.6 (2)	90.94	0.48*	n.sig.	0.819	n.sig.
Ta SPX2	F-test	$_{2,6}$=12.49	2,6=96.89	$_{2,6}$=8.35	n.sig.	n.sig.	n.sig.
	p-value	0.007	<0.001	0.018	0.004 (3)	n.sig.	n.sig.
	SED	0.47	0.08	3.89	n.sig.	n.sig.	n.sig.
	LSD	1.151	0.19	9.53	n.sig.	n.sig.	n.sig.
Ta MYB rel	F-test	n.sig.	n.sig.	$_{1,2}$=4.61*	n.sig.	n.sig.	n.sig.
	p-value	n.sig.	n.sig.	0.084 (2)*	n.sig.	n.sig.	n.sig.
	SED	n.sig.	n.sig.	0.124*	n.sig.	n.sig.	n.sig.
	LSD	n.sig.	n.sig.	0.319*	n.sig.	n.sig.	n.sig.

* Log_2 values used; n.e. = no expression; (1) = P_i availability, (2) = cv., (3) = interaction

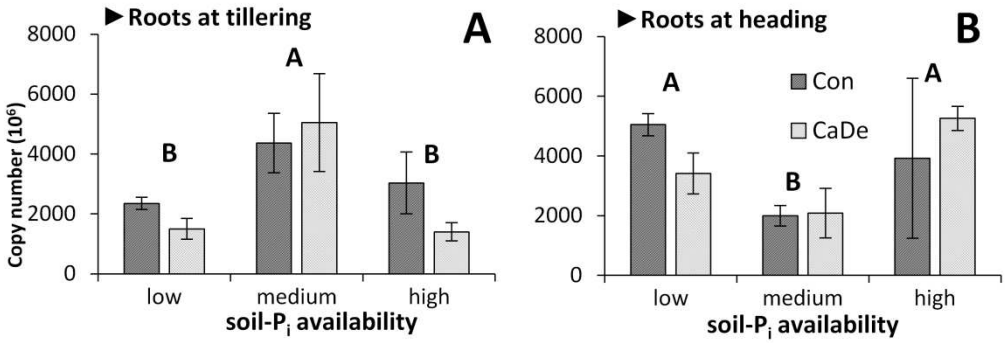

Figure 35: TaExt (b) expression (copy number in 0.1 µg of total RNA) in root tissues at tillering (A) and heading (B) from two different wheat genotypes at two physiological stages from the P_i field trial at Sawyers in 2013 and were exposed to three different soil-P_i availability concentrations (Olsen P).

Means were compared for expression differences through available soil-P_i (low: 3 Olsen P, medium: 15 Olsen P, high: 60 Olsen P; mg P_i kg^{-1} soil; Olsen et al. 1954) and wheat genotype (Con = Conqueror; CaDe= Capelle Desprez), using the SED and the LSD at 5 % level of significance from 3 biological replicates (n = 3) which are displayed in Table 44. Bars sharing the same letter are not statistically different (P>0.05) between transcript abundance influenced by soil-P_i availability (capital letters).

TaG3Pp2 expression increased in roots which were exposed to low and medium soil-P_i availability at tillering (Figure 36 A), heading (Figure 36 B) and at ripening (Figure 36 C; P-value = 0.051) compared to high P_i availability. TaG3Pp2 expression was only significantly influenced by the variety in roots at heading (Figure 36 B) and not at all in ear tissues (Figure 36 D, E and F). At heading TaG3Pp2 root expression was higher in Capelle Desprez compared to Conqueror independent from the available soil-P_i (Figure 36 B). Furthermore, TaG3Pp2 expression was highest in roots at heading (Figure 36 B) and even higher in rachis (Figure 36 D) and glume (Figure 36 E) at ripening and much lower in the grain (Figure 36 D).However, TaG3Pp2 transcription was not signficanly influenced by soil-P_i availability in ear tissues during maturity (Figure 36 D, E and F).

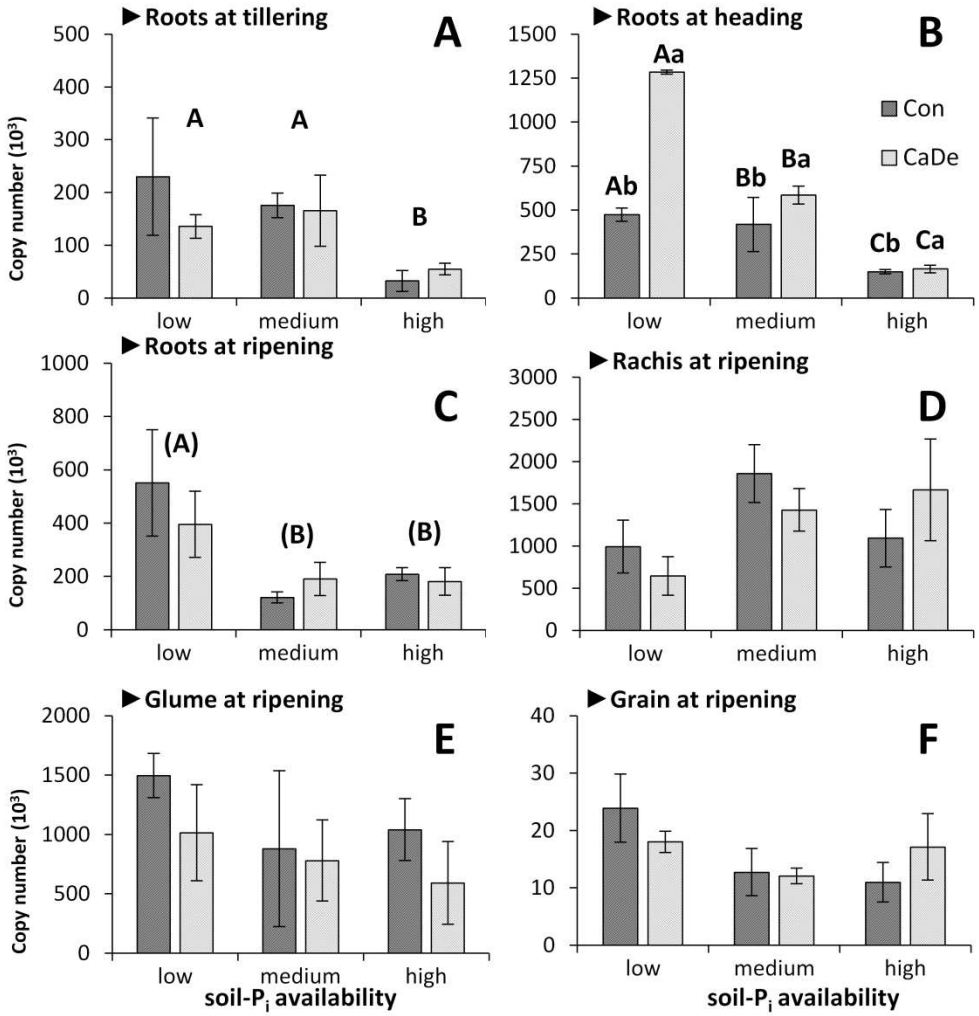

Figure 36: TaG3Pp2 expression (copy number in 0.1 µg of total RNA) in roots at tillering (A), heading (B) and ripening (C) and in ear tissues at ripening including rachis (D), glume (E) and grain (F) which are derived from two different wheat genotypes from the P_i field trial at Sawyers in 2013 and were exposed to three different soil-P_i availability concentrations (Olsen P).

Means were compared for expression differences through available soil-P_i (low: 3 Olsen P, medium: 15 Olsen P, high: 60 Olsen P; mg P_i kg^{-1} soil; Olsen et al. 1954) and wheat genotype (Con = Conqueror; CaDe= Capelle Desprez), using the SED and the LSD at 5 % level of significance from 3 biological replicates (n = 3) which are displayed in Table 44. Bars sharing the same letter are not statistically different (P>0.05) between transcript abundance influenced by soil-P_i availability (capital letters) or wheat genotype (small letters). The P-value for the influence of soil-P_i availability of TaG3Pp2 expression was 0.051 (letters therefore in brackets).

In 2013, varietal differences in the transcript abundance of TaPho1;3 were only significant in roots at tillering (Figure 37 A) and glume at ripening (Figure 37 E). TaPho1;3 expression was higher in roots at tillering (Figure 37 A) and glume at ripening (Figure 37 E) in Conqueror compared to Capelle Desprez similar to 2012 (Figure 33 A). TaPho1;3 root expression was highest at heading (Figure 37 B) and was higher expressed in the roots (Figure 37 A, B and C) compared to the ear tissues (Figure 37 D, E and F) except the grain (Figure 37 F). Increasing TaPho1;3 root expression only appeared at very low soil-P_i availability (Figure 37 A, B and C).

In 2013, the transcript abundance of TaSPX2 in the roots increased at low soil-P_i availability at tillering (Figure 38 A), heading (Figure 38 B) and ripening (Figure 38 C). However, TaSPX2 root expression was also much lower in 2013 (Figure 38 A, B and C) compared to 2012 (Figure 33 C). In ear tissues, the wheat genotype determined the expression level in the rachis (Figure 38 D) in which it was generally low compared to the transcription levels in other tissues (Figure 38 A, B, C, E and F). However, this varietal effect was not consistent across soil-P_i concentations in this experiment or with the results obtained in 2012 (Figure 33 C). TaSPX2 expression was particularly high in the ears (Figure 38 D, E and F) compared to the roots (Figure 38 A, B and C).

TaMYBrel expression was unaltered by soil-P_i availability or genotype in root (Figure 39 A, B and C) or ear tissues (Figure 39 D, E and F) during the growing period in 2013. This is again a inconsistent finding when taking the validation data which showed an up-regulation of TaMYBrel expression by low soil-P_i availability (Figure 32 H) or the 2012 data into account when TaMYBrel was only up-regulated in P_i replete plants (Figure 33 D). Only at ripening, there was a small genotypic effect on TaMYBrel root expression ($p = 0.084$) (Table 44).

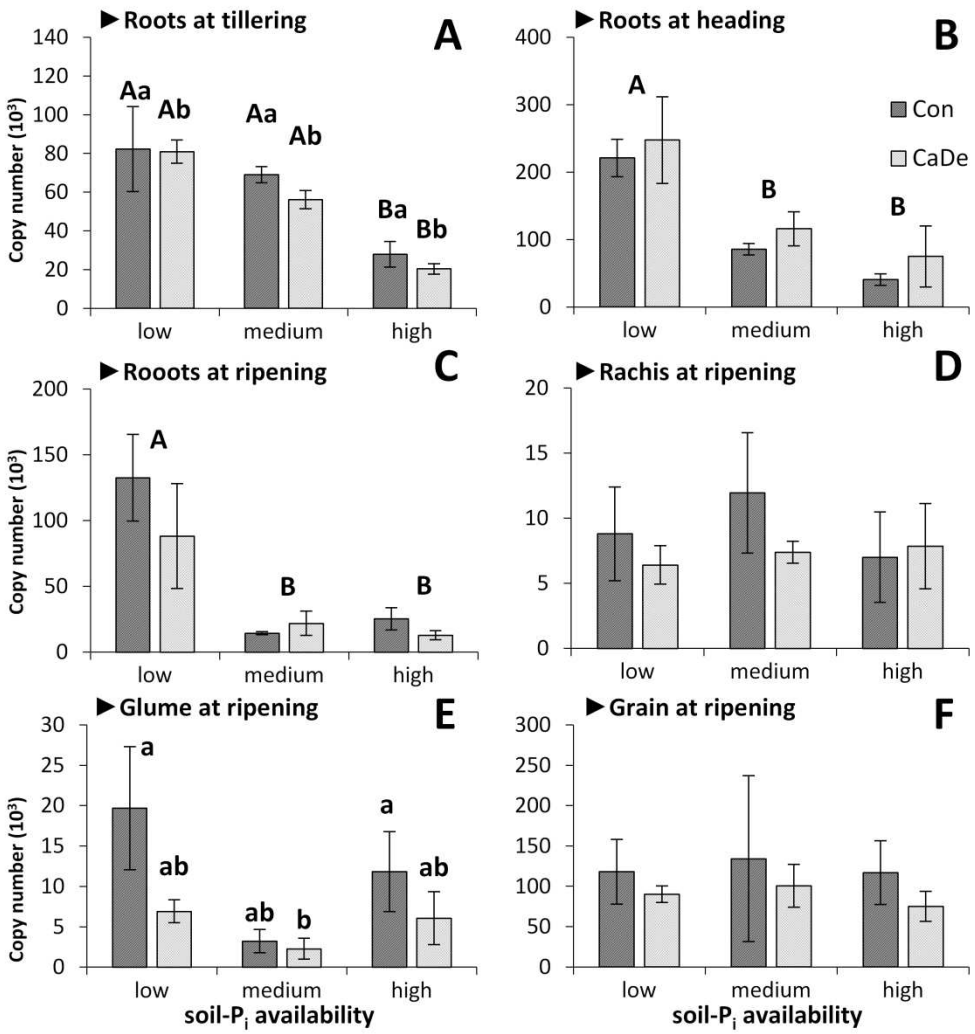

Figure 37: TaPho1;3 expression (copy number in 0.1 µg of total RNA) in roots at tillering (A), heading (B) and ripening (C) and in ear tissues at ripening including rachis (D), glume (E) and grain (F) which are derived from two different wheat genotypes from the P_i field trial at Sawyers in 2013 and were exposed to three different soil-P_i availability concentrations (Olsen P).

Means were compared for expression differences through available soil-P_i (low: 3 Olsen P, medium: 15 Olsen P, high: 60 Olsen P; mg P_i kg^{-1} soil; Olsen et al. 1954) and wheat genotype (Con = Conqueror; CaDe= Capelle Desprez), using the SED and the LSD at 5 % level of significance from 3 biological replicates (n = 3) which are displayed in Table 44. Bars sharing the same letter are not statistically different (P>0.05) between transcript abundance influenced by soil-P_i availability (capital letters) or wheat genotype (small letters).

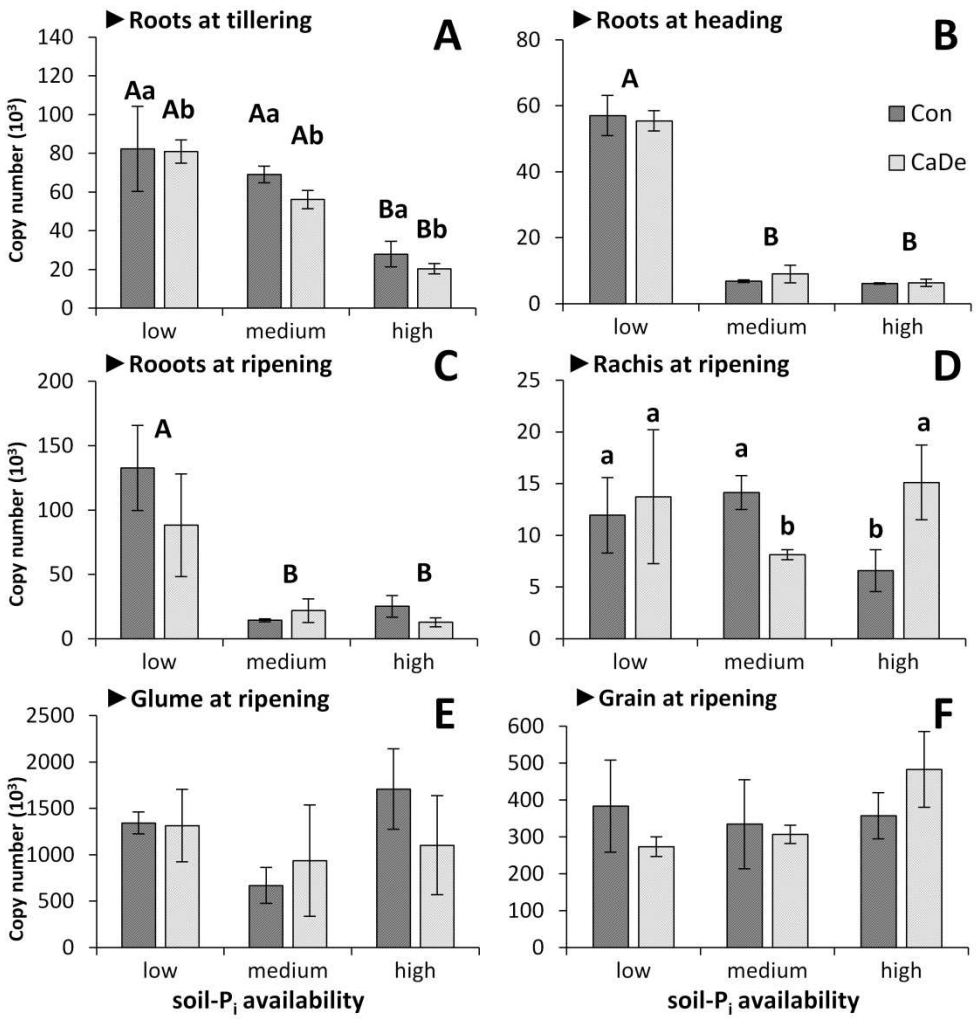

Figure 38: TaSPX2 expression (copy number in 0.1 μg of total RNA) in roots at tillering (A), heading (B) and ripening (C) and in ear tissues at ripening including rachis (D), glume (E) and grain (F) which are derived from two different wheat genotypes from the P_i field trial at Sawyers in 2013 and were exposed to three different soil-P_i availability concentrations (Olsen P).

Means were compared for expression differences through available soil-P_i (low: 3 Olsen P, medium: 15 Olsen P, high: 60 Olsen P; mg P_i kg^{-1} soil; Olsen et al. 1954) and wheat genotype (Con = Conqueror; CaDe= Capelle Desprez), using the SED and the LSD at 5 % level of significance from 3 biological replicates (n = 3) which are displayed in Table 44. Bars sharing the same letter are not statistically different (P>0.05) between transcript abundance influenced by soil-P_i availability (capital letters) or wheat genotype (small letters).

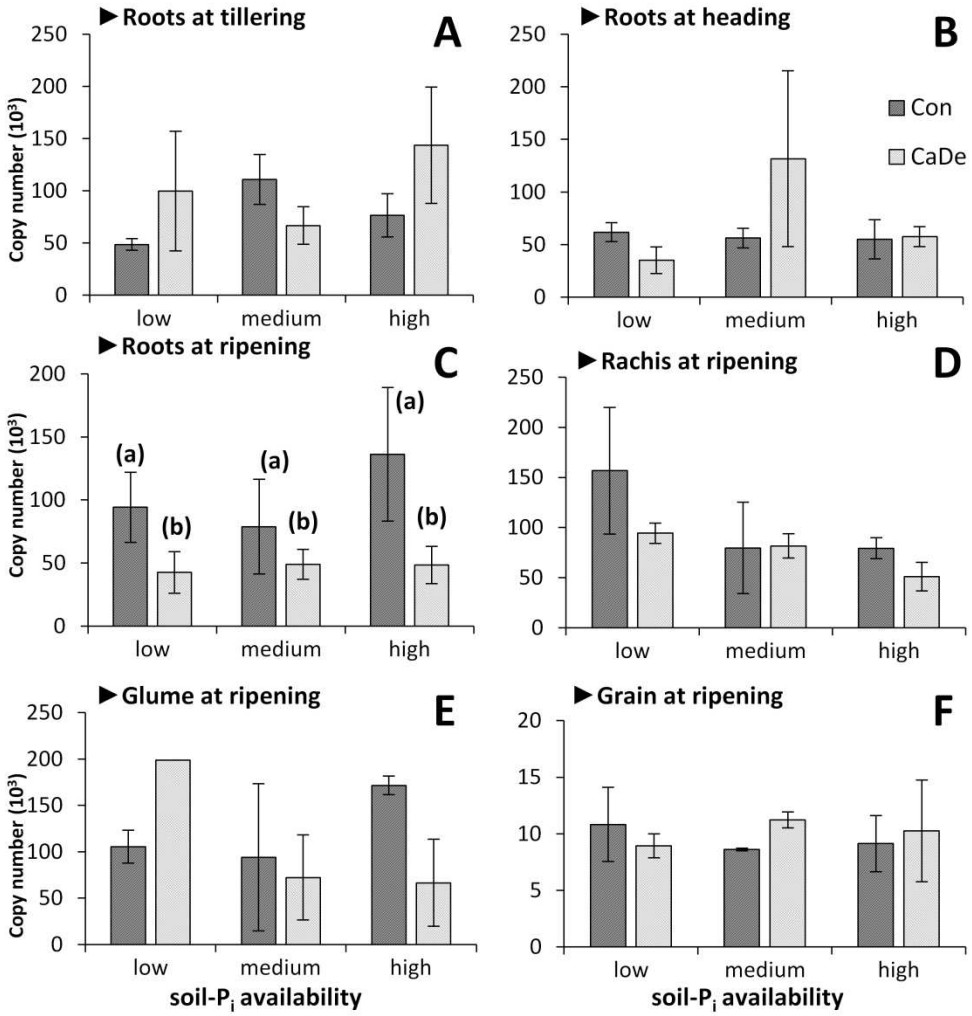

Figure 39: TaMYBrel expression (copy number in 0.1 μg of total RNA) in roots at tillering (A), heading (B) and ripening (C) and in ear tissues at ripening including rachis (D), glume (E) and grain (F) which are derived from two different wheat genotypes from the P_i field trial at Sawyers in 2013 and were exposed to three different soil-P_i availability concentrations (Olsen P).

Means were compared for expression differences through available soil-P_i (low: 3 Olsen P, medium: 15 Olsen P, high: 60 Olsen P; mg P_i kg^{-1} soil; Olsen et al. 1954) and wheat genotype (Con = Conqueror; CaDe= Capelle Desprez), using the SED and the LSD at 5 % level of significance from 3 biological replicates (n = 3) which are displayed in Table 44. Bars sharing the same letter are not statistically different (P>0.05) between transcript abundance of different wheat genotypes. P-value for the significance of Pi availability on TaMYBrel expression was 0.084.

In conclusion, the transcriptome data was successfully validated using real-time qPCR analysis (Figure 32). The root transcriptome responded in a more differentiated manner to soil-P_i availability compared to the ear transcriptome, for instance as shown for TaPP$_i$ase3 (Figure 34) and TaG3Pp2 (Figure 36). However, TaPho1;3 (Figure 37 A, B and C) and TaSPX2 (Figure 38 A, B and C) transcription in roots responded predominantly to severe soil-P_i depletion. Genotypic dependent expression was observed for TaPP$_i$ase3 (Figure 34 B and F), TaPho1;3 (Figure 37 A and E) and TaSPX2 (Figure 38 D) in the rachis, glume and grain respectively which is indicative for a genotypic influence of these genes on grain filling. TaExp (b) and TaMYBrel transcription determined in the P_i field trial at Sawyers (Figure 35 and 39) and was very different from the expression patterns observed in the transcriptome analysis (Figure 32 H and J). Both genes seemed to be expressed independently from soil-P_i availability (Figure 35 and 39). Therefore, TaG3Pp2, TaPP$_i$ase3 and TaPho1;3 are the most promising candidates for investigating a potential linkage of these genes to P_i efficiency traits which were assessed previously (Chapter 4, Section 3.1. to 3.5.).

4.3.8. Correlation of target gene expression to shoot P concentrations

The correlation of root transcription (copy number in 0.1 µg of total RNA) to shoot P concentrations (total P mg g^{-1} DM) of wheat grown at two field trials (Broadbalk, Sawyers), and at different physiological stages in 2012 and 2013 was determined for five target genes (Figures 40 to 45, Table 45).

The percentage of explained variance (R^2) for the best model was high for TaG3PpP2 (Table 45 A) and TaSPX2 (Table 45 B), sufficient for TaPP$_i$ase3 (Table 45 C) and TaPho1;3 (Table 45 D) but very low for TaExt (b) (Table 45 E) and TaMYBrel (Table 45 F). For two genes, a theoretical expression minimum was significant but no theoretical minimum for P concentrations including TaG3Pp2 (Table 45 A) and MYBrel (Table 45 E) indicating that theses genes may have still other functions when soil-P_i is not limiting.

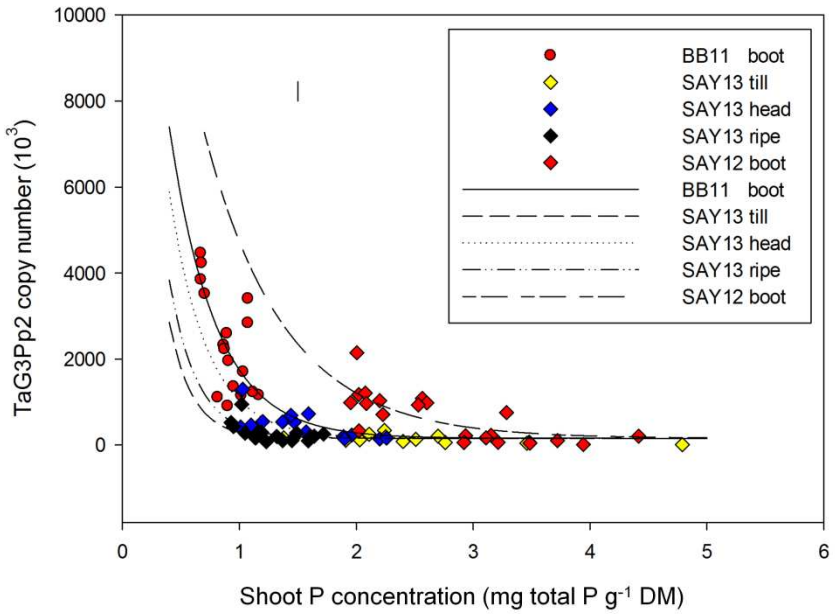

Figure 40: TaG3Pp2 expression in roots (copy number in 0.1 µg of total RNA) vs. total P concentrations (mg g^{-1} DM) in the shoots of wheat grown in two field trials, Broadbalk and Sawyers, at Rothamsted Research and sampled at different physiological stages in 2012 and 2013.
BB11 = Broadbalk 2011, SAY 12/13 = P_i field trial at Sawyers 2012/ 2013, elong = stem elongation (39/41), boot = booting (45), till = tillering (29/30), head = heading (51), ripe=ripening (75); model and parameters in Table 45 A.

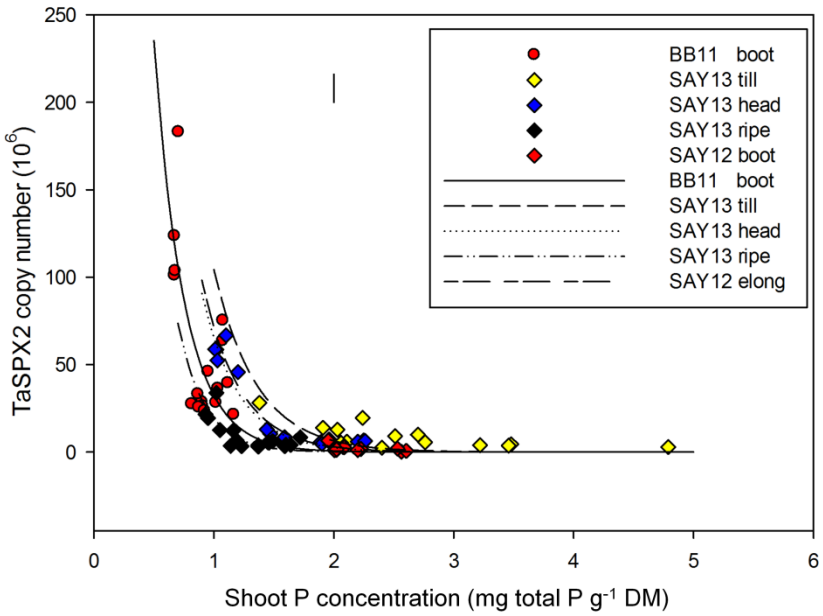

Figure 41: TaSPX2 expression in roots (copy number in 0.1 µg of total RNA) vs. total P concentrations (mg g-1 DM) in the shoots of wheat grown in two field trials, Broadbalk and Sawyers, at Rothamsted Research and sampled at different physiological stages in 2012 and 2013.
BB11 = Broadbalk 2011, SAY 12/13 = P_i field trial at Sawyers 2012/ 2013, elong = stem elongation (39/41), boot = booting (45), till = tillering (29/30), head = heading (51), ripe=ripening (75); model and parameters in Table 45 B.

Table 45: Models for correlation screen of candidate gene expression in roots vs. total shoot P concentrations of wheat grown in two field trials, Broadbalk and Sawyers, at Rothamsted Research and sampled at different physiological stages in 2012 and 2013 (Figures 42 to 47).

The model equation used was of the form: $y = a+Aexp^{(-B(P+c))}$ including y = target gene expression, a = theoretical lower minimal asymptotic gene expression as shoot P concentration increases, A = maximal possible gene expression above a, B = exponential rate of decline in gene expression with increasing shoot P concentration, c = minimal level of shoot P concentration. The statistical significance was tested for each variable of the model equation using F-tests and a FITNONLINEAR procedure (GenStat package). Abbreviations: BB11 = samples from Broadbalk 2011, SAY 12/13 = samples from the P_i field trial at Saywers 2012/ 2013, elong = stem elongation (39/41), boot = booting (45), till = tillering (29/30), head = heading (51), ripe=ripening (75), n.sig. = not significant.

Table 43 (A); Figure 40					
Ta G3Pp2	**Model**	**R^2**	**S^2**	**p-value (a)**	**p-value (B)**
	$y = a+Aexp^{(-Bi\ (P))}$	80.2%	205307; 76 df	<0.001	<0.001
	Model			**SE (a)** / **SE (A)**	**SE (B)**
	y (SAY13 till) = 154.6 + 19924*exp (-3.000*P)				0.988
	y (SAY12 elon) = 154.6 + 19924*exp (-1.471*P)				0.167
	y (BB11 boot) = 154.6 + 19924*exp (-2.530*P)			83.4 / 5485	0.536
	y (SAY13 head) = 154.6 + 19924*exp (-3.117*P)				0.399
	y (SAY13 ripe) = 154.6 + 19924*exp (-4.224*P)				0.808
Table 43 (B); Figure 41					
Ta SPX2	**Model**	**R^2**	**S^2 on_ df**	**p-value (A)**	**p-value (B)**
	$y = Aexp^{(-Bi\ (P))}$	75.1%	253; 69 df	n.sig.	0.017
	Model			**SE (A)**	**SE (B)**
	y (SAY13 till) = 1715*exp (-2.800*P)				0.369
	y (SAY12 elon) = 1715*exp (-3.180*P)				1.090
	y (BB11 boot) = 1715*exp (-3.974*P)			619	0.479
	y (SAY13 head) =1715*exp (-3.267*P)				0.350
	y (SAY13 ripe) = 1715*exp (-4.498*P)				0.493
Table 43 (C); Figure 42					
Ta Pho1;3	**Model**	**R^2**	**S^2**	**p-value (A)**	**p-value (B)**
	$y = Aexp^{(-Bi\ (P))}$	66.7%	31795 ; 79 df	n.sig.	0.006
	Model			**SE (A)**	**SE (B)**
	y (SAY13 till) = 2025*exp (-1.795*P)				0.563
	y (SAY12 elon) = 2025*exp (-2.032*P)				0.959
	y (BB11 boot) = 2025*exp (-1.215*P)			752	0.421
	y (SAY13 head) = 2025*exp (-2.000*P)				0.404
	y (SAY13 ripe) = 2025*exp (-3.015*P)				0.750
Table 43 (D); Figure 43					
Ta PP_iase 3	**Model**	**R^2**	**S^2**	**p-value (A)**	**p-value (B)**
	$y = Aexp^{(-Bi\ (P))}$	62.1 %	14737286; 78 df	0.013	n.sig.
	Model			**SE (A)**	**SE (B)**
	y (SAY13 till) = 1144113*exp (-4.360*P)				1.080
	y (SAY12 elon) = 1144113*exp (-3.287*P)				0.578
	y (BB11 boot) = 1144113*exp (-5.791*P)			731435	0.879
	y (SAY13 head) = 1144113*exp (-4.291*P)				0.616
	y (SAY13 ripe) = 1144113*exp (-4.895*P)				0.660

Table 43 (E); Figure 44						
Ta MYB rel	**Model**	**R^2**	**S^2**	**p-value (a)**	**p-value (A)**	**p-value (B)**
	$y = a+Aexp^{(-B(P))}$	52.2%	5484; 83 df	0.020	n.sig.	n.sig.
	Model			**SE (a)**	**SE (A)**	**SE (b)**
	y (all) = 77.4 + 96492*exp (-6.35*P)			31.5	73606	1.07

Table 43 (F); Figure 45					
Ta Ext (b)	**Model**	**R^2**	**S^2**	**p-value (A)**	**p-value (B)**
	$y = Aexp^{(-B(P))}$	24.7%	6537222 ; 65 df	n.sig.	n.sig.
	Model			**SE (A)**	**SE (B)**
	y (all) = 9618*exp (-0.3873*P)			1331	0.0871

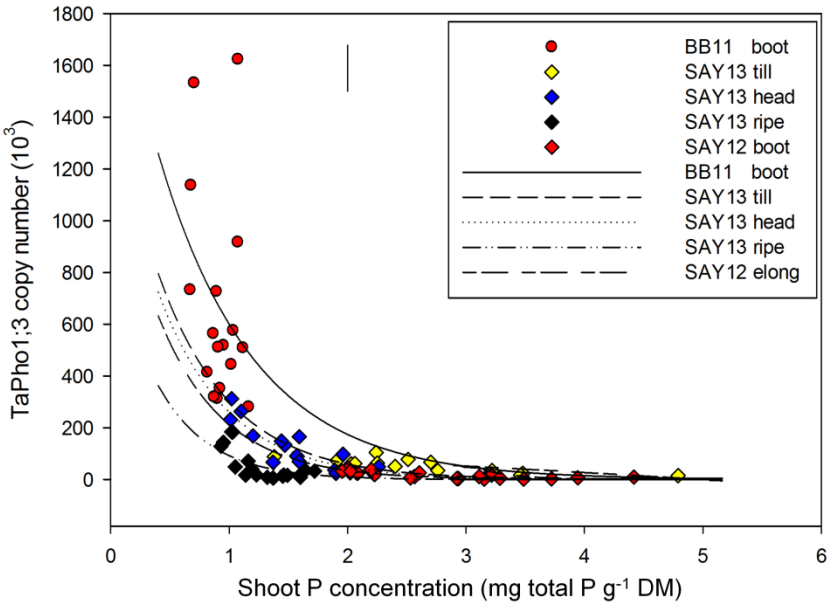

Figure 42: TaPho1;3 root expression (copy number in 0.1 µg of total RNA) vs. total P concentrations (mg g-1 DM) in the shoots of wheat grown in two field trials, Broadbalk and Sawyers, at Rothamsted Research and sampled at different physiological stages in 2012 and 2013.
BB11 = Broadbalk 2011, SAY 12/13 = P_i field trial at Sawyers 2012/ 2013, elong = stem elongation (39/41), boot = booting (45), till = tillering (29/30), head = heading (51), ripe=ripening (75); model and parameters in Table 45 C.

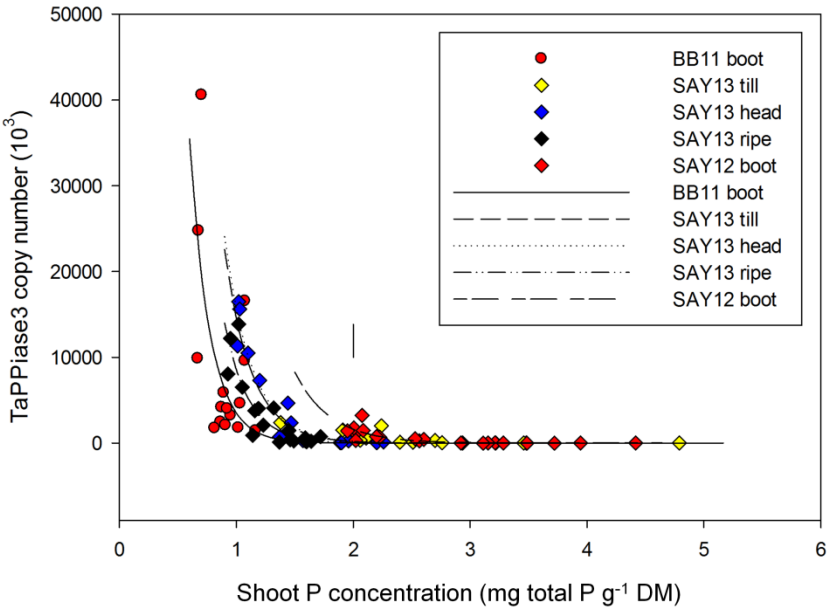

Figure 43: TaPP$_i$ase3 root expression (copy number in 0.1 µg of total RNA) vs. total P concentrations (mg g^{-1} DM) in the shoots of wheat grown in two field trials, Broadbalk and Sawyers, at Rothamsted Research and sampled at different physiological stages in 2012 and 2013.
BB11 = Broadbalk 2011, SAY 12/13 = P_i field trial trial at Sawyers 2012/ 2013, elong = stem elongation (39/41), boot = booting (45), till = tillering (29/30), head = heading (51), ripe=ripening (75); model and parameters in Table 45 D.

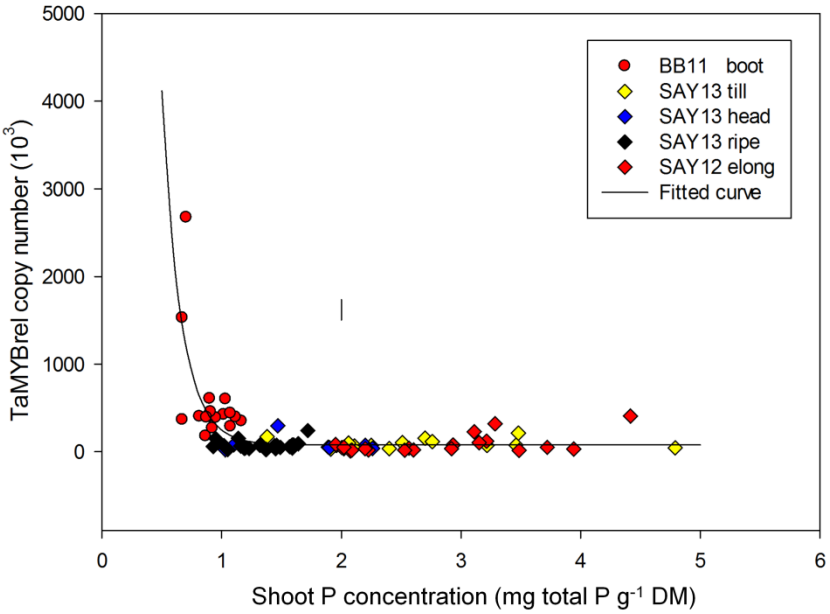

Figure 44: TaMYBrel root expression (copy number in 0.1 µg of total RNA) vs. total P concentrations (mg g-1 DM) in the shoots of wheat grown in two field trials, Broadbalk and Sawyers, at Rothamsted Research and sampled at different physiological stages in 2012 and 2013.
BB11 = Broadbalk 2011, SAY 12/13 = P_i field trial at Sawyers 2012/ 2013, elong = stem elongation (39/41), boot = booting (45), till = tillering (29/30), head = heading (51), ripe=ripening (75); model and parameters in Table 45 E.

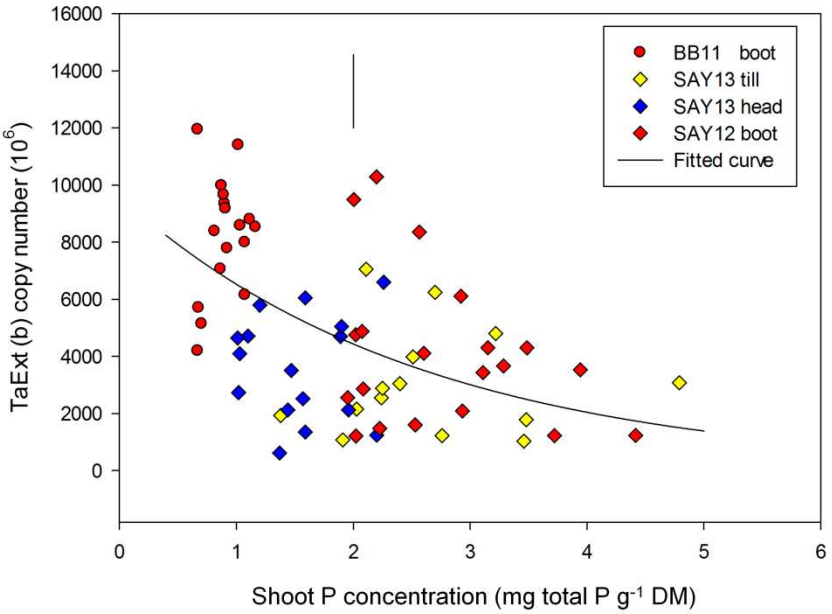

Figure 45: TaExt (b) root expression (copy number in 0.1 µg of total RNA) vs. total P concentrations (mg g^{-1} DM) in the shoots of wheat grown in two field trials, Broadbalk and Sawyers, at Rothamsted Research and sampled at different physiological stages in 2012 and 2013.
BB11 = Broadbalk 2011, SAY 12/13 = P_i field trial at Sawyers 2012/ 2013, elong = stem elongation (39/41), boot = booting (45), till = tillering (29/30), head = heading (51), ripe=ripening (75); model and parameters in Table 45 F.

There is a strong correlation of TaG3Pp2 expression to shoot P concentrations with different exponential rates across experiments and growth stages (Figure 40, Table 45 A). The declining exponential rates were greatest for samples from Sawyers at ripening in 2013 when shoot P concentrations were very low, and lowest for samples from Sawyers in 2012 at late stem elongation/early booting when shoot P concentrations were very high (Table 45 A). Furthermore, exponential rates for samples from Sawyers in 2013 (Table 45 A) indicate a decline with progressing plant growth. However, TaG3Pp2 shows the greatest responsiveness to the nutritional status in regards to soil-P_i availability during vegetative and pre-mature stages (Figure 40, Table 45 A).

For TaSPX2, there was no theoretical minimum for expression but a strong correlation of expression to shoot P concentrations and different exponential rates across experiments and growth stages (Figure 41, Table 45 B). The greatest decline rate for TaSPX2 occurred for samples from Sawyers in 2013 at ripening and the lowest for samples from Sawyers in 2013 at tillering with

increasing decline rates with progressing plant growth across experiments (Figure 41, Table 45 B). These findings indicate that TaSPX2 expression responded to altered shoot P concentrations across experiments and that the responsiveness was greater at later growth stages.

TaPho1;3 expression correlated to shoot P concentrations but with different exponential rates for each experiment (Figure 42, Table 45 C). These rates indicate that TaPho1;3 expression is most responsive to low shoot P concentrations during stem elongation and at later growth stages during maturation: the lowest decline rate occurred for samples from Broadbalk at booting and the highest for samples from Sawyers at ripening in 2013 (Figure 42, Table 45 C).

TaPP$_i$ase3 expression correlated to shoot P concentrations but with different exponential rates for each experiment (Figure 43, Table 45 D). However, decline rates were greater than for any other gene and were greatest for samples from Broadbalk in 2011 at booting and samples from Sawyers at ripening in 2013 (Figure 43, Table 45 D).

The expression of TaMYBrel and TaEx (b) was not related to changing shoot P concentrations in shoot tissue without having distinct decline rates for different samples, growth stages and years (Figures 44 and 45, Table 45 E and F). However, TaMYBrel had a minimum expression level (Table 45 E) indicating that it may have other functions apart from the observed up-regulation at low soil-P_i availability. Furthermore, soil-P_i dependent regulation occurred only in root samples at Broadbalk in 2011 (Figure 44, Table 45 E). There was considerable variation over shoot P concentrations for TaExt (b) expression and it cannot be considered to be correlated to it (Figure 45, Table 45 F).

4.3.9. Correlation of target gene expression to soil-P_i availability and P_i use efficiency

The correlation coefficients describe the relationship of shoot P concentrations or target gene expression with soil-P_i availability and P use efficiency (Figure 46 and 47, Table 46). There was a higher positive correlation with total shoot P concentrations in samples from the Sawyers in 2012 and 2013 compared to samples from Broadbalk in 2011 (Table 46). The relationship of shoot P concentrations with P use efficiency (PUE) decrease with later growth stages and was mostly higher for grain PUE than for total PUE (Table 46).

The correlation of target gene expression was also weaker to total P use efficiency to grain P use efficiency including TaG3Pp2, TaSPX2, TaPho1;3 and TaPP_iase3 (Table 46). TaMYBrel and TaExt (b) expression was not correlated to soil-P_i availability or P use efficiency or in all samples from the P_i field trial at Sawyers in 2012 and 2013 (Table 46). However, there was a strong negative correlation of TaMYBrel expression and a positive correlation with TaExt (b) expression soil-P_i availability at Broadbalk in 2011 (Table 46).

TaG3Pp2 expression was only moderately correlated with P use efficiency, being higher in samples from Sawyers in 2012 at elongation and lower in samples from Sawyers in 2013 at tillering, heading and ripening (Figure 46, Table 45). This indicates again that TaG3Pp2 may have additional roles in plant metabolism besides being regulated or influenced through the nutritional P status of the plants and its responsiveness increases with progressing growth (Figure 40, Table 45).

TaSPX2, TaPho1;3 and TaPP_iase were strongly correlated to P use efficiency in samples from Sawyers in 2012 at elongation, and moderately in samples from Sawyers in 2013 with increasing values from at tillering to heading and ripening (Figure 46, Table 46). Across these three genes, TaPho1;3 had the highest r values to P use efficiency at elongation in 2012 and tillering in 2013 (Figure 46, Table 46) TaSPX had a high r value at heading in 2013 and TaPP_iase at ripening in 2013 (Figure 46, Table 46). These three genes also exhibited a consistent negative relationship to soil-P_i availability (Table 46).

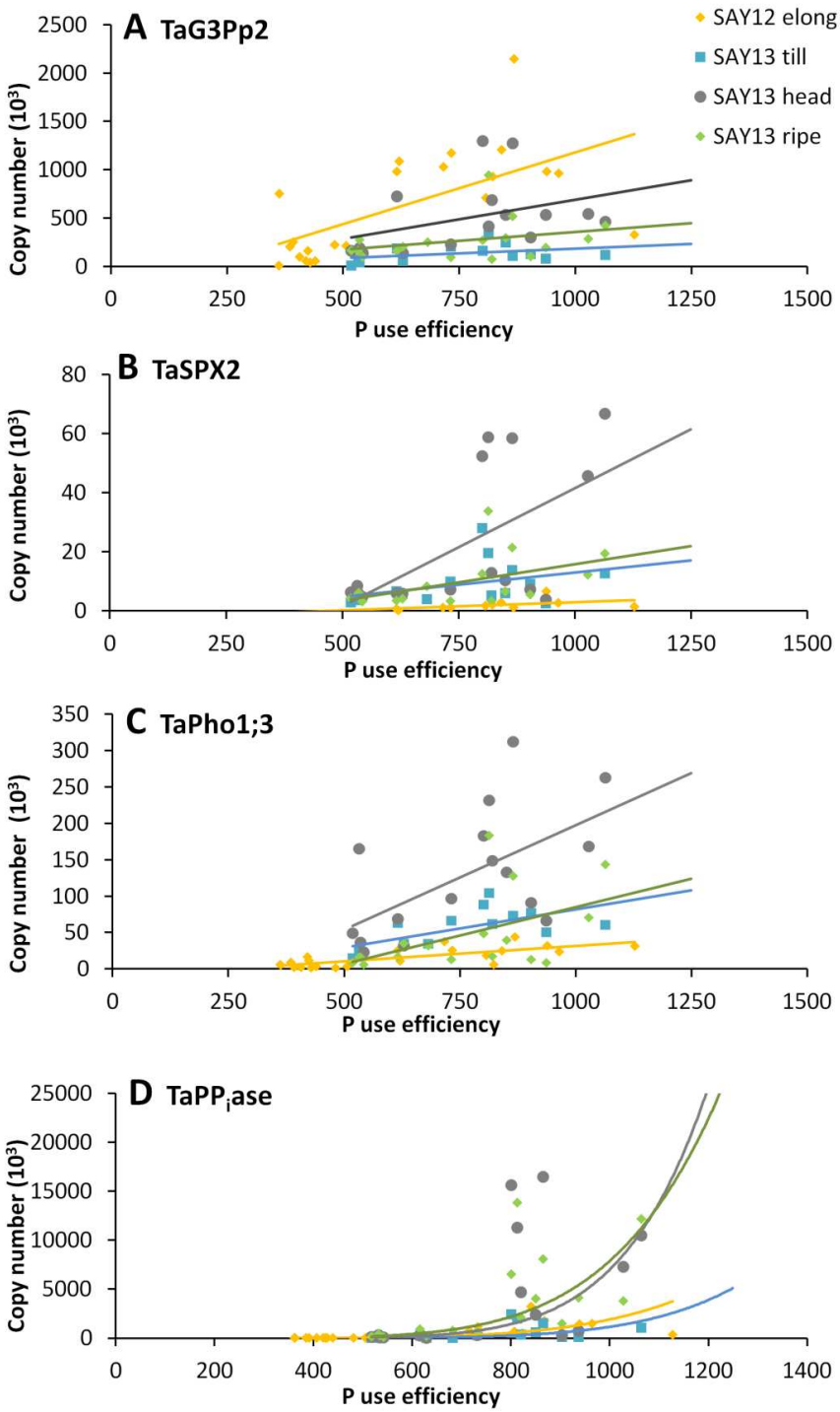

Figure 46: Relationships between candidate gene expression, inculding TaG3Pp2 (A), TaSPX2 (B), TaPho1;3 (C) and TaPP$_i$ase3 (D) in field-grown wheat roots and P use efficiency; data were acquired from two field trials, Broadbalk and Sawyers, at Rothamsted Research and sampled at different physiological stages in 2012 and 2013.

Abbreviations: gene expression = copy number in 0.1 µg of total RNA, P use efficiency = [kg grain+ straw / kg P taken up], SAY 12/13 = samples from the P_i field trial at Saywers 2012/ 2013, elong = stem elongation (39/41), till = tillering (29/30), head = heading (51), ripe=ripening (75). The correlation coefficients are displayed in Table 46.

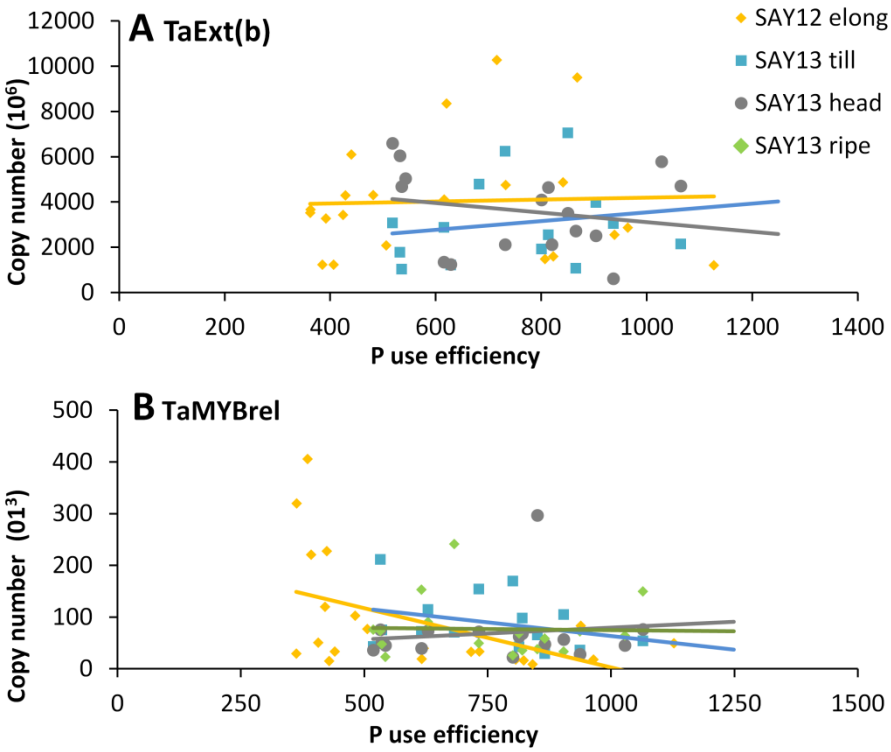

Figure 47: Relationships between candidate gene expression including TaMYBrel (A) and TaExt (b) (B) in field-grown wheat roots and P use efficiency; data were acquired from two field trials, Broadbalk and Sawyers, at Rothamsted Research and sampled at different physiological stages in 2012 and 2013.

Abbreviations: gene expression = copy number in 0.1 µg of total RNA, P use efficiency = [kg grain+ straw / kg P taken up], SAY 12/13 = samples from the P_i field trial at Saywers 2012/ 2013, elong = stem elongation (39/41), till = tillering (29/30), head = heading (51), ripe=ripening (75). The correlation coefficients are displayed in Table 46.

Table 46: Correlation coefficients (r and p-values) between candidate gene expression, soil-P_i availability (Olsen P) and P_i efficiency traits; data were acquired from two field trials, Broadbalk and Sawyers, at Rothamsted Research and sampled at different physiological stages in 2012 and 2013 (Figures 46 an 47).

Abbreviations: Olsen P = soil-P_i availability according to Olsen et al. (1954), P use efficieny = [kg grain+ straw / kg P taken up], grain P use efficiency = [kg grain/ kg P taken up]; Significance (P)* ≤ 0.05, ** ≤ 0.003, ***≤ 0.001

Gene expression vs. trait	Olsen P	P use efficiency	Grain P use efficiency
Shoot P conc.	0.76 ***		
TaG3Pp2	-0.69 **		
TaSPX2	-0.83 ***		
TaPho1;3	-0.49 *		
TaPP_iase3	-0.70 *		
TaMYBrel	-0.81 ***		
TaExt (b)	0.60 **		
Shoot P conc.	0.86 ***	-0.87 ***	-0.94 ***
TaG3Pp2	-0.79 ***	0.63 **	0.77 ***
TaSPX2		0.49	0.52
TaPho1;3	-0.78 ***	0.75 ***	0.82 ***
TaPP_iase3	-0.67 ***	0.66 ***	0.73 ***
TaMYBrel	0.53 *	-0.50 *	-0.53*
TaExt (b)	-0.27	0.04	0.26
Shoot P conc.	0.84 ***	-0.75 ***	-0.66 **
TaG3Pp2	-0.66 *	0.37	0.58 *
TaSPX2	-0.70 *	0.38	0.57 *
TaPho1;3	-0.90 ***	0.65 *	0.77 ***
TaPP_iase3	-0.77**	0.44	0.56 *
TaMYBrel	0.21	-0.33	-0.28
TaExt (b)	-0.06	0.18	0.05
Shoot P conc.	0.88 ***	-0.64 **	-0.70*
TaG3Pp2	-0.68 *	0.39	0.34
TaSPX2	-0.75 ***	0.60 *	0.73 **
TaPho1;3	-0.74 **	0.59 *	0.65 *
TaPP_iase3	-0.75 ***	0.53 *	0.58 *
TaMYBrel	-0.03	0.13	-0.06
TaExt (b)	0.20	-0.09	-0.10
Shoot P conc.	0.83 ***	-0.60 *	-0.66 *
TaG3Pp2	-0.47	0.31	0.50 *
TaSPX2	-0.62 *	0.50 *	0.64 *
TaPho1;3	-0.62 *	0.51 *	0.70 **
TaPP_iase3	-0.75 ***	0.64 *	0.74 ***
TaMYBrel	0.173	-0.03	0.22

4.4. Discussion

4.4.1. Data variation between methods, years and experiments

Both methods used for determining gene expression, microarray analysis (using the Affymetrix Genechip®) and real-time qPCR, delivered congruent and reproducible data (Figure 32, Table 42). However, candidate gene expression varied between years (Figures 33 to 39) and genotypic differences fluctuated for growth traits, nutritional measurements and P_i efficiency properties (Figures 24 to 31).

Major genotypic differences in phenotypic traits were predominant in 2012 at high soil-P_i availability (Figures 24 to 28); average P_i removal rates and COP were much higher than in 2013 (Figure 26, Tables 40 and 41). Furthermore, the correlation coefficients (r) between target gene expression, soil-P_i availability and P_i efficiency traits were lower in samples from Broadbalk in 2011 compared to samples from the P_i field trial at Sawyers in 2012 and 2013 (Figure 46, Table 46). Finally, target and actual Olsen P measured in autumn pre-sowing and COP fluctuated greatly (Tables 40 and 41). The main reasons for these fluctuations are likely to be abiotic factors affecting the interactions of P_i in the soil which influence the P_i delivery to the root system. This will be discussed in more detail in Chapter 5 (Section 2.2 and 2.3).

Another source of data variation occurred between the three field trials. Except TaMYBrel and TaExt (b), most target genes were highly responsive to soil-P_i availability across experiments (Figures 40 to 45, Table 45). However, even if they were used as low or high P treatments, Olsen P values of these plots varied greatly; particularly at Broadbalk where Olsen P values were very high (Table 2). Nonetheless, shoot P concentrations were lower in samples from Broadbalk (Table 12) compared to those at the P_i field trial at Sawyers (Figure 27). Reduced P_i acquisition of plants growing at Broadbalk in 2011 may have been the result of severely affected P_i replenishment in the soil solution toward the roots due to the dry weather conditions in 2011 (Figures 5 and 21). Although, shoot P concentrations were highly correlated to Olsen P (Table 45), this correlation was of a qualitative rather than a quantitative nature (Figure 48 A). Additionally, shoot P concentrations are usually asymptotic with increasing

Olsen P (Bollons and Barraclough 1999). Instead of linking the gene expression to available soil-P_i (Figure 48 B), linking it to shoot P concentrations (Figure 48 C) was the better approach for predicting if candidate genes could be used as markers for predicting when the critical soil-P_i or shoot P concentration are exceeded.

Plots used for the candidate gene screening at Sawyers in 2011/12 were selected on the assumption that plants exposed to strong starvation or high soil-P_i availability are most likely to exhibit genotypic differences. However, growing crops at such a high level of P_i fertilizer input without wasting fertilizer resources is not good agricultural practice (Defra 2010), causes large P_i losses in subsurface drainage (McDowell 2012) and is exceeding the COP. COP were considered being optimal at 9 Olsen P for winter wheat at Sawyers (Bollons and Barraclough 1999). However, COP values were 15 to 20 mg P_i kg^{-1} soil (Olsen P) higher than the proposed optimum in both experimental years (Table 40 and 41). Therefore, a plot with a medium Olsen P concentration just below the recommended level was used additionally in 2012/13. This soil-P_i level was used for evaluating potential target gene expression under appropriate agronomic conditions according to the proposed model for P_i efficiecy crop improvement (Figure 4).

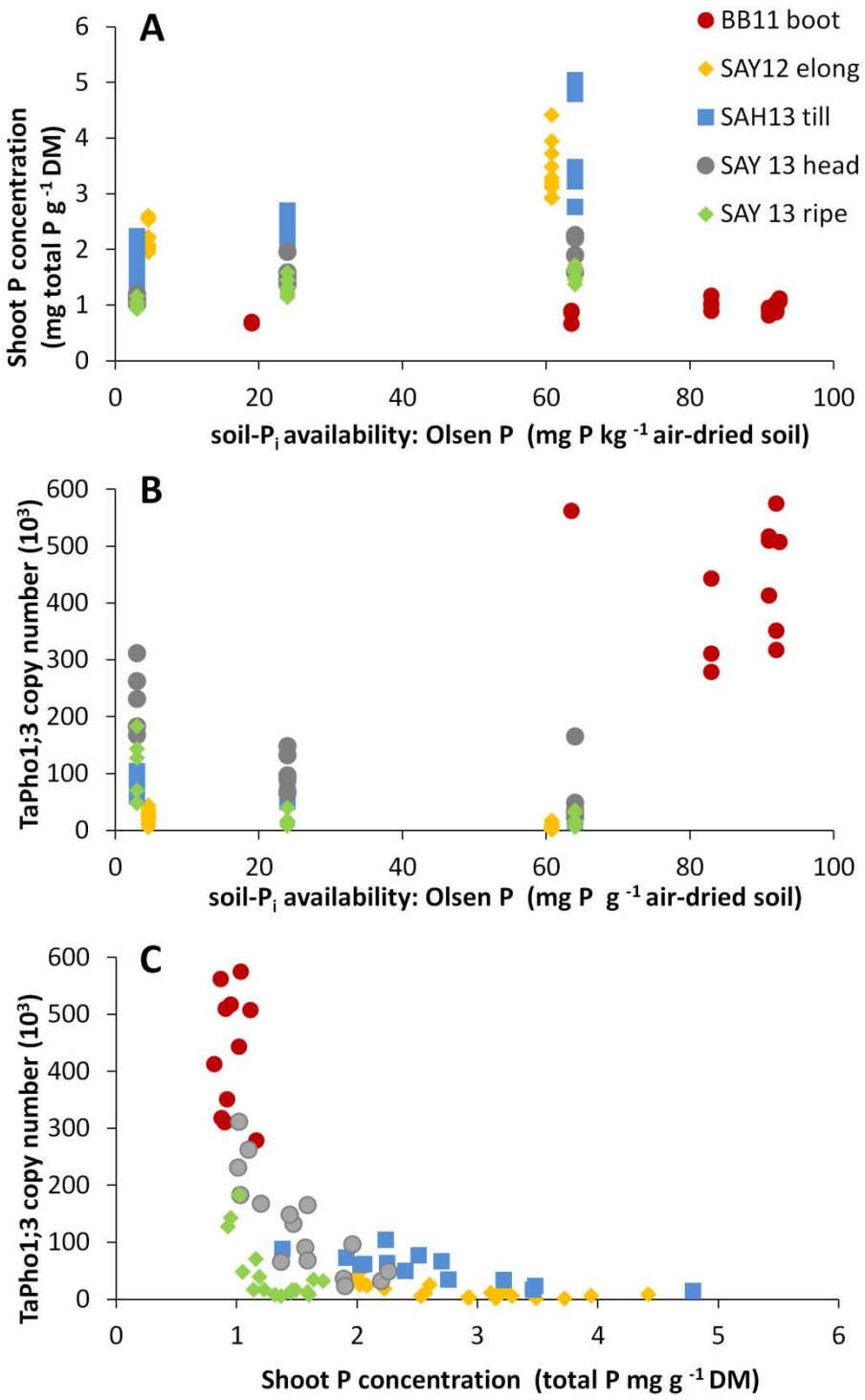

Figure 48: Relationship between (A) shoot P concentration and soil-P_i availability (B) candidate gene expression (e.g. TaPho1;3) in the roots and soil-P_i availability (C) candidate gene expression (e.g.TaPho1;3) in the roots and shoot P concentration of wheat.

Abbreviations: BB11 = Broadbalk in 2011, SAY 12/13 = P_i field trial at Sawyers in 2012/ 2013, elong = stem elongation (39/41), boot = booting (45), till = tillering (29/30), head = heading (51), ripe=ripening (75); correlations values (r) are displayed in Table 45.

4.4.2. Phenotypic data and variability in P_i efficiency traits

All phenotypic data collected from the P_i trial at Sawyers requires further validation in a third experimental year. Apart from the commercially available varieties, the wheat germplasm changed during the three experimental years (Table 33). Therefore, even if some cultivars exhibited interesting traits they could not all be used for further validation over a period of three years. Such interesting traits were seen for two contrasting AxC lines, including AxC line 49, which was selected due to an average major root length and short fine root development whereas AxC line 149 was selected due to its long major root and long fine roots (Table 33). AxC line 149 was selected due its long lateral roots (Table 32) and exhibited high shoot P concentrations (Figure 27 B), high P uptake rates at booting (Figure 26 A) and at harvest (Figure 26 E). In contrast, AxC line 49 and 93, an AxC line with average root architecture (Table 33), also had lower tiller densities (Figure 24 A), lower P concentrations at booting (Figure 27 B), low P_i removal rates at booting and harvest (Figure 26 A and F) and lower yields (Figure 30). Therefore, both AxC lines, 88 and 149, may have exploited a larger soil volume resulting in higher P_i acquisition rates (Figure 26 A).

Varieties with high P_i acquisition rates at booting in 2012, comprising AxC line 93, 149 and Conqueror, did not necessarily remove the most soil-P_i at harvest (Figure 26 E). For instance, the sping wheat variety Paragon had a low tiller density (Figure 24 A and B), high shoot P concentrations at booting (Figure 27), average shoot P concentrations in straw and grain (Figure 28 A to D), low TGW (Figures 28 E and F) but high yield per ha (Figure 30). Additionally, Paragon and Capelle Desprez, had low P_i removal rates at booting (Figure 26 A), but high P_i removal rates at harvest in 2012 (Figure 26 E).

P_i removal at harvest is mainly determined by the initial biomass (Figure 25), P concentrations in grain and straw (Figure 28 A to D) and the yield (Figures 30 and 31). In 2012, Conqueror had low shoot P concentrations at booting (Figure 27 B) and in straw and grain (Figure 28 A and C), mainly due to high biomass (Figure 25 A) and high yield (Figure 30), which caused a dilution effect on

nutrient shoot concentrations. At booting in 2012, high total P_i acquisition rates per area at booting in 2012 of Conqueror (Figure 26 A) were seen due to high initial biomass at booting (Figure 25 A) which compensated for the dilution effect on shoot P concentrations (Figure 27 A). AxC line 93 and 149 exhibited a similar pattern, having high biomass (Figure 25 A), low shoot P concentrations at booting (Figure 27 A) but high total P_i acquisition rates (Figure 26 A).

In 2012, TGW were lowest for Conqueror and AxC line 93 compared to Capelle Desprez and Maris Widgeon (Figure 28 E). AxC line 93 and 149 had higher P concentration in the grain compared to Conqueror (Figure 28 C), which is indicative for a higher P_i translocation into the grain. However, higher shoot (Figur 27 B) and grain P concentrations (Figure 28 C) in 2012 of Capelle Desprez, which also had less biomass (Figure 25 A), reveal a 'concentration effect'. However, total P_i acquisition of Capelle Desprez was lower compared to Conqueror at high soil-P_i at booting (Figure 26 A) but higher at harvest in 2012 (Figure 26 E). Furthermore, the yield of Capelle Desprez was lower compared to Conqueror (Figures 30 and 31, Table 39) resulting in higher amounts of available P for grains as sinks during maturity. In addition, even with higher grain size at high soil-P_i availability (Figure 28 E and F) and decreasing grain yield (Tables 39 to 41) of Capelle Desprez, P_i concentration in the grain (Figure 28 C and D) and P removal at harvest via the grain (Figure 26 E) was higher compared to Conqueror. Paragon exhibited similar P_i acquisition patterns but with lower P grain concentrations and lower TGW compared to Capelle Desprez (Figure 28 C to F), which is indicative for a weaker P_i translocation into the grain. This may explain the stronger responsiveness of Paragon compared to Capelle Desprez to increasing soil-P_i in 2012 in terms of yield (Figure 30, Table 39 A), but not necessarily in 2013 (Figure 31, Table 39 B).

AxC line 88, which had been selected in 2012 due its long fine roots (Table 33), had average biomass (Figure 25 A), average shoot P concentrations (Figure 27 B) but the highest grain P concentrations of all genotypes across soil-P_i availability levels (Figure 28 C) indicative for a very high P_i

translocation. AxC line 88 also responded well to increasing Olsen P with increasing yield (Figure 30, Tables 39 and 40). AxC line 49 exposed less pronounced patterns but a higher correlation of yield increase with increasing Olsen P concentrations (Figure 30, Tables 39 and 40). In 2012, Hereward was amonst the least P_i efficient variety exhibiting low biomass at booting (Figure 25 A), average yield (Figure 30, Table 39), and low shoot P concentrations (Figure 27 A). Maris Widgeon revealed a similar growth pattern (Figures 25 A and27 A) but its yield was higher and better related to increasing soil-P_i concentrations in both years (Figure 30, Table 39). Compared to Hereward, Maris Widgeon also exhibited higher P grain concentrations (Figure 28 C) resulting in significant higher P_i removal via the grain (Figure 26 E) which is indicative for a stronger P_i translocation. Hereward also had a stronger need for available P_i than Maris Widgeon, due to higher COP in 2012 (Figure 40).

In 2013, P concentrations for P_i acquisition and P_i translocation patterns were less obvious than in 2012. At tillering, shoot P concentrations were only determined by P_i availability (Figure 27 C). Varietal variation only occurred from heading to ripening in the shoot, not the ears (Figure 27 D to F) and in the grain at harvest (Figure 28 B). In 2013, shoot P concentration was highest in Conqueror at heading and ripening, in Maris Widgeon at heading at high P_i availability and in Paragon at heading and ripening at medium P_i availability (Figure 28 D and E). In contrast to 2012 data, Capelle Desprez had lower shoot P concentrations compared to Conqueror and Maris Widgeon at heading and ripening in 2013 (Figure 27 D and E). Therefore, the main conclusion for this data in 2013 is, that varietal growth differences were negligible (Figure 25) and had no consequences on shoot P concentrations as in 2012 (Figure 27). However, the varieties exhibited similar P_i translocation to the grain in 2012 (Figure 28 A and C) and 2013 (Figure 28 B and D). Maris Widgeon and Capelle Desprez had larger grain weights at high soil-P_i availability compared to Paragon and Conqueror at harvest in 2013 (Figure 29 E). It can be assumed that Capelle Desprez again, had a higher P_i translocation capability from the shoot to the grain than Conqueror. Therefore, Conqueror did not remove more P via the grain even if grain yield was highest for Conqueror across all three soil-P_i availability levels (Figure 26 E and F, Figure 28 A to D). Maris

Widgeon and Paragon did not exhibit any particular patterns in terms of P concentrations during the season 2013 (Figure 28 C to E) and P_i removal rates at harvest in both years (Figures 27 E and F).

In 2012, the COP was particularly high for Conqueror and Hereward compared to other cultivars, whereas it was ~11 mg Olsen P lower for Capelle Desprez (Tables 40 and 41) which reveals an effective P_i acquisition and partitioning ability or simply a lower requirement, particularly during maturity at low soil-P_i. Conqueror was a responsive variety which increased growth with increasing soil-P_i availability and was high yielding when well supplied with P_i (Figures 30 and 31, Table 39). However, this responsiveness resulted in high P_i acquisition rates per cropping area mainly at vegetative growth stages in 2012 (Figures 26 A and F), and in high COP in 2012 and 2013 (Table 40 and 41). Capelle Desprez reached the critical yield at a much lower soil-P_i availability (Tables 40 and 41), indicative for a weaker P_i requirement (Table 39 A) and therefore a higher P_i starvation tolerance, a stronger P_i translocation and sink capacity during maturity. However, Capelle Desprez had a weaker biomass development, at least in 2012, and lower yields and than Conqueror in both years (Figures 25 A, 30 and 31). Both varieties are therefore most likely to show contrasting expression patterns of candidate genes for PUE (Figure 29).

4.4.3. Selection of wheat genotypes for gene expression studies

The wheat varieties which were included in the study on P_i efficiency traits at the P_i field trial at Sawyers in 2012/13, were mainly selected according to shoot P concentrations at booting (Figure 27 B to F), grain P concentrations at harvest (Figure 28 C and D) and P_i efficiency properties in 2011/12 (Figure 29 A). Varietal variation in root and shoot architecture was not considered further due to the lack of validation data in addition to the pre-studies which lead to their selection (Table 33).

Tiller formation, tiller weights and shoot development are usually reduced when P is limiting (Römer and Schilling 1986, Bollons and Baraclough 1997,

Umehara et al. 2010). Therefore, tiller formation was, like in other studies (Yi et al. 2005), used for assessing the genetic response and tolerance to P_i starvation (Figure 24 A and B). However, the germplasm changed during the two seasons (Table 33). Additionally, the variety Hereward, which exhibited interesting "low P efficiency features" and was growing at Broadbalk in 2010/11, was grown only in 2011/12 in the P_i field trial at Sawyers (Table 33). Five commercially available wheat varieties were grown in the P_i field trial at Sawyers during all consecutive years (Table 33). Therefore, the most contrasting of them in terms of P_i acquisition and P partitioning patterns, Conqueror and Capelle Desprez, were used for identifying the potential linkage for target gene expression with the nutritional P status of the plants and P_i efficiency properties.

Capelle Desprez was considered the more P_i efficient variety compared to Conqueror in 2012 (Figure 29 A) with higher grain P_i concentrations (Figure 28 B and D) and a lower COP (Tables 40 and 41). Gene expression data revealed that in 2012, TaSPX2 was the only candidate showing a stronger up-regulation during limited P_i availability in Capelle Desprez compared to Conqueror (Figure 33 C). Even if there were no genotypic differences in P_i efficiency in 2013 (Figure 29 B), there was a significant up-regulation of TaPP$_i$ase3 (Figures 34 B) and TaG3Pp2 at P_i starvation in the roots at heading (Figure 36 B), and of TaSPX2 in the rachis at ripening in Capelle Desprez compared to Conqueror (Figure 36 D). In contrast, TaPho1;3 was significantly less up-regulated in Capelle Desprez compared to Conqueror in the roots at tillering and the glume at ripening (Figure 37 A and E) and, even if not significant, TaMYB in the roots at ripening (Figure 39 C). TaG3Pp2, TaPP$_i$ase3, TaPho1;3 and TaSPX2 were all correlated with P shoot concentrations (Figures 40, 41 and 43, Table 45) and P_i efficiency traits (Table 46). In conclusion, these four genes seem to have marker gene characteristics at the molecular level for assessing genotypic variation.

4.4.4. Candidate genes as target genes for P_i efficiency improvement

When the expression of candidate genes shifts towards lower levels with increasing P_i efficiency, they have potential use as target genes for predicting and improving P_i efficiency traits as suggested in the previously presented model (Chapter 1, Figure 4). Most of these genes were more responsive to decreasing soil-P_i concentrations (Figures 40 to 45, Tables 45 and 46). This may be due to the fact that critical shoot P concentrations decrease during the physiological development of the wheat plants with defining values below 0.4 % at tillering, 0.3 % at early booting and 0.2 % to 0.15 % towards maturity as indicative for P_i starvation (Finck 1991, Bollons and Barraclough 1999, Sanchez 2007). However, two candidates, TaMYBrel and TaExt (b) had no clear relationship to soil-P_i availability or shoot P concentration (Figures 33, 34, 35, 39, 44 and 45). In the following section, each potential target gene will be discussed individually.

4.4.5. The TaPho1;3 gene as target for P_i efficiency improvement

TaPho1;3 was up-regulated during P_i starvation (Figures 32 G, 33 A and 37). Pho1 genes are associated with P_i translocation from roots to shoot and triggering PSR in Arabidopsis and rice mutants (Poirier et al. 1991, Hamburger et al. 2002, Rouached 2011). However, there are only few studies reporting an up-regulation during P_i starvation (Morcuende et al. 2007, Secco et al. 2010, Oono et al. 2011) similar to the results shown here (Figures 32 G, 33 A and 37).

The expression of TaPho1;2 was not differentially regulated in the roots by any of the nutritional macronutrient deficiencies whereas TaPho1;3 was up-regulated in P_i starved and significantly down-regulated in N starved roots (Figure 32 G). Furthermore, high expression of TaPho1;3 was also found in the grain even without being influenced by nutritional status or P_i availability (Figure 37 F). The rice orthologue to TaPho1;2 is OsPho1;2 and to TaPho1;3 is OsPho1;3 and BdPho1;3 (results not shown). In contrast to wheat, OsPho1;2 expression was highest in roots and relatively low in other tissues whereas OsPho1;3 was the lowest gene expressed and slightly more in leaves and

flowers (Secco et al. 2010). In Arabidopsis, AtPho1 was also preferentially expressed in the roots (Hamburger et al. 2002, Morcuende et al. 2007) but less P specific than AtPho1:H1 even if they both belong to the same gene family and clade (Secco et al. 2010, Secco et al. 2012, Woo et al. 2012). These findings suggest, that TaPho1;3 may be the major Pho1 wheat gene responsible for P_i translocation from root to shoot and into the grain. Root-to-shoot P_i transfer is affected in the Ospho1;2 mutant (Secco et al. 2010), which implies a stronger up-regulation in the less P_i efficient wheat genotype Conqueror at tillering and even the glume (Figure 37 E) mirroring a stronger need of P_i translocation during P_i starvation. However, the correlation of TaPho1;3 to available soil-P_i at tillering in 2013 was high (Table 46) suggesting an additional signalling mechanism for TaPho1 regulation than just the internal nutritional P status. Particularly as in 2013, Conqueror did not exhibit lower shoot P concentrations at early growth stages or at ripening (Figure 27 C to F).

TaPho1;3 exhibited a high correlation to PUE at tillering, heading and ripening (Table 46). However, the responsiveness of TaPho1;3 in the roots to shoot P concentrations increased at ripening (Table 45) when grain P concentrations were actually lower in Conqueror compared to the more P_i efficient genotype Capelle Desprez (Figure 28 C and D). Therefore, internal P_i resources may have been used more efficiently by Capelle Desprez (as genes which promote internal P_i recycling are more responsive) which may have reduced the demand of enhancing P_i acquisition and translocation mechanisms through the roots, especially at maturation. To date, there are no other studies showing a link of Pho1 expression with genotypic P_i efficiency. However, P_i use efficiency in barley was correlated through the expression of HvPht1 transporters with HvIPS genes (Huang et al. 2011). These genes were less induced in the P_i acquisition efficient barley cultivars (Huang et al. 2011). Furthermore, Pho1 degradation is Pho2 dependent (Liu et al. 2012). However, the weaker response of the more P_i efficient wheat genotype Capelle Desprez may have been due to differences in this regulatory signalling network (weaker TaIPS gene expression, higher TaPho2 and lower TaPho1 expression) which needs consideration in future genotypic screens.

4.4.6. The TaSPX2 gene as target for P_i efficiency improvement

TaSPX2 was up-regulated in P_i starved roots (Figures 32 E, 33 E and 38 A, B and C), similarly to observations in rice (Wang et al. 2009a, Wang et al. 2009b, Liu et al. 2010, Oono et al. 2011), maize (Calderón-Vázquez et al. 2008, Schlüter et al. 2013) or Arabidopsis (Morcuende et al. 2007, Müller et al. 2007, Duan et al. 2008). TaSPX2 root expression was also correlated to shoot P concentrations (Table 45). TaSPX2 also seemed to be involved in a higher P_i use efficiency (Table 46) even if expression was particularly high in glume and grain (Figure 38 E and F). In contrast to rice or Arabidopsis (Duan et al. 2008, Wang et al. 2009a, Wang et al. 2009b, Liu et al. 2010, Yang et al. 2011), the SPX gene family in wheat has not been characterized, yet. Furthermore, none of the studies which assessed genotypic transcriptome or metabolic differences in P_i starvation tolerance identified SPX proteins as potential distinct regulators. Therefore, genotypic expression differences in wheat roots in both years with a stronger up-regulation in the P_i translocation efficient Capelle Desprez (Figures 33 C and 38 D) are new findings.

In rice, the interaction with the OsPHR1-Pho2 signalling pathways was suggested, implying that OsSPX proteins have different roles in different organelles (Wang et al. 2009a, Wang et al. 2009b). In Arabidopsis, AtSPX proteins are also regulated in a differential manner by P_i starvation (Duan et al. 2008) suggesting they have different roles. In wheat, over-expression of TaPHR1, the OsPHR1 homologue, increased TaIPS1.1 expression and enhanced lateral root branching (Wang et al. 2013a). However, it had no impact on TaSPX3 or TaPho2 expression patterns under P_i limitation which is indicative for another regulatory mechanism in wheat (Wang et al. 2013). In common bean, the over-expression of only one of the P responsive SPX proteins, PvSPX1, enhanced root hair development and the expression of other PSR genes (Yao et al. 2014). Therefore, more members of the TaSPX family need to be identified and their subcellular localization, spatial expression patterns and functions characterized in order to reveal their specific regulatory role in genotypic P_i efficiency in wheat.

The putative rice orthologue of TaSPX2 seem to be OsSPX3 and OsSPX5 which are repressors of OsPHR2 and root-shoot P_i translocation (Shi et al. 2014). Interestingly, Pho2 expression levels were reduced in the osspx3/5mutant and up-regulated in over-expressors in which IPS genes were significantly reduced (Shi et al. 2014). This leads to the assumption that in wheat plants with higher TaSPX2 expression, TaPho2 genes might have been expressed stronger and therefore TaPho1;3 weaker. This supports the previous hypothesis that the genotypic contrasting TaPho1;3 and TaSPX2 expression patterns were linked to changes in the signalling network for P root to shoot partitioning during constant soil-P_i depletion.

4.4.7. The TaG3Pp2 gene as target for P_i efficiency improvement

TaG3Pp2 was up-regulated in wheat roots in a differential manner when soil-P_i availability was limited (Figures 32 B, 34 B and 38 A to C), similarly to the up-regulation of G3Pps in Arabidopsis roots (Lan et al. 2012). Root TaG3Pp2 expression was also highly correlated to shoot P concentration (Figure 40, Table 45) and P_i use efficiency (Table 45). However, modelling TaG3Pp2 expression and P concentrations, implies additional roles apart from those during P_i limitation (Figure 40, Table 45). The G3Pp transport molecule G3P, a precursor for phospholipid biosynthesis (Ramaiah et al. 2011), is required to a certain extent during normal plant metabolism. However, roles in P_i homeostasis and P_i recycling have been suggested (Ramaiah et al. 2011).

A putative TaGDPD was up-regulated in P_i starved wheat roots (Tables 18 C and 19). Similarly TaGDPD was up-regulated in P_i starved rice (Wang et al. 2006), Arabidopsis (Morcuende et al. 2007) and white lupin (Cheng et al. 2011a). P_i starvation initiates the biosynthesis of sulfolipids and galactolipids which are derived from the conversion of glycerolipids, Sulfoquinovosyldiacylglycerol (SQDG) and digalactosyldiacylglycerol (DAG) (Nakamura 2013). There are three main pathways for the breakdown and conversion of phospholipids including the glycerophosphodiester phosphodiesterase (GDPD) and acyl hydrolase (LAH)-mediated pathway of

glycerol-3-phosphate (G3P) hydrolysis and the corresponding alcohol (choline, ethanolamine, inositol, glycerol etc.) (Nakamura 2013). TaGDPD up-regulation in P_i starved wheat roots (Tables 18 C and 19) indicates that this particular pathway, which is present in various subcellular compartments including plastids and vacuoles, is promoted (Nakamura 2013). However, it may predominantly degrade phospholipids rather than being involved in the membrane lipid remodelling process when P_i availability is limited (Cheng et al. 2011a; b, Morcuende et al. 2007). Glycerol-3-phosphatase can then dephosphorylate G3P which releases P_i (Cheng et al. 2011b) and enhances internal P_i recycling by increasing extracellular P_i. However, these processes have only recently been investigated in more detail, especially in plants, and remain elusive (Cheng et al. 2011, Nakamura 2013). The promoters of AtGDPD genes contain a cis-element to which the PHR1 transcription factor can bind (Rubio et al. 2001, Cheng et al. 2011b). G3P application restored the growth phenotype of the wild type (WT) when AtGDPD1, the main AtGDPD isoform expressed particularly in the roots of Arabidopsis during P_i starvation, was not functional in the mutant (Cheng et al. 2011b). Additionally, the products of the glycerophosphodiester phosphodiesterase (GDPD) and acyl hydrolase (LAH)-mediated pathway for phospholipid breakdown are involved in root architectural changes enhancing the P_i starvation tolerance. The silencing of GDPD in white lupin resulted in impaired root hair development (Cheng et al. 2011a). All these results underpin the involvement of the P_i responsive signalling pathway with phospholipid degradation.

Purple acid phosphatases were also among the up-regulated wheat genes in the transcriptome study and classified into cluster 3 (Tables 18 C and 19). Plants secrete phosphatases in order to make organic P forms in the soil available for the plant (Duff et al. 1994, Wang et al. 2011, Robinson et al. 2012). G3P actually had an up-regulating effect on the expression of purple acid phosphatases in Arabidopsis, AtPAP12 and AtPAP26, during P_i starvation (Robinson et al. 2012). In conclusion, G3Pp are important antiporter transporting molecules which are involved in the P_i lipid breakdown in order to improve P_i recycling during P_i limiting growth conditions. G3Pp may act as signalling molecules inducing changes in root architecture and root secretion in

order to enhance P_i acquisition. Therefore, the strong responsiveness towards soil-P_i availability and the enhanced expression in the more P_i starvation tolerant wheat genotype suggest that TaG3Pp2 belongs to the panel of target genes for enhancing genotypic P_i efficiency in crops.

4.4.8. The TaPP$_i$ase3 gene as target for P$_i$ efficiency improvement

TaPP$_i$ase3 was up-regulated during limited P_i availability in the microarray analysis and in the target gene screening (Figures 34, 35 and 36). It was not as strongly correlated to shoot P concentrations than for instance TaG3Pp2 expression, but it was the most responsive gene to decreasing total P concentrations (Table 43). PP_i acts as an alternative energy donor to replace ATP for sucrose mobilisation, glycolysis and tonoplast energisation (Stitt 1998). The expression of important PP_i dependent bypass enzymes such as sucrose synthase, phosphofructokinase, PEPC, PPDK, UDP-Glc-phyrophosphyrylase and H+ tonoplast PP$_i$ase (Stitt 1998, Plaxton and Tan 2011) was affected by the P nutritional status. For instance, phosphofructokinase was up-regulated in P_i starved roots of Arabidopsis roots (Lan et al. 2012), in P_i starved roots of rice without exhibiting genotype differences (Pariasca-Tanaka et al. 2009), and in maize additionally to the observed up-regulation of PEPC (Schlüter et al. 2013). Therefore, PP_i dependent processes are crucial for metabolic adaptation to P_i starvation, even if transcription of these seem to be less important than other more down-stream regulatory mechanisms in order to have an effect on the plants metabolism via these genes (Stitt 1998, Plaxton and Carswell 1999).

TaPP$_i$ase3 expression correlated to P_i use efficiency (Table 45) and was higher expressed in the grain of Conqueror at ripening (Figures 33 E and 36 F). PP$_i$ases are the enzymes controlling PP_i availability in the cells. They are usually found in plastids, not in the cytosol (Weiner et al. 1986, Sonnewald 1992). However, TaPP$_i$ase3 showed sequence similarity to the recently identified cytosolic AtPP$_i$ase in Arabidopsis (May et al. 2011). Increased AtPP$_i$ase (At1g73010) expression was seen in P_i starved Arabidopsis

(Morcuende et al. 2007, Müller et al. 2007, Lan et al. 2012) and May et al. (2011) assumed that increased activity of this particular AtPP$_i$ase would increase and stabilize intracellular P_i concentrations. Therefore, phosphohydrolases may be involved in the metabolic adaptation capability to P_i starvation in specific wheat genotypes. Over-expression of PP$_i$ase in the cytosol of potato led to sugar and amino acid accumulation and reduced phloem translocation into sink leaves (Sonnewald 1992, Jelitto et al. 1992). If PP_i metabolism affects sugar metabolism (Stitt 1998), it is potentially connected with in the sugar signalling of PSI genes determining the responsiveness of crops towards P_i starvation.

4.4.9. Rejection of TaMYBrel and TaExt (b) as target genes for P_i efficiency improvement

Except in samples from Broadbalk, when TaMYBrel expression was up- and TaExt (b) expression was down-regulated (Figure 32 H to J), both showed no relation to soil-P_i availability or shoot P concentration (Figures 33 E and F, 35, 39, 41, 44 and 45, Tables 45 and 46). The poor correlation of TaExt (b) expression to tissue P concentrations was mainly due to too much variation in the screening data (Figure 45). Like expansins, which modulate root hair elongation, extensins have been found to be involved in root hair formation (Kwasniewski et al. 2010, Velasquez et al. 2011). TaExt (b) was exclusively root-expressed during the early root growth period (Figure 35). However, root-excavation favours the removal of older root parts rather than root tip areas and root hairs. Hence, the potential loss of root hairs due to the sampling method could have contributed to these contradictory results of extensin expression. Extensins have been implicated to be influenced by ABA signalling (Bai et al. 2009) and involved in cessation of cell elongation giving the cell wall structure its rigidity (Cleland and Karlsnes 1967, Ito et al. 1998). ABA possesses a dual function inhibiting root growth but it can also act as a growth promoter during moderate stress (Niu et al. 2012). The other putative ABA responsive gene, TaMYBrel, was only up-regulated in P_i starved roots from Broadbalk (Figure 32 J) with shoot P concentrations (Table 12) below the critical P level (Finck

1991). However, despite being suggested, the connection of ABA signalling and P responses are still elusive (Niu et al. 2012, Woo et al. 2012).

There was no correlation of TaMYBrel and TaExt (b) expression to P_i efficiency traits (Figure 47, Table 45). Drought stress may reduce soil-P_i availability to a higher extent than those of other nutrients and increases ABA levels (Ji et al. 2011). MYB-TFs are involved in multiple cellular processes and responses to abiotic stress, not just P_i starvation (Zhan et al. 2012). Therefore, the dry conditions in which sampling was done in 2011 (Figure 5) may partly explain the data inconsistency for TaMYBrel expression. Despite all of these considerations, the conclusion remains elusive until TaMYB-TFs have been functionally characterized and further validations are done.

4.5. Conclusion

The reproducibility of microarray data (using the Affymetriy Genechip®) was checked and validated in a broader spectrum of cultivars, growth stages and tissues. Otherwise, microarray data can be ambiguous and lead to false conclusions e.g. in the case of TaExt and TaMYB-TFs genes. However, it was possible to link selected candidate genes that are regulated in wheat roots in response to P_i starvation with P_i acquisition and P_i translocation capability of distinct wheat genotypes. As a result, four potential target genes, TaPho1;3, TaPP$_i$ase3, TaSPX2 and TaG3Pp2, were identified in wheat, which are marker genes at the molecular level, and which exhibited genotypic expression differences. It would be worth identifying more members of these gene families as well as the determinants of their regulation. Further validation in more years and genotypes is required as well as an assessment of exploitability for incorporating them into breeding protocols.

Chapter 5: General Discussion

5.1. Verification of the thesis hypothesis

5.1.1. Determination of transcriptional responses to P_i starvation

The coordination of molecular responses to P_i starvation and the mechanisms of P_i starvation tolerance have been investigated predominantly in model plants (Chapter 1). Expression profiling was determined for many genes involved in the PSR for the first time in field-grown wheat roots (Chapter 2 and 3). These data improved the limited data availability for wheat research on PSR and P_i efficiency, which can now be used by other scientists for cross-comparison studies (GEO database[41]: Accession GSE61679) and make investigations more species targeted. Particularly, when the lack of gene annotation will be overcome, this data is a useful source in which P_i efficiency was investigated in more realistic scenarios as suggested by Manschadi et al. (2014). Transcriptome studies are useful but costly tools (Chapter 3, Section 1.1.). However, it has been shown that fertilizer regimes have effects on transcriptomes (Lu et al. 2005, Hammond et al. 2011, Tenea et al. 2012). Therefore, if regulated transcription is monitored, it may potentially be incorporated into mechanistic models for improving fertilizer recommendations.

However, transcriptional responses to macronutrient limitations in wheat were determined using the Affymetrix Genechip® Wheat Genome Array and real-time qPCR. The major challenge for this analysis was the lack of complete gene annotation of differentially altered transcripts and putative candidate genes. The gene annotation for wheat is the crucial step for identifying key genes in the PSR. However, the gene annotation for wheat is still extremely patchy and a complete reference genome is still missing (Leader et al. 2005, Choulet et al. 2010, Oono et al. 2013). Therefore, using a microarray approach instead of the most recent and expensive transcriptomics methods such as SAGE, MPSS, Roche 545 pyrosequencing technology or de novo assembly such as Oono et al. (2013), seems justified.

[41] http://www.ncbi.nlm.nih.gov/geo/

Several approaches including cluster analysis, cross- comparison with other studies and linking gene expression to the wheat ionome were used (Figures 17 to 19, Tables 18, 23 and 30) to compensate the lack of annotation by focusing on a crucial number of putative PSR key genes and their expression patterns across different macronutrient limitations. Furthermore, using absolute quantification (real-time qPCR) as validation technique allowed linking specific gene expression across all field experiments and years. This goes beyond most transcriptome studies validations of crops (Calderón-Vázquez et al. 2008, Pariaska-Tanaka et al. 2009, Li et al. 2010, Oono et al. 2011, Dai et al. 2012, Cai et al. 2013, Oono et al. 2011, Oono et al. 2013). Using wheat roots for a transcriptome study instead of shoot tissues revealed expression patterns related to structural, metabolic and signalling changes, predominantly induced through soil N and P_i availability (Table 18, Figure 16 and 17), similarly to results by Cai et al. 2013, Schlüter et al. 2013). For most genes such as peroxidases, cytochrome P450, glutathione-transferases, glycosyltransferases, MBY-TF, Lea genes, dehydrins, SPX genes, IPS genes, Pho-like transporter genes and APases, homologues have been been reported as being involved int the P_i starvation response in model plants and other cereal crops (Table 33) (Hammond et al. 2003, Uhnde-Stone et al. 2003, Morcuende et al. 2007, Calderón-Vázquez et al. 2008, Duan et al. 2008, Li et al. 2008, Wang et al. 2009b, Liu et al. 2010, Cheng et al. 2011, Oono et al. 2011, Huang et al. 2011, Dai et al. 2012, Secco et al. 2012, Woo et al. 2012). Interestingly, the SAMD gene was highly up-regulated (Table 18 B) and the NAS gene was highly down-regulated (Table 18 E). Both genes are potentially involved in the successful establishment of AM symbiosis (El-Ghachtouli et al. 1996, Kytoviita and Sarajala 1997, Higuchi et al. 199, Hussain et al. 2011, Chen et al. 2012). In conclusion, the acquired data revealed many similarities to previous studies on model plants but also some gene patterns unique to wheat and unique to the growing environment.

5.1.2. Determination of genes involved in P uptake and translocation processes

For determining the molecular responses to P_i availability in the roots focusing on up-take processes as well as translocation processes in ear tissues, transcript abundance was quantified for 14 P_i transporters genes of the TaPht1 family, which was nearly completely identified in wheat (Figures 6 and 7, Tables 7 and 8). Genome information on wheat is slowly becoming available, but complete assembly and annotation is still lacking (IWGSC 2014), emphasizing the timeliness of this study. The TaPht1 family is characterized by several gene duplications (Chapter 2, Section 3.1 and 3.2.) making it difficult to define precise homologues between wheat and other cereals species (Figure 7). Another novel aspect is the documentation of expression in field grown roots in relation to P_i availability. The unique and direct comparison of hydroponical (Figure 9) to field grown wheat Pht1 expression (Figure 10, 12 to 14), made possible due to absolute quantification (real-time qPCR), indicated a more complex regulation of P_i transporters under real agronomic conditions. However, these data suggest potential targets for crop improvement, including TaPht1;1, TaPht1;2, TaPht1;6, TaPht1;8 (Figures 10 and 15). Additionally, uptake and translocation peaks at tillering and post-anthesis (Römer and Schilling 1986) are reflected by P_i transporter expression (Figures 12 to 14) with consequences on sink strength for P_i during maturity, TGW and yield. In conclusion this study confirms what many previous studies in vitro studies suggested (Daram et al. 1998, Smith et al. 1999, Wang et al. 2002, Rae et al. 2003, Wasaki et al. 2003, Tittarelli et al. 2007, Calerón-Vázquez et al. 2008, Huang et al. 2008, Ai et al. 2009, Miao et al. 2009, Pariasca-Tanaka et al. 2009, Qin et al. 2012): that TaPht1 transporter are obvious targets for crop improvement when their subcellular localization, the biological functions, the molecular regulation of each member and the complex interaction amongst all family members are determined. Particularly, as varietal variation in TaPht1 expression patterns were already determined for TaPht1;1, TaPht1;2 and TaPht1;6 (Davies et al. 2002, Miao et al. 2009, Aziz et al. 2014) or for a barley homologues of TaPht1;6, HvPht1;6 (Huang et al. 2011).

5.1.3. Screening wheat germplasm for the expression of target genes and P_i efficiency traits

A wheat germplasm screen using the P_i trial at Sawyers successfully identified differences in P_i efficiency traits of investigated cultivars. However, not all phenotypic data was consistent across both years (Figures 24 to 29) and requires further validation in a third experimental year. This is particular unfortunate for varieties which exhibited a good correlation of known root architectural traits (Table 33) with P uptake and shoot P concentrations such as the AxC lines 88 and 149 (Figures 26 A and F, Figure 27 B, Figure 28 A and C). That P_i starvation tolerance was related to genotypic variability in root growth properties has been seen in many other studies (Gahoonia et al. 1996, Gahoonia et al. 1997, Zhu and Lynch 2004, Zhu et al. 2005, Li et al. 2008a, Hammond et al. 2009, Pariaska-Tanka et al. 2009, Yao et al. 2011). Therefore, it would be worth to screen those contrasting commercial varieties (Table 32) which has been used in the screening and exhibited phenotypic variation, for variation in root properties using a cigar roll system (Bai et al. 2013). Particulary Conqueror and Capelle Desprez, which exhibited clearly contrasting P_i requirements and P_i traits (Chaper 4, Section 4.2.).

Linking the gene expression of selected candidate genes to to shoot P concentrations (Figures 40 to 45) was a used to determine if putative candidate genes (Table 31) could be used as markers for predicting when the critical soil-P_i or shoot P concentration are exceeded. However, this had been done across experiments, years and varieties (Table 45). Particularly, as the variety was not statistically relevant for this model (Table 45). However, individual analysis in each experimental year of the P_i trial at Sawyers, reveals expressional differences of candidate genes in in the roots and ear tissues of the two selected wheat varieties, Conqueror and Capelle Desprez (Figures 33 C, 34 B and F, 36 B 37 A and E, 38 D). Therefore, this study complements previous P_i efficiency screenings in cereals which identified interesting genotypes in the field and those which used exactly these genotypes in molecular studies (Davies et al. 2002, Miao et al. 2009, Pariasca-Tanaka et al. 2009, Li et al. 2010, Aziz et al. 2014). It could further prove that transcriptome studies deliver marker genes for diagnosing a P_i deficiency (Hammond et al. 2011) and, additionally, show

genotypic variation in the P_i starvation response. Successfully validated candidate genes were involved in P_i starvation signalling cascades, P_i recycling and P_i stress reponses (Table 31).

Absolute quantification (real-time qPCR) further allowed linking gene expression directly to shoot P concentrations providing an even more comprehensive understanding of their role in the nutritional status of the plant (Figures 44 and 45) rather than remaining on the P_i starvation reponse level (Table 18, Figures 32 to 39). Until now, this is a unique procedure for validating transcriptome data. Interestingly, this validation approach revealed that two main candidate genes, TaMYBrel, which was highly up- and regulated (Table 18 A), and TaExt (b) which was highly down- regulated (Table 18 D) in the array study (Figure 32). However, both genes were actually not related to shoot P_i concentrations (Figures 44 and 45, Table 45) or P_i efficiency traits (Figure 47, Table 46). Most transcriptome studies used hydroponically or glass-house grown plant material (Wasaki et al. 2003, Pariaska-Tanaka et al. 2009) (Table 17) which are less susceptible to abiotic factor fluctuations compared to a field study. Therefore, the wheater conditions (Figures 5) may explain the occurrence of inconsistency between array data and validation data in this study (Chapter 5, Section 2.2 and 2.3.).

5.1.4. Identification of candidate genes for future crop improvement

Four potential target genes in wheat, TaSPX2, TaPP$_i$ase3, TaG3Pp2 and TaPho1;3, as well as TaPht1 transporters, were identified and discussed in Chapter 4 (Section 4.5. to 4.8.). The four genes can be used as marker genes at the molecular level (Figures 40 to 43), and exhibited genotypic expression differences (Figures 33 C, 34 B and F, 36 B, 37 A and E). Nevertheless, there remain frontlines for their application in crop breeding and crop production, which will be discussed in more detail in Chapter 5, Section 3.

5.2. The main influence factors on the thesis data

5.2.1. The transferability of hydroponical culture versus field studies

In regards to the TaPht1 expression study (Chapter 2) as well as the candidate genes expression study (Chapter 4), the question raises, how transferable are results from in vitro or hydroponical culture to soil studies and field trials? Results coming from field studies are more complex than data from hydroponics. This was already discussed for the observed TaPht1 expression patterns (Chapter 2, Section 4.4.). Often, results coming from in vitro studies are not transferable when plants are grown in soil. For instance, genotypic variation of root exuded phosphatases, measured in vitro, was not related to P_i uptake or P content in wheat (George et al. 2008). However, when phenotypic differences were already known between two genotypes in the field, phosphatase activity in soil samples correlated well with their P_i acquisitions abilities (Zhang et al. 2009).

On the other hand, enhanced P_i acquisition by overexpressing Pht1 transporter genes in P_i starved barley plants but could not be confirmed at the plant level, even when using a dilute flow culture system (Rae et al. 2004). The authors refered to a systemic down-regulation suppressing HvPht1;1 transcription by post-tranlational modification. It may be that the well-watered conditions reinforced this effect which could be different when plants are growing in a nutritionally heterogenous soil as hypothesised by Hayes et al. (2004). Hayes et al. (2004) compared two wheat cultivars for P_i efficiency differences in solution culture without seeing differences in P_i uptake kinetics. Nevertheless, in this study, there was a good relationship of TaPht1 expression in hydroponics with results from the field (Figures 9, 10 and 15). In order to confirm the hypothesis by Hayes et al. (2004), it would be nessecary to screen more than one wheat variety in vitro for potential differences in TaPht1 expression.

AM infection does not only affect P_i nutrition but also other abiotic factors in the soil. For instanct, arsenate uptake in plants is reduced when barley plants were colonized by AM (Christophersen et al. 2009). Particularly, due to the down-regulation of HvPht1;1 and HvPht1;2, homologues of the P_i transporters

TaPht1;1 and TaPht1;2 (Figure 7), which have been shown to be major contributors in direct P_i acquisition pathway by the roots (Figures 9,10 12 and 13) (Smith et al. 1999, Davies et al. 2002, Mudge et al. 2002, Paszkowski et al. 2002, Rae et al. 2003, Glassop et al. 2005, Nagy et al. 2006, Wang et al. 2013a). However, such interaction can only be investigated when the degree of colonization can be directly linked to gene expression using soil-experiments, particularly pot systems (Güimil et al. 2005, Glassop et al. 2005, Gaude et al. 2011).

Furthermore, there is an argument that you can only measure P_i use efficiency accurately between cultivars when you can ensure identical P_i uptake (Rose et al. 2011). Soil-based screenings may lead to confounding effects of P_i uptake on P_i use efficiency when more P_i uptake efficient cultivars suffer less from P_i starvation (Rose et al. 2011). To support this hypothesis, field screening results investigating P use efficiency (Figures 24 to 29, Tables 45 and 36), should be validated using a modified solution technique as suggested by Rose et al. (2011) with a fixed amount of available P_i leading to a uniform plant P_i starvation. For time reasons, this was not been done here. Particularly, as the main focus of this work was to link the expression of candidate genes with the genotypic response to P_i starvation and to describe the ability of cultivars to cope with P_i starvation. However, the application of this technique for further studies would be an important following up project.

5.2.2. The influence of weather fluctuations on P_i availability

Variations in soil-P_i availability, P_i uptake and therefore gene expression were seen. Such partly large inter-year and inter-experiments are mainly caused by abiotic factors. In hydroponics P_i starvation can be applied under very controlled conditions whereas P_i starvation in the field is subject to many different abiotic and biotic restrictions such as rainfall patterns, drought and climate change (McBeath et al. 2012, Norton 2012, Manschadi et al. 2014) and the impact of agricultural practices on microbial activity, which mineralize

organic soil-P sources to P_i (Richardson 1994), or on mycorrhiza symbioses (Abbott and Robson 1994).

Target and actual Olsen P measured in plots of the P_i trial at Sawyers 2011/12 and 2012/13 in autumn pre-sowing and COP fluctuated greatly (Tables 40 and 41). The main reasons for these fluctuations are likely to be such abiotic factors affecting the interactions of P_i in the soil which influence the P_i delivery to the root system and can cause a temporarily latent P_i starvation. On-site data revealed weather fluctuations between the three years, particularly in the amount of rainfall before sampling (Figures 5 and 21). Unfortunately, even if specific data was not available, rainfall pattern (Figure 5 and 21) show that there must have been differences in soil moisture content and field water capacity during the different sampling periods. Even if Pi availability is additionally affected chemical interactions in the rhizosphere, Pi delivery towards the roots proceeds mainly via diffusion in the soil solution (Hinsinger 2001). Therefore, soil-Pi availability largely depends on the buffering capacity and soil moisture which is, amongst other factors, largely determined by rainfall and temperature during the growing season. All these abiotic factors impair Pi availability, Pi acquisition processes and yield (Bahl and Singh 1986, Leigh and Johnston 1986, Holford 1997, Strong et al. 1997, McBeath et al. 2012). Results from Boadbalk in 2011 prove this hypothesis: despite the very high soil-Pi concentrations at Broadbalk (Table 2), shoot P concentrations across the entire experiment were low, even for plants growing in control plots (Table 12). However, the weather conditions in 2011 were much drier than in 2012 (Figures 5 and 21) for which shoot P concentrations were much higher in the control (Figure 11). Reduced P tissue concentrations in drier years were also observed by Bollons and Barraclough (1999) when using the Pi field experiment at Sawyers.

5.2.3. The influence of weather fluctuations on P_i fertilizer treatments

There is another caveat when comparing results from field studies where fertilizer applications were used as treatments (Table 1). The agronomic practices uses in such trial vary largely but they crucially influence soil-P_i

availability. For instance, shoot P concentrations at the Broadbalk experiment (Figure 18) reflected the applied fertilizer treatments across the trial (Table 1). However, the control plot had Olsen P concentrations within Index 4/5 (Table 2), which is far above the recommended target Index of 2 (Defra 2012). This was the reason why P_i fertilizer applications were stopped since 2000 on this control plots. Additionally, plots used as P_i starvation treatments at Broadbalk, plot 19 and plot 20 (Table 1), exhibit large variation in soil-P_i concentrations (Olsen P) (Table 2). Plot 19 was used as P_i starvation plot but received castor meal as organic N fertilizer until 2001, which contains significant amounts of P (Lima et al. 2011). This explains Olsen P concentrations in plot 19 at Index 2 and at Index 1 in plot 20, which never received any P_i fertilizer (Table 2). However, a sustainable fertilization strategy maintains soil-P_i concentrations at particular target and the amount of applied P_i fertilizer corresponds to the amount of harvest product take off (Figure 3 C). Fertilizer use by the plants, particularly the use of subsoil P_i, increased with increasing rainfall and irrigation (McBeath et al. 2012). Nontheless, topsoil P_i uptake is the favoured P_i foraging stragey of plants (Lynch and Brown 2001, Williamson et al. 2001, Pérez-Torres et al. 2008, McBeath et al. 2012) which makes them vulnerable to drought stress.

However, plants growing at Broadbalk in 2011 unlikely suffered from drought stress. Several genes were specifically induced by P_i starvation, including MYB-TF, LEA proteins and dehydrins genes (Table 18 A). Theise genes are either ABA responsive or involved in the ABA signalling pathway such as serine/threonine phosphatases (Table 18 A). Drought stress increases ABA levels (Ji et al. 2011). Additionally, the ABA responsive LEA proteins respond to conditions of drought, osmotic or salt stress (Zhu et al. 2000, Rampino et al. 2006). Dehydrins are also involved in drought tolerance of wheat (Lopez et al. 2003). Therefore, it seems that weather conditions specifically affected P_i availability without causing drought stress to the entire experiment.

5.3. Application of results in plant breeding and crop production

5.3.1. Global front lines of phosphate supply and phosphate nutrition

This project was focused on gene expression in wheat as a response to nutrient availability, emphasising P_i nutrition. In an arable system, P_i fertilizers supply the plants with this essential macronutrient. These P_i fertilizers are derived from rock P_i and are mainly imported into major grain crop producing countries in Asia, America and Europe (FAO 2011, Jasinski 2011). However, more than two thirds of rock phosphate is mined in only a few countries, China, Russia, Morocco and the United States, of which many are considered as geopolitically problematic (Cordell et al. 2009, Jasinski 2011). Furthermore, it is controversial how much rock P_i is still available for how many years (Cordell et al. 2009, Jasinski, 2011). In addition, once P_i becomes more limiting in the future, market forces will cause increasing prices (Cordell et al. 2009, Vaccari 2009). Many global P_i resources are not readily exploitable and currently no economical technologies exist to extract P_i from these sources (Vaccari 2009). However, stimulating prices may promote exploitation of new resources (Vaccari 2009). This is a reason why the main focus of much research on P_i efficiency in agricultural systems focusses on the environmental impact rather than on future P_i fertilizer scarcity.

Globally, food consumption will increase with the currently rapid growing population, which increases the need for maintaining or even increasing grain yields. This will push the amount of applied P_i fertilizer rates up further (Schröder et al. 2011). However, increasing fertilizer use (Figure 1 C) is no indication of an optimum fertilizer management in many countries which increase wheat productivity through higher fertilizer inputs (Phillips and Norton 2012). Additionally, in contrast to mineral fertilizers, there is not much global data available about organic P sources and their use and losses (Cordell et al. 2009, Schröder et al. 2011).

5.3.2. Global front lines of phosphate nutrition in crop production

It might be that P_i fertilizer scarcity and the need for higher fertilizer use P_i efficiency are not the only challenges which crop production has to face in the long term. Soil moisture and soil structure are important determinants for P_i acquisition and P_i use of crops (Bahl and Singh 1986, McBeath et al. 2012). Drought, as a consequence of predicted climate change, may therefore severely decrease P_i efficiency in cropping systems (Manchadi et al. 2014). Furthermore, the removal from and the poor return of nutrients to arable land, large global P imbalances (Figure 3) and anthropogenic P emissions leading to the eutrophication of water bodies may become even more problematic (Capenter 2008, Vaccari 2009, MacDonald et al. 2012). Therefore, increasing nutrient recycling, e.g. urban waste (water), has been suggested (Cordell et al. 2009). However, these solutions must deal with contamination and lack of infrastructure to provide better recycling systems (Keyzer 2010). A panel of concepts has also been suggested by Syers et al. (2008) to improve the poor recovery of fertilizer application; this panel includes the avoidance of soil compaction by applying zero- or minimum tillage systems, liming to overcome P_i limiting Al toxicity, maintaining more organic matter, minimising surface run-off and erosion by contour planting or soil cover, grazing management and appropriate manure application etc. (Syers et al. 2008, Schröder et al. 2011). Improving fertilizer management may be achieved by better timing, precise fertilizer placement (Sanchez 2007), using GPS (Global Positioning System) guided precision farming tools which relate yield maps to soil and plant analysis (Syers et al. 2008), or using the previously mentioned critical value concept (Kikby and Johnston 2008), which determines most fertilizer recommendations (Jordan-Meille et al. 2012). For instance, fertilizer bands increase the root development towards the subsoil, which would improve fertilizer use and even drought tolerance (McBeath et al. 2012).

5.3.3. Bottlenecks for P_i efficient crops in the breeding process

Unfortunately, only minor progress has been made forward to breed P_i efficient cultivars (Rose and Wissuwa 2012), which these authors attribute to inconsistent terminology and confounding effects of PAE and PUE in

genotypic screens, different levels of applied P_i starvation and a focus on PSR mechanisms rather than genotypic P_i starvation tolerance. These thoughts were discussed in the introduction (Chapter 1 and Chapter 4) and have been taken as guideline for this project on wheat. However, there may be additional reasons as to why the availability of P_i efficient cultivars is currently limited, which are mainly commercially and policy driven (Schröder et al. 2011). Firstly, nutrient efficiency is a complex and multi-genetic trait with low heritability, which is also influenced by many environmental and management factors (Manschadi et al. 2014). Therefore, it must be viable to put effort into including nutrient efficiency as selection criteria in breeding protocols (Schröder et al. 2011). The results in Figures 30, 31 and 32 showed that genotypic variability was seen during P_i depletion. Batten (1992) suggested evaluating for nutrient efficient varieties on sup-optimal levels which enhances indirectly the selection towards a higher varietal P_i starvation tolerance. However, P_i efficiency corresponds to a better tolerance during unfavourable growing conditions (Figure 3) and would not necessarily increase yield potential. Therefore, such screening would result in cultivars which secure yield potential, reduce P_i losses from the field, increase fertilizer usage etc. This may be another reason why nutrient efficiency is still not a main breeding goal, unlike resistance or quality. It is also not a test criterion in variety suggestions for farmers (HGCA Recommended List 2014/15)[42]. A root or rhizosphere index could describe rooting properties by combining evaluation methods described by Chaignon and Hinsinger (2003), George et al. (2004), Trachsel et al. (2011), Santner et al. (2012), de Sousa et al. (2012) and Bai et al. (2013). Such an initiative could create a demand and willingness to pay for nutrient efficiency properties in a cropping system. This could benefit the breeders and may push their efforts towards delivering varieties with improved nutrient related traits. Nevertheless, interest in efficient and reduced use of inputs may rise with increasing P_i fertilizer prices and stricter legislative policies, which internalize the negative costs effects of agriculture and reward high P_i use efficiency (Schröder et al. 2011).

[42] http://www.hgca.com/varieties/hgca-recommended-lists.aspx

Another angle was considered by Manschadi et al. (2014), who suggested an interdisciplinary research framework for developing P_i efficient crop varieties, addressing trait dissection (heritability, metabolic and other trade-offs, QTL identification), efficient phenotyping platforms for evaluating these traits and identifying of P_i efficient genotypes and their effects on and in various, realistic cropping systems. This approach would improve P_i use efficiency of the plant itself by integrating molecular biology and plant breeding tools (Manschadi et al. 2014).

5.3.4. Bottlenecks for P_i efficient crops in fertilizer recommendation schemes

The implementation of more P_i efficient crops would require changes in the fertilizer recommendation schemes. Fertilizer recommendations rely on empiric models which are based on field trials and calibrated against soil testing or nutrient concentrations in plant tissues (Hammond and White 2008). However, the reliability of fertilizer recommendations is limited. Methods used for estimating the available soil-P_i together with appropriate application schemes differ widely across European countries (Neyroud and Lischer 2003, Jordan-Meille et al. 2012). Firstly, there was a huge inter-laboratory bias even when identical methods had been used for similar soil testing (Neyroud and Lischer 2003, Jordan-Meille et al. 2012). Secondly, soil analysis does not necessarily represent the P available for the plant and some extractants under- or overestimate the bio-available soil-P_i (Neyroud and Lischer 2003). Thirdly, there were apparent contradictions in how these data was interpreted, recommendations were given and how soil and crop rotations were included in the calibrations (Jordan-Meille et al. 2012). Certainly, mechanistic models are available but require much more and accurate information about the crop, weather and soil etc. (Hammond and White 2008). However, environmental constraints and P transfer to water bodies could be considered, calibration methods improved and plant responses to changing soil-P_i better monitored by establishing such mechanistic models (Jordan-Meille et al. 2012, Mollier et al. 2008). Apart from the lack of standardization, another major aspect is that

fertilizer recommendations do not always account for the crop sensitivity and do not as yet account for variation among cultivars (Sanchez 2007).

Given this current background, implementing more P_i efficient genetic material into practice, as a suggested strategy to increase fertilizer use, would perhaps not have an immediate and significant effect. Finally, it can be concluded that there are bottlenecks for P_i efficient crops and agronomic strategies which have to be overcome before the application of molecular tools such as marker genes can successfully affect the supply of P_i efficient cereal crops to farmers.

5.3.5. Exploitability of identified marker genes

Generally, more information is required for the identified candidate genes (Chapter 5, Section 1.4.) in order to ascertain their localization, functional regulation, their onset of transcription and if target genes are actually useful to monitor the onset of P_i starvation, to enhance the ability for tolerating P_i limited conditions (decrease fertilizer inputs) or to increase P_i efficiency by a more efficient internal use. It would also be useful to test if any of the identified genes are associated with a known QTL for P_i starvation tolerance (Su et al. 2006, Su et al. 2009). This is particularly interesting for the TaPht1 transporter family in order to ascertain their impact on P_i starvation tolerance more accurately. This would require investigating homologues genes in additional species, for instance maize or rice. However, using the candidates as marker genes requires fine mapping and identifying the underlying genes of a known QTL (Collard and Mackill 2008, Gamuyao et al. 2012). Therefore, it is still a long way until the identified genes here could actually be used in MAS.

Another requirement for future genotypic screens on the molecular level are more uniform screening definitions in order to validate the viability of the identified marker genes and to estimate the magnitude of P_i efficiency gain. P_i fertilizers are usually estimated and applied before the actual demand exists (Gregory and George 2011). This pre-knowledge is therefore an absolute

requirement to anticipate when P_i fertilizer acquisition efficiency should be enhanced by more P_i use efficient crops through target genes.

If marker genes are successfully validated, these single key genes could be used together with other biotechnological tools within a platform such as Traitmill™ which enables large-scale transgenesis and high-throughput phenotypic evaluation (Reuzeau et al. 2006). This platform focuses on plant performance for delivering commercial products rather than discovering gene functions. The concept of using marker genes in "smart plant systems" has been suggested by Hammond et al. (2003) and could be implemented in precision farming practices: marker genes are transformed in plants with an appropriate promoter-marker gene construct and reporter genes such as GFP (green fluorescent protein) or GUS (β-glucuronidase) (Hammond and White 2008). However, this concept only works when marker genes respond specifically to limited P, earlier than using tissue analysis, and before it is not already too late to remedy e.g. with foliar application (Bollon and Barraclough 1997). Furthermore, a technological system which recognises fluorescent plant responses has to be implemented for agricultural machinery and has to be viable for farmers. Nonetheless, distinct public opinions in different countries (Hails and Kinderlerer 2003, Oeschger and Silva 2007, Ahteensuu 2012) towards genetic engineering (GM) technologies or other transgenic approaches (Gaxiola et al. 2011) have to be considered when targeting such approaches for solving the P_i efficiency problem globally.

5.4. Final conclusion

Nutrient efficiency is a very complex trait (Chapter 1). The identification of genetic regulators of this trait is an important contribution to future agricultural sustainability. Genes involved in the PSR were determined and members of the TaPht1 P_i transporter family 1 were identified for the first time in field-grown wheat roots (Chapter 2 and 3). Wheat germplasm screening via real-time qPCR techniques showed evidence that there is varietal expression of four selected candidates which could be used as marker genes for monitoring responses to soil-P_i availability (Chapter 4). To ascertain if these genotypic differences are consistent, more investigations on the genotypic effects of P_i starvation tolerance and yield are required. However, agronomic bottlenecks may still impede the implementation of P_i efficient crops and the application of molecular tools such as marker genes.

References

Abbott, L.K. and Robson, A.D. (1994) The impact of agricultural practices on mycorrhizal fungi. In: Soil biota: management in sustainable farming systems (Pankhurst, C.E., ed.), CSIRO, East Melbourne, Australia, pp. 88-95.

Ahteensuu, M. (2012) Assumptions of the deficit model type of thinking: ignorance, attitudes, and science communication in the debate on genetic engineering in agriculture. J. Agric. Environ. Ethics 25: 295-313.

Ahuja, I., Voas, R.C.H., Bones, A.M. and Hall, R. (2010) Plant molecular stress responses face climate change. Trend Plant Sci. 15: 664-674.

Ai, P., Sun, S., Zhao, J., Fan, X., Xin, W., Guo, Q., Yu, L., Shen, Q., Wu, P., Miller, A.J. and Xu, A. (2009) Two rice phosphate transporters, OsPht1;2 and OsPht1;6, have different functions and kinetic properties in uptake and translocation. Plant J. 57: 798-809.

Akhtar, M.S., Oki, Y. and Adachi T. (2008) Genetic variability in phosphorus acquisition and utilization efficiency from sparingly soluble P-sources by Brassica cultivars under P-stress environment. J. Agron. Crop Sci. 194: 380-392.

Alexova, R. and Millar, A.H. (2013) Proteomics of phosphate use and deprivation in plants. Proteomics 13: 609-623.

Allen, A.M., Barker, G.L.A., Berry, S.T., Coghill, J.A., Gwilliam, R., Kirby, S., Robinson, P., Brenchley, R.C., D´Amore, R., McKenzie, N., Waite, D., Hall, A., Bevan, M., Hall, N. and Edwards (2011) Transcript-specific, single-nucleotide polymorphism discovery and linkage analysis in hexaploid bread wheat (Triticum aestivum L.). Plant Biol. J. 9: 1086-1099.

Altschul, S.F., Gish, W., Miller, W., Myers, E.W. and Lipman, D.J. (1990) Basic local alignment search tool. J. Mol. Biol. 215: 403-410.

Amtmann, A. and Armengaud, P. (2009) Effects of N, P, K and S on metabolism: new knowledge gained from multi-level analysis. Curr. Opin. Plant Biol. 12: 275-283.

Andersson, M.X., Stridh, M.H., Larsson, K.E., Liljenberg, C. and Sandelius, A.S. (2003) Phosphate-deficient oat replaces a major portion of the plasma membrane phospholipids with the galactolipid digalactosyldiacylglycerol. FEBS Letters 537: 128-132.

Aung, K., Lin, S.I., Wu, C.C., Huang, Y.T., Su, C.L. and Chiou, T.J. (2006) Pho2, a phosphate overaccumulator, is caused by a nonsense mutation in a microRNA399 target gene. Plant Physiol. 141: 1000-1011.

Aversano, R., Ercolano, M.R., Caruso, I., Fasano, C., Rosellini, D. and Carputo, D. (2012) Molecular tools for exploiting polyploidy genomes in plants. Int. J. Mol. Sci. 13: 10316-10335.

Aziz, T., Finnegan, P.M., Lambers, H. and Jost, R. (2014) Organ-specific phosphorus-allocation patterns and transcript profiles linked to phosphorus efficiency in two contrasting wheat genotypes. Plant Cell and Environ. 37: 943-960.

Bai, C., Liang, Y. and Hawkesford, M.J. (2013) Identification of QTLs associated with seedling root traits and their correlation with plant height in wheat. J. Exp. Bot. 64: 1745-1753.

Bagge, M, Xia, X. and Lübberstedt, T. (2007) Functional markers in wheat. Curr. Opin. Plant Biol. 10: 211-216.

Bahl, G.S. and Singh, N.T. (1986) Phosphorus diffusion in soils in relation to some edaphic factors and its influence on P uptake by maize and wheat. J. Agric. Sci. 107: 335-341.

Bai, L., Zhou, Y. and Song, C.P. (2009) Arabidopsis proline-rich extensin-like receptor kinase 4 modulates the early event toward abscisic acid response in root tip growth. Plant Signal. Behav. 4: 1075-1077.

Barber, S.A. (1984) Phosphorus. In: Soil Nutrient Bioavailability – A Mechanistic Approach. John Wiley & Sons, New York, USA, pp. 201-228.

Bari, R., Pant, B.D., Stitt, M. and Scheible, W.R. (2006) PHO2, microRNA399, and PHR1 define a phosphate-signaling pathway in plants. Plant Physiol. 141: 988-999.

Bates, T.R. and Lynch, J.P. (1996) Stimulation of root hair elongation in Arabidopsis thaliana by low phosphorus availability. Plant Cell Environ.19: 529-538.

Bates, T.R. and Lynch, J.P. (2001) Root hairs confer a competitive advantage under low phosphorus availability. Plant Soil 236: 243-250.

Batten, G.D. and Khan, M.A. (1987) Uptake and utilization of phosphorus and nitrogen by bread wheats grown under natural rainfall. Aust. J. Exp. Agr. 27: 405-410.

Batten, G.D. (1992) A review of phosphorus efficiency in wheat. Plant Soil 146: 163-168.

Bayle, V., Arrighi, J.F., Creff, A., Nespoulous, C., Vialaret, J., Rossignol, M., Gonzalez, E., Paz-Ares, J. and Nussaume, L. (2011) Arabidopsis thaliana high-affinity phosphate transporters exhibit multiple levels of posttranslational regulation. Plant Cell 23: 1523-1535.

Bieleski, R.L. (1968) Effect of phosphorus deficiency on levels of phosphorus compounds in Spirodela. Plant Physiol. 43: 1309-1316.

Bieleski, R.L. (1973) Phosphate pools, phosphate transport, and phosphate availability. Ann. Rev. Plant Physiol. 24: 225-252.

Biltz, D.F. and Mellon, M.G. (1948) Spectrophotometric determination of phosphorus as molydiphosphoric acid. Anal. Chem. 20: 749-751.

Bollons, H.M. and Barraclough, P.B. (1997) Inorganic orthophosphate for diagnosing the phosphorus status of wheat plants. J. Plant Nutr. 20: 641-655.

Bollons, H.M. and Barraclough, P.B. (1999) Assessing the phosphorus status of winter wheat crops: inorganic orthophosphate in whole shoots. J. Agric. Sci. 133: 285-295.

Bolstad, B.M., Irizarry, R.A., Astrand, M. and Speed, T.P. (2003). A comparison of normalization methods for high density oligonucleotide array data based on bias and variance. Bioinformatics 19: 185-193.

Brady, S.M., Song, S., Dhugga, K.S., Rafalski, J.A. and Benfey, P.N. (2007) Combining expression and comparative evolutionary analysis. The COBRA gene family. Plant Physiol. 143: 172-187.

Brazma, A., Hingamp, P., Quackenbush, J., Sherlock, G., Spellman, P., Stoeckert, C., Aach, J., Ansorge, W., Ball, C.A., Causton, H.C., Gaasterland, T., Glenisson, P., Holstege, F.C.P., Kim, I.F., Markowitz, V., Matese, J.C., Parkinson, H., Robinson, A., Sarkans, U., Schulze-Kremer, S., Stewart, J., Taylor, R., Vilo, J. and Vingron., M. (2001) Minimum information about a microarray experiment (MIAME)-towards standard for microarray data. Nature Genetics 29: 365-371.

Brenchley, R., Spannagl, M., Pfeifer, M., Barker, G.L.A., D'Amore, R., Allen, A.M., McKenzie, N., Kramer, M., Kerhornou, A., Bolser, D., Kay, S., Waite, D., Trick, M., Bancroft, I., Gu, Y., Huo, N., Luo, M.C., Sehgal, S., Gill, B., Kianian, S., Anderson, O., Kersey, P., Dvorak, J., McCombie, W.R., Hall, A., Mayer, K.F.X., Edwards, K.J., Bevan, M.W. and Hall, N. (2012) Analysis of the bread wheat genome using whole-genome shotgun sequencing. Nature 491: 705-710.

Bucher, M., Rausch, C. and Daram, P. (2001) Molecular and biochemical mechanisms of phosphate uptake into plants. J. Plant Nutr. Soil Sci. 164: 209-21.

Bustos, R., Castrillo, G., Linhares, F., Puga, M.I., Rubio, V., Pérez- Pérez, J., Solano, R., Leyva, A. and Paz-Ares, J. (2010) Central regulatory system largely controls transcriptional activation and repression responses to phosphate starvation in Arabidopsis. PLOS Genetics 6: e1001102. doi: 10.1371/journal.pgen.1001102

Byrne, S.L., Foito, A., Hedley, P.E., Morris, J.A., Stewart, D. and Barth, S. (2011) Early response mechanisms of perennial ryegrass (Lolium perenne) to phosphorus deficiency. Ann. Bot. 107: 243-254.

Chaignon, V. and Hinsinger, P. (2003) A biotest for evaluating copper bioavailability to plants in a contaminated soil. J. Environ. Qual. 32: 824-833.

Cai H., Xie, W.B., Lian and X.M. (2013) Comparative analysis of differentially expressed genes in rice under nitrogen and phosphorus starvation stress conditions. Plant Mol. Biol. Rep. 31: 160-173.

Calderón-Vázquez, C., Ilbarra-Laclette, E., Caballero-Perez, J. and Herrera-Estrella, L. (2008) Transcript profiling of Zea mays roots reveals responses to phosphate deficiency and the plant-species-specific level. J. Exp. Bot. 59: 2479-2497.

Calderón-Vázquez, C., Sawers, R.J.H. and Herrera-Estrella, L. (2011) Phosphate deprivation in maize: genetics and genomics. Plant Physiol. 156: 1067-1077.

Carpenter, S.R. (2008) Phosphorus control is critical to mitigating eutrophication. Proc. Nat. Acad. Sci. USA 105: 11039-11040.

Chen, J., Liu, Y., Ni, J., Wang, Y., Bai, Y., Shi, J., Gan, J., Wu, Z. and Wu, P. (2011) OsPhf1 regulates the plasma membrane localization of low- and high-affinity inorganic phosphate transporters and determines inorganic phosphate uptake and translocation in rice. Plant Physiol. 157: 269-278.

Chen, J.Y., Xu, L., Cai, Y.L. and Xu, J. (2009a) Identification of QTLs for phosphorus utilization in maize (Zea mays L.) across P levels. Euphytica 167: 245-252.

Chen, Y., Ma, W., Li, X.Y., Miao, W.Y., Zheng, L.L. and Cheng, B.J. (2012) Polyamines stimulate hyphal branching and infection in the early stage of Glomus etunicatum colonization. World J. Microbiol. Biotechnol. 28: 1615-1621.

Chen Y., Yang, X., He, K., Liu, M., Li, J., Gao, Z., Lin, Z., Zhang, Y., Wang, X., Qiu, X., Shen, Y., Zhang, L., Deng, X., Luo, J., Deng, X.-W., Chen, Z., Gu, H. and Qu, L.-J. (2006) The MYB transcription factor superfamily of Arabidopsis: expression analysis and phylogenetic comparison with the rice MYB family. Plant Mol. Biol. 60: 107-124.

Chen, Y.F., Li, L.Q., Xu, Q., Kong, Y.H., Wang, H. and Wu, W.H. (2009b) The WRKY6 transcription factor modulates PHOSPHATE1 expression in response to low Pi stress in Arabidopsis. Plant Cell 21: 3554-3566.

Chen, Z.H., Nimmo, G.A., Jenkins, G.I. and Nimmo, H.G. (2007) BHLH32 modulates several biochemical and morphological processes that respond to Pi starvation in Arabidopsis. Biochem. J. 405: 191-198.

Cheng, L., Bucciarelli, B., Liu, J., Zinn, K., Miller, S., Patton-Vogt, J., Allan, D., Shen, J. and Vance, C.P. (2011a) White lupin cluster root acclimation to phosphorus deficiency and root hair development involve unique glycerophosphodiester phosphodiesterases. Plant Physiol. 156: 1131-1148.

Cheng, Y. Zhou, W., El Sheery, N.I., Peters, C., Li, M., Wang, X. and Huang, J. (2011b) Characterization of the Arabidopsis glycerophosphodiester phosphodiesterase (GDPD) family reveals a role of the plastid-localized AtGDPD1 in maintaining cellular phosphate homeostasis under phosphate starvation. Plant J. 66: 781-795.

Chevalier, F. and Rossignol, M. (2011) Proteomic analysis of Arabidopsis thaliana ecotypes with contrasted root architecture in response to phosphate deficiency. J. Plant Physiol. 168: 1185-1890.

Chin, J.H., Lu, X., Haefele, S.M., Gamuyao, R., Ismail, A., Wissuwa, M. and Heuer, S. (2010) Development and application of gene-based markers for the major rice QTL phosphorus uptake 1. Theor. Appl. Genet. 120: 1073-1086.

Chiou, T.J., Aung, K., Lin, S.I., Wu, C.C., Chiang, S.F. and Sua, C.L. (2006) Regulation of phosphate homeostasis by microRNA in Arabidopsis. Plant Cell 18: 412-421.

Christophersen, H.M., Smith, F.A. and Smith, S.E. (2009) Arbuscular mycorrhizal colonization reduces arsenate uptake in barley via down-regulation of transporters in the direct epidermal phosphate uptake pathway. New Phytol. 184: 962-974.

Chiou, T.J. and Lin, S. (2011) Signaling network in sensing phosphate availability in plants. Annu. Rev. Plant Biol. 62: 185-206.

Chitwood, D.H. and Timmermans, M.C.P. (2007) Target mimics modulate miRNAs. Nat. Genet. 39: 935-936.

Cleland, R. and Karlsnes, A.M. (1967) A possible role of hydroxyproline-containing proteins in the cessation of cell elongation. Plant Physiol. 42: 669-671.

Collard, B.C.Y., Jahufer, M.Z.Z., Brouwer, J.B. and Pang, E.C.K. (2005) An introduction to markers, quantitative trait loci (QTL) mapping and marker-assisted selection for crop improvement: The basic concepts. Euphytica 142: 169-196.

Collard, B.C.Y. and Mackill, D.J. (2008) Marker-assisted selection: an approach for precision plant breeding in the twenty-first century. Phil. Trans. R. Soc. B 363: 557-572.

Coram, T.E., Brown-Guedira, G. and Chen, X. (2008) Using transcriptomics to understand the wheat genome. CAB Reviews: Perspectives in Agriculture, Veterinary Science, Nutrition and Natural Resources No. 083: 1-9.

Cordell, D., Drangert, J. and White, S. (2009) The story of phosphorus: global food security and food for thought. Global Environ. Change 12: 292-305.

Choulet, F., Wicker, T., Rustenholz, C., Paux, E., Salse, J., Leroy, P., Schlub, S., Paslier, M.C., Magdelenat, G., Gonthier, C., Couloux, A., Budak, H., Breen, J., Pumphrey, M., Liu, S., Kong, X., Jia, J., Gut, M., Brunel, D., Anderson, J.A., Gill, B.S., Appels, R., Keller, B. and Feuillet, C. (2010) Megabase level sequencing reveals contrasted organization and evolution patterns of the wheat gene and transposable element spaces. Plant Cell 22: 1686-1701.

Dai, X., Wang, Y., Yang, A. and Zhang, W. (2012) OsMYB2P-1, an R2R3 MYB transcription factor, is involved in the regulation of phosphate-starvation responses and root architecture in rice. Plant Physiol. 159: 169-183.

Daram, P., Brunner, S., Persson, B.L., Amrhein, N. and Bucher, M. (1998) Functional analysis and cell-specific expression of a phosphate transporter from tomato. Planta 206: 225-233.

Daram, P., Brunner, S., Rausch, C., Steiner, C. and Amrheim, N. (1999) Pht2;1 encodes a low-affinity phosphate transporter from Arabidopsis. Plant Cell 11: 2153-2166.

DaSilva, A.E. and Gabelman, W.H. (1992) Screening maize inbred lines for tolerance to low-P stress conditions. Plant Soil 146: 181-187.

Davies, T.G.E., Ying, J., Li, Z.S., Li, J. and Gordon-Weeks, R. (2002) Expression of analysis of putative high-affinity phosphate transporters in Chinese winter wheats. Plant Cell Environ. 25: 1325-1339.

Defra (2010) Principles of nutrient management and fertiliser use: phosphate, potash and magnesium for field crops. In: Fertilizer manual (RB209) 8th Edition, ISBN 9780112432869; www.defra.gov.uk

Delhaize, E. and Randall, P.J. (1995) Characterization of a phosphate-accumulator mutant of Arabidopsis-thaliana. Plant Physiol. 107: 207-213.

Delhaize, E., Hebb, D.M. and Ryan, P.R. (2001) Expression of a Pseudomonas aeruginosa citrate synthase gene in tobacco is not associated with either enhanced citrate accumulation or efflux. Plant Physiol. 125: 2059-2067.

Delhaize, E., Taylor, P., Hocking, P.J., Simpson, R.J., Ryan, P. R. and Richardson, A.E. (2009) Transgenic barley (Hordeum vulgare L.) expressing the wheat aluminium resistance gene (TaALMT1) shows enhanced phosphorus nutrition and grain production when grown on an acid soil. Plant Biotech. J. 7: 391-400.

DelPozo, J.C., Allona, I., Rubio, V., Layva, A., de la Pena, A., Aragoncillo, C. and Paz-Ares, J. (1999) A type 5 acid phosphatase gene from Arabidopsis is induced by phosphate starvation and by some other types of phosphate mobilization /oxidative stress conditions. Plant J. 19: 579-589.

De Sousa, S.M., Clark, R.T., Mendes, F.F., de Oliveira, A.C., de Vasconcelos, M.J.V., Parentoni, S.N., Kochian, L.V., Guimarães, C.T. and Magalhães, J.V. (2012) A role for root morphology and related candidate genes in P acquisition efficiency in maize. Funct. Plant Biol. 39: 925-935.

Devaiah, B.N., Karthikeyan, A.S. and Raghothama, K.G. (2007a) WRKY75 transcription factor is a modulator of phosphate acquisition and root development in Arabidopsis. Plant Physiol. 143: 1789-1801.

Devaiah, B.N., Nagarajan, V.K. and Raghothama, K.G. (2007b) Phosphate homeostasis and root development in Arabidopsis are synchronized by the zinc finger transcription factor ZAT6. Plant Physiol. 145: 147-159.

Devaiah, B.N., Madhuvanthi, R., Karthikeyan, A.S. and Raghothama, K.G. (2009) Phosphate starvation responses and gibberellic acid biosynthesis are regulated by the MYB62 transcription factor in Arabidopsis. Mol. Plant 2: 43-58.

Ding, G., Yang, M., Hu, Y., Liao, Y., Shi, L., Xu, F. and Meng, J. (2010) Quantitative trait loci affecting seed mineral concentrations in Brassica napus grown with contrasting phosphorus supplies. Ann. Bot. 105: 1221-1234.

Ding, G., Zhao, Z., Liao, Y., Hu, Y., Shi, L., Long, Y. and Xu, F. (2012) Quantitative trait loci for seed yield and yield-related traits, and their responses to reduced phoshorus supply in Brassica napus. Ann. Bot. 109: 747-759.

Dinkelacker, B., Römheld, V. and Marschner, H. (1989) Citric acid excretion and precipitation of calcium citrate in the rhizosphere of white lupin. Plant Cell Environ. 12: 285-292.

Doerner, P. (2008) Phosphate starvation signaling: a threesome controls systemic Pi homeostasis. Curr. Opin. Plant Biol. 11: 536-540.

Druka, A., Muehlbauer, G., Druka, I., Caldo, R., Baumann, U., Rostoks, N., Schreiber, A., Wise, R., Close, T. and Kleinhofs, A., Graner, A., Schulman, A., Landridge, F, Sato, K., Hayes, F., McNicol, J., Marshall, D. and Waugh, R. (2006). An atlas of gene expression from seed through barley development. Funct. Integr. Genomics 6: 202-2011.

Duan, K., Yi, K., Dang, L., Huang, H., Wu, W. and Wu, P. (2008) Characterization of a sub-family of Arabidopsis genes with the SPX domain reveals their diverse functions in plant tolerance to phosphorus starvation. Plant J. 54: 965-975.

Duff, S.M.G., Moorhead, G.B.G., Lefebre, D.D. and Plaxton, W.C. (1989) Phosphate starvation inducible `bypasses` of adenylate and phosphate dependet glycolytic enzymes in Brassica nigra suspension cells. Plant Physiol. 90: 1275-1278.

Duff, S.M.G., Sarath, G. and Plaxton, W.C. (1994) The role of acid-phosphatases in plant phosphorus-metabolism. Physiol. Plantarum 90: 791-800.

Egle, K., Manske, G., Römer, W. and Vlek, P.L.G. (1999) Improved phosphorus efficiency of three new wheat genotypes from CIMMYT in comparison with an older Mexican variety. J. Plant Nutr. Soil Sci. 162: 353-358.

El-Ghachtouli, N., Paynot, M., Matin-Tanguy, J., Dorandi, D. and Gianinazzi, S. (1996) Effect of polyamines and polyamines biosynthesis on spore germination and hyphal growth of Glomus mosseae. Mycol. Res. 100: 697-600.

eRA data (2010; 2011; 2012; 2013) http://www.era.rothamsted.ac.uk/ [online] electronic Rothamsted Archive.

Essigmann, B., Güler, S., Narang, R.A., Linke, D. and Benning, C. (1998) Phosphate availability affects the thylakoid lipid composition and the expression of SQD1, a gene required for sulfolipid biosynthesis in Arabidopsis thaliana. Proc. Natl. Acad. Sci. USA 95: 1950-1955.

FAOStat (2012) http://faostat.fao.org/site/291/default.aspx [online] (from September 2014: http://faostat3.fao.org/faostat-gateway/go/to/home/E [online]) Food and Agricultural Organization of the United Nations Statistical Database

Felsenstein, J. (1985). Confidence limits on phylogenies: An approach using the bootstrap. Evolution 39: 783-791.

Finck, A. (1991) Düngermenge nach Pflanzenanalyse. In: Düngung (Baumeister, W., ed.), Ulmer, Stuttgart, Germany, pp. 96-101.

Fitter, A.H. (2006) What is the link between carbon and phosphorus fluxes in arbuscular mycorrhizas? A null hypothesis for symbiotic function. New Phytol. 172: 3-6.

Food and Agriculture Organization of The United Nations: Current world fertilizer trends and outlook to 2015. Rome 2011

Franco-Zorrilla, J.M., Valli, A., Todesco, M., Mateos, I., Puga, I.M., Rubio-Somoza, I., Leyva, A., Weigel, D., Garcia, J.A. and Paz-Ares, J. (2007) Target mimicry provides a new mechanism for regulation of microRNA activity. Nat. Genet. 39: 1033-1037.

Fujii, H., Chiou, T.J., Lin, S.I., Aung, K. and Zhu, J.K. (2005) A miRNA involved in phosphate-starvation response in Arabidopsis. Curr. Biol. 15: 2038-2043.

Furihata, T., Suzuki, M. and Sakurai, H. (1992) Kinetic characterization of two phosphate uptake systems with different affinities in suspension-cultured Catharanthus roseus protoplasts. Plant Cell Physiol. 33: 1151-1157.

Gahoonia, T.S., Care, D. and Nielsen, N.E. (1996) Variation in acquisition of soil phosphorus among wheat and barley genotypes. Plant Soil 178: 223-230.

Gahoonia, T.S., Care, D. and Nielsen, N.E. (1997) Root hairs and phosphorus acquisition of wheat and barley cultivars. Plant Soil 1991: 181-188.

Gahoonia, T.S. and Nielsen, N.E. (1998) Direct evidence on participation of root hairs in phosphorus (^{32}P) uptake from soil. Plant Soil 198: 147-152.

Gahoonia, T.S., Nielsen, N.E. and Lyshede, O.B. (1999) Phosphorus (P) acquisition of cereal cultivars in the field at three levels of P fertilization. Plant Soil 211: 269-281.

Gahoonia, T.S., Nielsen, N.E., Joshi, P.A. and Jahoor, A. (2001) A root hairless barley mutant for elucidation genetic of root hairs and phosphorus uptake. Plant Soil 235: 211-219.

Gamuyao, R., Chin, J.H., Pariasca-Tanaka, J., Pesaresi, P., Catausan, S., Dalid, C., Slamet-Loedin, I., Tecson-Mendoza, E.M., Wissuwa, M. and Heuer, S. (2012) The protein kinase Pstol1 from traditional rice confers tolerance of phosphorus deficiency. Nature 488: 535-539.

Gao, C., Zhao, X., Liu X., Zhan L., Gu J., Li, X., Lu, W. and Xiao, K (2013) Function of wheat phosphate transporter gene TaPHT2;1 in Pi translocation and plant growth regulation under replete and limited Pi supply conditions. Planta 237: 1163-1178.

Gao, N., Su, Y., Mi, J., Shen, W. and Shi, W. (2010) Transgenic tomato overexpressing ath-miR399d has enhanced phosphorus accumulation through increased acid phosphatase and proton secretion as well as phosphate transporters. Plant Soil 334: 123-136.

Gaude, N., Tippmann, H., Flemetakis, E., Katinakis, P., Udvardi, M and Dörmann, P. (2004) The galactolipid digalactosyldiacylglycerol accumulates in the peribacteroid membrane of nitrogen-fixing nodules of soybean and lotus. J. Biol. Chem. 279: 34624-34630.

Gaude, N., Bortfeld, S., Duensing, N., Lohse, M. and Krajinski, F. (2012) Arbuscule-containing and non-colonized cortical cells of mycorrhizal roots undergo extensive and specific reprogramming during arbuscular mycorrhizal development. Plant J. 69: 510-528.

Gaxiola, R.A., Edwards, M. and Elser, J.J. (2001) A transgenic approach to enhance phosphorus use efficiency in crops as part of a comprehensive strategy for sustainable agriculture. Chemosphere 84: 840-845.

George, T.S., Richardson, A.E., Hadobas, P.A. and Simpson, R.J. (2004) Characterization of transgenic Trifolium subterraneum L. which expresses phyA and releases extracellular phytase: growth and P nutrition in laboratory media and soil. Plant Cell Environ. 27: 1351-1361.

George, T.S., Simpson, R.J., Hadobas, P.A. and Richardson, A.E. (2005) Expression of a fungal phytase gene in Nicotiana tabacum improves phosphorus nutrition of plants grown in amended soils. Plant Biotechnol J. 3: 129-140.

George, T.S. and Richardson, A.E. (2008) Potential and limitations to improving crops for enhanced phosphorus utilization. In: The Ecophysiology of Plant-Phosphorus Interactions, Vol. 7. (White, P.J. and Hammond. J.P., eds), Springer, Dordrecht, Netherlands, pp. 247-270.

George, T.S., Gregory, P.J., Hocking, P. and Richardson, A.E. (2008) Variation on root-associated phosphatase activities in wheat contributes to the utilization of organic P substrates in vitro, but does not explain differences in the P-nutrition of plants when grown in soils. Environ. Exp. Bot. 64: 2239-249.

Gerke, J., Römer, W. and Jungk, A. (1994) The excretion of citric and malic-acid by proteoid roots of Lupines albus L. - effects on soil solution concentrations of phosphate, iron, and aluminum in the proteoid rhizosphere in samples of an oxisol and a luvisol. Z. Pflanz. Bodenkunde 157: 289-294.

Glassop, D., Smith, S.E. and Smith, F.W. (2005) Cereal phosphate transporters associated with the mycorrhizal pathway of phosphate uptake in roots. Planta 222: 688-698.

Golstein, A.H., Baertlein, D.A. and Danon, A. (1989) Phosphate starvation stress as an experimental system for molecular analysis. Plant Mol. Biol. 7: 7-16.

Gomez-Roldan, V., Fermas, S., Brewer, P.B., Puech-Pagès, V., Dun, E.A., Pillot, J.P., Letisse, F., Matusova, R., Danoun, S., Portais, J.C., Bouwmeester, H., Bécard, G., Beveridge, C.A., Rameau, C. and Rochange, S.F. (2008) Strigolactone inhibition of shoot branching. Nature 455: 189-195.

González, E., Solano, R., Rubio, V., Leyva, A. and Paz-Ares, J. (2005) Phosphate transporter traffic facilitator1 is a plant-specific sec12-related protein that enables the endoplasmic reticulum exit of a high-affinity phosphate transporter in Arabidopsis. Plant Cell 17: 3500-3512.

Gregory, A.L., Hurley, B.A., Tran, H.T., Valentine, A.J., She, Y.M., Knowles, V.L. and Plaxton, W.C. (2009) In vivo regulatory phosphorylation of the phosphoenolpyruvate carboxylase AtPPC1 in phosphate-starved Arabidopsis thaliana. Biochem J. 420: 57-65.

Gregory, P.J. and George, T.S. (2011) Feeding nine billion: the challenge to sustainable crop production. J. Exp. Bot. 62: 5233-5239.

Greenwood, D.J., Karpinets, T.V. and Stone, D.A. (2001) A dynamic model for the effects of soil P and fertilizer P on crop growth, P uptake and soil P in arable cropping: model description. Ann. Bot. 88: 279-291.

Gu, M., Xu, K., Chen, A., Zhu, Y., Tang, G. and Xu, G. (2010) Expression analysis suggests potential roles of micro RNAs for phosphate and arbuscular mycorrhizal signaling in Solanum lycopersicum. Physiol. Plant 138: 226-237.

Guénin, S., Mauriat, M., Pelloux, J., Wuytswinkel, O.V., Bellini, C. and Gutierrez, L. (2009) Normalization of qRT-PCR data: the necessity of adopting a systematic, experimental condition-specific, validation of references. J.Exp. Bot. 60: 487-493.

Güimil, S., Chang, H.S., Zhu, T., Sesma, A., Osbourn, A., Roux, C., Ioannidis, V., Oakeley, E.J., Docquier, M., Descombes, P., Briggs, S.P. and Paszkowski, U. (2005) Comparative transcriptomics of rice reveals an ancient pattern of response to microbial colonization. Proc. Natl. Acad. Sci. USA 102: 8066-8070.

Gunes, A., Inal, A., Alpaslan, M. and Cakmak, I. (2006) Genotypic variation in phosphorus efficiency between wheat cultivars grown under greenhouse and field conditions. Soil Sci. Plant Nutr. 52: 470-478.

Guo, B., Jin, Y., Wussler, C., Blancaflor, E.B., Moter, C.M. and Versaw, W.K. (2008) Functional analysis of the Arabidopsis PHT4 family of intracellular phosphate transporters. New Phytol. 177: 889-898.

Guo, C., Zhao, X., Liu, X., Zhang, L., Gu, J., Li, X., Lu, W. and Xiao, K. (2013) Function of wheat phosphate transporter gene TaPHT2;1 in Pi translocation and plant growth regulation under replete and limited Pi supply conditions. Planta 237: 1163-1178.

Guo, W., Zhao, J., Li, X., Qin, L., Yan, X. and Hong Liao, H. (2011) A soybean β-expansin gene GmEXPB2 intrinsically involved in root system architecture responses to abiotic stresses. Plant J. 66: 541-552.

Gutjahr, C., Banba, M., Croset, V., An, K., Miyao, A., An, G., Hirochika, H., Imaizumi-Anraku, H. and Paszkowski, U. (2008) Arbuscular mycorrhiza–specific signaling in rice transcends the common symbiosis signaling pathway. Plant Cell 20: 2989-3005.

Hails, R. and Kinderlerer, J. (2003) The GM public debate: context and communication strategies. Nature Rev. Genet. 4: 819-825.

Han, Y.Y, Zhou, S., Chen, Y.H., Kong, X., Ying Xu, Y. and Wang, W. (2014) The involvement of expansins in responses to phosphorus availability in wheat, and its potentials in improving phosphorus efficiency of plants. Plant Physiol. Biochem. 78: 53-62.

Hamburger, D., Rezzonico, E., Petetot, J.M., Somerville, C. and Poirier, Y. (2002) Identification and characterization of the Arabidopsis Pho1 gene involved in phosphate loading to the xylem. Plant Cell 14: 889-920.

Hammond, J.P., Bennet, M.J., Bowen, H.C., Broadley, M.R., Eastwood, D.C., May, S.T., Rahn, C.R., Swarup, R., Woolaway, K.E. and White, P.J. (2003) Changes in gene expression in Arabidopsis shoots during phosphate starvation and the potential for developing smart plants. Plant Physiol. 132: 578-596.

Hammond, J.P., Broadley, M.R. and White, P.J. (2004) Genetic responses to phosphorus deficiency. Ann. Bot. 94: 323-332.

Hammond, J.P, Broadley, M.R., Craigon, D.J., Higgins, J., Emmerson, Z.F., Townsend, H.J., White, P.J. and May, S.T. (2005) Using genomic DNA-based probe-selection to improve the sensitivity of high-density oligonucleotide arrays when applied to heterologous species. Plant Methods 1: 10 doi:10.1186/1746-4811-1-10.

Hammond, J.P. and White, P.J. (2008) Sucrose transport in the phloem: integrating root responses to phosphorus starvation. J. Exp. Bot. 59: 93-109.

Hammond, J.P., Broadley, M.R., White, P.J., King, G.J., Bowen, H.C., Hayden, R., Meacham, M.C., Mead, A., Overs, T., Spracklen, W.P. and Greenwood, D.J. (2009) Shoot yield drives phosphorus use efficiency in Brassica oleracea and correlates with root architecture traits. J. Exp. Bot. 60: 1953-1968.

Hammond, J.P. and White, P.J. (2011a) Sugar signaling in root responses to low phosphorus availability. Plant Physiol. 156: 1033-1040.

Hammond, J.P., Broadley, M.R., Bowen, H.C., Spracklen, W.P., Hayden, R.M. and White, P.J. (2011b) Gene expression changes in phosphorus deficient potato (Solanum tuberosum L.) leaves and the potential for diagnostic gene expression markers. PLOS one 6: e24606. doi: 10.1371/journal.pone.0024606

Hammond, J.P. and White, P. J. (2012) Diagnosing phosphorus deficiency in crop plants. In: The Ecophysiology of Plant-phosphorus Interactions, Vol. 7. (White, P.J. and Hammond, J.P., eds). Springer Science+Business media B.V., Dordrecht, Netherlands, pp. 177-223.

Haran, S., Logendra, S., Saskar, M., Bratanova, M. and Raskin, I. (2000) Characterization of Arabidopsis acid phosphatase promoter and regulation of acid phosphatase expression. Plant Physiol. 124: 615-626.

Harrison, M.J., Dewbre, G.R. and Liu, J. (2002) A phosphate transporter from Medicago truncatula involved in the acquisition of phosphate released by arbuscular mycorrhizal fungi. Plant Cell 14: 2413-2429.

Hayes, J.E., Zhu, Y.G., Mimura, T. and Reid, R.J. (2004) An assessment of the usefulness of solution culture in screening for phosphorus efficiency in wheat. Plant Soil 261: 91-97.

Helal, H.M. (1990) Varietal differences in root phosphatases activity as related to the utilization of organic phosphates. Plant Soil 123: 161-163.

Hensel, L.L., Grbic, V., Baumgarten, D.A. and Bleecker, A.B. (1993) Developmental and age-related processes that influence the longevity and senescence of photosynthetic tissues in Arabidopsis. Plant Cell 5: 553-564.

Hermans, C., Hammond, J.P., White, P.J. and Verbruggen, N. (2006) How do plants respond to nutrient shortage by biomass allocation? Trend Plant Sci.11: 610-617.

HGCA (2014) http://www.hgca.com/varieties/hgca-recommended-lists.aspx [online] Recommended List for winter wheat and spring wheat varieties.

Higuchi, K., Suzuki, K., Nakanishi, H., Yamaguchi, H., Nishizawa, N. and Mori, S. (1999) Cloning of nicotianamine synthase genes, novel genes involved in the biosynthesis of phytosiderophores. Plant Physiol. 119: 471-479.

Himelblau, E. and Amasino, R.M. (2001) Nutrients mobilized from leaves of Arabidopsis thaliana during leaf senescence. J. Plant Physiol. 158: 1317-1323.

Hinsinger, P. (2001) Bioavailability of soil inorganic P in the rhizosphere as affected by root-induced chemical changes: a review. Plant Soil 237: 173-195.

Hochholdinger, F. and Zimmermann, R. (2008) Conserved and diverse mechanisms in root development. Curr. Opin. Plant Biol. 11: 70-74.

Hochholdinger, F., Wen, T.J., Zimmermann, R., Chimot-Marolle, P., Silva, O.D.E., Bruce, W., Lamkey, K.R., Wienand, U. and Schnable, P.S. (2008) The maize (Zea mays L.) roothairless3 gene encodes a putative GPI-anchored, monocot specific, COBRA-like protein that significantly affects grain yield. Plant J. 54: 888-898.

Holford, I.C.R. (1997) Soil phosphorus: its measurement, and its uptake by plants. Aust. J. Soil Res. 35: 227-239.

Hong, J.J., Park, Y.S., Bravo, A., Bhattarai, K.K., Daniels, D.A. and Harrison, M.J. (2012) Diversity of morphology and function in arbuscular mycorrhizal symbioses in Brachypodium distachyon. Planta 236: 851-865.

Hou, X.L., Wu, P., Jiao, F. C., Jia, Q. J., Chen, H. M., Yu, J., Song, X. W. and Yi, K.K. (2005) Regulation of the expression of OsIPS1 and OsIPS2 in rice via systemic and local Pi signalling and hormones. Plant Cell Environ. 28: 353-364.

Hsieh, L.C., Lin, S.I., Shih, A.C.C., Chen, J.W., Lin, W.Y., Tseng, C.Y., Li, W.H. and Chi, T.J. (2009) Uncovering small RNA-mediated responses to phosphate deficiency in Arabidopsis by deep sequencing. Plant Physiol. 151: 2120-2132.

Huang, C.Y., Roessner, U., Eickmeier, I., Gene, Y., Callahan, D.L., Sirley, N., Langridge, P. and Bacie A. (2008) Metabolite profiling reveals distinct changes in carbon and nitrogen metabolism in phosphate-deficient barley plants (Hordeum vulgare L.). Plant Cell Physiol. 49: 691-703.

Huang, C.Y., Shirley, N., Genc, Y., Shi, B. and Langridg, P. (2011) Phosphate utilization efficiency correlates with expression of low-affinity phosphate transporters and noncoding RNA, IPS1, in barley. Plant Physiol. 156: 1217-1229.

Huang, Y.F.,Lemieux, M.J., Song, J.M., Auer, M. and Wang, D.N. (2003) Structure and mechanism of the glycerol-3-phosphate transporter from Escherichia coli. Science 301: 616-620.

Huang, X. and Madan, A. (1999) CAP3: A DNA sequence assembly program. Genome Res. 9: 868-877.

Hürlimann, H.C., Pinson, B., Stadler-Waibel, M., Zeeman, S.C. and Freimoser, F.M. (2009) The SPX domain of the yeast low-affinity phosphate transporter Pho90 regulates transport activity. EMBO Rep. 10: 1003-1008.

Hussain, S.S., Ali, M., Ahmad, M. and Siddique, K.H.M. (2011) Polyamines: natural and engineered abiotic and biotic stress tolerance in plants. Biotechnol. Adv. 29: 300-311.

Irizarry, R.A., Bolstad, B.M., Collin, F., Cope, L.M., Hobbs, B. and Speed, T.P. (2003a) Summaries of Affymetrix GeneChip probe level data. Nucleic Acids Research 31: e15.

Irizarry, R.A., Hobbs, B., Collin, F., Beazer-Barclay, Y.D., Antonellis, K.J., Scherf, U. and Speed, T.P. (2003b) Exploration, normalization, and summaries of high density oligonucleotide array probe level data. Biostatistics 4: 249-264.

Irigoyen, S., Karlsson, P. M., Kuruvilla, J., Spetea, C. and Versaw W.K. (2011) The sink-specific plastidic phosphate transporter PHT4;2 influences starch accumulation and leaf size in Arabidopsis. Plant Physiol. 157: 1765-1777.

Ismail, A.M., Heuer, S.,Thomson, M.J. and Wissuwa M. (2007) Genetic and genomic approaches to develop rice germplasm for problem soils. Plant Mol. Biol. 65: 547-570.

Ito, M., Kodama, H., Komamine, A. and Watanabe, A. (1998) Expression of extensin genes is dependent on the stage of the cell cycle and cell proliferation in suspension-cultured Catharanthus roseus cells. Plant Mol. Biol. 36: 343-351.

IWGSC (2014) A chromosome-based draft sequence of the hexaploid bread wheat (Triticum aestivum) genome. Science 345: 1251788; 1-11.

Jain, A., Poling, M.D., Karthikeyan, A.S., Blakeslee, J.J., Peer, W.A., Titapiwatanakun, B., Murphy, A.S. and Raghothama, K.G. (2007) Differential effects of sucrose and auxin on localized phosphate deficiency-induced modulation of different traits of root system architecture in Arabidopsis. Plant Physiol. 144: 232-247.

Jakobsen, I., Abbott, L.K. and Robson, A.D. (1992) External hyphae of vesicular-arbuscular mycorrhizal fungi associated with Trifolium subterraneum L. 1. Spread of hyphae and phosphorus inflow into roots. New Phytol. 120: 371-380.

Jasinski, S.M. (2011) Phosphate rock. In: U. S. Geological Survey Minerals Yearbook-2010., pp. 56.1-56.10.

Jellito, T., Sonnewald, U., Willmitzer, L., Hajirezaei, M. and Stitt, M. (1992) Inorganic pyrophosphate content and metabolites in leaves and tubers of potato and tobacco plants expressing E. coli pyrophosphatase in their cytosol. Planta 188: 238-244.

Ji, X., Dong, B., Shiran, B., Talbot, M.J., Edlington, J. E., Hughes, T.,White, R.G., Gubler, F. and Dolferus, R. (2011) Control of abscisic acid catabolism and abscisic acid homeostasis is important for reproductive stage stress tolerance in cereals. Plant Physiol. 156: 647-662.

Jia, H., Ren, H., Gu, M., Zhao, J., Sun, S., Zhang, X., Chen,J., Wu, P. and Xu, G. (2011) The phosphate transporter gene OsPht1;8 is involved in phosphate homeostasis in rice. Plant Physiol. 156: 1164-1175.

Johnson, J.F., Vance, C.P. and Allan, D.L. (1996) Phosphorus deficiency in Lupinus albus. Plant Physiol. 112: 31-41.

Jones, G.P.D., Jessop, R.S. and Blair, G.J. (1992) Alternative methods for the selection of phosphorus efficiency in wheat. Field Crops Res. 30: 29-40.

Jordan-Meille, L., Rubæk, G. H. , Ehlert, P. A. I., Genot, V., Hofman, G., Goulding, K., Recknagel, J., Provolo, G. and Barraclough P. (2012) An overview of fertilizer-P recommendations in Europe: soil testing, calibration and fertilizer recommendations. Soil Use Manage. 28: 419-435.

Jungk, A. (2001) Root hairs and the acquisition of plant nutrients from soil. J. Plant Nutr. Soil Sci. 164: 121-129.

Juszczuk, I., Malusa, E. and Rychter, A. (2001). Oxidative stress during phosphate deficiency in roots of bean plants (Phaseolus vulgaris L.). J. Plant Physiol. 158: 1299-1305.

Kanda, H., Kasukabe, Y., Fujita, H., Washino, T. and Tachibana, S. (1994) Effect of low root temperature on ribonucleic-acid concentrations in figleaf gourd and cucumber roots differing in tolerance to chilling temperature. J. Jpn. Soc. Hortic. Sci. 63: 611-618.

Karthikeyan, A.S., Varadarajan, D.K., Jain, A., Held, M.A., Carpita, N.C. and Raghothama, K.G. (2007) Phosphate starvation responses are mediated by sugar signaling in Arabidopsis. Planta 225: 907-918.

Keyzer, M. (2010) Towards a closed phosphorus cycle. Economist-Netherlands 158: 411-425.

Kirkby, E.A. and Johnston, A.E.J. (2008) Soil and fertilizer phosphorus in relation to crop nutrition. In: The Ecophysiology of Plant-phosphorus Interactions, Vol. 7. (White, P.J. and Hammond, J.P., eds). Springer Science+Business media B.V., Dordrecht, Netherlands, pp. 177-223.

Koide, R.T. and Kabir, Z. (2000) Extraradical hyphae of the mycorrhizal fungus Glomus intraradices can hydrolyse organic phosphate. New Phytol. 148: 511-517.

Koyama, H., Kawamura, A., Kihara,T., Hara, T., Takita, E. and Shibata, D. (2000) Overexpression of mitochondrial citrate synthase in Arabidopsis thaliana improved growth on a phosphorus-limited soil. Plant Cell Physiol. 41: 1030-1037.

Krugman, T., Peleg, Z., Quansah, L., Chagué, V., Korol, A.B., Nevo, E., Saranga, Y., Fait, A., Chalhoub, B. and Fahima, T. (2011) Alteration in expression of hormone-related genes in wild emmer wheat roots associated with drought adaptation mechanisms. Funct. Integr. Genomics 11: 565-583.

Kwasniewski, M., Janiak, A., Mueller-Roeber, B. and Szarejko, I. (2010) Global analysis of the root hair morphogenesis transcriptome reveals new candidate genes involved in root hair formation in barley. J. Plant Physiol. 167: 1076-1083.

Kytoviita, M.M. and Sarajala, T. (1997) Effects of defoliation and symbiosis on polyamine levels in pine and birch. Mycorrhiza 7: 107-111.

Lagudah, E.S., Dubcovsky, J. and Powell, W. (2001) Wheat genomics. Plant Physiol. Biochem. 39: 335-344.

Lan, P., Li, W. and Schmidt, W. (2012) Complementary proteome and transcriptome profiling in phosphate-deficient Arabidopsis roots reveals multiple levels of gene regulation. Mol. Cell. Proteomics 11: 1156-1166.

Larkin, M.A., Blackshields, G., Brown, N.P., Chenna, R., McGettigan, P.A., McWilliam, H., Valentin, F., Wallace, I.M., Wilm, A., Lopez, R., Thompson, J.D., Gibson, T.J. and Higgins, D.G. (2007) Clustal W and Clustal X version 2.0. Bioinformatics 23, 2947-2948.

Lauer, M.J., Blevins, D.G. and Sierzputowska-Gracz, H. (1989) ^{31}P-Nuclear magnetic resonance determination of phosphate compartmentationin leaves of reproductive soybeans (Glycine max L.) as affected by phosphate nutrition. Plant Physiol. 89: 1331-1336.

Leader, D.J. (2005) Transcriptional analysis and functional genomics in wheat. J. Cereal Sci. 41: 149-163.

Lee, R.B. (1988) Phosphate influx and extracellular phosphatase activity in barley roots and rose cells. New Phytol. 109: 141-148.

Lefebvre, D.D., Duff, S.M.G., Fife, C.A., Inalsingh, J.C. and Plaxton, W.C. (1990) Response to phosphate deprivation in Brassica nigra suspension cells. Plant Physiol. 93: 504-511.

Lei, M., Liu, Y., Zhang, B., Zhao, Y., Wang, X., Zhou, Y., Raghothama, K.G. and Liu, D. (2011) Genetic and genomic evidence that sucrose is a global regulator of plant responses to phosphate starvation in Arabidopsis. Plant Physiol. 156: 1116-1130.

Leigh, R. A. and Johnston, A. E. (1986) An investigation of the usefulness of phosphorus concentrations in tissue water as indicators of the phosphorus status of field-grown spring barley. J. Agric. Sci. Camb. 107: 329-333.

Li, K., Xu, C., Li, Z., Zhang, K., Yang, A. and Zhang, J. (2008a) Comparative proteome analyses of phosphorus responses in maize (Zea mays L.) roots of wild-type and a low-P-tolerant mutant reveal root characteristics associated with phosphorus efficiency. Plant J. 55: 927-939.

Li, L., Liu, C. and Lian, X. (2010) Gene expression profiles in rice roots under low phosphorus stress. Plant Mol. Biol. 72: 423-432.

Li, Y., Tong, Y., Bin, L., Zhao, H., Zhang, X. and Li, Z. (2008b) Expression of TaIPS Genes in wheat seedlings with nitrogen and phosphorous starvation. Acta Bot. Boreal Occident. Sin. 27: 1303-1307.

Liao, M., Hocking, P.J., Dong, B., Delhaize, E., Richardson, A.E. and Ryan, P.R. (2008) Variation in early phosphorus-uptake efficiency among wheat genotypes grown on two contrasting Australian soils. Aust. J. Agric. Res. 59: 157-166.

Liang, Q., Cheng, X., Mei, M., Yan, X. and Liao, H. (2010) QTL analysis of root traits as related to phosphorus efficiency in soybean. Ann. Bot. 106: 223-234.

Liang, C., Tian, J. and Liao, H. (2013) Proteomics dissection of plant responses to mineral nutrition deficiency. Proteomics, 13: 624-636.

Lin, W.Y., Lin, S.I. and Chiou, T.J. (2009) Molecular regulators of phosphate homeostasis in plants. J. Exp. Bot. 60: 1427-1438.

Lima, R.L.S., Severino, L.S, Sampaio, L.R., Safiatti, V., Gomes, J.A. and Beltrão, N.E.M. (2011) Blends of castor meal and castor husks for optimized use as organic fertilizer. Ind. Crops and Prod. 33: 364-368.

Liu, C., Muchhal, U.S., Uthappa, M., Kononowicz, A.K., Raghotama, K.G. (1998) Tomato phosphate transporter genes are differentially regulated in plant tissues by phosphorus. Plant Physiol. 116: 91-99.

Liu, F., Wang, Z., Ren, H., Shen, C., Li, Y., Ling, H.Q., Wu, C., Lian, X. and Wu, P. (2010) OsSPX1 suppresses the function of OsPHR2 in the regulation of expression of OsPT2 and phosphate homeostasis in shoots of rice. Plant J. 62: 508-517.

Liu, F., Chang, X.-J., Ye, Y., Xie, W.-B., Wu, P. and Lian, X.-M. (2011) Comprehensive sequence and whole-life-cycle expression profile analysis of the phosphate transporter gene family in rice. Mol. Plant 4: 1105-1122.

Liu, T.Y., Huang, T.K., Tseng, C.Y., Lai, Y.S., Lin, S.I., Lin, W.Y., Chen, J.W. amd Chiou, T.J. (2012) PHO2-dependent degradation of PHO1 modulates phosphate homeostasis in Arabidopsis. Plant Cell 24: 2168-2183.

Lloyd, J.C. and Zakhleniuk, O.V. (2004) Responses of primary and secondary metabolism to sugar accumulation revealed by microarray expression analysis of the Arabidopsis mutant, Pho3. J. Exp. Bot. 55: 1221-1230.

Long, X.-Y., Wang, J.R., Ouellet, T., Rocheleau, H., Wei, Y.-M, Pu, Z.-E., Jiang, Q.-T., Lan, X.J. and Zheng, Y.L. (2010) Genome-wide identification and evaluation of novel internal control genes for q-PCR based transcript normalization in wheat. Plant Mol. Biol. 74:307–311.

Lopez, C.G., Banowetz, G.M., Peterson, C.J. and Kronstad, W.E. (2003) Dehydrin expression and drought tolerance in seven wheat cultivars. Crop. Sci. 43: 577-582.

López-Bucio, J., de la Vega, O.M., Guevara-García, A. and Herrera-Estrella, L. (2000) Enhanced phosphorus uptake in transgenic tobacco plants that overproduce citrate. Nat. Biotechnol. 18: 450-453.

Lott, J.N.A., Bojarski, M., Kolasa, J., Batten, G.D. and Campbell, L.C. (2009) A review of the phosphorus content of dry cereal and legume crops of the world. Int. J. Agric. Resources Govern. Ecol. 8: 351-370.

Lu, C., Hawkesford, M.J., Barraclough, P.B., Poulton, P.R., Wilson, I.D., Barker, G.L., and Edwards, K.J. (2005) Markedly different gene expression in wheat grown with organic or inorganic fertilizer. Proc. R. Soc. B. 272: 1901-1908.

Luan, S. (2003) Protein phosphatases in plants. Annu. Rev. Plant Biol. 54: 63-92.

Lundmark, M., Kørner, C.J. and Nielsen, T.H. (2010) Global analysis of microRNA in Arabidopsis in response to phosphate starvation as studied by locked nucleic acid-based microarrays. Physiol. Plant. 140: 57-68.

Lynch, J. and Brown, K.M. (2001) Topsoil foraging - an architectural adaptation of plants to low phosphorus availability. Plant Soil 237: 225-237.

Lynch, J. (1995) Root architecture and plant productivity. Plant Physiol. 109: 7-13.

Lynch, J.P. and Ho, M.D. (2005) Rhizoeconomics: Carbon costs of phosphorus acquisition. Plant Soil 269: 45-56.

Lysøe, E., Seong, K.Y. and Kistler, H.C. (2011) The transcriptome of Fusarium graminearum during the infection of wheat. Mol. Plant Microb. Inf.. 24: 995-1000.

Maathuis, F.J.M. and Amtmann, A. (2005) Transcriptional profiling of membrane transporters. In: Plant Nutritional Genomics. Blackwell-Publishing, Oxford, UK, pp. 170-200.

MacDonald, G.K., Bennet, E.M., Potter, P.A. and Ramakutty, N. (2011) Agronomic phosphorus imbalances across the word`s croplands. Proc. Natl. Acad. Sci. USA 108: 3086-3091.

MacKintosh, C., Coggins, J. and Cohen, P. (1991) Plant protein phosphatases-subcellular distribution, detection of protein phosphatase 2C and identification of protein phosphatase 2A as the major quinate dehydrogenase phosphatase. Biochem. J. 273: 733-738.

Manschadi, A.M., Kaul, H.P., Vollmann, J., Eitzinger, J. and Wenzel W. (2014) Developing phosphorus-efficient crop varieties - an interdisciplinary research framework. Field Crops Res. 162: 87-98.

Manske, G.G.B., Ortiz-Monasterio, J.I., van Ginkel, M., González, R.M., Fischer, R.A., Rajaram, S and Vlek, P.L.G. (2001) Importance of P uptake efficiency versus P utilization for wheat yield in acid and calcareous soils in Mexico. Eur. J. Agron. 14: 261-274.

Marschner, P. (2012) Phosphorus. In: Marschner`s Mineral Nutrition of Higher Plant, 3rd Edition (Marschner, P., ed.), Academic Press, Elsevier Ltd., London, U.K.

May, A., Berger, S., Hertel, T. and Köck, M. (2011) The Arabidopsis thaliana phosphate starvation responsive gene AtPPsPase1 encodes a novel type of inorganic pyrophosphatase. Biochem. Biophys. Acta 1810: 178-185.

Mengel K and Kirkby EA. (2001) Principles of plant nutrition. 5th edn. Dordrecht: Kluwer Academic Publishers, 849 pp.

McBeath, T. M., McLaughlin, M. J. , Kirby, J. K. and Armstrong, R. D. (2012) The effect of soil water status on fertiliser, topsoil and subsoil phosphorus utilisation by wheat. Plant Soil 358: 337-348.

McDowell, R.W. (2012) Minimising phosphorus losses from the soil matrix. Curr. Opin. Biotech. 23: 860-865.

Miao, J., Sun, J., Liu, D., Li, B., Zhang, A. and Li, Z. (2009) Characterization of the promoter of phosphate transporter TaPHT1.2 differentially expressed in wheat varieties. J. Genet. Genomics 36: 455-466.

Michael, B., Zink, F. and Lantzsch, H.J. (1980) Effect of phosphate application of phytin-P and other phosphate fractions in developing wheat grains. Z. Planzenernähr. Bodenk. 143: 369-376.

Miller, S.S., Liu, J., Allan, D.L., Menzhuber, C.J., Fedorova, M. and Vance, C.P. (2001) Molecular control of acid phosphatase secretion into the rhizosphere of proteoid roots from phosphorus-stressed white lupin. Plant Physiol. 127: 594-606.

Mimura, T., Sakano, K. and Shimmen, T. (1996) Studies on the distribution, re-translocation and homeostasis of inorganic phosphate in barley leaves. Plant Cell Environ. 19: 311-320.

Mimura, T. (2001) Physiological control of phosphate uptake and phosphate homeostasis in plant cells. Aust. J. Plant Physiol. 28: 653-658.

Mitsukawa, N., Okumura, S., Shirano, Y., Sato, S., Kato, T., Harashima, S. and Shibata, D. (1997) Overexpression of an Arabidopsis thaliana high-affinity phosphate transporter gene in tobacco cultured cells enhances cell growth under phosphate-limited conditions. Pro. Natl. Acad. Sci. USA 94: 7098-7102.

Misson, J., Raghothama, K.G., Jain, A., Jouhet, J., Block, M.A., Bligny, R., Ortet, P., Creff, A., Somerville, S., Rolland, N., Doumas, P., Nacry, P., Herrerra-Estrella, L., Nussaume, L. and Thibaud, M.C. (2005) A genome-wide transcriptional analysis using Arabidopsis thaliana Affymetrix gene chips determined plant responses to phosphate deprivation. Proc. Nat. Acad. Sci. USA 102: 11934-11939.

Miura, K., Rus, A., Sharkhuu, A., Yokoi, S., Karthikeyan, A.S., Raghothama, K.G., Baek, D., Koo, Y.D., Jin, J.B., Bressan, R.A., Yun, D.J. and Hasegawa, P.M. (2005) The Arabidopsis SUMO E3 ligase SIZ1 controls phosphate deficiency responses. Proc. Natl. Acad. Sci. USA 102: 7760-7765.

Miura, M., Lee, J., Gong, Q., Ma, S., Jin, J.B., Yoo, C.Y., Miura, T., Sato, A., Bohnert, H.J. and Hasegawa, P.M. (2011) SIZ1 regulation of phosphate starvation-induced root architecture remodeling involves the control of auxin accumulation. Plant Physiol. 155: 1000-1012.

Mollier, A. and Pellerin, S. (1999) Maize root system growth and development as influenced by phosphorus deficiency. J. Exp. Bot. 50: 487-497.

Mollier, A., De Willigen, P., Heinen, M., Morel, C., Schneider, A. and Pellerin, S. (2008) A two-dimensional simulation model of phosphorus uptake including crop growth and P-response. Ecological Modelling 210: 453-464.

Morcuende, R., Bari, R., Gibon, Y., Zhen, W., Pant, B.D., Bläsing, O., Usadel, B., Czechowski, T., Udvardi, M.K., Stitt, M. and Scheible, W.-R. (2007) Genome-wide reprogramming of metabolism and regulatory networks of Arabidopsis in response to phosphorus. Plant Cell. Environ. 30: 85-112.

Muchhal, U.S., Pardo, J.M. and Raghothama, K.G. (1996) Phosphate transporters from the higher plant Arabidopsis thaliana. Proc. Natl. Acad. Sci. USA 93: 10519-10523.

Muchhal, U.S. and Raghothama, K.G. (1999) Transcriptional regulation of plant phosphate transporters. Proc. Natl. Acad. Sci. USA 96: 5868-5872.

Mudge, S.R., Rae, A.L., Diatloff, E. and Smith, F.W. (2002) Expression analysis suggests novel roles for members of the Pht1 family of phosphate transporters in Arabidopsis. Plant J. 31: 341-353.

Müller, R., Nilsson, L., Krintel, C. and Nielsen, T.H. (2004) Gene expression during recovery from phosphate starvation in roots and shoots of Arabidopsis thaliana. Physiol. Plant. 122: 233-243.

Müller, R., Nilsson, L., Nielsen, L.K. and Nielsen, T.H. (2005) Interaction between phosphate starvation signalling and hexokinase-independent sugar sensing in Arabidopsis leaves. Physiol. Plant. 124: 81-90.

Müller, R., Morant, M., Jarmer, H., Nilsson, L. and Nielsen, T.H. (2007) Genome-wide analysis of the Arabidopsis leaf transcriptome reveals interaction of phosphate and sugar metabolism. Plant Physiol. 143: 156-171.

Nagarajan, V.K., Jain, A., Poling, M. D., Lewis, A. J., Raghothama, K. G. and Smith, A.P. (2011) Arabidopsis Pht1;5 mobilizes phosphate between source and sink organs and influences the interaction between phosphate homeostasis and ethylene signalling. Plant Physiol. 156: 1149-1163.

Nagy, R., Vasconcelos, M.J.V., Zhao, S., McElver, J., Bruce, W., Amrhein, N., Raghothama, K.G. and Bucher, M. (2006) Differential regulation of five Pht1 phosphate transporters from maize (Zea mays L.). Plant Biol. 8: 186-197.

Nakamura, Y. (2013) Phosphate starvation and membrane lipid remodelling in seed plants. Prog. Lipid Res. 52: 43-50.

Nei, M. and Kumar, S. (2000). Molecular evolution and phylogenetics. New York: Oxford University Press.

Neumann, G. and Römheld, V. (1999) Root excretion of carboxylic acids and protons in phosphorus-deficient plants. Plant Soil 211: 121-130.

Neumann, G. and Martinoia, E. (2002) Cluster roots – an underground adaptation for survival in extreme environments. Trends Plant Sci. 7: 162-167.

Neyroud, J.A. and Lischer, P. (2003) Do different methods used to estimate soil phosphorus availability across Europe give comparable results. J. Plant Nutr. Soil Sci. 166: 422-431.

Ni, J.J., Wu, P., Senadhira, D. and Huang, N. (1998) Mapping QTLs for phosphorus deficiency tolerance in rice (Oryza sativa L.) Theor. Appl. Genet. 97: 1361-1369.

Nicholas, K.B. and Nicholas, H.B (1997) GenDoc: a tool for editing and annotating multiple sequence alignments. Distributed by the author.

Nielsen, T.H., Krapp, A., Röper-Schwarz, U. and Stitt, M. (1998) The sugar-mediated regulation of genes encoding the small subunit of Rubisco and the regulatory subunit of ADP glucose pyrophosphorylase is modified by phosphate and nitrogen. Plant Cell Environ. 12: 443-454.

Nilsson, L., Müller, R. and Nielsen, T.H. (2007) Increased expression of the MYB-related transcription factor, PHR1, leads to enhanced phosphate uptake in Arabidopsis thaliana. Plant Cell Environ. 30: 1499-1512.

Nilsson, L., Müller, R. and Nielsen, T.H. (2010) Dissecting the plant trascriptome and the regulatory response to tomato deprivation. Physiol. Plant. 139: 129-143.

Nilsson, L., Lundmark, M., Jensen, P.E. and Nielsen, T.H. (2012) The Arabidopsis transcription factor PHR1 is essential for adaptation to high light and retaining functional photosynthesis during phosphate starvation. Physiol. Plant. 144: 35-47.

Niu, Y.F., Chai, R.S., Jin, G.L., Wang, H., Tang, C.X. and Zhang, Y.S. (2012) Responses of root architecture development to low phosphorus availability: a review. Ann. Bot. 112: 391-408.

Norton, R. (2012) Nutrient management for wheat in a variable climate. Better Crops with plant food 96 (3): 16-17.

Oeschger, M.P. and Silva, C.E. (2007) Genetically modified organisms in the United States: Implementation, concerns, and public perception. In: Green Gene Technology: Research in an area of social conflict. (Fiechter, A. and Sautter, C., eds.), Springer, pp. 57-68.

Olsen, R. A., Cole, C. V., Watanabe, F. S. and Dean, L.A. (1954) Estimation of available phosphorus in soils by extraction with sodium bicarbonate. USDA Circ. 939. U.S. Gov. Print. Office, Washington DC.

Oono, Y., Kawahara, Y., Kanamori, H., Mizuno, H., Yamagata, H., Yamamoto, M., Hosokawa, S., Ikawa, H., Akahane, I., Zhu, Z., Wu, J., Itoh, T. and Matsumoto, T. (2011) mRNA-seq reveals a comprehensive transcriptome profile of rice under phosphate stress. Rice 4: 50-65.

Oono, Y., Kobayashi, F., Kawahara, Y., Yazawa, T., Handa, H., Itoh, T. and Matsumoto, T. (2013) Characterisation of the wheat (Triticum aestivum L.) transcriptome by de novo assembly for the discovery of phosphate starvation-responsive genes: gene expression in Pi-stressed wheat. BMC Genomics 14: 77. doi:10.1186/1471-2164-14-77.

Osborne, L.D. and Rengel, Z. (2002) Screening cereals for genotypic variation in efficiency of phosphorus uptake and utilisation. Aust. J. Agric. Res. 53: 295-303.

Ozturk, L., Eker, S., Torun, B. and Cakmak, I. (2005) Variation in phosphorus efficiency among 73 bread and durum wheat genotypes grown in a phosphorus-deficient calcareous soil. Plant Soil 269: 69-80.

Palma, D.A., Blumwald, E. and Plaxton W.C. (2000) Upregulation of vacuolar H^+-translocating pyrophosphatase by phosphate starvation of Brassica napus (rapeseed) suspension cell cultures. FEBS Letters 486 155-158.

Panara, F., Pasqualini, S. and Antonielli, M. (1990) Multiple isoforms of barley root acid phosphatase: purification and some characteristics of the major cytoplasmic isozyme. Biochem. Biophys. Acta 1037: 351-357.

Pao, S.S., Paulsen, I.T. and Saier, M.H. (1998) Major facilitator superfamily. Microbiol. Mol. Biol. Rev. 63: 1-134.

Pariasca-Tanaka, J., Satoh, K., Rose, T., Mauleon, R. and Wissuwa, M. (2009) Stress response versus stress tolerance: a transcriptome analysis of two rice lines contrasting in tolerance to phosphorus deficiency. Rice 2: 167-185.

Paszkowski, U., Kroken, S., Roux, C. and Briggs, S.P. (2002) Rice phosphate transporters include an evolutionarily divergent gene specifically activated in arbuscular mycorrhizal symbiosis. Proc. Natl. Acad. Sci. USA 99: 13324-13329.

Peleg, Z., Cakmak, I., Ozturk, L., Yazici, A., Jun, Y., Budak, H., Korol, A.B., Fahim, T.A. and Saranga, Y. (2009) Quantitative trait loci conferring grain mineral nutrient concentrations in durum wheat x wild emmer wheat RIL population. Theor. Appl. Genet. 119: 353-369.

Peng, J., Richards, D.E., Hartley, N.M., Murphy, G.P., Devos, K.M., Flintham, J.E., Beales, J., Fish, L.J., Worland, A.J., Pelica, F., Sudhakar, D., Christou, P., Snape, J.W., Gale, M.D. and Harberd, N.P. (1999)`Green revolution' genes encode mutant gibberellin response modulators. Nature 400: 256-261.

Pérez-Torres, C.A., López-Bucio, J., Cruz-Ramírez, A., Ibarra-Laclette, E., Dharmasiri, S., Estelle, M. and Herrera-Estrella, L. (2008) Phosphate availability alters lateral root development in Arabidopsis by modulating auxin sensitivity via a mechanism involving the TIR1 auxin receptor. Plant Cell 20: 3258-3272.

Phillips, S. and Norton, R. (2012) Global wheat production and fertilizer use. Better Crops with plant food 96 (3): 4-6.

Plaxton, W. and Tran, H.T. (2011) Metabolic adaptation of phosphate-starved plants. Plant Physiol. 156: 1006-1015.

Plaxton, W.C. and Carswell, M.C. (1999) Metabolic aspects of the phosphate starvation response in plants. In: Plant responses to environmental stresses: from phytohormones to genome reorganization (Books in Soils, Plants, and the Environment) (Lerner, H.R., ed.), CRC Press, pp. 349-372.

Poirier, Y., Thoma, S., Somerville, C. and Schiefelbein, J. (1991) A mutant of Arabidopsis deficient in xylem loading of phosphate. Plant Physiol. 97: 1087-1093.

Poole, R., Barker, G., Wilson, I.D., Coghill, J.A. and Edwards, K.J. (2007) Measuring global gene expression in polyploidy; a cautionary note from allohexaploid wheat. Funct. Integr. Genomics 7: 207-219.

Preuss, C., Huang, C.Y., Gilliham, M. and Tyerman, S.D. (2010) Channel-like characteristics of the low-affinity barley phosphate transporter Pht1;6 when expressed in xenopus oocytes. Plant Physiol. 152: 1431-1441.

Qin, L., Guo, Y., Chen, L., Liang, R., Gu, M., Xu, G., Zhao, J., Walk, T. and Liao, H. (2012). Functional characterization of 14 Pht1 family genes in yeast and their expression in response to nutrient starvation in soybean. PLOS One 7: e47726. doi: 10.1371/journal.pone.0047726.

Raboy, V. (2009) Approaches and challenges to engineering seed phytate and total phosphorus. Plant Sci. 177: 281-296.

Rae, A.L., Cybinski, D.H., Jarmey, J.M. and Smith, F.W. (2003) Characterization of two phosphate transporters from barley; evidence for diverse function and kinetic properties among members of the Pht1 family. Plant Mol. Biol. 53: 27-36.

Rae, A.L., Jarmey, J.M., Mudge, S.R. and Smith, F.W. (2004) Over-expression of a high-affinity transporter in transgenic barley plants does not enhance phosphate uptake rates. Funct. Plant Biol. 31: 141-148.

Raghothama, K.G. (1999) Phosphate acquisition. Annu. Rev. Plant Physiol. Plant Mol. Biol. 50: 665-693.

Raghothama, K.G. (2005) Phosphorus. In: Plant Nutritional Genomics (Broadley, M.R., White, P.J., eds.), Blackwell Publishing Ltd., Oxford, UK, pp. 112-126.

Ramaiah, M., Jain, A., Baldwin, J.C., Karthikeyan, A.S. and Raghothama K.G. (2011) Characterization of the phosphate starvation-induced glycerol-3-phosphate permease gene family in Arabidopsis. Plant Physiol. 157: 279-291.

Ramakers, C., Ruijter, J.M., Deprez, R.H. L. and Moorman, A.F.M (2003) Assumption-free analysis of quantitative real-time polymerase chain reaction (PCR) data. Neurosci. Lett. 339: 62-66.

Rampino, P., Pataleo, S., Gerardi, C., Mita, G. and Perrotta, C. (2006) Drought stress response in wheat: physiological and molecular analysis of resistant and sensitive genotypes. Plant Cell Environ. 29: 2143-2151.

Rashotte, A. M., DeLong, A. and Muday, G.K. (2001) Genetic and chemical reductions in protein phosphatase activity alter auxin transport, gravity response, and lateral root growth. Plant Cell 13: 1683-1697.

Rausch, C. and Bucher, M. (2002) Molecular mechanisms of phosphate transport in plants. Planta 216: 23-37.

Raven, J.A. (2008) Phosphorus and the future. In: The Ecophysiology of Plant-Phosphorus Interactions, Vol. 7. (White, P.J. and Hammond, J.P., eds.), Springer, Dordrecht, Netherlands, pp. 271-283.

Raven, J.A. (2012) Protein turnover and plant RNA and phosphorus requirements in relation to nitrogen fixation. Plant Sci. 188: 25-35.

Rebafka, F.P., Bationo, A. and Marschner, H. (1993) Phosphorus seed coating increases phosphorus uptake, early growth and yield of pearl-millet (Pennisetum glaucum (L.) R. Br.) grown on an acid sandy soil in Niger, West-Africa. Fertilizer Res. 35: 151-160.

Reddy, S.K., Weng,Y., Rudd, J.C., Akhunova, A. and Liu, S. (2013) Transcriptomics of induced defense responses to greenbug aphid feeding in near isogenic wheat lines. Plant Sci. 212: 26-36.

Ren, F., Guo, Q.Q., Chang, L.L., Chen, L., Zhao, C.Z., Zhong, H. and Li, X.B. (2012a) Brassica napus PHR1 gene encoding a myb-like protein functions in response to phosphate starvation. Plos One 7: e44005.doi: 10.1371/journal.pone.0044005

Ren, Y., He, X., Liu, D., Li, J., Zhao, X., Li, B., Tong, Y., Zhang, A. and Li, Z. (2012b) Major quantitative trait loci for seminal root morphology of wheat seedlings. Mol. Breeding 30: 139-148.

Reuzeau, C., Fankard, V., Hatzfeld, Y., Sanz, A., Van Camp, W., Lejeune, P., De Wilde, C., Lievens, K., De Wolf, J., Vranken, E., Peerbolte, R. and Broekaert, W. (2006) Traitmill™: a functional genomics platform for the phenotypic analysis of cereals. Plant Genetic Resources 4: 20-24.

Reymond, M., Svistoonof, F.S., Loudet, O., Nussaume, L. and Desnos, T. (2006) Identification of QTL controlling root growth response to phosphate starvation in Arabidopsis thaliana. Plant Cell Environ. 29: 115-125.

Richardson, A.E. (1994) Soil Microorganisms and phosphorus availability. In: Soil biota: management in sustainable farming systems (Pankhurst CE, Doube BM, Gupta VVS, Grace PR, eds.), CSIRO Australia, Melbourne, Australia, pp. 50-62.

Richardson, A.E., Hadobas, P.A. and Hayes, J.E. (2000) Acid phosphomonoesterase and phytase activities of wheat (Triticum aeativum L.) roots and utilization of organic phosphorus substrates by seedings grown in sterile culture. Plant Cell Environ. 23: 397-405.

Robinson, W.D., Park, J., Tran, H.T., Del Vecchio, H.A., Ying, S., Zins, J.L., Patel, K., McKnight, T.D. and Plaxton, W.C. (2012) The secreted purple acid phosphatase isozymes AtPAP12 and AtPAP26 play a pivotal role in extracellular phosphate-scavenging by Arabidopsis thaliana. J. Exp. Bot., 63: 6531-6542.

Römer, R. and Schilling, G. (1986) Phosphorus requirements of the wheat plant in various stages of its life cycle. Plant Soil 91: 221-229.

Rose, T.J., Rengel, Z., Ma, Q. and Bowden, J.W. (2007) Differential accumulation patterns of phosphorus and potassium by canola cultivars compared to wheat. J. Plant Nutr. Soil Sci. 170: 404-411.

Rose, T.J., Rose, M.T., Pariasca-Tanaka, J., Heuer, S. and Wissuwa, M. (2011) The frustration with utilization: why have improvements in internal phosphorus utilization efficiency in crops remained so elusive? Front Plant Sci. 2: 7. doi: 10.3389/fpls.2011.00073.

Rose, T.J. and Wissuwa, M. (2012) Rethinking internal phosphorus utilization efficiency: A new approach is needed to improve PUE in grain crops. In: Advances in Agronomy (Sparks, D.L., ed.), Elsevier, London, UK, pp. 185-218.

Rouached, H., Arpat, A.B. and Poirier, Y. (2010) Regulation of phosphate starvation responses in plants: signaling players and cross-talks. Mol. Plant 3: 288-299.

Rouached, H. (2011) Multilevel coordination of phosphate and sulfate homeostasis in plants. Plant Signal. Behav. 6: 952-955.

Rothamsted Research (2006) Guide to the Classical and other Long-term Experiments, Datasets and Sample Archive, Lawes Agricultural Trust Co. Ltd, ISBN 0951445693.

Rubio, V., Linhares, F., Solano, R., Martín, A.C., Iglesias, J., Leyva, A. and Paz-Ares, J. (2001) A conserved MYB transcription factor involved in phosphate starvation signaling both in vascular plants and in unicellular algae. Gene Dev. 15: 2122-2133.

Saitou, N. and Nei, M. (1987) The neighbor-joining method: A new method for reconstructing phylogenetic trees. Mol. Biol. Evol. 4: 406-425.

Sanchez, C.A. (2007) Phosphorus. In: Handbook of Plant Nutrition (Barker, A.V. E. and Pilbeam, D.J., eds.), Taylor & Francis Group, pp.51-90.

Sánchez-Calderón, L., López-Bucio, J., Chacón-López, A., Cruz-Ramírez, A., Nieto-Jacobo, F., Dubrovsky, J.G. and Herrera-Estrella, L. (2005) Phosphate starvation induces a determinate developmental program in the roots of Arabidopsis thaliana. Plant Cell Physiol. 46: 174-184.

Sánchez-Calderón, L., López-Bucio, J., Chacón-López, A., Gutiérrez-Ortega, A., Hernández-Abreu, E. and Herrera-Estrella, L. (2006) Characterization of low phosphorus insensitive mutants reveals a crosstalk between low phosphorus-induced determinate root development and the activation of genes involved in the adaptation of Arabidopsis to phosphorus deficiency. Plant Pysiol. 140: 879-889.

Santner, S., Zhang, H., Leitner, D., Schnepf, A., Prohaska, T., Puschenreiter, M. and Wenzel, W.W. (2012) High-resolution chemical imaging of labile phosphorus in the rhizosphere of Brassica napus L. cultivars. Environ. Exper. Bot. 77: 219-226.

Sattelmacher, B., Horst, W.J. and Becker, H.C. (1994) Factors that contribute to genetic variation for nutrient efficiency of crop plants. Z. Pflanzen. Bodenk. 157: 215-24.

Schachtman, D.P., Reid, R.J. and Ayling, S.M. (1998) Phosphorus uptake by plants: from soil to cell. Plant Physiol. 116: 447-453.

Schachtman, D.P. and Shin, R. (2007) Nutrient sensing and signaling: NPKS. Annu. Rev. Plant Biol. 58: 47-69.

Schlüter, U., Mascher, M., Colmsee, C., Scholz, U., Bräutigam, A., Fahnenstich, H. and Sonnewald, U. (2012) Maize source leaf adaptation to nitrogen deficiency affects not only nitrogen and carbon metabolism but also control of phosphate homeostasis. Plant Physiol. 160: 1384-1406.

Schlüter, U., Colmsee, C., Scholz, U., Bräutigam, A., Weber, A.PM., Zellerhoff, N., Bucher, M., Fahnenstich, H. and Sonnewald, U. (2013) Adaptation of maize source leaf metabolism to stress related disturbances in carbon, nitrogen and phosphorus balance. BMC Genomics 14: 442. doi: 10.1186/1471-2164-14-442.

Schröder, J.J., Smit, A.L., Cordell, D. and Rosemarin, A. (2011) Improved phosphorus use efficiency in agriculture: A key requirement for its sustainable use. Chemosphere 84: 822-831.

Schünmann, P.H.D., Richardson, A.E., Smith, F.W. and Delhaize, E. (2004) Characterization of promoter expression patterns derived from the Pht1 phosphate transporter genes of barley (Hordeum vulgare L.). J. Exp. Bot. 55: 855-865.

Secco, D., Baumann, A. and Poirier, Y. (2010) Characterization of the rice PHO1 gene family reveals a key role for OSPHO1;2 in phosphate homeostasis and the evolution of a distinct clade in dicotyledons. Plant Physiol. 152: 1693-1704.

Secco, D., Wang, C., Arpat, B.A., Wang, Z., Poirier, Y., Tyerman, S.D., Wu, P., Shou, H. and Whelan, J. (2012) The emerging importance of the SPX domain-containing proteins in phosphate homeostasis. New Phytol. 193: 842-851.

Seo, P.J., Xiang, F., Qiao, M., Park, J.Y., Lee, Y.N., Kim, S.G., Lee, Y.H., Park, W.J. and Park, C.M. (2009) The MYB96-transcription factor mediates abscisic acid signaling during drought stress in Arabidopsis. Plant Physiol. 151: 275-289.

Shane, M.W. and Lambers, H. (2005) Cluster roots: A curiosity in context. Plant Soil 274: 101-125.

Shewry, P. (2009) Wheat. J.Exp. Bot. 60: 1537-1553.

Shewry, P.R., Mitchell, R.A.C., Tosi, P., Wan, Y., Underwood, C., Lovegrove, A., Freeman, J., Toole, G.A., Mills, E.N. and Ward, J.L. (2012) An integrated study of grain development of wheat (cv. Hereward). J. Cereal Sci. 56: 21-30.

Shi, T., Li, R., Zhao, Z., Ding, G., Long, Y., Meng, J., Xu, F. and Shi, L. (2013) QTL for yield traits and their association with functional genes in response to phosphorus deficiency in Brassica napus. PLOS One 8: e54559. doi: 10.1371/journal.pone.0054559

Shi, J., Hu, H., Zhang, K., Zhang, W., Yu, Y., Wu, Z. and Wu, P. (2014) The paralogous SPX3 and SPX5 genes redundantly modulate Pi homeostasis in rice. J. Exp. Bot. 65: 859-870.

Shih, C.Y. and Kao, C.H. (1996) Growth inhibiton in suspension-cultured rice cells under phosphate deprivation is mediated through putrescin accumulation. Plant Physiol. 111: 721-724.

Shin, H., Shin, H.S., Chen, R. and Harrison, M.J. (2006) Loss of At4 function impacts Phosphate distribution between the roots and the shoots during phosphate starvation. Plant J. 45: 712-726.

Sisaphaithong, T., Kondo, D., Matsunaga, H., Kobae, Y. and Hata, S (2012) Expression of plant genes for arbuscular mycorrhiza-inducible phosphate transporters and fungal vesicle formation in sorghum, barley, and wheat roots. Biosci. Biotechnol. Biochem. 76: 2364-2367.

Smith, S.E. and Smith F.A. (2012) Fresh perspectives on the roles of arbuscular mycorrhizal fungi in plant nutrition and growth. Mycologia 104: 1-13.

Smith, F.W., Cybinski, D.H. and Rae, A.L. (1999) Regulation of expression of genes encoding phosphate transporters in barley roots. In: Plant Nutrition-Molecular Biology and Genetics (Gissel-Nielsen, G., Jensen, A., eds.), Kluwer Academic Publisher, Dordrecht, Netherlands, pp. 145-150.

Solaiman, Z., Marschner, P., Wang, D. and Rengel, Z. (2007) Growth, P uptake and rhizosphere properties of wheat and canola genotypes in an alkaline soil with low P availability. Biol. Fertil. Soils 44: 143-153.

Sonnewald, U. (1992) Expression of E. coli inorganic pyrophosphatase in transgenic plants alters photoassimilate partitioning. Plant J. 2: 571-581.

Stangoulis, J.C.R., Huynh, B.L., Welch, R.M., Choi, E.Y. and Graham, R.D. (2007) Quantitative trait loci for phytate in rice grain and their relationship with grain micronutrient content. Euphytica 154: 289-294.

Stefanovic, A., Ribot, C., Rouached, H., Wang, Y., Chong, J., Belbahri, L., Delessert, S. and Poirier, Y. (2007) Members of the PHO1 gene family show limited functional redundancy in phosphate transfer to the shoot, and are regulated by phosphate deficiency via distinct pathways. Plant J. 50: 982-994.

Stitt, M. (1998) Pyrophosphate as an energy donor in the cytosol of plant cells: an enigmatic alternative to ATP. Bot. Acta 111: 167-175.

Strong, W.M., Best, E.K. and Cooper, J.E. (1997) Phosphate fertilizer residues in wheat-growing soils of the western downs, Queensland. Aust. J. Soil Res. 35: 341-354.

Su, J., Xiao, Y., Li, M., Liu, Q., Li, B.,Tong, Y., Jia, J. and Li, Z. (2006) Mapping QTLs for phosphorus-deficiency tolerance at wheat seedling stage. Plant Soil 281: 25-36.

Su, J., Zheng, Q., Li, H.W., Li, B., Jing, R.L., Tong, Y.P. and Li, Z.S. (2009) Detection of QTLs for phosphorus use efficiency in relation to agronomic performance of wheat grown under phosphorus sufficient and limited conditions. Plant Sci. 176: 824-836.

Sun, S., Gu, M., Cao, Y., Huang, X., Zhang, X., Ai, P., Zhao, J., Fan, X. and Xu, G. (2012) A constitutive expressed phosphate transporter, OsPht1;1, modulates phosphate uptake and translocation in phosphate-replete rice. Plant Physiol. 159: 1571–1581.

Suzuki, Y., Kihara-Doi, T., Kawazu, T., Miyake, C. and Makino, A. (2010) Differences in rubisco content and its synthesis in leaves at different positions in Eucalyptus globulus seedlings. Plant Cell Environ. 33: 1314-1323.

Svistoonoff, S., Creff, A., Reymond, M., Sigoillot-Claude, C., Ricaud, L., Blanchet, A., Nussaume, L. and Desnos, T. (2007) Root tip contact with low-phosphate media reprograms plant root architecture. Nat. Genet. 39: 792-796.

Syers, J.K., Johnston, A.E. and Curtin, D. (2008) Efficiency of soil and fertilizer phosphorus use – Reconciling changing concepts of soil phosphorus behaviour with agronomic information. FAO Fertilizer and Plant Nutrition Bulletin 18, pp. 27-44.

Tamura, K., Peterson, D., Peterson, N., Stecher, G., Nei, M. and Kumar, S. (2011) MEGA5: Molecular Evolutionary Genetics Analysis using Maximum Likelihood, Evolutionary Distance, and Maximum Parsimony Methods. Mol. Biol. Evol. 28: 2731-2739.

Tarafdar, J.C. and Marschner, H. (1994) Phosphatase activity in the rhizosphere and hydrosphere of a mycorrhizal wheat supplied with inorganic and organic phosphorus. Soil Biol. Biochem. 26: 387-395.

Tenea, G.N., Raposo, F.C. and Maquet, A. (2012) Comparative transcriptome profiling in winter wheat grown under different agricultural practices. J. Agric. Food Chem. 60: 10970-10978.

Teng, W., Deng, Y., Chen, Y.P., Xu, X.F., Chen, R.Y., Lv, Y., Zhao, Y.Y., Zhao, X.Q., He, X., Li, B., Tong, Y.P., Zhang, F.S. and Li, Z.S. (2013) Characterization of root response to phosphorus supply from morphology to gene analysis in field-grown wheat. J. Exp. Bot. 64: 1403-1411.

Tesfaye, M., Temple, S.J., Allan, D.L., Vance, C.P. and Samac D.A. (2001) Overexpression of malate dehydrogenase in transgenic alfalfa enhances organic acid synthesis and confers tolerance to aluminium. Plant Physiol. 127: 1836-1844.

Tesfaye, M., Liu, J., Allan, D.L. and Vance C.P. (2007) Genomic and genetic control of phosphate stress in legumes. Plant Physiol. 144: 594-603.

Theodorou, M.E. and Plaxton, W.C. (1993) Metabolic adaptations of plant respiration to nutritional phosphate deprivation. Plant Physiol. 101: 339-344.

Thonar, C., Erb, A. and Jansa, J. (2012) Real-time PCR to quantify composition of arbuscular mycorrhizal fungal communities-marker design, verification, calibration and field validation. Mol. Ecol. Res. 12: 219-232.

Tian, J., Wang, C., Zhang, Q., He, X., Whelan, J. and Shou, H. (2012) Overexpression of OsPAP10a, a root-associated acid phosphatase, increased extracellular organic phosphorus utilization in rice. J. Integr. Plant Biol. 54: 631-639.

Tiessen, H. (2008) Phosphorus in a global environment. In: The Ecophysiology of Plant-Phosphorus Interactions, Vol. 7. (White, P.J. and Hammond, J.P., eds.). Springer, Dordrecht, Netherlands, pp. 1-7.

Ticconi, C.A., Delatorre, C.A., Lahner, B., Salt, D.E. and Abel, S. (2004) Arabidopsis pdr2 reveals a phosphate-sensitive checkpoint in root development. Plant J. 37: 801-814.

Tittarelli, A., Milla, L., Vargas, F., Morales, A., Neupert, C., Meisel, L.A., Salvo-G, H., Peñaloza, E., Muñoz, G., Corcuera, L.J. and Silva, H. (2007) Isolation and comparative analysis of the wheat TaPT2 promoter: identification in silico of new putative regulatory motifs conserved between monocots and dicots. J. Exp. Bot. 58: 2573-2582.

Torabi, S., Wissuwa, M., Heidari, M., Naghavi, M.-R., Gilany, K., Mohammad-Reza Hajirezaei, M.-R., Omidi, M., Yazdi-Samadi, B., Ismail, A.M.and Salekdeh, G.H.(2009) A comparative proteome approach to decipher the mechanism of rice adaptation to phosphorous deficiency. Proteomics 9: 159-170.

Trachsel, S., Kaeppler, S.M., Brown, K.M. and Lynch, J.P. (2011) Shovelomics: high throughput phenotyping of maize (Zea mays L.) root architecture in the field. Plant Soil 341: 75-87.

Tran, H.T., Hurley, B.A. and Plaxton, W.C. (2010) Feeding hungry plants: The role of purple acid phosphatases in phosphate nutrition. Plant Sci.179: 14-27.

Tuomi, J.M., Voorbraak, F., Jones, D.L. and Ruijter, J.M. (2010) Bias in the Cq value observed with hydrolysis probe based quantitative PCR can be corrected with the estimated PCR efficiency value. Methods 50: 313-322.

Udvardi, M., Czechowski, T. and Scheible, W.R. (2008). Eleven golden rules of quantitative RT-PCR. Plant Cell 20: 1736-1737.

Uhde-Stone, C., Zinn, K.E., Ramirez-Yanez, M., Li, A. and Vance, C.P. (2003) Nylon filter arrays reveal differential gene expression in proteoid roots of white lupin in response to phosphorus deficiency. Plant Physiol. 131: 1064-1079.

Ullrich-Eberius, C.I., Novacky, A., Fischer, E. and Lüttge, U. (1981) Relationship between energy-dependent phosphate uptake and the electrical membrane potential in Lemna gibba G1. Plant Physiol. 67: 797-801.

Umehara, M., Hanada, A., Magome, H., Takeda-Kamiya, N. and Yamaguchi, S. (2010) Contribution of strigolactones to the inhibition of tiller bud outgrowth under phosphate deficiency in rice. Plant Cell Physiol. 51: 1118-1126.

Van Mooy, B.A.S., Fredricks, H.F., Pedler, B.E., Dyhrman, S.T., Karl, D.M., Koblizek, M., Lomas, M.W., Mincer, T.J., Moore, L.R., Moutin, T., Rappe, M.S. and Webb, E.A. (2009) Phytoplankton in the ocean use non-phosphorus lipids in response to phosphorus scarcity. Nature 458: 69-72.

Vaccari, D.A. (2009) Phosphorus: A looming crisis. Scientific American. 300: 42-47.

Van Mooy, B.A.S., Rocap, G., Fredricks, H.F., Evans, C.T. and Devol, A.H. (2006) Sulfolipids dramatically decrease phosphorus demand by picocyanobacteria in oligotrophic marine environments. P. Natl. Acad. Sci. USA 103: 8607-8612.

Vance, C.P., Uhde-Stone, C. and Allan, D.L. (2003) Phosphorus acquisition and use: critical adaptations by plants for securing a non-renewable resource. New Phytol. 157: 423-447.

Velasquez, S.M., Iusem, N.D. and Estevez, M.J. (2011) Root hair sweet growth. Plant Signal. Behav. 6: 1600-1602.

Veneklaas, E.J., Lambers, H., Bragg, J., Finnegan, P.M., Lovelock, C.E., Plaxton, W.C., Price, C.A., Scheible, W.R., Shane, M.W., White, P.J. and Raven, J.A. (2012) Opportunities for improving phosphorus-use efficiency in crop plants. New Phytol. 195: 306-320.

Versaw, W.K. and Harrison, M.J. (2002) A chloroplast phosphate transporter PHT2;1 influences allocation of phosphate within the plant and phosphate-starvation responses. Plant Cell 14: 1751-1766.

Vreugdenhil, D, Aarts, M.G.M. and Koornneef, M. (2005) Exploring natural genetic variation to improve plant nutrient content. In: Plant Nutritional Genomics. Blackwell-Publishing, Oxford, UK, pp. 170-200.

Waines, J.G. and Ehdaie, B. (2007) Domestication and crop physiology: roots of green-gevolution wheat. Ann. Bot. 100: 991-998.

Walinga, I., van Vark, W., Houba, V. J. G. and van Lee, L.L. (1989) Plant analysis procedures, Part 7. Department of Soil Science and Plant Nutrition, Wageningen Agricultural University Syllabus: 138-141.

Walters, D.R. (2000) Polyamines in plant-microbe interactions. Plant Mol. Plant Pathol. 57: 137-146.

Wan, Y., Poole, R.L., Huttly, A.K., Toscano-Underwood, C., Feeney, K., Welham, S.,Gooding, M.J., Mills, C., Edwards, K.J., Shewry, P.R. and Mitchell, R.A.C. (2008) Transcriptome analysis of grain development in hexaploid wheat. BMC Genomics 9: 121. doi: 10.1186/1471-2164-9-121.

Wang, C., Ying, S., Huang, H., Li, K., Wu, P. and Shou, H. (2009a) Involvement of OsSPX1 in phosphate homeostasis in rice. Plant J. 57: 895-904.

Wang, J., Sun, J., Miao, J., Guo, J., Shi, Z., He, M., Chen, Y., Zhao, X., Li, B., Han, F.P., Tong, Y. and Li, Z. (2013) A wheat phosphate starvation response regulator Ta-PHR1 is involved in phosphate signalling and increases grain yield in wheat. Ann. Bot. 6: 1139-1153.doi:10.1093/aob/mct080.

Wang, L., Chen, F., Zhang, F. and Mi, G. (2010) Two strategies for achieving higher yield under phosphorus deficiency in winter wheat grown in field conditions. Field Crops Res. 118: 36-42.

Wang, L., Li, Z., Qian, W., Guo, W. Gao, X., Huang, L., Wang, H., Zhu, H.,Wu, J.W., Wang, D. and Liu, D. (2011) The Arabidopsis purple acid phosphatase AtPAP10 is predominantly associated with the root surface and plays an important role in plant tolerance to phosphate limitation. Plant Physiol. 157: 1283-1299.

Wang, X., Yi, K., Tao, Y., Wang, F., Wu, Z., Jiang, D., Chen, X., Zhu, L. and Wu, P. (2006) Cytokinin represses phosphate-starvation response through increasing of intracellular phosphate level. Plant Cell Environ. 29: 1924-1935.

Wang, X., Shen, J. and Liao, H. (2010) Acquisition or utilization, which is more critical for enhancing phosphorus efficiency in modern crops? Plant Sci. 179: 302-306.

Wang, J., Sun, J., Miao, J., Guo, J., Shi, Z., He, S., Chen, Y., Zhao, X., Li, B., Han, F., Tong, Y. and Li, Z. (2013a) A wheat phosphate starvation response regulator Ta-PHR1 is involved in phosphate signalling and increases grain yield in wheat. Ann. Bot. 6: 1139-53 doi: 10.1093/aob/mct080.

Wang, X., Liu, Y., Chen, L., Zhao, D., Wang, X. and Zhang, Z. (2013b) Wheat resistome in response to barley yellow dwarf virus infection. Funct. Integr. Genomics 13: 155-165.

Wang, Y., Ribot, C., Rezzonico, E., Poirier, Y. (2004) Structure and expression profile of the Arabidopsis PHO1 gene family indicates a broad role in inorganic phosphate homeostasis. Plant Physiol. 135: 400-411.

Wang, Y.H., Garvin, D.F. and Kochian, L.V. (2002) Rapid induction of regulatory and transporter genes in response to phosphorus, potassium, and iron deficiencies in tomato roots. Evidence for cross talk and root/rhizosphere-mediated signals. Plant Physiol. 130: 1361-1370.

Wang, Z., Hu, H., Huang, H., Duan, K.,Wu, Z. and Wu, P. (2009b) Regulation of OsSPX1 and OsSPX3 on expression of OsSPX domain genes and Pi-starvation signaling in rice. J. Integr. Plant Biol. 51: 663-674.

Wasaki, J., Yonetani, R., Kuroda, S., Shinano, T., Yazaki, J., Fujii, F., Shimbo, K., Yamamoto, K., Sakata, K., Sasaki, T., Kishimtot, N., Kikuchi, S., Yamagishi, M.Y. and Osaki, M. (2003) Transcriptomic analysis of metabolic changes by phosphorus stress in rice roots. Plant Cell Environ. 26: 1515-1523.

Watts, C.W., Clark, L.J., Poulton, P.R., Powlson, D.S. and Whitmore, A.P. (2006) The role of clay, organic carbon and long-term management on mouldboard plough draught measured on the Broadbalk wheat experiment at Rothamsted. Soil Use Manage. 22: 334-341.

Weiner, H., Stitt, M. and Heldt, H.W. (1987) Subcellular compartmentation of pyrophosphate and alkaline pyrophosphatase in leaves. Biochim. Biophys. Acta 893: 13-21.

White P.J. and Veneklaas, E.J. (2012) Nature and nurture: the importance of seed phosphorus content. Plant Soil 357: 1-8.

White, P.J., Broadley, M.R. and Gregory, P.J. (2012) Managing the nutrition of plants and people. Appl. Envir. Soil Sci. 2012: Article ID 104826.

Williamson, L.C., Ribrioux, S.P.C.P., Fitter, A.H. and Leyser, H.M.O. (2001) Phosphate availability regulates root system architecture in Arabidopsis. Plant Physiol. 126: 875-882.

Wingen, L.U., Orford, S., Goram, R., Leverington-Waite, M., Bilham, L., Patsiou, T.S., Ambrose, M., Dicks, J. and Griffiths, S. (2014) Establishing the A.E. Watkins landrace cultivar collection as a resource for systematic gene discovery in bread wheat. Theor. Appl. Genet. 127: 1831-1842.

Wissuwa, M., Yano, M. and Ae, N. (1998) Mapping of QTLs for phosphorus-deficiency tolerance in rice (Oryza sativa L.). Theor. Appl. Genet. 97: 777-783.

Wissuwa, M. and Ae, N. (2001) Further characterization of two QTLs that increase phosphorus uptake of rice (Oryza sativa L.) under phosphorus deficiency. Plant Soil 237: 275-286.

Wissuwa, M., Wegner, J., Ae, N. and Yano, M. (2002) Substitution mapping of Pup1: a major QTL increasing phosphorus uptake of rice from a phosphorus-deficient soil. Theor. Appl. Genet. 105: 890-897.

Wissuwa, M., Gamat, G. and Ismail, A.M. (2005) Is root growth under phosphorus deficiency affected by source or sink limitations? J. Exp. Bot. 56: 1943-1950.

Wissuwa, M., Mazzola, M. and Picard, C. (2009) Novel approaches in plant breeding for rhizosphere-related traits. Plant Soil 321: 409-430.

Woo, J., MacPherson, C.R., Liu, J., Wang, H., Kiba, T., Hannah, M.A., Wang, X.J., Bajic, V.B. and Chua, N.H. (2012) The response and recovery of the Arabidopsis thaliana transcriptome to phosphate starvation. BMC Plant Biol. 12: 62. doi: 10.1186/1471-2229-12-62.

Wu, P., Ma, L.G., Hou, X.L., Wang, M.Y., Wu, Y.R., Liu, F.Y. and Deng, X.W. (2003) Phosphate starvation triggers distinct alterations of genome expression in Arabidopsis roots and leaves. Plant Pysiol. 132: 1260-1271.

Wu, P. and Wang, X.M. (2008) Role of OsPHR2 on phosphorus homeostasis and root hairs development in rice (Oryza sativa L.). Plant Signal Behav. 3: 674-675.

Xue, G.P., Drenth, J., Glassop, D., Kooiker, M. and McIntyre, C.L. (2013) Dissecting the molecular basis of the contribution of source strength to high fructan accumulation in wheat. Plant Mol. Biol. 81: 71-92.

Yang, M., Ding, G., Shi, L., Feng, J., Xu, F. and Meng, J. (2010) Quantitative trait loci for root morphology in response to low phosphorus stress in Brassica napus. Theor. Appl. Genet. 121: 181-193.

Yang, M., Ding, G., Shi, L., Xu, F. and Meng, J. (2011) Detection of QTL for phosphorus efficiency at vegetative stage in Brassica napus. Plant Soil 339: 97-111.

Yang, S.Y., Grønlund, M., Jakobsen, I., Suter-Grotemeyer, M., Rentsch, D., Miyao, A., Hirochika, H., Kumar, C.S., Sundaresan, V., Salamin, N., Catausan, S., Mattes, N., Heuer, S. and Paszkowski, U. (2012) Nonredundant regulation of rice arbuscular mycorrhizal symbiosis by two members of the phosphate transporter 1 gene family. Plant Cell 24: 4236-4251.

Yang, Y.S. and Paszkowski, U. (2011) Phosphate import at the arbuscule: just a nutrient? Mol. Plant Microb. Inf. 24: 1296-1299.

Yao, Y., Sun, H., Xu, F., Zhang, X. and Liu, S. (2011) Comparative proteome analysis of metabolic changes by low phosphorus stress in two Brassica napus genotypes. Planta 233: 523-537.

Yao, Z.F., Liang, C.Y., Zhang, Q., Chen, Z.J., Xiao, B.X., Tian, J. and Liao, H. (2014) SPX1 is an important component in the phosphorus signalling network of common bean regulating root growth and phosphorus homeostasis. J. Exp. Bot. 65: 3299-3310.

Yi, K., Wu, Z., Zhou, J., Du, L., Guo, L., Wu, Y. and Wu, P. (2005) OsPTF1, a novel transcription factor involved in tolerance to phosphate starvation in rice. Plant Physiol. 138: 2087-2096.

Yu, Y., Guo, G., Lv, D., Hu, Y., Li, J., Li, X. and Yan, Y. (2014) Transcriptome analysis during seed germination of elite Chinese bread wheat cultivar Jimai 20. BMC Plant Biol. 14: 20. doi: 10.1186/1471-2229-14-20.

Yu, Z., Kang, B., He, X., Lv, S., Bai, Y., Ding, W., Chen, M., Cho, H. and Wu, P. (2011) Root hair-specific expansins modulate root hair elongation in rice. Plant J. 66: 725-734.

Zadoks, J.C., Chang, T.T. and Konzak, C.F. (1974) A decimal code for the growth stage of cereals. Weed Research 14: 415-421.

Zakhleniuk, O.V., Raines, C.A. and Lloyd, J.C. (2001) Pho3: a phosphorus-deficient mutant of Arabidopsis thaliana (L.) Heynh. Planta 212: 529-534.

Zeng, H.Q., Zhu, Y.Y., Huang, S.Q. and Yang, Z.M. (2010) Analysis of phosphorus-deficient responsive miRNAs and cis-elements from soybean (Glycine max L.). J. Plant Physiol. 167: 1289-1297.

Zhang, H. and Forde, B.G. (2000) Regulation of Arabidopsis root development by nitrate availability. J. Exp. Bot. 51: 51-59.

Zhang, K., Greenwood, D.J., White P.J. and Burns, I.G. (2007) A dynamic model for the combined effects of N, P and K fertilizers on yield and mineral composition; description and experimental test. Plant Soil 298:81-98.

Zhang, H., Huang, Y., Ye, X., Shi, L. and Xu, F. (2009) Genotypic differences in phosphorus acquisition and the rhizosphere properties of Brassica napus in response to low phosphorus stress. Plant Soil 320: 91-102.

Zhang, L., Zhao, G., Jia, J., Liu, X. and Kong, X. (2012) Molecular characterization of 60 isolated wheat MYB genes and analysis of their expression during abiotic stress. J. Exp. Bot. 63: 203-214.

Zhao, J., Jamar, D.C.L., Lou, P., Wang, Y., Wu, J., Wang, X., Bonnema, G., Koornneef, M. and Vreugdenhil, D. (2008) Quantitative trait loci analysis of phytate and phosphate concentrations in seeds and leaves of Brassica rapa. Plant Cell Environ. 31: 887-900.

Zhao, M.R., Han, Y.Y., Feng, Y.N., Li, F. and Wang, W. (2012) Expansins are involved in cell growth mediated by abscisic acid and indole-3-acetic acid under drought stress in wheat. Plant Cell Rep. 31: 671-685.

Zhao, X., Liu, X., Guo, C., Gu, J. and Xiao, K. (2013) Identification and characterization of microRNAs from wheat (Triticum aestivum L.) under phosphorus deprivation. J. Plant Biochem. Biotechnol. 22: 113-123.

Zhou, J., Jiao, F.C., Wu, Z., Li, Y., Wang, X., He, X., Zhong, W. and Wu, P. (2008) OsPHR2 is involved in phosphate-starvation signaling and excessive phosphate accumulation in shoots of plants. Plant Physiol. 146: 1673-1686.

Zhu, B., Choi, D.W., Fenton, R. and Close, T.J. (2000) Expression of the barley dehydrin multigene family and the development of freezing tolerance. Mol. Gen. Genet. 264: 145-53.

Zhu, J. and Lynch, J.P. (2004) The contribution of lateral rooting to phosphorus acquisition efficiency in maize (Zea mays) seedlings. Funct. Plant Biol. 31: 949-958.

Zhu, Y.G. and Smith, S.E. (2001) Seed phosphorus (P) content affects growth, and P_i uptake of wheat plants and their association with arbuscular mycorrhizal (AM) fungi. Plant Soil 231: 105-112.

Zhu, J., Shawn, M., Kaepple, S.M. and Lynch, J.P. (2005a) Mapping of QTL controlling root hair length in maize (Zea mays L.) under phosphorus deficiency. Plant Soil 270: 299-310.

Zhu, J., Shawn, M., Kaepple, S.M. and Lynch, J.P. (2005b) Mapping of QTLs for lateral root branching and length in maize (Zea mays L.) under differential phosphorus supply. Theor. Appl. Genet. 111: 688-695.

Zhu, J, Mickelson, S.M., Kaeppler, S.M. and Lynch, J.P. (2006) Detection of quantitative trait loci for seminal root traits in maize (Zea mays L.) seedlings grown under differential phosphorus levels. Theor. Appl. Genet. 113: 1-10.

Zhu, J., Zhang, C. and Lynch, J.P. (2010) The utility of phenotypic plasticity of root hair length for phosphorus acquisition. Funct. Plant Biol. 37: 313-322.